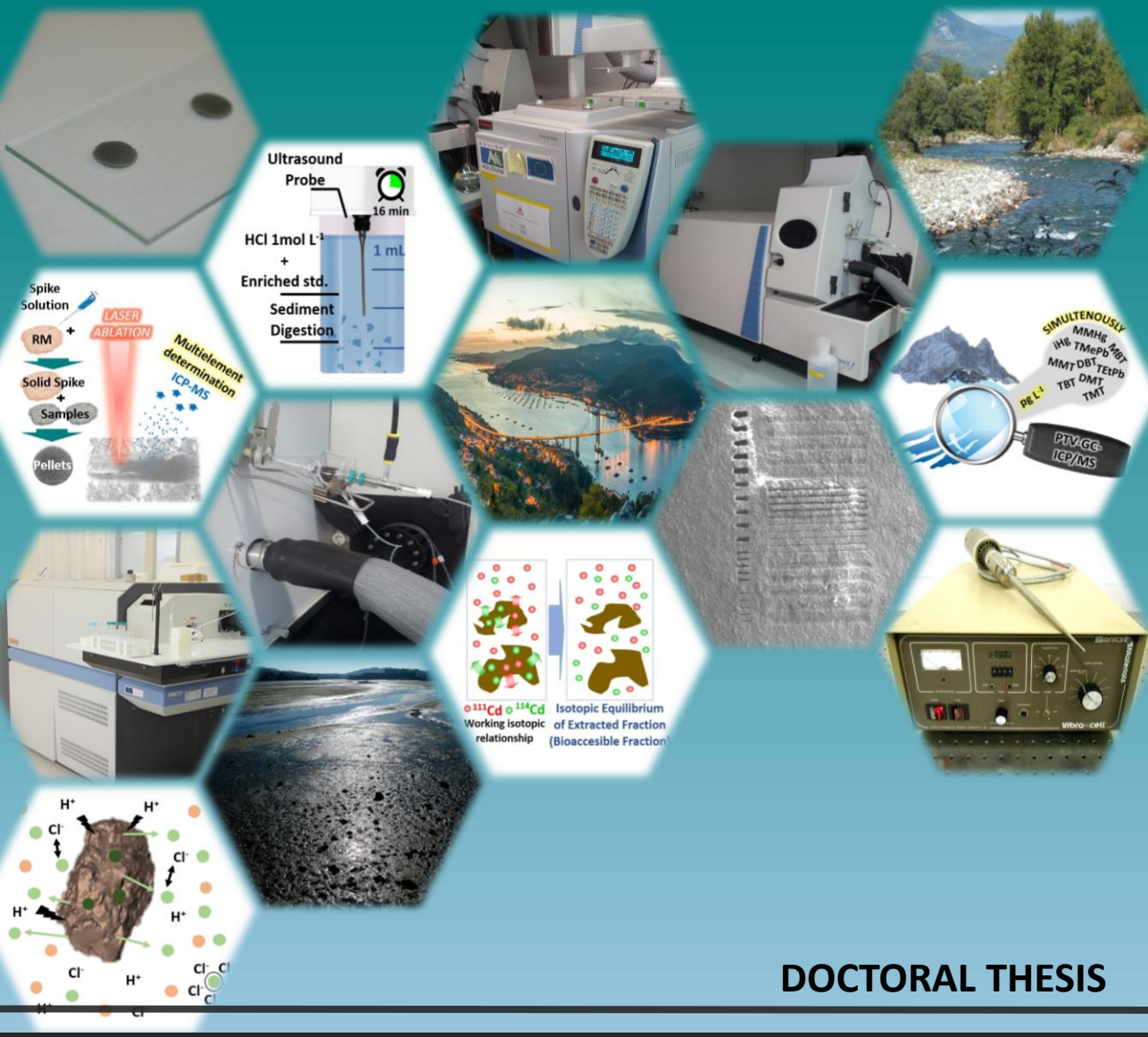

DOCTORAL THESIS

Analytical strategies to study metals in environmental matrices by inductively coupled plasma mass spectrometry

JAVIER TERÁN BAAMONDE

UNIVERSIDADE DA CORUÑA

UNIVERSIDADE DA CORUÑA

PhD “Química Ambiental y Fundamental”
(RD 1393/2007). Área de Química Analítica.

ANALYTICAL STRATEGIES TO STUDY METALS IN ENVIRONMENTAL MATRICES BY INDUCTIVELY COUPLED PLASMA MASS SPECTROMETRY

Author

Javier Terán Baamonde

Advisors

Dra. Rosa María Soto Ferreiro

Dra. Alatzne Carlosena Zubieta

A Coruña, 2017

INSTITUTO UNIVERSITARIO DE MEDIO AMBIENTE
UNIVERSIDADE DA CORUÑA

CICA | CENTRO DE INVESTIGACIONES CIENTÍFICAS AVANZADAS

UNIVERSIDADE DA CORUÑA

Dra. Dña. ROSA MARÍA SOTO FERREIRO y **Dra. Dña. ALATZNE CARLOSENA ZUBIETA,** Profesoras Titulares del Área de Química Analítica de la Universidade da Coruña,

CERTIFICAN

Que la presente memoria titulada *"Analytical Strategies to Study Metals in Environmental Matrices by Inductively Coupled Plasma Mass Spectrometry"* ha sido realizada por D. Javier Terán Baamonde bajo su dirección en el Departamento de Química Analítica de la Universidade da Coruña, y constituye su Tesis Doctoral para optar al grado de Doctor con Mención Internacional.

Y para que así conste, firman la presente en A Coruña a 3 de abril de 2017.

Dra. Dña. Rosa Soto Ferreiro Dra. Dña. Alatzne Carlosena Zubieta

RESEARCH PROJECTS & GRANTS

This doctoral Thesis has been carried out within the research group of Química Analítica Aplicada (QANAP) of the Universidade da Coruña and has been supported by the Galician and the Spanish Governments through the Research Projects:

"Programa de Consolidación y Estructuración de Unidades de Investigación Competitivas" (GRC2013-047, 2013-2016; 52/2010, 2010-2012; Xunta de Galicia). Researcher head: Darío Prada Rodríguez.

"Impacto de microplásticos, contaminantes regulados y emergentes de ecosistemas marinos y establecimiento de sus criterios de calidad ambiental (IMPACTA)" (CTM201348194-C3-2-R, 2014-2016; Ministerio de Economía y Competitividad). Researcher head: Soledad Muniategui Lorenzo.

J. Terán-Baamonde thanks the following financial supporting:

"Contrato Predoctoral de la Universidade da Coruña" (Universidade da Coruña); 2013-2015.

"Subvención para estancias de movilidad de estudiantes en el marco de estrategias institucionales de formación doctoral de las Universidades y de la consolidación de programas de doctorado con Mención a la Excelencia" (Ministerio de Educación); mayo a julio 2012; Grupo de Espectroscopia Atómica y Molecular (GEAM), Universidad de Oviedo.

"Ayudas UDC-Inditex para la realización de estancias en el extranjero" (Universidade da Coruña y Inditex S.A.) y ***"Ayudas para estancias en el extranjero de la Red Galega de Tratamento de Augas"*** (Red REGATA); septiembre a diciembre 2015; Laboratoire de Chimie Analytique Bio-Inorganique et Environnement (IPREM) – CNRS/Université de Pau et des Pays de l´Adour; Pau – Francia.

"Ayudas para estancias de investigación en el extranjero" (Agrupación CICA-INBIC); septiembre a noviembre 2016; Ultra Trace Analyses Aquitaine (UT2A); Pau – Francia.

AGRADECIMIENTOS

¿Cómo puede ser que después de escribir todo lo que viene a continuación, me siente delante de esta hoja en blanco durante tanto tiempo? Dándole vueltas y vueltas a cómo empezar estos agradecimientos, repasando mentalmente a las personas a las que darles las gracias… pero, sobre todo, como expresar esos sentimientos y recuerdos con unas simples palabras. Es imposible escribir más de una frase sin sorprenderse a uno mismo repasando mentalmente los recuerdos compartidos y las experiencias vividas… pero supongo que eso es lo que hace que esta etapa sea única e irrepetible.

Empezaré dándole las gracias al grupo de **Química Analítica Aplicada** de la UDC, a todos sus integrantes sin excepción, tanto de la Facultad como del IUMA o del departamento en Ferrol (aunque no voy a poner la lista porque como se me olvide alguno por nombrar... venga os lo merecéis…😖 *Darío*, *Sol*, *Puri*, *Isa*, *Jorge*, *Elisa*, *Mariajo*, *MariCarmen*, *Fanny*, *Vero*, *Carmen*, *Gloria*, *MariPaz*, *Elia*, *Maribel*, *Flavia*, *María*, *Pili*, *Silvia*, *Manolo*, *Victoria*, *Solís*…); porque sin duda he podido comprobar durante este tiempo que es más que un mero grupo de investigación, donde da igual los años que hayan pasado, el camino que haya elegido cada uno… porque llega el día de la comida de Navidad, o cualquier otro tipo de celebración, y las conversaciones, bromas, risas, complicidades, etc., que tienen lugar, hacen imposible decir que aquello es una simple reunión de compañeros de trabajo.

Muchísimas gracias a mis directores de tesis **Alatzne**, **Rosa** y **Andrade** (ya sé que oficialmente no lo eres, pero después de toda la ayuda prestada, enseñanzas transmitidas, cálculos realizados, disponibilidad para ayudarnos ante cualquier problema o situación… por mi parte hace mucho tiempo que te considero como tal). Gracias por confiar en mí hace ya algunos años atrás para iniciar mi carrera investigadora con vosotros, por adentrarnos juntos en partes de la Química Analítica que eran nuevas para todos nosotros, por el tiempo dedicado para tratar de entender los resultados alcanzados… pero, sobre todo, por vuestra disponibilidad, ayuda y cercanía desde el primer día hasta el último. Sin duda, sin vosotros todo habría sido mucho más difícil.

Gracias a las personas que hicieron posible mis diferentes estancias de investigación. Al profesor *Alfredo Sanz Medel* por permitirme pasar esos meses, al principio de esta tesis, en su grupo de investigación en **Oviedo**, quedando impresionado por su nivel científico y donde creo que acabé de convencerme para empezar mi carrera investigadora. Al profesor *Jorge Ruiz* por su amabilidad,

cercanía y formación en el campo de la dilución isotópica, algo totalmente nuevo para mí; y que debió hacer muy bien viendo la temática final de esta tesis. Y, sobre todo, al impresionante grupo de personas y compañeros de laboratorio que pude conocer, que me recibieron con los brazos abiertos desde el primer día y que siempre estaban dispuestos a ayudarme y a que viera cosas nuevas con ellos. Siguiendo con estancias de investigación, también querría dar las gracias a *David*, *Sylvain* y *Manu*, del **IPREM** (Pau – Francia; ¡fantástico centro de investigación!); por hacer que mi primera experiencia en el extranjero en el año 2015 fuera tan fructífera, que aprendiera cosas que de otra forma alomejor nunca hubiera conocido y por todo el trabajo invertido en la culminación del último apartado de esta tesis. También a todas las personas de este centro que siempre estuvieron dispuestas a ayudar y echar una mano. Y, por último, al equipo del **UT2A** (Pau – Francia), entre ellos a *Fabienne*, *Mathieu* y *Marlène*; porque durante el tiempo que pude pasar trabajando con ellos durante unos meses en el 2016, siempre estuvieron dispuestos a enseñarme y ayudarme en todo lo que pudieran, despertando mi curiosidad ante el fascinante nanomundo.

Agradecer a **Alicia**, de los Servicios de Apoyo a la Investigación de la UDC, y a esta institución en sí misma, toda su ayuda y paciencia cada vez que íbamos a asaltar los ICP, proponiéndole y plateándole las mil y una dudas e ideas que se nos pasaban por la cabeza.

También a todas las *instituciones* y *organismos* que hicieron posible la realización de este trabajo: al Instituto Español Oceanográfico de Vigo por la cesión de las muestras estudiadas en esta tesis; y a la Red REGATA, la Agrupación CICA-INIBIC, el programa de ayudas INDITEX-UDC, el Ministerio de Educación y a la propia Universidade da Coruña, por la financiación concedida en forma de ayudas o contratos para la realización de las estancias de investigación y de la propia tesis doctoral.

Especial mención a mis compis de mesa/laboratorio, **María**, **Noe S.** y **Noe R.**; al fin y al cabo, con alguna podría considerarme compañeros de piso… después de taaaaantas horas uno pierde la noción de los conceptos casa y laboratorio! Porque no nos dejan, pero los problemas del mundo de la investigación, de la universidad, etc. ya estaban más que solucionados… pero las risas que nos echamos 😆. Y porque se sigan repitiendo nuestras jornadas de escapismo seguidas de cenas, comidas y demás actividades de ocio…

Muchísimas gracias a todos mis amigos (**Pablo** y **Paula**, **Eva**, **Cris** y **Luigi**, **Ana**, **Sara**, **Chema**, **Arán**…), a lo que conozco desde la guardería, del colegio, del instituto, de la universidad… Que los puedes ver todos los días y siempre hay algo de qué hablar, o puedes pasar una temporada sin verlos, pero la distancia

o el tiempo no cambian nada. Por gente como vosotros la vida vale la pena, y siempre estaré ahí para ayudaros.

A nuestra familia *Paloise*, esa mágica conexión *"franco-venezolana-galega"* (**Patri** y **Jérôme**, **Vic**, **Nico** e **Inma**). Porque los que dicen que la distancia afecta a las relaciones no saben de lo que hablan, porque nos despedimos una vez pensando en el tiempo que pasaría hasta la siguiente vez que nos viésemos y ya van tres más (¡y las que quedan! Y mamá llorará más que en la anterior…😭), y porque hicisteis que Pau pasase de ser una simple ciudad más en el mapa a estar marcada con colores fosforitos para siempre. Muchas gracias chic@s, nuestra casa será la vuestra siempre y donde sea que estemos.

Gracias también a mi **familia** y **familia política**, a los que están y a los que no, por su apoyo durante todo este tiempo.

La palabra *gracias* ya se queda corta a la hora de mencionar a mis **padres**, y todo se resume a que todos los agradecimientos anteriores habría que borrarlos si no fuese por su ayuda, ánimo, apoyo y comprensión. Este trabajo también es fruto de vuestro esfuerzo y espero que estéis orgullosos de él como yo también lo estoy de vosotros.

Y como lo más importante siempre hay que dejarlo para el final… ahí estás tú, **Cris**. Cumpliendo más de media vida juntos, pasando otra etapa más uno junto al otro, y todo sigue como el primer día… Nada sería igual si no fuese contigo a mi lado. Muchas gracias Cristinita. 🫶

¡Muchísimas gracias a todos!
Con esto he querido dejar constancia de vuestro granito de arena en esta Tesis Doctoral, espero que estéis orgullosos de vuestro trabajo…

Javi

P.D.: Aunque el primer párrafo me quedó muy bonito, tener presente que me acordaba de todos y cada uno de vosotros antes de empezar a escribir estos agradecimientos…😉

INDEX

LIST OF FIGURES

CHAPTER II: INTRODUCTION

CHAPTER III: INTERPOLATION IN THE STANDARD ADDITION METHODS

CHAPTER V: ISOTOPE DILUTION ANALYSIS FOR METAL QUANTIFICATION BY ICP-MS

V.1.- A simple procedure to select a model for mass discrimination correction in isotope dilution inductively coupled plasma mass spectrometry

V.2.- A fast approach to evaluate the bioaccessible fraction of cadmium in sediments using isotope dilution inductively coupled plasma mass spectrometry (ID-ICP-MS)

V.3.- An isotope dilution inductively coupled plasma mass spectrometry (ID-ICP-MS) procedure to assess the bioaccessible fraction of chromium in sediments

V.4.- Direct and simultaneous determination of Cd and Cr in sediments by solid-spiking matrix matched isotope dilution laser ablation ICP-MS

LIST OF TABLES

CHAPTER V: ISOTOPE DILUTION ANALYSIS FOR METAL QUANTIFICATION BY ICP-MS

V.1.- A simple procedure to select a model for mass discrimination correction in isotope dilution inductively coupled plasma mass spectrometry

V.2.- A fast approach to evaluate the bioaccessible fraction of cadmium in sediments using isotope dilution inductively coupled plasma mass spectrometry (ID-ICP-MS)

V.3.- An isotope dilution inductively coupled plasma mass spectrometry (ID-ICP-MS) procedure to assess the bioaccessible fraction of chromium in sediments

V.4.- Direct and simultaneous determination of Cd and Cr in sediments by solid-spiking matrix matched isotope dilution laser ablation ICP-MS

CHAPTER VI: SIMULTANEOUS SPECIATION OF MERCURY, TIN AND LEAD COMPOUNDS IN NATURAL WATERS BY ISOTOPIC DILUTION AND PROGRAMMED TEMPERATURE VAPORIZATION INJECTION-GAS CHROMATOGRAPHY HYPHENATED WITH INDUCTIVELY COUPLED PLASMA-MASS SPECTROMETRY

LIST OF ACRONYMS

AAS	***A**tomic **A**bsorption **S**pectrometry*.
ADL	***A**bsolut **D**etection **L**imit.*
AFS	***A**tomic **F**luorescence **S**pectrometry.*
ANOVA	***A**nalysis **o**f **V**ariance.*
ASTM	***A**merican **S**ociety for **T**esting and **M**aterials*.
AVS	***A**cid **V**olatile **S**ulfide.*
BCR	***C**ommunity **B**ureau of **R**eference.*
BLM	***B**iotic **L**igand **M**odel.*
BOE	***B**oletín **O**ficial del **E**stado.*
CCQM	***C**omité **C**onsultative por la **Q**uantité de **M**atière.*
CEN	***E**uropean **C**ommitte for **N**ormalization*.
CI	**C**onfidence **I**nterval.
CRM	***C**ertified **R**eference **M**aterial*.
DBT	***Di**buty**lt**in.*
DLLME	***D**ispersive **L**iquid-**l**iquid **M**icro-**e**xtraction.*
DMT	***Dim**ethyl**t**in.*
DOC	***D**issolved **O**rganic **C**arbon.*
EEC	***E**uropean **E**conomic **C**ommunity.*
EqP	***E**quilibrium **P**artitioning **A**pproach.*
EQS	***E**nvironmental **Q**uality **S**tandards.*
ESA	***E**lectrostatic **A**nalyzer.*
ETAAS	***E**lectrothermal **A**tomic **A**bsorption **S**pectrometry*.
ETV	***E**lectrothermal **V**aporization*.
EU	***E**uropean **U**nion.*
FAAS	***F**lame **A**tomic **A**bsorption **S**pectrometry*.
FIAM	***F**ree **I**on **A**ctivity **M**odel.*
FID	***F**lame **I**onization **D**etection.*
GC	***G**as **C**romatography*.
GFAAS	***G**raphite **F**urnace **A**tomic **A**bsorption **S**pectrometry*.
HPLC	***H**igh **P**erformance **L**iquid **C**hromatography*.

ICMM	***I**nternational **C**ouncil of **M**ining and **M**etals.*
ICP	***I**nductively **C**oupled **P**lasma*.
ICP-AES	***I**nductively **C**oupled **P**lasma **A**tomic **E**mission **S**pectrometry.*
ICP-OES	***I**nductively **C**oupled **P**lasma **O**ptical **E**mission **S**pectrometry*.
ICP-MS	***I**nductively **C**oupled **P**lasma **M**ass **S**pectrometry*.
IDA	***I**sotope **D**ilution **A**nalysis.*
IDMS	***I**sotope **D**ilution **M**ass **S**pectrometry.*
IEO	***I**nstituto **E**spañol de **O**ceanografía, Oceanographic Spanish Institute.*
IHg	***I**norganic mercury.*
IRMM	***I**nstitute for **R**eference **M**aterials and **M**easurements.*
IUPAC	***I**nternational **U**nion of **P**ure and **A**pplied **C**hemistry*.
ISO	***I**nternational **O**rganization for **S**tandardization*.
KED	***K**inetic **E**nergy **D**iscrimination.*
LA	***L**aser **A**blation*.
LOD	***L**imit **o**f **D**etection.*
LOF	***L**ack-**o**f-**f**it.*
LOQ	***L**imit **o**f **Q**uantification.*
LLE	***L**iquid-**l**iquid **E**xtraction.*
LS	***L**east-**s**quares*.
LVI	***L**arge **V**olume **I**njection.*
MASE	***M**embrane **A**ssisted **E**xtraction.*
MBT	***M**ono**b**utyl**t**in.*
MDL	***M**ethodological **D**etection **L**imit.*
MMHg	***M**ono**m**ethylmercury.*
MMT	***M**ono**m**ethyl**t**in.*
MS	***M**ass **S**pectrometry*.
MSMS	***M**ass **S**pectrometry in tandem mode.*
MSEP	***M**agnetic **S**tirring-assisted **E**xtraction **P**rocedure.*
MW	***M**icro**w**ave.*
NIST	***N**ational **I**nstitute of **S**tandars and **T**echnology*.
OLS	***O**rdinary **L**east-**s**quares*.
PFPD	***P**ulsed **F**lame **P**hotometric **D**etector.*
PTFE	***P**oly**t**etra**f**luoro**e**thylene*.

PT	***P**urge and **T**rap.*
PTV	***P**rogrammed **T**emperature **V**aporization.*
Pyr	***P**yrolysis.*
QC	***Q**uality **C**ontrol*.
RIDMS	***R**everse **I**sotope **D**ilution **M**ass **S**pectrometry.*
RSD	***R**elative **S**tandard **D**eviation*.
RSDF	***R**elative **S**tandard **D**eviation of the **F**it.*
SD	***S**tandard **D**eviation*.
SAM	***S**tandard **A**ddition **M**ethod*.
SBSE	***S**tir-**b**ar **S**orptive **E**xtraction.*
SEM	***S**imultaneously **E**xtracted **M**etals.*
SM&T	***S**tandards, **M**easurements and **T**esting Programme.*
SPE	***S**olid **P**hase **E**xtraction.*
SQG	***S**ediment **Q**uality **G**uidelines.*
SI	*International **S**ystem of **U**nits.*
SRM	***S**tandard **R**eference **M**aterial*.
SS-IDA	***S**pecies-**s**pecific **I**sotope **D**ilution **A**nalysis.*
TBT	***T**ri**b**utyl**t**in.*
TMAOH	***T**etramethylammonium **H**ydroxide.*
TMT	***T**ri**m**ethyl**t**in.*
TMePb	***T**ri**m**ethyllead.*
TEtPb	***T**ri**e**thyllead.*
TOF	***T**ime **O**f **F**light*.
UBEP	***U**ltrasound **B**ath-assisted **E**xtraction **P**rocedure.*
UPEP	***U**ltrasound **P**robe-assisted **E**xtraction **P**rocedure.*
USEPA	***U**nited **S**tates **E**nvironmental **P**rotection **A**gency.*
UV	***U**ltra**v**iolet.*
WER	***W**ater-**e**ffect **R**atio.*
WFD	***W**ater **F**ramework **D**irective.*

SUMMARY

This Doctoral Thesis presents validated analytical strategies to assess metallic contamination (metals and their chemical forms) in marine sediments and river waters by ICP-MS applying the principles of the Green Analytical Chemistry. Thus, several studies were performed in sediment samples of two Galician rias. The metallic bioaccessible fraction was accurately evaluated through the simultaneously extracted metals (SEM) and the acid volatile sulfides (AVS). The SEM-AVS ratio was calculated to evaluate the metallic contamination risk. The isotope dilution analysis allowed to improve the results in the determination of the bioaccessible fractions of cadmium and chromium, since is not affected by analyte losses and in addition is a low time-consuming procedure. The total content of these elements was determined by the direct analysis of the solid samples with laser ablation coupled to ICP-IDMS synthetizing a unique solid spike. River water samples were analyzed for the simultaneous determination of organometallic compounds of mercury, tin and lead using large volume injections in a programmable temperature vaporizer coupled to GC-ICP-MS. This new methodology provided detection limits well below the actual directive requirements.

Also, it is addressed a statistical study of the standard addition method in classical calibration and the mass discrimination factor in isotope dilution.

RESUMEN

Esta Tesis Doctoral presenta estrategias analíticas para evaluar la contaminación metálica en sedimentos marinos y aguas naturales mediante ICP-MS aplicando los principios de la Química Analítica Verde. Así, se realizaron varios estudios en muestras de sedimentos procedentes de dos rías gallegas. Se evaluó la fracción metálica bioaccesible a través de los metales extraídos simultáneamente (SEM) y de los sulfuros ácidos volátiles (AVS). Se calculó la relación SEM-AVS para evaluar el riesgo de contaminación. El análisis por dilución isotópica mejoró los resultados en la determinación de la fracción bioaccesible de cadmio y cromo ya que no está afectado por pérdidas de analitos e implica menos tiempo. Se determinó el contenido total de cadmio y cromo mediante análisis directo de muestras sólidas con ablación láser ICP-IDMS, sintetizando un único trazador sólido. Se analizaron muestras de aguas de río para la determinación simultánea de compuestos organometálicos de mercurio, estaño y plomo inyectando volúmenes grandes de muestra en un inyector de temperatura programable acoplado con GC-ICP-IDMS. Esta nueva metodología proporcionó límites de detección inferiores a los requerimientos de la directiva actual.

También se realizó un estudio estadístico del método de adiciones estándar en calibración clásica y del factor de discriminación de masas en dilución isotópica.

RESUMO

Esta Tese Doctoral presenta estratexias analíticas para evaluar a contaminación metálica en sedimentos marinos e augas naturais mediante ICP-MS aplicando os principios da Química Analítica Verde. Así, realizaronse varios estudos en mostras de sedimentos procedentes de dúas rías galegas. Evaluouse a fracción metálica bioaccesible a través dos metalais extraídos simultáneamente (SEM) e dos sulfuros ácidos volátiles (AVS). Calculouse a relación SEM-AVS para avaliar o risco de contaminación. A análise por dilución isotópica mellerou os resultados na determinación da fracción bioaccesible de cadmio e cromo xa que non está afectado por pérdidas dos analitos e implica menos tempo. Determinouse o contido total de cadmio e cromo mediante a análise directa de mostras sólidas con ablación láser ICP-IDMS, sintetizando un único trazador sólido. Analizáronse mostras de augas de río para a determinación simultánea de compostos organometálicos de mercurio, estaño e chumbo inxectando volúmenes grandes de mostra nun inxector de temperatura programable acoplado con GC-ICP-IDMS. Esta nova metodoloxía proporcionou límites de detección inferiores aos requerimientos pola directiva actual.

Tamén se realizou un estudo estadístico do método de adicións estándar na calibración clásica e do factor de discriminación de masas en dilución isotópica.

CHAPTER

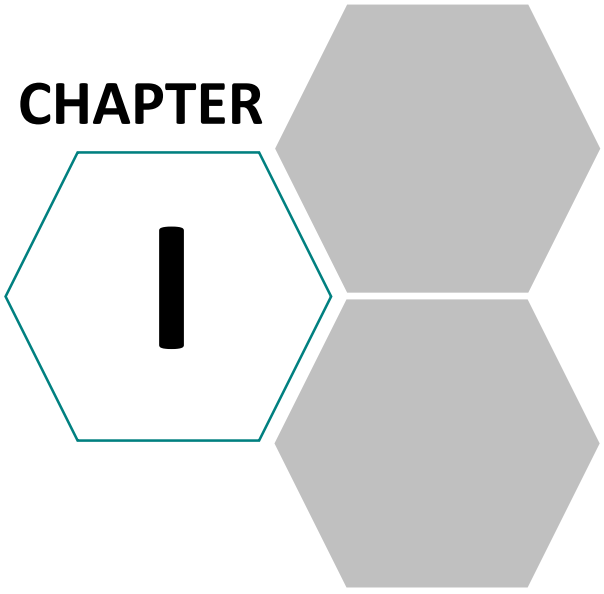

I

OBJECTIVES AND STRUCTURE OF THE THESIS

OBJECTIVES and STRUCTURE of the THESIS

The main objective of this Doctoral Thesis, entitled *"Analytical strategies to study metals in environmental matrices by inductively coupled plasma mass spectrometry",* is to develop new analytical methods to detect and quantitate trace metals and their chemical forms applying the principles of the Green Analytical Chemistry. Of course, the goal is to get simple, fast and accurate methods that yield validated information for decision-making. In particular, analytical methods will be established to measure the total concentration and the bioaccessible fractions. This work has been developed in the research group of Química Analítica Aplicada (QANAP) of the Universidade da Coruña.

This PhD is focused on two different environmental matrices, water and sediments. For the former, clear and strict laws were enforced under the Water Framework Directive (WFD), the lists of "potentially hazardous" (PHS), "priority" (PS) and "of emerging concern" compounds; as well as the establishment of Environmental Quality Standards (EQS) for each substance. All they bring paramount importance to the development of new analytical procedures, involving suitable and modern extraction techniques and cutting-edge analytical equipment to be able to detect and quantify low amounts of the pollutants. For sediments case it is known that the quantitation of the bioaccessible fraction is a good indication on their quality. Unfortunately, many different viewpoints over the past years about the definition of this (and related) terms, and the lack of a uniform methodology for its assessment, made it necessary to develop new, simple analytical methodologies to determine this fraction. Hopefully, they would contribute to the simplification and harmonization of "Sediment Quality Guidelines" (SQGs).

According to all these considerations, the following specific objectives were posed:

- To perform a preliminary statistical study of the most common classical calibration modes as a necessary stage in any quantitative analysis.
- To develop and validate a simple procedure to assess the bioaccessible metallic fraction through the simultaneously extracted metals (SEM) in marine sediments employing inductively coupled plasma mass

spectrometry (ICP-MS), as well as to propose a simple approach to determine the acid volatile sulfides (AVS).

- To apply the isotope dilution (ID) analysis to assess both the extraction process of the bioaccessible fraction of cadmium and chromium in sediments and to quantify them with an absolute method. For this, the best approach to calculate the mass discrimination factor in ICP-IDMS needs to be evaluated.
- To develop a simple and reliable methodology to quantify the total content of cadmium and chromium in sediments by laser ablation ICP-IDMS.
- To implement an analytical method for the simultaneous speciation of organometallic compounds of mercury, tin and lead in natural water samples using Programmed Temperature Vaporization Gas Chromatography coupled with ICP-IDMS.

The experimental work of this PhD and the results gathered from it were organized in dedicated chapters that are summarized below:

- **Chapter II** is a critical review. It includes an overview of the metals and their properties and characteristics, their aquatic and sediment chemistry, a suite of definitions of essential terms and references to various risks assessments. Procedures for sample treatments and instrumental measurements are also presented. Finally, common quantification approaches are addressed.
- **Chapter III** presents a mathematical and thorough demonstration about the optimal way to quantify analytes, in classical terms through the standard addition method. For this, two common practices, extrapolation and interpolation, are studied in terms of the variances associated with the predictions.
- **Chapter IV** reports on a procedure to assess the bioaccessible metallic fraction through the simultaneously extracted metals (SEM) and the acid volatile sulfides in marine sediments. The SEM-AVS ratio is further used to evaluate the metallic contamination risk of real sediment samples.
- **Chapter V** addresses the use of isotope dilution analysis to determine metals by ICP-MS. First, a procedure to select the best approach to set

one of the parameters that affects accuracy (mass bias) is established. Next, the methods developed to quantitate and evaluate the extraction of the bioaccessible fractions of cadmium and chromium from sediments by ICP-IDMS are presented.

The methodology developed for determining total cadmium and chromium in sediments by laser ablation ICP-IDMS is detailed. It is based on the synthesis of a unique solid spike.

- **Chapter VI** presents results from the research stay realized in the *Laboratoire de Chimie Analytique Bio-inorganique et Environnement* (LCABIE – *Institut Pluridisciplinaire de Recherche sur l´Environnement et les Matériaux* – Pau, France). It reports on analytical method to the simultaneous speciation of organometallic compounds of mercury, tin and lead in water samples by a Programmed Temperature Vaporization (PTV) gas chromatography coupled with ICP-IDMS.

CHAPTER

II

INTRODUCTION

INTRODUCTION

The use of metals has increased exponentially from the Industrial Revolution. As result, metals can reach high concentrations, especially near the discharge zone. The large increase in the circulation of these elements through the environment and their inevitable transfer to the human food chain remains an important environmental issue, which entails some unknown health risks for future generations. In fact, different international organisms and institutions are focused on the development of updated scientific principles and guidelines for assessing ecological risks of chemical substances, among which are metals, for freshwater and marine sediments [1].

1. Metals/metalloids and organometallic compounds

Inorganic metals and metal compounds have special characteristics in comparison with organic substances, and they should be taken into account when assessing their risks [2]. Some of these unique characteristics are:

1. Not created and destroyed by biological or chemical processes. They only suffer transformations to another chemical form.
2. Native or zero valence forms are not soluble. On this way, the toxicity and bioavailability studied by toxicity tests based on soluble salts may be overestimated.
3. Some metals are nutritionally essential elements (for humans, animals, plants or microorganisms) at low levels but toxic at high levels; others have no known biological functions. Besides, their toxicokinetics and toxicodynamics depend on the metal, the form and the organism´s ability to regulated and/or store it.
4. Be naturally occurring, so organisms have evolved mechanisms to regulate accumulations.
5. Present concentration variations across geographic regions, and they could be introduced into the environment as mixtures. Their environmental chemistry strongly influences their fate and effects on human and ecological receptor.

In environmental chemistry, it is necessary to clarify some metal related terms. **Speciation** was used to refer to the reaction specificity, i.e., changes during natural cycles (species transformation), analytical activity of measuring the distribution of an elements among species in a sample (speciation analysis), and to the distribution itself of an element among different species (species distribution). It was defined as "the occurrence of an elements in separate, identifiable form (chemical, physical or morphological state)". As an attempt to harmonize this term, IUPAC [3] formulated the following definitions:

- **Speciation**: distribution of an element among defined chemical species in a system.
- **Specie**: specific form of an element defined as to isotopic composition, electronic or oxidation state, and/or complex or molecular structure (in a toxicology point of view, some aspects are more important than other).

Related to this, another term is **fractionation**. It can be defined as the process of classification of an element according to physical (e.g. size or solubility) or chemical (e.g. bonding or reactivity) properties [4].

1.1. Aquatic chemistry: metals complexes

Metals dissolved in water may be presented as free ions, or aquo-ions (surrounded by coordinating water molecules) or complexes. On this way, the total analytical concentration measured of a metal in water is the sum of: (concentration of its free ion + concentration of its complexes + concentration of metal associated with suspended organic or mineral solids) [2]. These complexes formation is important to understand the availability and fate of metals in environment, because an increase of the metal that is complexed results on an increase of the solubility of minerals of that metal [5].

Complexes are formed between metals (acids) and ligands (bases), both in solution and at the surface of minerals and organisms; and the toxic reaction of organisms to metals can be related to the nature of these metal complexes. A useful tool to understand the strength of metal complexing and toxicity was introduced by Pearson (1973) [6]. Here, metals cations are Lewis acids (electron acceptor) and ligands are Lewis bases (electron donor). "Soft" term means that

species have a deformable or polarizable electron cloud, and the electrons are mobile and easily moved; on this way, these species prefer to participate in covalent bonds. “Hard” species are present in ionic bonds due to their nondeformable and low polarizable electron cloud with strongly held electrons [5]. Hard acids form strong bonds with hard bases (by ionic bonding), and soft acids form strong complexes with soft bases (by covalent bonding); in contrast, the bonds formed between hard-soft or soft-hard acids and bases are weak, and their complexes are not frequent.

Hard metals, which are the least toxic and play an important health role as macronutrients, preferentially bind with hard bases that contain oxygen, forming weaker bonds with soft nitrogen or sulfur species. The strength of binding between hard metals and hard ligands is related to the pH. Soft metals bind normally with S and N ligands, forming weaker bonds with hard base species such as hydroxide and sulfate. Soft borderline metals, and Mn^{2-} (which is hard), form bonds of decreasing strength with soft ligands such as sulfide in the order: $Pb^{2+} > Cu^{2+} > Cd^{2+} > Co^{2+} \approx Fe^{2+} > Ni^{2+} > Zn^{2+} > Mn^{2+}$. For other hand, the tendency of metals to bind to soft ligands or to organic substrates (usually soft) is greatest or soft and borderline metals (soft acids), followed by the hard metals (hard acids): $Pb^{2+} > Cu^{2+} > Cd^{2+} > Zn^{2+} > Ca^{2+} > Mg^{2+} >> Na^{+}$ [7].

The transformation process of metals and metalloids occur through interactions with other chemicals and biota in the environment; and the cycling and distribution of organometallic compound between terrestrial, aquatic and atmospheric phases may be physically, chemically or biologically mediated. Table 1 shows some of the most commonly and stable organometallic compounds in the environment.

Table 1. Most common occurring environment stable organometallic compounds.

Metal/metalloid	Organometallic compounds
Arsenic	Methylarsenic acid, dimethyl arsenic acid, trimethyl arsine, trimethylarsine oxide
Lead	Tetramethyl/ethyl lead, trimethyl/ethyl lead, dimethyl/ethyl lead
Mercury	Methyl mercury, dimethyl mercury
Selenium	Dimethyl selenide, dimethyl diselenide, seleno-amino acids
Tin	Tributyltin, bis(tributyltin) oxide

Metal mobility and toxicity may be affected by the organometallic environmental transformations, and these transformations (and their products) are dependent on the environmental conditions (e.g. pH, temperature, reduction and oxidation potential, organic matter content, dissolved oxygen, nutrient availability, salinity, complexing rates, etc., many of which are interrelated), the microorganism population and the distribution of the metal between compartments (sediment, water, gaseous) [2].

One of the most important process that metals and metalloid suffer in the environment is the methylation/demethylation process, which can take place through biotic or abiotic transformations. The biotic transformation is the process for which the organisms transfer alkyl groups to bioavailable metals by their bacterial community (i.e. the sulfate-reducing bacteria *SRB*). The main compartment in which this transformation occurs is the sediment column, but due to the higher volume of water column, the methylation process here it is also important. Note that, the methylation rates decrease with increasing the sediment depth, probably due to a decrease in biotic habitat [8, 9].

In general terms, the metal-methylation process is stimulated by high temperatures and anaerobic conditions (on the contrary for the demethylation process). Although the pH effect is complex, organometallic compounds tends to increase in the water column in low pH environment but probably due to the release of metals from the soils and sediments. In low sulfate concentrated media, such as freshwater ecosystems, an increase of sulfate concentration

reveals an increase of the methylation rates. This might be explained by the formation of less bioavailable metal-sulfur complex, and not by the metal sulfide formation. Finally, a high dissolved organic carbon (DOC) content, which may bind with metals/metalloids and making them unavailable, reduces the biotic methylation rates. A brief of this tendencies are showed in Table 2 [2].

Table 2. Trends of environmental factor on the methylation/demethylation rates.

Parameter	**Tª**		**pH**		**SO_4^{2-}**	**Org. matter**	**Redox**		**Salinity**
Value of parameter	**↑**	**↓**	**↑**	**↓**	**↑**		**Oxic**	**Anoxic**	**↑**
Total methylation	↑	↓	?	?	?	?	↓	↑	↓
Aquatic	↑	↓	↓	↑	↓	↓↑	↓	↑	↓
Sediment	↑	?	↑	↓	↓	?	?	?	?
Demethylation	↓	↑	↓	↑	?	?	↑	↓	?

Regarding abiotic transformations, there are three main mechanism, namely, transmethylation between mercury and tin/lead alkyls, reactions with humic/fulvic substances and photochemical reactions. Organometallic compounds with electronegativity greater than 1.7 are stable under environmental conditions but carbon-metal bonds with metal electronegativity lower than 1.7 will undergo hydrolysis.

1.2. Sediment chemistry: dissolved and labile metal pools

Sediments (bed or bottom) are found at the bottom of lakes, rivers, and estuaries. Its chemistry is determined by their location and characteristics of the water body in which they are hosted.

Because of their large capacity to "hold" metals (up to a million times more metal than an equivalent volume of water), sediments have been characterized as "sinks"; and trough which metals can enter in ecological and human food webs [10]. Accumulation in benthic organisms (those that live in the sediments or that feed from the sediment bed; see Figure 1) is the main entry and uptake route [11].

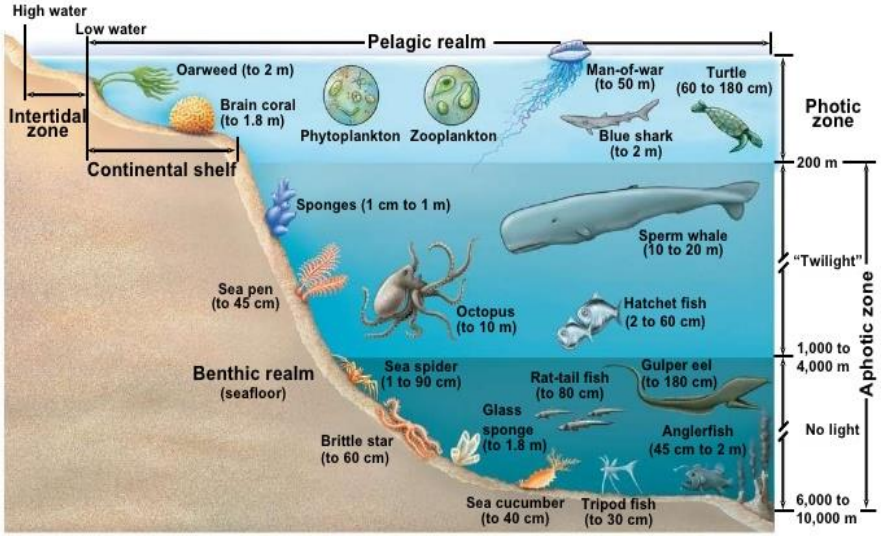

Figure 1. Representation of ocean habitats (Pearson Education Inc. 2009).

For humans, the route of entry of metals from the sediments is by water used for drinking, bathing and swimming; and their availability is mediated by sediment-water exchange processes that can result in the release or remobilization of chemicals from the sediment bed [2]. But it is truth that is some cases, for examples for mercury and its capacity to bioaccumulate as monomethyl form, fish consumption is the critical route of exposure.

Two kinds of pools should be considered for the metal risks assessment in sediments:

- Metals found within the mineral matrix of sediments soils. It is not available to biota and its release only occur over geological time scales by diagenetic process.

- "Exchangeable" or "labile". Aqueous or dissolved metal species bounded to colloids or to sediment particles through an exchangeable binding

process. The origin of these metals are in weathering and diagenetic process, or in anthropogenic activities. This exchangeable poll of metals is subject to speciation in the aqueous phase and sorption to solid phases, where sorption is a term that includes (see Figure 2):

- Adsorption, accumulation of matter at the solid-water interface or a two-dimensional process.
- Absorption, inclusion in a three-dimensional matrix.

This sorption process can occur rapidly, but desorption and dissolution of metal from the solid phase may be a two-step process, where the second step is rate limiting [12].

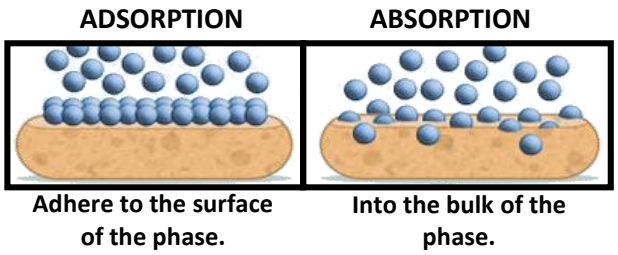

Figure 2. Difference between adsorption and absorption process.

Several speciation/complexation model are available to perform the distribution of metals among aqueous species and between the aqueous phase and the solid phase [13, 14]; but they do not work well under anoxic conditions, where metals are controlled by the solubility of metals sulfides, or when the reaction is governed by microbial processes (e.g. Hg methylation). Thus, extremely insoluble metals sulfides are formed in anoxic sediments by soft acid metal cations, whereas borderline hard and hard metal cations dorm slightly more soluble metal sulfides [15].

In oxic sediments pore waters, metals will exist as aqueous species, that means, freely dissolved ions or metals complexes and associated with colloids. Solid-phase reactions are controlled by iron oxyhydroxides and manganese oxides that are present as colloids, sediment particles or surface coatings of particles; organic matter and clay colloids and particles. These solid-phase

manganese oxides are the first to be reduced and dissolved, releasing metals that are sorbed or coprecipitated. Then, these metals will be adsorbed by iron(III) oxyhydroxides. Under reducing conditions, particularly as sulfate is consumed and the sulfur is converted to sulfide, metal concentrations in poor water again drop as solid-phase metal sulfides are formed [2].

As a result of redox chemistry (Figure 3), metals can undergo seasonal redox-driven cycling between the water column and sediments or within the sediments:

1. Adsorption and coprecipitation of metals with iron and manganese hydroxides under oxidizing conditions.
2. Under moderate reducing conditions; reduction and dissolution of the manganese and iron oxyhydroxides with the release of the associated metals into the water or pore water.
3. Metal diffusion upward toward the zone of low metal concentration under oxidizing conditions or downward toward the zone of low metal concentration owing to their precipitation as sulfides.

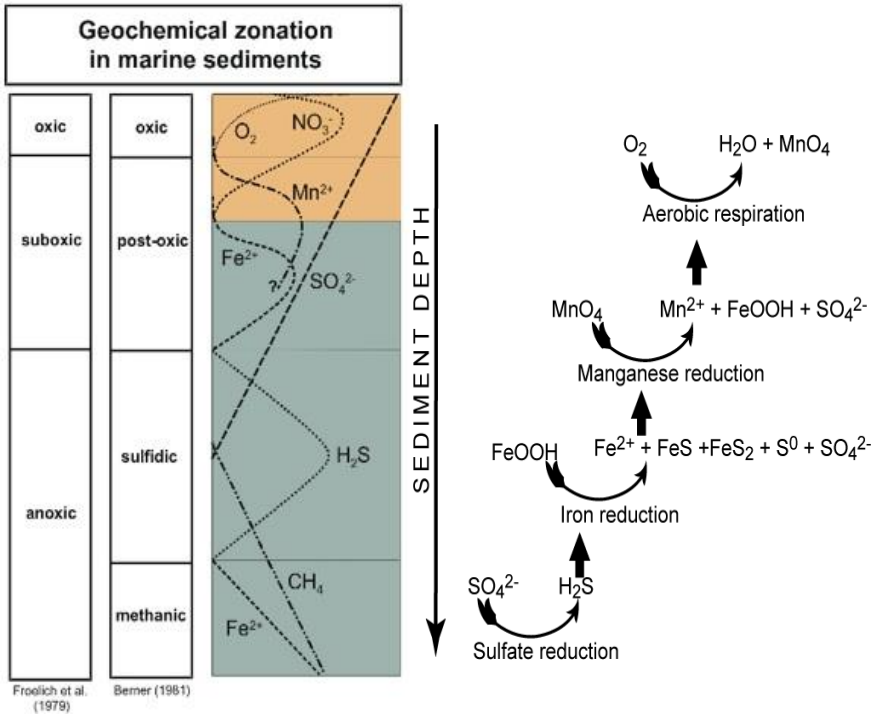

Figure 3. Scheme for redox cascade in marine sediments [16].

As a result of this vertical cycling, the depth profile of metals in pore water may not be the same that of the solid phase. Additionally, pH affects the species distribution of dissolved ligands and the surface charge of binding sites on dissolved organic matter and solid phase (e.g. iron oxyhydroxides); on this way, this parameter plays an important role on metal speciation and binding. Thus, at low pH surface sites are protonated and the sorption of cationic metal decreases, increasing the metal mobility.

1.3. Bioavailability or bioaccesibility?

In recent years, there are many efforts are focused on the development of updated scientific principles and guidelines for assessing ecological risks of chemical substances for freshwater and marine sediments. In the case of metals, the associated risks vary according to the physical, chemical and biological conditions under which an organism is exposed, and to their bioavailability.

Taking into account the critical importance of the bioavailability and bioaccessibility for the risk assessment process, these terms must be clearly understood. The numerous research works related to these concepts for decades with different definitions and interpretations created more than a *semantic stumbling block*. For example, in the case of bioavailability concept, some of these definitions (sometimes depending on the discipline) are [17]: (i) Fraction of a chemical accessible to an organism for absorption, the rate at which a substance is absorbed into a living system, or a measure of the potential to cause a toxic effect; (ii) Fraction of chemical absorbed and able to reach the systemic circulation in an organism; (iii) Chemical crossing a cell membrane and becoming available at a site of biological activity, etc.

On this way and taking the point of view of IUPAC recommendations, it is possible to differentiate these two terms as [18]:

- **Bioavailability**: extent of absorption of a substance or compounds (freely available) by a living organism compared to a standard system.
- **Bioaccessibility**: potential for a substance or compounds to come in contact with a living organism and then interact with it if the organism has access to the chemical. Contaminants can become available within the order of second from some locations (and hence are bioavailable), following release from labile or reversible pools, or the organism can move into contact with the substance/compound. To sum up, bioaccessible encompasses what is actually bioavailable now plus what is potentially bioavailable [17].

One important advantage of these definitions are their multi-functionality, as they can be applied to contaminants being available or accessible to microorganisms, fungi, plants, invertebrates and higher animals; because the portion of a chemical bioavailable or bioaccessible in a given sample can differ substantially between organisms. Before bioavailability becomes relevant, substance must be accessible to the living organisms at risk. The cases that need careful consideration are those where living organisms occur, but where essential nutrients or toxicants are locked into physical or chemical compartments which inhibit or prevent contact with the living organisms. Here,

the bioaccessibility is the limiting factor that determines the possibility of exposure and resultant adequate nutrition or potential toxicity.

Figure 4 shows the distribution of a chemical in sediments. They can be divided into an irreversibly bound pool (i.e. non-extractable, bound residues), reversibly bounds, and freely dissolved pool. The reversibly bound and the freely dissolved pool constitute the bioaccessible pool. This accessible pool (operationally defined) defines the fraction of total concentration that can undergo degradation, be mobilized or taken up by organisms. However, it is a poor measure for the actual diffusion, partitioning or uptake process, which is rather driven by the freely dissolved concentration or the chemical activity. Bioavailability is linked to bioaccessibility and the freely dissolved concentration (or the chemical activity), and also includes the uptake of a chemical by the organisms; so it not only depends on the characteristics of the sediment, but also on the organism.

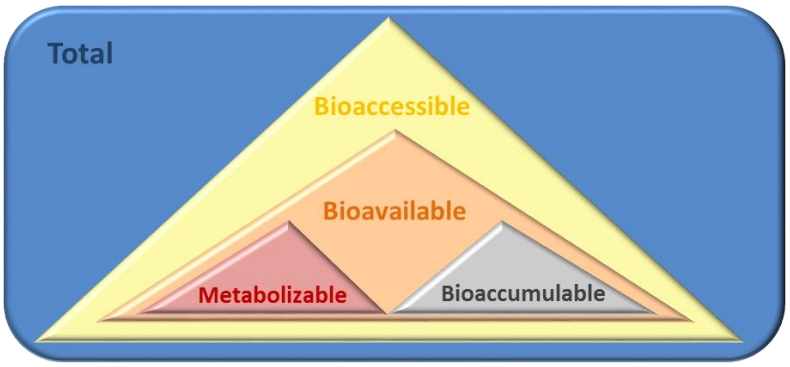

Figure 4. Distribution of a chemical in sediments.

A detailed scheme of these fractions into the marine sediments is shown in Figure 5.

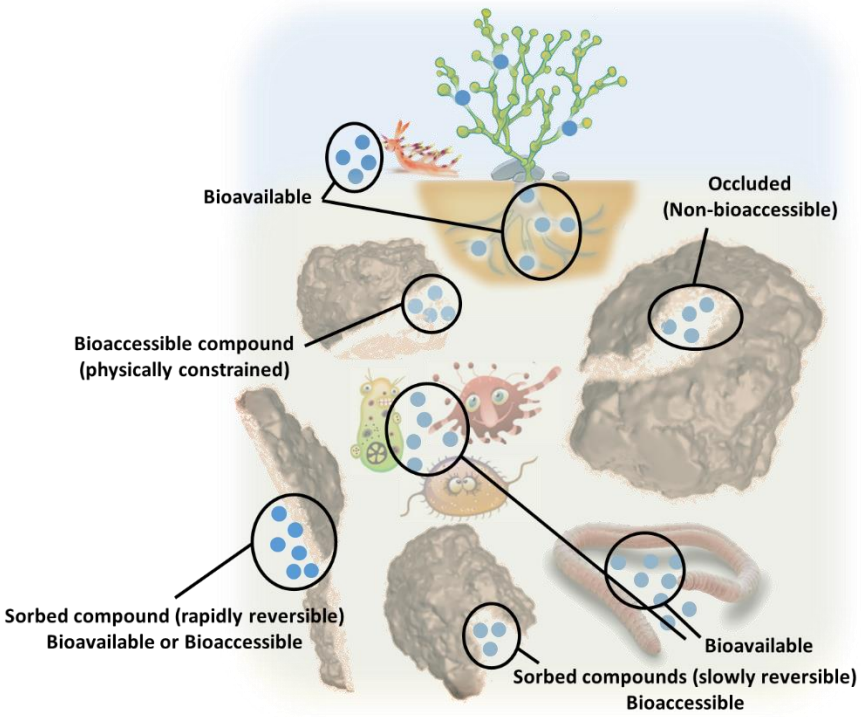

Figure 5. Bioavailable and bioaccessible fractions in marine sediments.

In the case of metals, *non-ionic* and *uncombined form* are mostly non bioaccessible or bioavailable. An exception is mercury vapor, because it is lipid-soluble and is able to dissolve in cell membranes. Besides, the cationic forms (dimetilmercury and mercury ions) are much less able to pass into/trough biological membranes; but on the other hand, the mercury chloride can exist in a unionized lipid-soluble form or converted to methylmercury chloride, which are readily absorbed by living organisms.

Metallic elements that form *hydrated ions* are accessible to living cells, but elements that form insoluble precipitates in water may not be bioaccessible.

For *complexed ions* (by inorganic or organic ligands), their bioavailability varies with the nature of the complex. Often, aqueous complexes are in an equilibrium state that may fluctuate considerably with environmental

conditions, and any change of these conditions lead to important consequents for the affected ecosystem.

Referring to the bioaccessible and bioavailable terms through the food chain, they vary between elements and the environmental chemical species, how they are stored and their sinks. Besides, it is assumed that proportions of chemical species remain constant in the different environmental compartments, but this is not always true.

Some organisms accumulate elements and compounds from the environment (**bioconcentration)** or from their prey (**bioaccumulation**), causing them to have very high body load relative to outside concentrations. Besides, how each successive trophic level in a predator-prey relationship has a lower biomass or a lower productivity, a process of **biomagnification** is presented. Figure 6 shows these processes in aquatic environment.

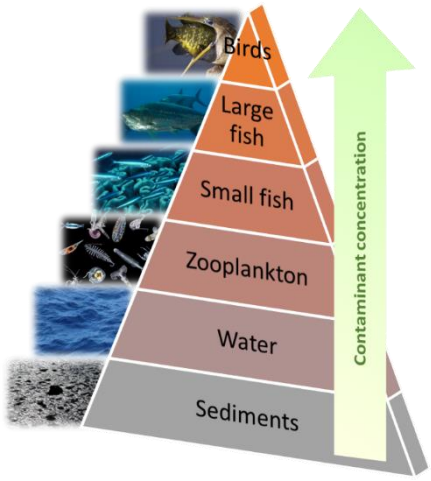

Figure 6. Biomagnification process in the food web for aquatic environment.

1.4. Criteria for risk assessment

All these terms are very important in an environmental risk assessment (ERA) process, defined as: identification and quantification of the risk resulting from a specific use or occurrence of a chemical or physical agent, taking into

account possible harmful effects on individuals or populations exposed to the agent in the amount and manner proposed and all the possible routes of exposure. Normally, these terms are included into a risk assessment management process, that is the whole process from hazard identification to risk management (combination of risk evaluation, emission and exposure control and risk monitoring), with the final goal to reduce the risks to acceptable minimum levels.

There are four steps in risks assessment:

1. Hazard identification.
2. Risk characterization (potential effects and quantify dose-effect/response relationships).
3. Exposure assessment.
4. Risk estimation.

The chemical status protection is defined in terms of compliance with all environmental quality standards (EQS) established for the chemical substances of the European list of priority. These EQS are concentrations derived in water column, sediment and biota that should protect human health and the environment. The Directive 2008/105/EC and the new Directive 2013/39/EC, gives a useful role to sediment: member states have the possibility to derive environmental quality standards for the priority substances in sediment compartment for specific water bodies (no specific guidance for sediment risk assessment has been developed). Furthermore, the analysis of sediment for specific priority substances is useful for the analysis of the trend [19].

It is generally recognized that total metal concentrations are often poor predictor of metal bioavailability and the risk posed by metals. Although bioavailability assessments would be more preferable, the only real way for measuring bioavailability is by exposing relevant species to sediment and obtaining the tissue residues and toxicokinetics estimations. For other hand, bioaccessibility can be measured using other techniques and extraction approach, but what is really needed, is a unified scheme.

In the case of metals, the bioaccessibility can be modelled with the SEM-AVS approach. AVS in the sediment react with dissolved metals to form an insoluble metal sulphide, non-bioaccessible to benthic organism via the dissolved route. The AVS and SEM are operationally defined terms and refer to the sulfide and metal fractions that are released upon a cold, weak acid extraction. The amount of AVS in sediments, which is determined by the anaerobicity and the availability of sulfur in the sediment, serves as a critical parameter to determine metal bioaccessibility and toxicity in sediments. Metals will exist in the form of their respective metal sulfide if the AVS is present in excess of the reactive forms of the sediment metals (SEM), and as long as anaerobic conditions persist. On the other hand, some fraction of metals may occur in the pore water and other complexation processes in the pore water becomes relevant (e.g. binding to dissolved organic carbon, clays, Fe/Mn oxides, etc.).

Metals have specific environmental and biotic attributes that should be considered in all risk assessments [2]:

- Background levels.

Although this term is object of several discussions [20, 21], it is possible define it as "the concentration of a hazardous substance (metals in this case) that provides a defensible reference point that can be used to evaluate whether or not a release from the site has occurred (derived from natural or anthropogenic sources but that are not the goal of the risk assessment)" [22]. Taking into account that certain essential metals can be bioaccummulated in some aquatic ecosystems, or even some nonessential metals due to mimicry of essential metals or sequestration and storage; it is important to know background concentration in order to differentiate risk associated to metal sources already in the environment from those of concern.

Several author published different methods to present the background level concentrations: as a range (*minimum, 25th percentile, median, 75th percentile or maximum*) or as a single value "*baseline*" [23, 24]; but as important as establishing background concentration it is to determine the threshold (upper limit to differentiate background variability from anomalies [23].

- Form of metals.

The physical and chemical form of metals affect exposure, bioavailability and subsequent effect, and are influenced by physicochemical environmental conditions. It is important note that all assessments transitions from national, to regional or local sites should be accompanied by the *site-specific sediment and water quality parameters* that influence metal speciation, complexation and sorption (e.g. pH, organic carbon, inorganic ligands, Ca, Mg, sulfide, etc.).

- Exposure pathway analysis.

Potential routes of exposure to metals include absorption across respiratory organs, dermal absorptions, sediment ingestion and food ingestion; and the quantification of these exposure and the metals uptake is very complex [2]. The use of *stable isotope technique* has contributed to evaluating the role of diet in metal accumulation by defining trophic interactions [25].

- Toxicokinetics and toxicodynamics (bioavailability and bioaccumulation):
    - In aqueous phase:

In dissolved phase, metals can exist as free ions or in a variety of complexed forms or species; and are of key importance in understanding bioavailability and the hazard and risk assessment. Moreover, though metals species could differ in their toxicological properties, it is the free ionic form that is most responsible for toxicity.

There are a variety of methods to account for relative bioavailability of metals in the aquatic systems, such as *water-effect ratio* (WER), *free ion activity model* (FIAM) and *aquatic Biotic Ligand Models* (BLMs) [26].

- In sediment phase:

Several approaches have been developed to estimate exposures to sediment-associated metals. The *equilibrium partitioning approach* (EqP) assumes that chemical activity in the sediment (indexed by chemical concentration in the interstitial water) is proportional to the chemical´s bioavailability to sediment-dwelling organisms.

In the case of anoxic sediments, sulfides are the primary binding phase for many cationic metals; and the metal sulfides formed are highly insoluble and

are thought to have low toxicity. On this way, if the sediment has more content of sulfide than metal, these cationic metals should be presented as insoluble and nontoxic metal sulfides. The procedurally defined content of reactive sulfide, when sediment is extracted with 1N HCl, is called *Acid Volatile Sulfide* (AVS). On the same way, the amount of reactive metal in the acid extract is knows as *Simultaneously Extracted Metal* (SEM).

- If SEM-AVS < 0 means that there is sufficient sulfide to bind all SEM and metal toxicity is not expected.
- If SEM-AVS > 0 means that the binding capacity of sulfides is exceeded and the toxicity may occur (if there are no other binding phases).

Several works have been published with this model for many metals (References AVS) [27 - 30].

Other methods applied to contribute to sediment risk assessments are based on the metal concentrations in the chemical, acid and biomimetic extracts [31-33], and from sequential chemical extraction schemes [34].

- Bioaccumulation and trophic transfer.

Interest in metals bioaccumulation originates from concerns regarding the direct impact of metals on organisms accumulating the metal and indirect impacts on their consumer (i.e. trophic transfer) [2].

Inorganic metals compounds rarely biomagnify across three or more trophic levels [35], but some organometallics can biomagnify in aquatic food chain. But it is still important not interpret lack of biomagnification as lack of exposure or concern, because aquatic organisms are able to bioaccumulate large amount of metals and become an important source of dietary metal to their predators [36].

2. Analytical methodologies for metal analysis

2.1. Sample preparation

Sample preparation procedures are necessary to isolate the desired compounds from complex liquid or solid matrices, and also because most of analytical instruments cannot directly handle the liquid or solid sample. On this way, the aim of the different sample treatment approaches is to convert real matrix samples into samples suitable for analysis. This process almost inevitably changes the interactions of analytes with their matrices. These interactions are determined by the physical and chemical properties of both analytes and matrices, and they affect the applicability of different sample pre-treatment techniques and analytical methods as well as their efficiency and repeatability. Independently of the complexity, sample treatment methods have the same goals [4]:

- Increase the selectivity of the analytical techniques by removing potential interferences (e.g. high saline matrices in seawater samples).
- Improve the sensitivity of the analytical techniques by increasing the analyte concentration (e.g. trace metal analysis).
- Analyte conversion into a more suitable form (e.g. organometallic compounds derivatization into apolar volatile species).
- Transfer the analyte to a compatible solvent for a certain analytical technique.
- Isolation of certain species (e.g. in speciation studies).
- Establishment of a robust and reliable method that is not affected by variations in the sample matrix.

In addition to these targets, there is a need nowadays to develop analytical procedures based on the main principles and strategies which support the green practices in analytical chemistry. Thus Green Analytical Chemistry is becoming a movement which can modify our perspective and praxis in the analytical field in future years [37]. Aside from the development in instrumentation and methodologies, which are necessary for improvements in

the quality of chemical analyses, efforts are being made to reduce the negative impact of chemical analyses on the environment and to enable implementation of sustainable development principles to analytical laboratories. The most important challenge to the future of this discipline is to reach a compromise between the increasing quality of the results and the improving environmental friendliness of analytical methods. Guidelines that provide the framework for Green Analytical Chemistry are needed to meet this challenge. Galuszka et al. [38] proposed the 12 principles that are listed in Figure 7.

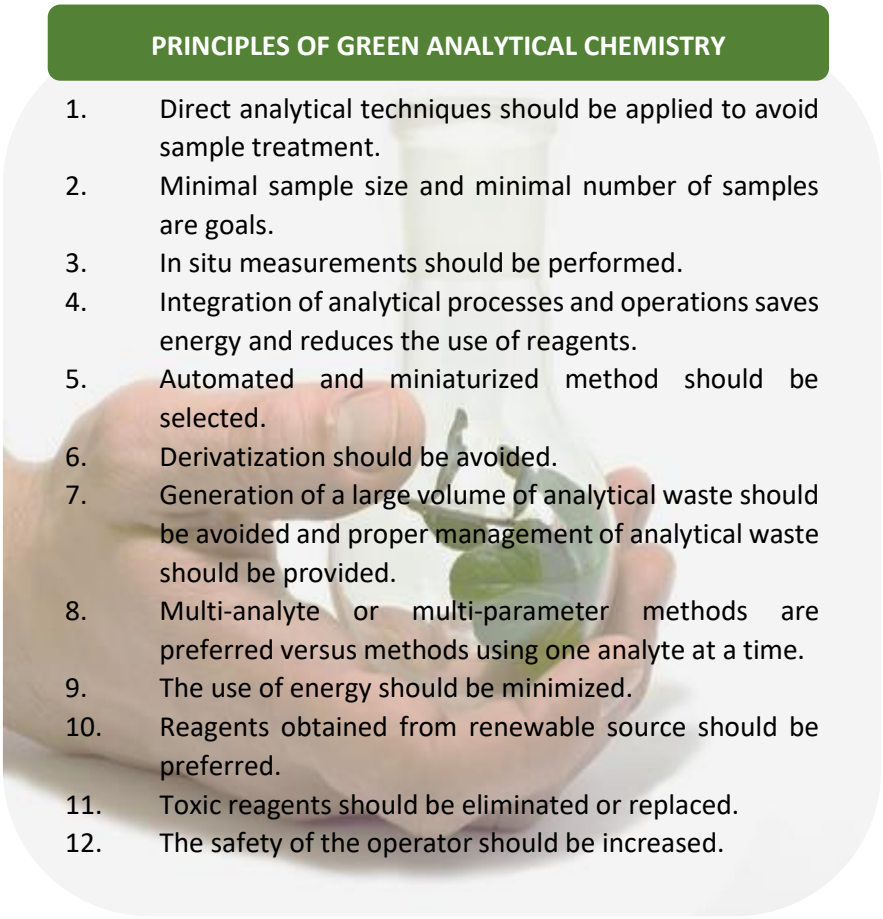

Figure 7. Principles of Green Analytical Chemistry.

2.1.1. Total and bioaccessible metal determination in sediments

a) Procedures for the determination of total metal contents

The determination of total metal contents in solid samples, as sediments, implies the total matrix dissolution since it ensures complete availability of the analytes for the analysis. Moreover, the techniques commonly utilized for metal determination traditionally required the sample to be as an aqueous solution. However, it is a lengthy process in many cases and is an important source of contamination and/or analyte losses. There exist other methods which may achieve useful analytical samples with less time and labor. Slurry sampling is one such method. If the sample can be finely powdered and the powder taken up in a fluid slurry, it may give satisfactory analytical results. Direct solid analysis can be also performed coupled with certain metal determination techniques if the appropriate introduction device is available.

The common methods used to dissolve samples for metal analysis are acid digestions, nowadays mostly performed in closed vessels and with microwave energy. This combination accomplishes the complete dissolution of the sample quickly and efficiently preventing contamination and the losses of volatile species, in comparison with classical open digestion procedures.

Microwave ovens consist basically of a magnetron the generation of microwaves which are then injected and distributed into the microwave cavity. A turntable is needed so that the vessels are exposed to uniform microwave energy. Closed vessels provide higher temperatures by the pressure produced inside. Vessel materials must be transparent to microwave radiation (low dissipation factors) so that the energy will not be absorbed by the vessel and will pass directly to the solution inside. PTFE is generally the material of choice due to its good thermal and chemical resistance.

The microwave energy is a no ionizing radiation that not causes changes in the molecular structure, and is characterized by the rapid and uniform heating of the sample solution. Microwave chemistry is based on the efficient heating of materials (in most cases solvents) by dielectric effects. Dielectric heating works by two major mechanisms:

- Dipolar polarization: for a substance to be able to generate heat when irradiated with microwaves it must to be a dipole. Since the microwave field is oscillating, the dipoles in the field align to the oscillating field. This alignment causes rotation, that results in friction and ultimately in heat energy.

- Ionic conduction: dissolved ions oscillate back and forth under the influence of microwave irradiation. This oscillation caused collisions of the charged particles with neighboring molecules or atoms, which are ultimately responsible for creating heat energy.

These two processes occur simultaneously and the dominance of one or another mechanism is highly dependent on the temperature. Therefore, for solvents such as water, the dielectric loss to a sample due to dipole rotation decreases as the temperature increases. In contrast, dielectric loss due to ionic migration increases as sample temperature increases.

All of this provides microwaves acting as a source of intense energy to rapidly heat the sample. However, a chemical reaction is still necessary to complete the dissolution of the sample. Several acids or acid mixtures can be used to achieve this task for metal analysis, and Table 3 presents a resume of their principal applications.

Table 3. List and uses of different acids and reagents for sample decompositions.

Acid	Matrix type
Hydrochloric acid	Carbonates, phosphates, oxides and sulfides.
Sulfuric acid	Inorganic (ores, alloys, oxides and hydroxides).
	High organic matter content.
Nitric acid	Carbonates, phosphates, oxides and sulfides.
Perchloric acid	Organic matter (violent reaction).
Hydrofluoric acid	Siliceous matrices.

Sulfuric acid/ nitric acid (5/20)	Nitric acid attacks most of organic matter and sulfuric acid destroys last traces
Nitric acid/ hydrochloric acid (1/3) "Aqua regia"	Combine the oxidizing media of nitric and complexing character of hydrochloric

Figure 8 shows the different mechanism occurring in conventional and microwave heating and the temperature distribution inside the digestion vessel. Microwave heating is internal while conventional heating is only external, thus better contact between the sample particles and the acids is the key to rapid dissolution achieved with the former.

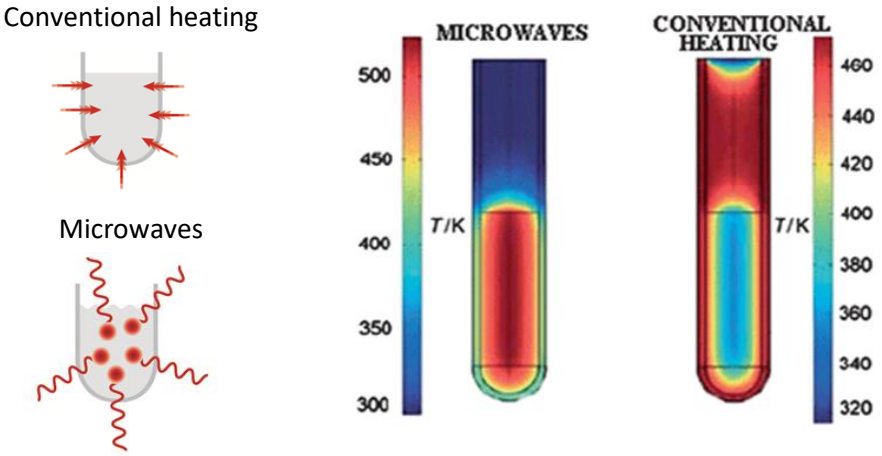

Figure 8. Schematic diagram of microwave and conventional heating, and temperature distribution comparison.

b) Procedures for the determination of bioaccessible fractions

As it was mentioned in the first part of this introductory section the total content of metals in sediments does not provide totally useful information since the environmental ecotoxicity and mobility of metals is strongly dependent upon their specific chemical forms or way of binding. In practice, environmental studies on sediment analysis are often based on leaching or extraction

procedures, enabling broader forms or phases to be measured (e.g. bioaccessible fractions of elements).

The first sequential extraction procedures developed at the end of the 1970s have been adapted and are still widely used. Besides the usefulness of these schemes, it is recognized that the lack of uniformity in the procedures used does not allow the results to be compared world-wide not the methods validated. Indeed, the results obtained are "operationally-defined" which means that the "forms" of pollutants are defined by the determination of extractable contents using a given procedure and therefore, the significance of the analytical results is highly dependent on the extraction procedures used [39].

Extraction or lixiviation methods are based on the use of diluted reagents to extract or to leach trace elements from a solid sample. These procedures do not involve the total matrix sample destruction but the breakdown of the chemical bonds between the trace elements and the matrix sample constituents [40]. A wide variety of single and sequential extraction procedures were reported in the literature using different reagents and modes of heating. For single extractions the agents mostly used are thylenediaminetetraacetic acid (EDTA), diethylenetriaminepentaacetic acid (DTPA), calcium chloride, dilute hydrochloric acid, etc. Regarding sequential schemes, one of the most representatives is that proposed by the Standards, Measurements and Testing Programme, SM&T (formerly BCR) of the European Commission, which fractionate metals using three reagents of increasing reactivity: acetic acid, hydroxylamine hydrochloride and hydrogen peroxide.

Sequential extraction procedures involve a lot of work and time, which is even more evident when using conventional stirring, also, but to a lesser extent, single approaches can be considered time-consuming procedures with this type of agitation.

Ultrasound energy has been currently used for assisting and/or accelerating the extraction of both organic and inorganic compounds from solid samples. The induced cavitation processes occurring in a medium containing suspended particles promotes asymmetric collapses of bubbles leading high-speed microjets toward the solid phase (Figure 9). Under these conditions analyte transport from the solid particles to the liquid phase is more efficient

and extractions in short times can be expected. In addition, due to a best interaction between the solid sample and the extracting solution, chemical bonds between the analytes and the matrix components can be broken by the action of diluted acids [41]. The ultrasound energy can be applied to the samples by means of ultrasonic baths and ultrasonic probes.

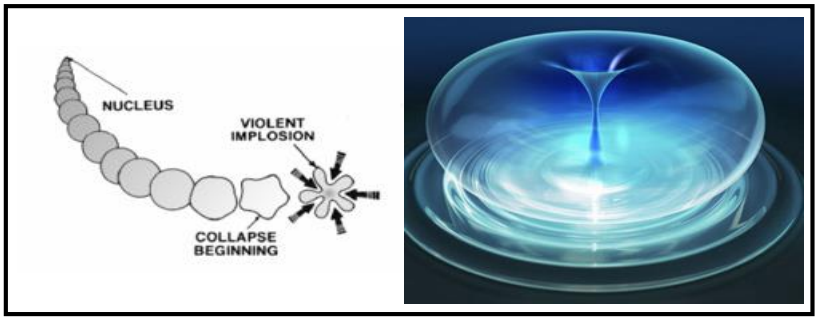

Figure 9. Representation of the growth and collapse of a cavitation bubble produced by ultrasound energy.

The ultrasonic baths are widely used in the laboratories but are not very efficient in the extraction of metal species due to their low operation power. Additionally, since the ultrasound transducer is situated at the bottom of the tank the ultrasound energy will be transferred to the liquid contained in the tank and only a small fraction of this liquid (which is near the transducer) will undergo the cavitation phenomena. Therefore the energy transfer will depend on the position of sample vessel inside the bath, the number of vessels, the material of the wall and its thickness, the tank volume/dimensions, etc [42].

Conversely, ultrasonic probes utilize higher power and they have the ultrasound transducer coupled to a metal probe or tip which is introduced into the sample. Thus, they focus their energy to specific zones, so the cavitation, and hence the dissolution are favored.

2.1.2. Liquid sample treatment: metal speciation in superficial waters

Levels of metal species in waters are very low and some of them are included in the Water Framework Directives (WFD) due to their potential environmental and biological risk. Therefore their quantitation and

monitorization is a challenging task for laboratories involved in environmental analysis.

Sample preparation procedures applicable to aqueous samples imply the separation of analytes from water and they are usually combined with their preconcentration, and often with their derivatization. Extraction procedures include classical solvent (liquid–liquid) extraction, solid-phase extraction (SPE), solid-phase microextraction (SPME), liquid–gas extraction (purge and trap), etc. The procedures are classified according to the order of extraction and derivatization steps. When analytes are present at the ng L^{-1} level in relatively clean water samples, in situ derivatization followed by an extraction technique with a high preconcentration factor (purge and trap, SPE or SPME) are preferred. In the case of dirty matrices with higher concentrations of analytes, the latter are usually extracted as nonpolar complexes (with DDTC, dithizone or tropolone) which are later derivatized [43].

Wasik and Namiesnik declaimed [44] that an ideal extraction/separation treatment should offer the following characteristics:

- Isolate the analyte from the matrix, reduce or eliminate the interferences and yield an appropriate enrichment factor.

- Obtain low sample blanks and hence detection limits by minimizing the use of reagents and simplifying the process.

- Produce a final solution matrix matched with the solutions of the calibration method.

a) Extraction procedures

***Liquid-liquid extraction*:** liquid-liquid extraction procedures are based on the relative solubility of the target compounds in two immiscible phases. An ideal liquid-liquid extraction procedure must guarantee a quantitative isolation of the analyte from the aqueous matrix sample while interference species remain in the aqueous phase. This leads to an improvement on the selectivity and to an increase on sensitivity by transferring the analyte to a small solvent volume. The extraction of metal species from aqueous samples is normally

performed using an organic immiscible nonpolar solvent as the extractant phase. The desirable characteristics of such solvents are [4]:

- They must extract the metals species by using one or few extraction steps.
- They must be immiscible with the aqueous solution.
- They must not form emulsions because emulsion formation hinders phase separation.
- They must enhance the signal sensitivity as compared to the sensitivity in water.
- The extracted species must be stable in the organic solvent.

The aqueous and organic phases are well mixed and then are allowed to separate. The analyte distributes itself between both phases accordingly with its solubility, and its concentration in each phase will be defined by the Nernst distribution (or partition) law, where K_D is the distribution coefficient:

$$X_{aq} \leftrightarrow X_{org}$$

$$K_D = [X_{org}] / [X_{aq}]$$

The efficiency of the liquid-liquid extraction depends on the affinity of the analytes for the extracting solvent, the pH of the aqueous phase, the number of the successive extractions and the shaking times.

The main advantages of liquid-liquid extractions are their simplicity and the fact that they allow rapid method development, but on the other hand, they are time consuming and commonly use relatively high amounts of toxic solvents. Nonetheless, these extraction procedures are still widely used for metal speciation analysis.

***Solid-phase extraction (SPE)*:** the analytes are extracted by sorption, eluted with a small amount of an organic solvent and derivatized. Its advantages over liquid–liquid extraction include a higher enrichment factor, lower solvent consumption and risk of contamination, and the ease of application to field sampling and automation. Solid-phase extraction is particularly suitable for the

analyte preconcentration prior to HPLC; by using an appropriate eluent the analytes can be separated on the SPE cartridge itself or on a connected HPLC column. Sorbents with immobilized chelating reagents, such as dithiocarbamate, dithizone or diphenylthiocarbazone, have widely been used.

***Solid-phase microextraction (SPME)*:** is based on the sorption of analytes present in a liquid phase or, more often, in a headspace gaseous phase, on a microfibre coated with a chromatographic sorbent. After the extraction process the fiber is then transferred either to a GC injector where the analytes are thermally desorbed or to an HPLC interface where they are solubilized in the mobile phase used as solvent. The absorptive-type polydimethylsiloxane (PDMS) coatings are the most popular in speciation analysis. This solvent-free technique offers numerous advantages such as simplicity, the use of a small amount of liquid phase, low cost and the possibility of an on-line analytical procedure [43].

***Stir-bar sorptive extraction (SBSE)*:** a bar coated with polydimethylsiloxane is introduced into an aqueous sample and stirred during a predetermined time. Then, the stir-bar is desorbed thermally or with a liquid solvent. The main advantage of this methodology is that a drying step is not needed, therefore there is no risk to lose volatile analytes but on the contrary the variety of stationary phases is limited.

***Membrane assisted extraction (MASE)*:** this is a three-phase system. A small volume of solvent is placed inside a non-porous membrane and immersed into the aqueous solution. The analyte will dissolve into the membrane, cross it and achieve the extractant. Emulsion formation is avoided compared with liquid-liquid extraction.

***Dispersive liquid-liquid micro-extraction (DLLME)*:** is based on the cloudy solution formed between an extraction solvent (immiscible in aqueous phase) and a disperser solvent (miscible in both phases). The extraction solvent

is rapidly injected in the disperser solvent producing a high turbulence, which leads to small droplets dispersed in the aqueous sample. The extraction of the analytes from the aqueous medium into the dispersed organic droplets takes place very rapidly. The main drawback is the limited number of extractants that form stable cloudy solutions, that can be easily removed and that extract the analyte.

b) Derivatization procedures

Derivatization consists of the modification of the analyte to obtain similar or closely related structures as the original compound, but adequate for gas chromatographic separation. Several derivatization methods were investigated and employed with the purpose to render the analytes less polar, more volatile or to otherwise differentiate between organometallics of similar gas chromatographic behavior.

The methods of derivatization for gas chromatography can be divided in two categories: pre- and on-column methods. In pre-column mode, derivatization of analytes is performed prior to injection of components into the GC column. This method is suitable for thermally unstable samples and polar/ionic analytes. For example, the volatile derivatives are usually prepared before injection (pre-column). Some of the general shortcomings of this mode are introduction of contaminants arising from impurities, reagent excess and side-reaction products, which may interfere with the analytes, and the possibility of incomplete reactions. In the case of injection-port or on-column derivatization, the analytes and the derivatization reagent are mixed and injected together into the gas chromatographic system and the derivatization reaction occurs in hot injection port [45].

Regarding the derivatization reactions can be carried out before extraction (pre-extraction) when derivatization is necessary for the extraction since analytes have low partition coefficients; after extraction (post-extraction) when the analytes are first concentrated in the acceptor phase and then exposed to the reagents for separation and detection; or simultaneously with extraction when the derivatization reagents are added to the liquid sample at the same time that the extraction reagent.

Various chemical reactions can be employed to derivatize the analytes of interest and facilitate their further separation by chromatographic techniques. The alkylation/arylation reactions using sodium tetraalkylborate are currently the most commonly applied derivatization procedures for metal speciation analysis by GC, due to their more reproducible results, low detection limits and reagent stability in water when the derivatization is performed in aqueous media.

In an alkylation reaction, an alkyl or aryl group replaces the active hydrogen of polar functional groups resulting in a less polar derivate or alternatively leads to a new specie form more volatile than the initial one. The main limitations of these reactions are: the pH adjustment according to the studied analyte, the reaction time (around 5 – 30 min), the purity and the stability of the reagents. Figure 10 shows, as an example, the reactions involved for mercury speciation.

$$R - COOH \longrightarrow R - COO^- \xrightarrow{R'X} R - COOR' + HX$$

$$2NaBEt_4 + Hg^{2+} \longrightarrow 2BEt_3 + HgEt_2 + 2Na^+$$

$$NaBEt_4 + MeHg^+ \longrightarrow BEt_3 + MeHgEt + Na^+$$

$$2NaBPr_4 + Hg^{2+} \longrightarrow 2BPr_3 + HgPr_2 + 2Na^+$$

$$NaBPr_4 + MeHg^+ \longrightarrow BPr_3 + MeHgPr + Na^+$$

Figure 10. Alkylation reactions for mercury speciation.

2.2. Instrumental techniques

2.2.1. Inductively coupled plasma mass spectrometry (ICP-MS)

Inductively coupled plasma mass spectrometry (ICP-MS) can be considered one of the most powerful techniques available nowadays for elemental analysis. Strengths of the technique include [46]:

- Virtually all elements can be measured by ICP-MS, including alkali and alkaline earth elements, transition and other metals and metalloids, rare earth elements, most of the halogens and some of the non-metals.
- High sensitivity and low background signals combine to give very low detection limits (sub ng L^{-1} in most cases).
- Wide analytical working range: up to 9 orders in a single acquisition.
- Isotopic information.

2.2.1.1. Interferences

One of the critical aspects in ICP-MS is the occurrence of spectral interferences since they will determine the selection of the mass spectrometer utilized and the operational conditions as well. Spectral interferences are produced by the overlap of ions that have the same mass/charge ratio (m/z) than the isotope of interest of the analyte. There are two types of spectral interferences:

Isobaric interferences: there is a direct overlap between some isotope from an element other than the analyte and the isotope of interest at the same nominal m/z ratio, e.g., $^{54}Fe^{+}$ overlaps with $^{54}Cr^{+}$;

Polyatomic interferences: due to polyatomic ions with the same m/z ratio as the nominal one of the analyte, these ions can proceed from species of the plasma (mainly Ar), some components of the sample and/or the reagents employed during sample pretreatment; e.g., $^{40}Ar^{35}Cl^{+}$ overlaps with $^{75}As^{+}$.

Isobaric overlaps cannot be resolved using spectrometric methods, not even with high resolution spectrometers. In order to avoid them, either an alternative isotope of the analyte can be measured or mathematical corrections may be applied. The effect of polyatomic ions can be managed using high resolution analyzers or as it was mentioned above, including a collision/reaction cell in quadrupole instruments.

2.2.1.2. Instrumentation

The basic components of an ICP-MS instrument are sample introduction system, ion source, interface, mass analyzer and detector.

a) Sample introduction system

Samples are usually introduced as solutions in ICP-MS instruments. The general way of introducing a liquid into an ICP mass spectrometer is the generation of a fine aerosol of the sample so it can be efficiently ionized in the plasma discharge. The sample introduction area is the weakest component of the instrument, with only 1 - 2 % of the sample finding its way into the plasma. The generation of the aerosol is achieved with a nebulizer and a spray chamber. The sample is normally pumped by a peristaltic pump into the nebulizer to ensure a constant flow of liquid, then, it is broken up into a fine aerosol and enters the spray chamber. The function of the spray chamber is to allow only the small droplets to enter the plasma and to smooth out pulses that occur during the nebulization process, due mainly to the peristaltic pump.

Pneumatic nebulizers are most commonly utilized in ICP-MS, being concentric and crossflow the most popular designs. Basically two spay chamber designs are used in commercial ICP-MS instrumentation: double pass spray chambers, by far the most common, and cyclonic, gaining in popularity.

b) Ion source

The vaporization, atomization and ionization of the sample aerosol are produced in the inductively coupled plasma (ICP). Argon is used to generate the plasma due to its high first ionization potential (15.8 eV), which causes the ionization of most elements. The basic components of the ion source are a

plasma torch, a radio frequency (RF) coil, and a RF power supply. The torch consists of three concentric tubes usually made from quartz through which argon flows. The total argon consumption of an ICP is around 20 L min^{-1}. The first step that takes place when the aerosol reaches the plasma is desolvation of the droplet, becoming a very small solid particle. As the sample moves further into the plasma, the solid particle changes first, into a gaseous form and then, into a ground-state atom. Finally, the conversion of an atom to an ion is achieved mainly by collisions of energetic argon electrons (and to a lesser extent by argon ions) with the groundstate atom. The ion is then directed into the interface of the mass spectrometer.

c) Interface

The ions generated in the plasma are brought efficiently, consistently, and with electrical integrity, into the mass spectrometer via an interface constituted by metal cones. Such an interface transfer the ions from the argon stream, which is at atmospheric pressure (760 torr), to the low pressure region of the mass spectrometer ($< 1 \cdot 10^{-5}$ torr). The ions pass through the sampler cone which has an orifice of 0.8 - 1.2 mm i.d., travel a short distance to the next cone (skimmer) with a smaller orifice (0.4 - 0.8 mm i.d.) and finally are directed through the ion optics to mass analyzer.

d) Mass analyzer

Before entering into the mass analyzer the ions are directed to the ion-focusing system whose main function is to transport the maximum number of analyte ions from the interface region to the mass separation device, while rejecting as many of the matrix components and nonanalyte-based species as possible. A secondary but also very important role of the ion optic system is to stop particulates, neutral species, and photons from getting through to the mass analyzer and the detector. These species cause signal instability and contribute to background levels, which ultimately affect the performance of the system. These ion optics typically consists of one or more electrostatically controlled lens components (metallic plates, barrels or ion mirrors) maintained at a vacuum of approximately 10^{-3} torr with a turbomolecular pump. Ions emerging from the ion optics will be separated in the mass analyzer according to their mass-to-charge ratio (m/z).

ICP-MS instruments include mainly double-focusing magnetic sector spectrometers and cuadrupole filters. Recently, triple quadrupoles are also commercialized.

Double-focusing magnetic sector spectrometers consist of an electrostatic filter combined with a magnetic analyzer to focus the ion beam. The system also uses narrow entry and exit slits which allow ions to pass through detector. The ions are sampled from the plasma in a conventional manner and accelerated in the ion optic region to a few kV. The magnetic field, which is dispersive with respect the ion energy and mass, focuses all the ions with diverging angles of motion from the entrance slit. The electrostatic analyzer, which is only dispersive with respect the ion energy, focuses all the ions onto the exit slit, where the detector is positioned. The main characteristics of magnetic sector analyzers are high resolution (better than the unit mass) which resolves most of polyatomic interferences, high sensitivity and high ion transmission.

Quadrupole mass spectrometers consist of four cylindrical or hyperbolic metallic rods of the same length and diameter. Combined direct current and time-dependent alternating current of radiofrequency can be set on opposite pairs of rods to pass only a selected mass-to-charge ratio. All other ions do not have a stable trajectory through the quadrupole mass analyzer and will collide with the quadrupole rods never reaching the detector. The scanning process is repeated for another analyte with a different mass-to-charge ratio. The main advantages of cuadrupole filters are high speed scanning, simplicity and low cost. Regarding drawbacks the most important are low transmission of high masses and low resolution (0.7 - 1 amu) being inadequate for the correction of spectral interferences produced by Ar, the solvent and/or the matrix.

The problem of polyatomic interferences in cuadrupole instruments have led to the commercialization of collision/reaction cells, which are positioned prior the mass analyzer. A collision/reaction gas (e.g. He, H_2, NH_3 or O_2) is introduced into the cell containing a multipole (quadrupole, hexapole or octapole). By different collision and reaction mechanisms, polyatomic interfering ions are converted to noninterfering species or the analyte is converted to another ion that is not interfered with. There are basically two

approaches being the major differences between them how the gaseous molecules interact with the interfering species and what type of multipole is used in the cell. These dictate whether it is an ion-molecule collision or reaction mechanism taken place.

- ***Collision mechanism using nonreactive gases and kinetic energy discrimination (KED)*** [47]: the analyte and the polyatomic interfering ions enter in the pressurized cell and suffer multiple collisions with the nonreactive gas. Because the cross-sectional area of the polyatomic ions is usually larger than the analyte ion, they undergo more collisions. This has the effect of lowering the kinetic energy of theses interfering species and then are rejected or discriminated by the potential energy barrier at the cell exit. On the other hand, analyte ions, which have a higher kinetic energy, are transmitted to the mass analyzer.

- ***Reaction mechanism using highly reactive gases*** [48]: here, a highly reactive gas is bled into the cell, which is a catalyst for ion-molecule chemistry to take place. These gaseous molecules react with the interfering ions to convert them into either an innocuous species different from the analyte mass or a harmless neutral species. The analyte mass then emerges from the cell free of its interference and is steered into the analyzer cuadrupole.

Triple cuadrupole analyzers are recently developed for ICP-MS which placed an additional quadrupole prior to the collision/reaction cell, in addition to the analyzer cuadrupole. In this configuration the first cuadrupole acts as a simple mass filter to allow only the analyte masses to enter the cell, while rejecting all other masses. The second cuadrupole is the analyzer cuadrupole, and the middle multipole device is actually an octopole collision/reaction cell.

e) Detector

The detector is responsible for detecting and quantifying the number of ions emerging from the mass analyzer. The detector converts the ions into electrical pulses, which are then counted using its integrated measurement circuitry. The magnitude of the electrical pulses corresponds to the number of analyte ions present in the sample, which is then used for trace element

quantification by comparing the ion signal with known calibration or reference standards [49].

Faraday cup: the ion beam from the mass analyzer is directed into a simple metal electrode. Thus, there is no control over the voltage, so it is only used for high ion currents. They are not used as the only detector due to the limited sensibility that provide, but they are used in conjunction with a channeltron or discrete dynode detector to extend the dynamic range of the instrument. Faraday cups are also used in multicollector detection instruments.

Channel electron multiplier (channeltron): consists of an open glass cone (coated with a semiconductor type-material) to generate electrons from ions that impinge on its surface. The potential gradient inside the tube varies based on position, so the secondary electrons move further down the tube. As these electrons strike new areas of the coating, more secondary electrons are emitted. This process is repeated many times. The result is a discrete pulse that contains many millions of electrons generated from an ion that first hits the cone of the detector.

***Discrete dynode electron multiplier*:** it works in a very similar way to channel electron multiplier, but uses discrete dynodes to carry out the electron multiplication. Because of the materials used in the discrete dynode detector and the difference in the way electrons are generated, it is typically 50 - 100 % more sensitive than channeltron.

2.2.2. Laser Ablation Inductively Coupled Plasma Mass Spectrometry (LA-ICP-MS)

The basis of this technique is the use of high-powered lasers to ablate the surface of a solid and sweep the sample aerosol into the ICP-MS to perform a conventional analysis. As it is shown in Figure 11, a laser ablation device coupled to a ICP-MS instrument consists of an ablation chamber fitted with fused silica windows, where the sample is placed, a lens to allow focusing, an adjustable platform for positioning in the three *x*, *y* and *z* directions, a camera for remote viewing of the sample, and a laser source. Once the sample is ablated, an argon carrier gas transports the ablated material to the torch [4].

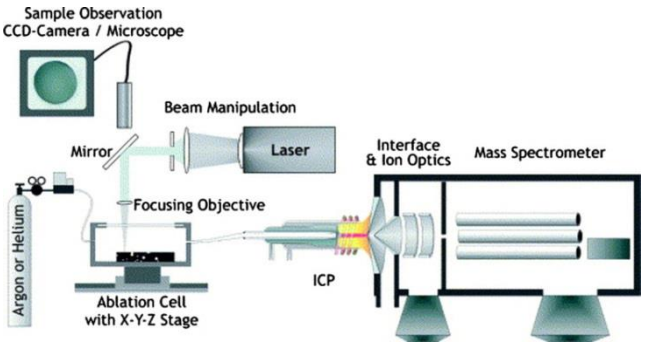

Figure 11. Schematic diagram of a commercial available laser ablation ICP-MS system [50].

There are a number of commercial laser ablation systems on the market designed specifically for ICP-MS, including 266 nm and 213 nm Nd:YAG and 193 nm ArF excimer lasers. They all have varying output energy, power density, and beam profiles, and even though each one has different ablation characteristics, they all work very satisfactorily, depending of the types of samples being analyzed and the data quality requirements. Laser ablation is now considered a very reliable sampling technique for ICP-MS that is capable of producing data of high quality directly on solid samples and powders. Some of the benefits offered by this technique include the following [4, 49]:

- Small amount of sample to perform the analysis.
- Applicable to virtually any kind of solid material and powders by pelletizing.
- Does not require complicated sample preparation procedures, so the risk of contamination or sample loss can be avoided. Reagent consumption and waste generation are minimized.
- Sensitive in the ppb to ppt range, directly in the solid.
- Reduction in the spectral interferences compared to conventional pneumatic nebulization.
- Permits microanalysis, depth profiling analysis and 2-dimensional elemental mapping.

However, two fundamental aspects constrain the ability of LA-ICP-MS to act as a universal method for direct analysis of solid samples [51]:

- ***Elemental fractionation*** is produced due to the abundances of the ions detected, after m/z separation, are not often entirely representative of the composition of the original sample. Besides the ablation process itself (e.g. non-stoichiometric effects due to the preferred ablation of more volatile compounds), the transport of the aerosol particles from the ablation chamber into the ICP and the vaporization, atomization and ionization in the ICP, are also important contributors to fractionation effects.

- ***Difference in the interaction between the laser beam and the sample surface*** observed for various matrices, causing changes in the mass of analyte ablated per pulse due to differences in the properties of the matrices investigated (e.g. absorptivity, reflectivity, and thermal conductivity). These sample-related "matrix effects" impair the accuracy of LA-ICP-MS analysis and complicate quantification.

The experimental parameters used for the laser ablation process were investigated in recent years in order to understand better and minimize the mentioned limitations. Most of the work carried out has been focused on the sampling process in terms of the laser wavelength (infrared versus ultraviolet), the pulse duration (nanosecond versus femtosecond), the carrier gas (Ar versus He or Ne), and the cell design; since these parameters play an important role in the properties of the laser-generated aerosol. In this sense the developments in the laser area have mainly been driven in two directions, shorter wavelengths and shorter pulses [52].

2.2.3. Gas Chromatography Inductively Coupled Plasma Mass Spectrometry (GC-ICP-MS)

Gas chromatography inductively coupled plasma mass spectrometry (GC-ICP-MS) combines the high separation efficiency of this separation technique with the unmatched sensitivity, elemental specificity and multi-element measurement capability of the atomic spectrometry technique. Thus

GC-ICP-MS constitutes a powerful laboratory technique, with the ability to separate and quantitate ultra-trace levels of metals and organometallic compounds. This fact has been reflected in the growing importance of ICP-MS as an element-specific detector for gas chromatography and the increasing number of applications in speciation analysis. Some of the characteristics provided by this hyphenated technique are briefly commented below [43]:

- High sample introduction efficiency, since it can be assumed that 100% of the sample will be transported to the plasma.
- Efficient use of plasma energy. When He is used as carrier gas, the analytes are carried to the plasma by monoatomic gases so the plasma energy can be used more efficiently for atomization and ionization.
- Separation of the solvent from the analytes during the chromatographic run, so there is no need to volatilize and atomize solvent molecules as it is for liquid sample introduction, and no distortion of the plasma will be produced.
- Low signal drift due to the amount of material reaching the sampler and skimmer cones is very small so there is less chance of cone blocking.
- Stable plasma conditions during chromatographic run. The chromatographic separation takes place using temperature programming, and no by gradient elution as is typical of HPLC, so the sensitivity remains constant during the separation, a stable baseline is obtained and, hence, low detection limits can be achieved.

The interfacing of GC with ICP-MS is quite straightforward. Basically, the effluent from the GC column must be transported to the inlet of the torch. The main requirement is that the volatilized analytes remain in the gas phase during the transport from the GC column to the plasma. Therefore, any condensation of the analytes should be avoided to assure no loss of the analyte and also the peak sharpness necessary for high sensitivity and low detection limits [53]. This can be achieved by two general approaches [43]:

- Heating the entire transfer line to avoid any cold region. This implies removing the conventional spray chamber and inserting the transfer line into the central channel of the torch (dry plasma conditions). Since the normal flows used in GC are on the order of a few mL min^{-1}, a carrier or

make-up gas flow is also introduced to allow introduction of the analytes into the plasma.

- Using an aqueous aerosol carrier that is mixed with the GC column effluent prior to their introduction into the plasma (wet plasma conditions). This approach is needed when continuous introduction of an internal standard is required. Its main disadvantage is the loss of plasma energy due to the desolvation of the aerosol and the subsequent deterioration in sensitivity compared with dry plasma conditions.

The interface forces the disassembly and reassembly of the conventional sample introduction system for ICP, and does not allow the continuous introduction of an internal standard required in some applications. Different approaches were developed that circumvent the removal of the spay chamber, allow constant internal standard introduction and avoid the inconvenience of switching the assembly to analyze liquid or gaseous flows. In most of these devices, an aqueous aerosol, formed in a regular introduction system with a concentric nebulizer and a spray chamber, is mixed with the GC effluent by means of a T-piece connection (Figure 12a). Consequently, the analytes in the gas phase and an internal standard in the aerosol can be simultaneously mixed and transferred to the plasma (Figure 12b).

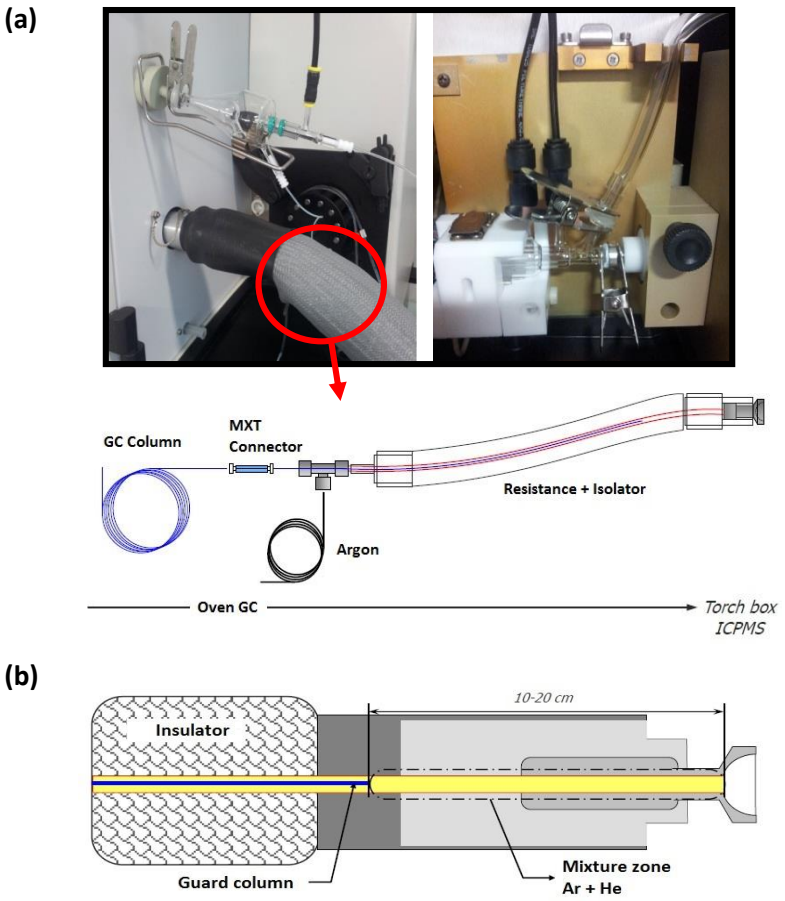

Figure 12. T-piece connection interface for the introduction of the GC effluent and the aqueous aerosol (a). Details of the interface (b).

Sample introduction is of primary importance in gas chromatography. The performance of the sample introduction system is crucial for the overall chromatographic separation. Its function is to introduce a representative portion of the sample as a narrow band onto the chromatographic column. The following features are required: does not cause more band broadening than the analytical column, provides good accuracy and precision, the sample injected is representative of the original one, does not produce discrimination based on

differences in boiling point, polarity, concentration or thermal/catalytic instability, be applicable to trace analysis as well as to undiluted samples.

The most common inlet for capillary GC is known as the split/splitless inlet, where the liquid sample in vaporized into the gas phase prior the transference onto the capillary column. In the split mode only a small part of the diluted sample enters the column and most of the sample will flow out via the split line (useful for high concentrations); while in the splitless mode the whole sample is transferred to the capillary column by the carrier gas (used for trace analysis).

Programmed Temperature Vaporization (PTV) inlet (Figure 13) combines the advantages of split and splitless modes and is especially useful for thermolabile samples. This sample introduction system makes an efficient control of the temperature and permits setting a temperature program. The main differences with the split/splitless approach are that the inlet is kept cool during sample introduction, allowing the analyte to condense onto the liner walls or packing, while the solvent is vented via the split line; and in addition, the inlet has a very low thermal mass, which allows rapid heating to transfer the analyte to the GC column after the solvent has been vented.

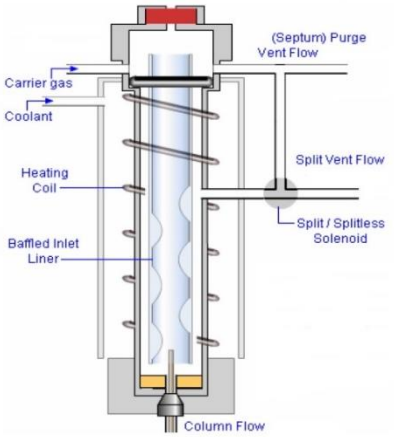

Figure 13. Schematic diagram of a Programmed Temperature Vaporization (PTV) inlet for gas chromatography [54].

The PTV solvent injection process consists of two main steps. Figure 14 shows the temperature and the split status during these steps:

- ***Solvent elimination***: when the sample is introduced by a syringe a small liquid droplet forms at the tip of the needle. This start to evaporate, but evaporation is very slow due to the small surface area of the droplet. The droplet grows until it exceeds the critical size and falls into the liner, creating a thin liquid film on the wall of the injector. At this moment, the split line is open and a high flow of gas is flowing across the liquid film that will be evaporated by the carrier gas. First the solvent is evaporated due its lowest boiling point, and the mixture carrier gas and solvent vapor passes along the column inlet (only a small fraction will enter the column and the bulk of gas will be discharged via the split exit). When all solvent is evaporated, the evaporation of the other components starts.

- ***Splitless transfer***: the components that remained in the liner are transferred to the column in a splitless mode. For this, the split exit is closed and the components can only escape via the column. To obtain a good re-focussing, low initial oven temperatures are needed (equal or slightly above the initial temperature of the PTV injector), and the final temperature of the injector should be high enough to yield a rapid and quantitative transport of

the components of interest within the splitless time selected (to avoid discrimination of high boiling point components).

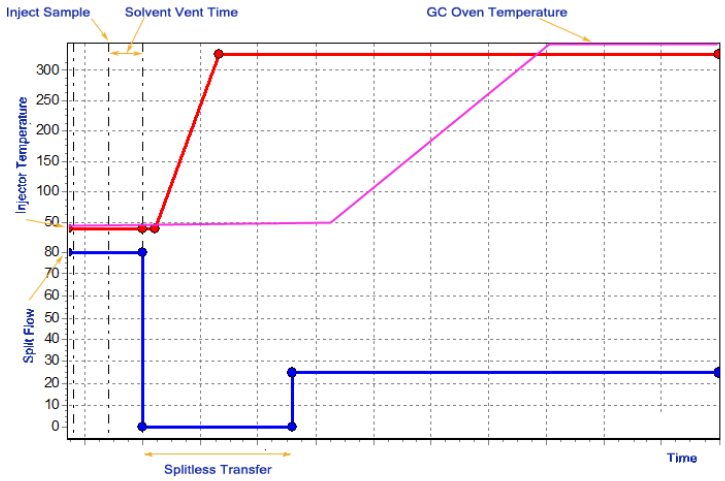

Figure 14. Graphical representation of temperature and split status during PTV injection [54].

The parameters that should be controlled with Programmed Temperature Vaporization (PTV) inlets are: sample flow rate, liner type and packing which depend on the volume of sample injected, PTV flow and temperature (best results will be achieved with boiling point differences between the solvent and the analytes of around 150 °C) and PTV solvent elimination when polar solvents are introduced in non-polar columns, or are not compatible with the detector.

The PTV injector is a very flexible injector that can be used for a wide range of different sample introduction techniques. Large volume injection using a PTV can be performed in mainly three different ways [55].

- ***Multiple injection mode***: multiple aliquots of the sample are injected at time intervals which allow the solvent evaporation and evacuation before next injection. This method is not really suited for automated routine applications. It is, however, a simple way to increase the injection volume and sensitivity by a factor of up to ten. As no

instrumental modifications are required, it is a good method when an increased sensitivity is only required once in a while.

- ***Rapid or "at once" injection***: the sample is injected rapidly, and is evaporated in the liner filled with a packing material to increase its capacity to retain the liquid sample. Although the principle of the rapid injection method for large volume sampling is extremely simple, a number of parameters have to be optimized before a large volume injection can be performed successfully (choice the packing material, determination of the maximum sample volume that can be accommodated by the packed bed, determination of the solvent-elimination time, etc.).

- ***Speed controlled mode***: the sample is introduced into the liner at a constant and controlled rate. During sample introduction the liner is kept at a low temperature and the split exit is open. Upon injection of the sample a liquid film of sample is created on the wall of the injector or on the packing material. This film starts to evaporate from its top side. The sample vapors formed are discharged from the injector via the split exit. This mode is slightly more complicated to optimize than the other but shares with then the advantage of a good ruggedness.

The main advantages of the Programmed Temperature Vaporization (PTV) inlets can be resumed as follows:

- Large sample volumes (until 200 µL) may be injected at controlled speeds into the inlet.
- Discrimination effects, due to differences in analyte boiling points, are eliminated.
- Matrix and solvent effects are reduced.
- In general improvement of chromatographic performance and analytical characteristics.

3. Quantitation approaches

Quantifying analyte(s) is usually the primary object of any laboratory. There are different quantitation methods which allow determination from sub-ppt up to high ppm-levels. Next, conventional methods are briefly described and isotope dilution, as absolute method of quantitation, is explained.

3.1. Conventional methods

Conventional methods of quantitation employ a suite of instrumental electronic signals which must be related mathematically to the amount of substance or property we are interested in.

External standardization: the instrument is calibrated by measuring the intensity of all elements of interest in a number of known calibration pure standards that represent a range of concentrations similar to those founded in the unknown samples. Then, a calibration curve is constructed with the measured intensities and the concentrations of each element. Finally, the unknown samples are analyzed and the element intensities are read against their respective calibration curves. Does not compensate for matrix effects (except if matrix-matched calibration solutions are used), fluctuations or drifts in sensitivity.

Standard additions method: is based on spiking aliquots of the sample solution with known and increasing concentrations of the target element(s), and also the unspiked sample is analyzed. A calibration curve is built from the signals obtained. Based on the slope of the calibration curve and where it intercepts the y-axis, it is possible to determine the concentration of the unknown sample [56]. It is an effective approach to overcome the matrix effects that modify the analytical signal. Thus, it enables the analyst to obtain unbiased results when the matrix of the test solution varies unpredictably among test materials in a run [57, 58]. It is more robust and reliable than conventional external calibration, but is more time consuming and costly since it must be theoretically applied to every sample to be analyzed.

Internal standardization: an internal standard is a non-analyte element that is added to the blank solutions, standards and samples to be analyzed. It is selected on the basis of the similarity of their ionization characteristics, mass and/or chemical behavior with the analyte. It is mainly used to correct for signal drift and instrumental fluctuations, as well as to compensate changes in analyte sensitivity caused by variation in the concentration and type of matrix. The correction is achieved by the calculation of the ratio between the analyte and the internal standard signals and plotting them against the concentration of the analyte.

3.2. Absolut method: isotope dilution

Isotope dilution analysis (IDA) is a well-known analytical technique based on the measurement of isotope ratios in samples where the isotopic composition of an endogenous element is altered by the addition of a known amount of an isotopically enriched element (spike) [59, 60]. The element to be analyzed must have, therefore, at least two stable or long-lived radioactive isotopes able to be measured in a mass spectrometer free of spectral interferences. This principle is illustrated in Figure 15 for an element containing two different isotopes *a* and *b*. As can be observed, the isotope *a* is the most abundant in the sample whereas the spike is isotopically enriched in the isotope *b*. It is clear that the abundance of the two isotopes and, hence, the isotope ratio in the mixture will be intermediate between those in the sample and the spike and it will depend both on the amount of spike added and on the initial amount of the element in the sample.

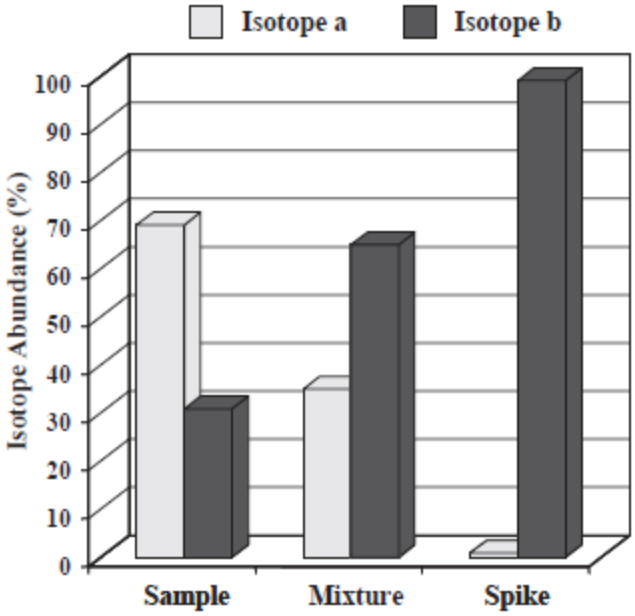

Figure 15. Illustration of the principle of isotope dilution analysis for an element containing two different isotopes.

These relations can be expressed mathematically using the isotope dilution equation. If N_S represents the number of moles of a poly-isotopic element in the sample and N_{Sp} those of the same element in the spike, the number of moles of the element in the resulting mixture, N_m, can be expressed by

$$N_m = N_s + N_{sp} \qquad (1)$$

In the same way we can express similar mass balances for those two isotopes:

$$N_m^a = \mathrm{N}_s^a + \mathrm{N}_{sp}^a \qquad (2)$$

$$N_m^b = \mathrm{N}_s^b + \mathrm{N}_{sp}^b \qquad (3)$$

When we divide equations 2 and 3 the isotope ratio (R_m) is obtained for both isotopes in the mixture:

$$R_m = \frac{N_m^a}{N_m^b} = \frac{N_s^a + N_{sp}^a}{N_s^b + N_{sp}^b} \qquad (4)$$

If we know the isotope abundances for the given isotopes *a* and *b* both in the sample ($A^a{}_s$, $A^b{}_s$) and the spike ($A^a{}_{sp}$, $A^b{}_{sp}$) equation 4 can be expressed as:

$$R_m = \frac{N_s A_s^a + N_{sp} A_{sp}^a}{N_s A_s^b + N_{sp} A_{sp}^b} \qquad (5)$$

Rearranging equation 5 for N_s we obtain:

$$N_s = N_{sp} \frac{R_m A_{sp}^b - A_{sp}^a}{A_s^a - R_m A_s^b} \qquad (6)$$

Equation 6 is the most basic form of the isotope dilution equation. As can be observed, if we know the number of moles added with the spike and the isotope composition of both sample and spike we can calculate easily the number of moles in the sample only by measuring *Rm* in the mixture. This expression can be adapted to express concentrations (mass/mass) instead of number of moles, defining $R_s = (A_s{}^b)/(A_s{}^a)$ as the isotope ratio (*b/a*) in the sample and $R_{sp} = (A_{sp}{}^a)/(A_{sp}{}^b)$ the isotope ratio (*a/b*) in the spike, so equation 6 can be expressed as follows:

$$N_s = N_{sp} \frac{A_{sp}^b}{A_s^a} \left(\frac{R_m - R_{sp}}{1 - R_m R_s} \right) \qquad (7)$$

This final expression can be converted in concentrations by using the expressions $N_s = (C_s \cdot m_s)/(M_s)$ and $N_{sp} = (C_{sp} \cdot m_{sp})/(M_{sp})$ being:

- c_S and c_{Sp} the concentrations of the element in the sample and the spike, respectively,
- m_S and m_{Sp} the mass taken from sample and spike in the mixture, respectively, and

- M_S and M_{Sp} the elemental atomic weights of the element in the sample and the spike, respectively.

By substitution, the final isotope dilution equation is obtained:

$$c_s = c_{sp} \frac{m_{sp}}{m_s} \frac{M_s}{M_{sp}} \frac{A_{sp}^b}{A_s^a} \left(\frac{R_m - R_{sp}}{1 - R_m R_s} \right) \qquad (8)$$

In this equation the concentration of the element in the sample c_S is determined just by measuring R_m by mass spectrometry as all other parameters in the equation are known.

This method has several advantages in comparison with the other calibration strategies:

- Signal drifts or matrix effects will have no influence in the value calculated for the element concentration in the sample, because there is no parameter regarding to instrumental sensitivity in the isotope dilution equation.
- The uncertainty in the concentration measurement (c_S) depends only on the measurement of the isotope ratios (R_m) in the mixture, since the elemental atomic weights in the sample and spike (M_S and M_{Sp}) are known and the mass taken from sample and spike (m_S and m_{Sp}) can be gravimetrically determined. In most cases, except for certain elements which show natural variations in their isotope abundances, R_S is known and this is also the case for R_{Sp} if a certified tracer or spike is used.
- If the isotope equilibration is achieved in the mixture, possible loss of substances of the isotope-diluted sample will have no influence on the final result. This is due to the fact that any aliquot of the isotope-diluted sample will contain the same R_m, and therefore, there is no need to know the pre-concentration or dilution factor of the sample or to take into account any non-quantitative separation or evaporation step.

Nevertheless, several considerations are required in order to ensure the above affirmations:

- Any loss of substance (either sample or spike) before the complete isotope equilibration is achieved will involve an important error.
- Once isotope equilibration is reached, the enriched isotope added to the sample should behave identically to the natural element throughout the whole analytical procedure.
- The target isotopes, *a* and *b*, must be free of spectral interferences when measuring them in the mass spectrometer and the factors affecting the accuracy in the measurement of the isotope ratios (such as mass bias and detector dead time) must be under control.
- Blank values must be exhaustively controlled since any kind of contamination affecting the isotope diluted sample will lead to wrong R_m values.

The application of isotope dilution analysis for elemental speciation can be performed under two different modes (the so-called "species-specific" and "species-unspecific" spiking mode), depending on when and in which chemical form the isotope tracer (spike) is added to the sample. It is worth nothing that elemental speciation requires a previous separation of the species to be determined before mass spectrometric determination.

Species-unspecific mode: the addition of the spike is performed after the complete separation of the naturally occurring species in the sample (post-column spiking). Here, the spike may exist in a chemical form different from that of the species to be determined, so this mode is useful when the structure or composition of the species is not well known or when the isotopically labelled compounds are not commercially available or cannot be synthesized. It is important to consider that this spiking mode does not offer the full range of advantages of the isotope dilution analysis, because of any loss of sample prior or during the chromatographic separation will not be corrected for.

Species-specific mode: requires the use of a spike solution containing the species to be analyzed in an isotopically labelled form, so the composition and the structure of the species must be exactly known in order to either synthesize the enriched species or acquire the proper spike solution if it is commercially available. Here, the spike is added at the beginning of the analytical procedure to ensure that all advantages of isotope dilution analyses can be fully exploited. Besides, when several species of the same element are analyzed, each compound can be enriched in a different isotope of the element allowing new forms of quantitation and correction of species interconversion reactions [59].

References

[1] Tarazona, J.V.; Versonnen, B.; Janssen, C.; De Laender, F.; Vangheluwe, M.; Knight, D. Principles for environmental risk assessment of the sediment compartment. Proceeding of the topical scientific workshop (Helsinki, 7-8 May 2013). European Chemicals Agency, Helsinki (Finland), 2014.

[2] U.S. EPA (Environmental Protection Agency). Framework for metals risks assessement. Office of the Science Advisor, Risk Assessment Forum, Washington DC (USA), EPA120/R-07/001, 2007.

[3] Templeton, D.M.; Ariese, F.; Cornelis, R.; Danierlson, L.G.; Muntau, H.; Van Leeuwen, H.P.; Lobinski, R. Guidelines for terms related to chemical speciation and fractionation of elements. Definitions, structural aspects, and methodological approaches. Pure Appl.Chem. 2000, 72:1453-1470.

[4] Moreda-Piñeiro, A.; Moreda-Piñeiro, J. *Cadmium Speciation*, in: Analytical Chemistry of Cadmium. Sample pre-treatments and determination methods. Chemistry Research and Applications. Nova Science Publishers Inc., New York (USA), 2010.

[5] Langmuir, D. Aqueous environmental chemistry. Prentice-Hall, Upper Saddle River, NJ (USA), 1997.

[6] Pearson, R.G. Hard and soft acids and bases. Hutchinson & Ross, Stroudsburg, PA (USA), 1973.

[7] Pickering, W.F. Metal ion speciation in soils and sediments (a review). Ore Geology Rev. 1996, 1:83-146.

[8] Ullrich, S.M.; Tanton, T.W.; Abdrashitova, S.A. Mercury in the aquatic environment: a review of factor affecting methylation. Cri.Rev.Environ.Sci.Tech. 2001, 31:241-293.

[9] Shao, D.; Knag, Y.; Wu, S.; Wong, M.H. Effect of sulfate reducing bacteria and sulfate concentrations on mercury methylation in freshwater sediment. Sci.Total Environ. 2012, 424:331-336.

[10] Diamond, M.L. Application of a mass balance model to assess in-place arsenic pollution. Environ.Sci.Technol. 1995, 29:29-42.

[11] Morrison, H.A.; Whittle, D.M.; Haffner, G.D. The relative importance of species invasions and sediments disturbance in regulating chemical dynamics in western Lake Erie. Ecol.Modeling, 2000, 125:279-294.

[12] Nyffler, U.P.; Santschi, P.H.; Li, Y-P. The relevance of scavenging kinetics to modeling of sediment water interactions in natural water. Limmol.Oceanogr. 1986, 31:277-292.

[13] Schecher, W.D.; McAvoy, D.C. MINEQL+ - A chemical equilibrium modelling system, version 4.5 for windows user´s manual. Environmental Research Software, Hallowell, ME (USA), 2001.

[14] Lofts, S.; Tipping, E. An assemblage model for cation binding by natural particulate matter. Geochom.Cosmochim.Acta, 1998, 62:2609-2625.

[15] Di Toro, D.M.; Mahony, J.D.; Hansen, D.J.; Scott, K.J.; Hicks, M.B.; Mayr, S.M.; Redmond, M.S. Toxicity of cadmium in sediments: the role of acid volatile sulfide. Environ.Toxicol.Chem. 1990, 9:1487-1502.

[16] Bruland, K.; Paytan, A. OCEA 290A Ocean redox chemistry. Present and Past. http://www.pmc.ucsc.edu/~apaytan/290A/, 2012.

[17] Sempre, K.T.; Doick, K.J.; Jones, K.C.; Burauel, P.; Craven, A.; Harms, H. Defining bioavailability and bioaccessibility of contaminated soil and sediment is complicated. Environ.Sci.Tech. 2004, 15:229A-231A.

[18] Nordberg, M.; Duffus, J.H.; Templeton, D.M. Explanatory dictionary of key terms in toxicology: Part II (IUPAC Recommendations 2010). Pure Appl.Chem. 2010, 82:679-751.

[19] ECHA (European Chemicals Agency. Principles for environmental risk assessment of the sediment compartment. Proceedings of the topical scientific workshop. Helsinki, 2013.

[20] Ander, E.L.; Johnson, C.C.; Cave, M.R.; Palumbo-Roe, B.; Nathanail, C.P.; Lark, R.M. Methodology for the determination of normal background concentrations of contaminants in English soil. Sci.Total Environ. 2013, 454-455:604-618.

[21] Reimann, C.; Garrett, R.G. Geochemical background – concept and reality. Sci.Total Environ. 2005, 350:12-27.

[22] U.S. EPA (Environmental Protection Agency). Establishing background levels. Office of Soild Waste and Emergency Response, Washington DC (USA), EPA/540/F-94/030, 1995.

[23] Reimann, C.; Filzmoser, P.; Garrett, R.G. Background and threshold: critical comparison of methods of determination. Sci.Total Environ. 2005, 346:1-16.

[24] Vestenius, M.; Leppänen, S.; Anttila, P.; Kyllönen, K.; Hatakka, J.; Hellén, H.; Hyvärinen, A. P.; Hakola, H. Background concentrations and source apportionment of polycyclic aromatic hydrocarbons in south-eastern Finland. Atmos.Environ. 2011, 45:3391-3399.

[25] Jarman, W.M.; Hobson, K.A.; Sydeman, W.J.; Bacon, C.E.; McLaren, E.B. Influence of trophic position and feeding location on contaminant levels in the Gulf of the Farallones food web revealed by stable isotope analysis. Environ.Sci.Technol. 1996, 30:654-660.

[26] Paquin, P.R.; Gorsuch, J.W.; Apte, S.; Batley, G.E.; Bowles, K.C.; Campbell, P.G.; Delos, C.G.; Di Toro, D.M.; Dwyer, R.L.; Galvez, F.; Gensemer, R.W.; Goss, G.G.; Hostrand, C.; Janssen, C.R.; McGeer, J.C.; Naddy, R.B.; Playle, R.C.; Santore, R.C.; Schneider, U.; Stubblefield, W.A.; Woodm C.M.; Wu, K.B. The biotic ligand model: a historical overview. Special issue: The biotic ligand model for metals: current research, future directions and regulatory implications. Comp.Biochem.Physicol.C.Toxicol.Pharmacol. 2002, 133:3-35.

[27] Machado, W.; Carvalho, M.F.; Santelli, R.E.; Maddock, J.E.L. Reactive sulfides relationship with metals in sediments from a eutrophicated estuary in Southeast Brazil. Mar.Pollut.Bull. 2004, 49:89-92.

[28] Zhuang, W.; Gao, X.L. Acid-volatile sulfide and simultaneously extracted metals in surface sediments of the southwestern coastal Laizhou Bay, Bohai Sea: Concentrations, spatial distributions and the indication of heavy metal pollution status. Mar.Pollut.Bull. 2013, 76:128-138.

[29] Rickard, D.; Morse, J.W. Acid volatile sulfide (AVS). Mar.Chem. 2005, 97:141-197.

[30] U.S. EPA (Environmental Protection Agency). Analytical method for determination of acid volatile sulfide in sediments. Office of Science and Technology Health and Ecological Criteria, Washington DC (USA), EPA-821R-91-100, 1991.

[31] Fan, W.; Wang, W-X. Sediments geological controls on Cd, Cr and Zin assimilation by tge calm Ruditapes philippinarum. Environ.Toxicol.Chem. 2001, 20:2309-2317.

[32] Langston, W.J. Arsenic in U.K. estuarine sediments and its availability to benthic organisms. J.Marine Biol.Assn. 1980, 60:869-881.

[33] Weston, D.P.; Maruya, K.A. Predicting bioavailability and bioaccumulation with in vitro digestive fluid extraction. Environ.Toxicol.Chem. 2002, 21:962-971.

[34] Tessier, A.; Campbell, P.G.C.; Bisson, M. Sequential extraction procedure for the speciation of particulate trace metals. Anal.Chem. 1979, 51:844-851.

[35] McGeer, J.; Henningsen, G.; Lanno, R.; Fisher, N.; Sappington, K.; Drexler, J. Issue paper on the bioavailability and bioaccumulation of metals. http://cfpub1.epa.gov/ncea/raf/recordisplay.cfm?deid=86119, 2004.

[36] Reinfelder, J.R.; Fisher, N.S.; Luoma, S.N.; Nichols, J.W.; Wang, W.X. Trace element trophic transfer in aquatic organisms: a critique of the kinetic model approach. Sci.Total Environ. 1998, 219:117-135.

[37] de la Guardia, M.; Garrigues, S. Handbook of Green Analytical Chemistry. Jonh Wiley & Sons, Ltd., Chichester (UK), 2012.

[38] Galuszka, A.; Migaszewski, Z.; Namiesnik, J. The 12 principles of green analytical chemistry and the significance mnemonic of green analytical practices. Trend Anal.Chem. 2013, 50:78-84.

[39] Quevauviller, P. Methodologies for soil and sediment fractionation studies. Royal Society of Chemistry, Cambridge (UK), 2002.

[40] Bermejo-Barrera, P.; Moreda-Piñeiro, A.; Bermejo-Barrea, A. Sample pre-treatment methods for the trace elements determination in seafood products by atomic absorption spectrometry. Talanta, 2002, 57:969-984.

[41] Moreda-Piñeiro, A.; Barciela-Alonso, M.C.; Domínguez-González, R.; Peña-Vázquez, E.; Herbello-Hermelo, P.; Bermejo-Barrera, P. Alternative solid sample pre-treatment methods in green analytical atomic spectrometry. Spectrosc.Lett. 2009, 42:394-417.

[42] Mason, T.J.; Lorimer, J.P. Applied sonochemistry: uses of power ultrasounds in chemistry and processing. Wiley-VCH, Weinheim (Germany), 2002.

[43] Cornelis, R.; Crews, H.; Caruso, J.; Heumann, K. Handbook of elemental speciation: techniques and methodology. John Wiley & Sons, Ltd., Chichister (UK), 2003.

[44] Wasik, A.; Namiesnik, J. Speciation of organometallic compounds of tin, lead and mercury. Polish J.Environ.Studies, 2001, 10:405-413.

[45] Farajzadeh, M.A.; Nouri, N.; Khorram, P. Derivatization and microextraction methods for determination of organic compounds by gas chromatography. Trends Anal.Chem. 2014, 55:14-23.

[46] Inductively coupled plasma mass spectrometry – a primer. Agilent Technologies, Publication Nº5989-3526EN, 2005.

[47] Thermo Electron Corporation. X Series ICP-MS: enhanced collision cell technology (CCT). Thermo Scientific Product Specifications, http://www.thermo.com/eThermo/CMA/PDFs/Articles/articlesFile_24138.pdf, 2004.

[48] Tanner, S.D.; Baranov, V.I. A dynamic reaction cell for inductively plasma mass spectrometry (ICP-DRC-MS). II. Reduction of interferences produced within the cell. J.Am.Soc.Mass Spectrom. 1999, 10:1083-1094.

[49] Thomas, R. Practical Guide to ICP-MS. A tutorial for beginners. CRC Press Taylor & Francis Group, Boca Raton, FL (USA), 2013.

[50] Orellana, F.A.; Gálvez, C.G.; Roldán, M.T.; García-Ruiz, C. Applications of laser-abaltion-inductively-coupled plasma-mass spectrometry in chemical analysis of forensic evidence. Trend Anal.Chem. 2013, 42:1-34.

[51] Limbeck, A.; Galler, P.; Bonta, M.; Bauer, G.; Nischkauer, W.; Vanhaecke, F. Recent advances in quantitative LA-ICP-MS analysis: challenges and solutions in the life science and environmental chemistry. Anal.Bioanal.Chem. 2015, 407:6593-6617.

[52] Fernández, B.; Claverie, F.; Pécheyran, C.; Donard, O.F.X. Direct analysis of solid samples by fs-LA-ICP-MS. Trends Anal.Chem. 2007, 26:951-966.

[53] Wuilloud, J.C.A.; Wuilloud, R.G.; Vonderheide, A.P.; Caruso, J.A. Gas chromatography/plasma spectrometry – an important analytical too for elemental speciation studies. Spectromchim.Acta Part B, 2004, 59:755-792.

[54] CHROMacademy. Theory and instrumentation of gas chromatography. Sample introduction. http://www.chromacademy.com.

[55] GL Science. Large volume injections in capillary gas chromatography. https://www.glsciences.eu/optic/LVI-training-manual.pdf.

[56] Andrade, J.M.; Terán-Baamonde, J.; Soto-Ferreiro, R.M.; Carlosena, A. Interpolation in the standard additions method. Anal.Chim.Acta, 2013, 780:13-19.

[57] Andrade-Garda, J.M.; Carlosena-Zubieta, A.; Soto-Ferreiro, R.M.; Terán-Baamonde, J.; Thompson, M. *Classical línear regression by the least squares method*, in Basic Chemometric Techniques in Atomic Spectroscopy, ed. Andrade-Garda, J.M. RSC Publishing, Cambridge (UK), 2013.

[58] Ellison, S.L.R.; Thompson, M. Standard additions: myth and reality. Analyst, 2008, 133:992-997.

[59] Rodríguez-González, P.; Marchante-Gayón, J.M.; García Alonso, J.I.; Sanz-Medel, A. Isotope dilution analysis for elemental speciation: a tutorial review. Spectrochim.Acta Part B, 2005, 60:151-207.

[60] Rodríguez-González, P.; García Alonso, J.I. Isotope dilution mass spectrometry. Royal Society of Chemistry, Cambridge (UK), 2013.

CHAPTER

III

INTERPOLATION IN THE STANDARD ADDITION METHOD

INTERPOLATION IN THE STANDARD ADDITION METHOD

1. Abstract

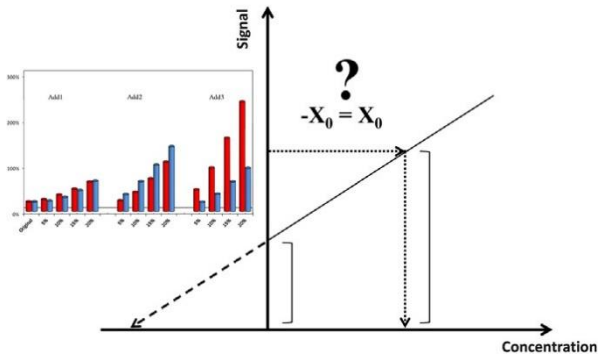

The standard additions method (SAM) has traditionally been performed by using extrapolation. This practice is suboptimal because predictions are affected by even slight departures of calibration points from a straight line. Despite this, most textbooks and papers in analytical chemistry still refer exclusively to extrapolation. In contrast, the use of interpolation is recommended in this paper as a way to get predictions on the central part of the regression line and thus minimize the bias in the prediction and the variance associated with the analytical result. Several scenarios were studied, with concentration errors simulated in different calibration solutions. It was found that translational effects due to variations at the central part of the calibration caused the lowest disturbances on the predicted concentrations. The differences between the interpolated and extrapolated predictions can be as large as ±30%. The confidence interval associated with the extrapolation result is wider than that due to interpolation by as much as 100%. It is shown that commonly used equations underestimate the correct confidence intervals. Both, absence of bias and improved precision, are of relevance in quality assurance, method validation and error propagation.

The results discussed in this chapter are summarized in the scientific publications cited below:

Interpolation in the standard additions method.

J.M. Andrade, J. Terán-Baamonde, R.M. Soto-Ferreiro and A. Carlosena.

Analytica Chimica Acta, 2013, 780, 13-19.

Classical Linear Regression by the Least Squares Method, in: Basic Chemometric Techniques in Atomic Spectroscopy (2nd Edition).

José Manuel Andrade-Garda, Alatzne Carlosena-Zubieta, Rosa María Soto-Ferreiro, Javier Terán-Baamonde and Michael Thompson.

Royal Society of Chemistry, 2013, pp. 52-122.

2. Introduction

Analytical chemists develop measurement methods that almost always are indirect, i.e. the analytical signal is related to the amount of analyte by means of a mathematical functional relationship [1,2]. When pairs of values adhere closely to a mathematical model it is said that a 'calibration function' was found. Although this sounds definitely familiar and routine, serious errors are often underestimated which may yield interlaboratory inaccuracies in the 20–100% range [3], some of which are due to the misuse of regression equations [4]. It is worth stressing that determining the concentration of an analyte in a problem sample is only half the work as the confidence interval associated with that prediction must also be evaluated. Hence, it is the analyst's responsibility to validate the calibration model [5] and the main aspects to be studied were reviewed recently [6].

Most routine calibrations assume a zero-order behavior which considers that the signal is not interfered by concomitants [7]. How-ever, often signal interferences cannot be eliminated. Calibration by means of the standard additions method (SAM) is intended to overcome the problem of the matrix effects that modify the sensitivity, that is, the slope of the calibration function. It enables the analyst to obtain unbiased results when the matrix of the test solution varies unpredictably among test materials in a run [8,9]. This difficulty renders matrix matching the calibrators to the test solutions impossible to apply. SAM is presented frequently as a way to optimize the precision of the results while avoiding certain causes of bias, providing a constant standard deviation or a proportional standard deviation occur [8].

Several limitations of SAM may reduce its good performance. First, SAM may be inadequate whether the behavior of the incurred analyte and the added analyte is not the same. Slight differences on how they link to the matrix can yield different performances, although that depends on the nature of the analytical method. For instance, in an ICP-based method all of the analyte will be atomized irrespective of its source or the nature of its chemical bonding. In GFAAS, in contrast, differences in how they are combined with the matrix concomitants can make an analytical signal present an initial shoulder because of slightly different atomization mechanisms. In general, we also need to ask whether the signal is dependent on the speciation of the analyte. If we look for

total concentration these differences may be irrelevant, but whenever speciation is concerned it becomes a critical issue.

A critical limitation of SAM that analysts must always bear in mind is that it corrects only for rotational matrix effects, not for translational matrix effects. A translational effect is a systematic variation of the measured signal produced by an extra signal caused by concomitant substances present in the test solution, and it is frequently called 'background or baseline interference'. This affects the intercept of a calibration function, but not its slope. On the other hand, a rotational effect arises when non-analyte constituents of the test solution affect the size of the signal from the analyte, giving rise to a change in sensitivity [8]. Both effects can occur simultaneously and often do. Translational effects therefore have to be eliminated by the analyst as a separate step of the procedure.

When discussing both phenomena Ellison and Thompson showed that a 'one-point addition' should be considered instead of the classical separate additions of several different equally spaced amounts of analyte (obviously, this involves being sure that the system follows a straight line behavior). Advantages of a one-point addition are: (i) it simplifies the analyst's benchwork, thereby reducing the cost of the analysis and the possibility of mistakes; (ii) it obviates the need for regression: a simple straight line extrapolation gives the same result as regression, either simple or weighted;(iii) multi-level addition provides no useful information about linearity: tests for deviation from straight line calibration in standard additions have low power unless an impracticable amount of time is spent on the measurement; (iv) it was shown that loss of precision in standard additions is negligible in a well-designed protocol [8].

In relation to point (i) above, common practice is to develop a SAM calibration for each test solution. However, Perkin-Elmer has long implemented the so-called 'addition-calibration method' which is based on developing a SAM calibration for several test solutions: for each one its ordinate is considered to get a new pre-diction by adapting the regression equation [10,11]. Nevertheless, one must be certain on the straight line behavior of the calibration and, moreover, on the true similarity on the composition of the unspiked and spiked solutions; otherwise it should not be applied.

Finally, SAM has traditionally been used as an extrapolation method [1,6,12] whose predictions may be affected (biased) by this practice. However, despite every scientist acknowledge that no model can be applied outside its boundaries, extrapolation is applied ubiquitously in analytical chemistry. This has major con-sequences on method validation and quality assurance systems subjected to external audits intended to certify technical competence. To the best of the author's knowledge this issue has been mostly overcome in the field and it will be discussed in this paper.

To evaluate how the predictions (bias) and the associated confidence intervals (precision) generated by SAM are affected by errors in a calibrator constitutes the objective of the next paragraphs. A case study will be presented to reflect on the problems that may arise when an incorrect use of some common equations is made.

2.1. Interpolation vs. extrapolation

A representation of the data obtained from SAM and how the concentration of interest is predicted commonly by extrapolation is depicted in Fig. 1. A seemingly more adequate alternative is also depicted there, which is an interpolation. The latter is to be dis-cussed below and then compared to extrapolation in a practical example.

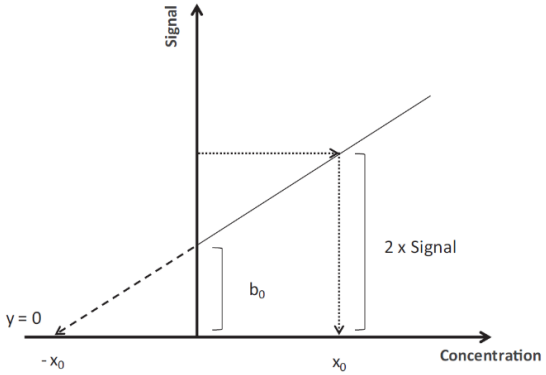

Figure 1. Graphical representation of extrapolation (broken line) and interpolation (dotted line) to predict the concentration of a sample (x_0) after calibration by the standard additions method; b_0 is the ordinate of the calibration function.

Meier and Zünd [13] referred some time ago to SAM. They claimed that interpolation was more precise than extrapolation. Besides, they prevented us from extrapolating always to a zero signal level because in case a matrix component interfered the signal, one should extrapolate to a higher signal value. On the other hand, Miller [12,14] and Miller and Miller [15,16] referred to the extrapolation method stating simply that errors in the slope and intercept contribute to the uncertainty of the calculated concentration. How-ever, when providing the equation of the variance associated to the prediction, they explained merely that the measurand was not determined from a single measured value of the analytical signal (y) and, for the homoscedastic case, set the standard error of the predicted value as [12]:

$$s_{\hat{x}_0} = \frac{s_{y/x}}{b_1}\sqrt{\left(\frac{1}{N} + \frac{\bar{y}^2}{b_1^2\sum_{i=1}^{N}(x_i - \bar{x})^2}\right)} = \frac{s_{y/x}}{b_1}\sqrt{\left(\frac{1}{N} + \frac{(\hat{x}_0 - \bar{x})^2}{\sum_{i=1}^{N}(x_i - \bar{x})^2}\right)} \quad (1)$$

Here $\hat{x}_0$ is the value predicted by the extrapolation of *x* when its associated signal (y_0) becomes $y_0 = 0$; $s_{\hat{x}_0}$ is its standard error; b_1 the slope of the regression line; $s_{y/x}$ is the residual variance of the regression and xi corresponds to each of the calibrators. *N* is the number of calibration solutions, assuming that there are no replicates (although that is not made explicit and the original notation was retained here). Massart et al. [17] used Miller's equations with-out further comments although they warned against the drawbacks associated to extrapolation and their adverse effects in precision.

The International Union of Pure and Applied Chemistry (IUPAC) [1] expounds the extrapolation by SAM in more detail. It recommends adding amounts of x_i (the analyte) equimolar that expected for the test solution, so that $x_1 \sim x_0$; $x_2 \sim 2 \cdot x_1$; . . . $x_p \sim p \cdot x_1$ (*p* is the number of levels of the addition; frequently $p = 3$ or 4). A preliminary estimate of x_0 would be needed. The estimated standard error for the predicted concentration from the true mean value of the extrapolated signal ($y_0 = 0$) was proposed as Eq. (2) [1,6]. This is wider than the error yielded by interpolation with a normal calibration (see Eq. (4)) because of the extrapolation to $x_i = -x_0$, where *m* is the total number of

calibration solutions. Many scientists do not consider the term $-x_0$ (they consider only the absolute value) and, so, they estimate an unduly small standard error.

$$s_{\hat{x}_0} = \frac{s_{y/x}}{b_1}\sqrt{\left(\frac{1}{m} + \frac{(-\hat{x}_0 - \bar{x})^2}{\sum_{i=1}^{N}(x_i - \bar{x})^2}\right)} \qquad (2)$$

IUPAC sets $m = m_0 + pm_i$, where m_0 is the number of replicated measures performed on the test solution; mi is the number of replicates for each addition, and p is the number of levels of additions used to establish the regression. This clarifies any ambiguity in the correct use of N in Eq. (1).

Ortiz et al. [6] studied also this question and compared the equations of the variances associated to the estimated value for the concentration of the test solution: when extrapolating, the quantity of analyte in the test solution is obtained by setting the signal $y_0 = 0$, $x_0 = -(b_0/b_1)$ where b_0 is the intercept of the regression line. Its standard error is calculated as:

$$s_{\hat{x}_0} = \frac{s_{y/x}}{b_1}\sqrt{\left(1 + \frac{1}{m} + \frac{(-(b_0/b_1) - \bar{x})^2}{\sum_{i=1}^{N}(x_i - \bar{x})^2}\right)} \qquad (3)$$

There, m includes all spiked and unspiked calibrators. The term '*1*' within the parenthesis stems from error propagation. Note that both Eqs. (1) and (2) lack from this term because they were defined for true mean signals (which in daily practice are not known).

The alternative is to perform interpolation, and they proposed to calculate the regression line from the data $(x_i, y_i - b_0)$, $i = 1, \ldots, N$. It is clear that the slope of the new regression line is the same as before. The concentration of the test solution corresponds to the subtracted ordinate y_0. The estimated concentration has the standard error given in Eq. (4).

$$s_{\hat{x}_0} = \frac{s_{y/x}}{b_1}\sqrt{\left(1 + \frac{1}{m} + \frac{((b_0/b_1) - \bar{x})^2}{\sum_{i=1}^{N}(x_i - \bar{x})^2}\right)} \qquad (4)$$

It is clear again that the standard error, and therefore the confidence interval (C.I.), of the extrapolation mode is larger than for interpolation (due to the differences in the numerators). The C.I. for interpolation and extrapolation can be derived from both equations or, as it is more common, from the measured signals as it is shown in Eqs. (5) and (6) for interpolation and extrapolation ($y_0 = 0$), respectively:

$$\hat{x}_0 \pm t_{(\alpha/2,N-2)} \cdot \frac{s_{y/x}}{b_1} \sqrt{\left(1 + \frac{1}{m} + \frac{(y_0 - \bar{y})^2}{b_1^2 \sum_{i=1}^{N} (x_i - \bar{x})^2}\right)} \quad (5)$$

$$\hat{x}_0 \pm t_{(\alpha/2,N-2)} \cdot \frac{s_{y/x}}{b_1} \sqrt{\left(1 + \frac{1}{m} + \frac{\bar{y}^2}{b_1^2 \sum_{i=1}^{N} (x_i - \bar{x})^2}\right)} \quad (6)$$

These equations assume an underlying normal distribution for the results of the repeats. However, results from extrapolation can be strongly biased (in particular, skewed), but results from interpolations are likely to be much closer to normally distributed.

The use of the transformed ($y - b_0$) values to interpolate contradicts conceptually the well-known fact that in general it is not recommended to remove the intercept (blank) from the calibrations [5,18,19]. This contradiction is solved easily and we propose to apply a practice based on simple geometry, see Fig. 1, which consists of interpolating twice the signal generated by the test solution ($y_0 = 2 \cdot$ *signal of the unspiked test solution*, note that this is not always necessarily the same as $2 \cdot b_0$). The calculations of the confidence intervals reduced to Eq. (5) (the precision for the measurements of the test solutions and calibrators are assumed equal) [20]. In this respect, it is worth noting that the Ortiz et al. [6] approach and our own one yield predictions in the central part of the regression straight line. Therefore, bias due to extrapolation is avoided and the variance associated to the interpolated value is minimized, contrary to classical SAM. It is also worth noting that, in many situations where extrapolation has been performed, Eq. (4) (or Eq. (1)) was used to calculate the confidence interval associated to the prediction, which is not consistent with the rest of the procedure.

3. Experimental

The case study considered here deals with the determination of Ni in fuel oil using electrothermal atomic absorption spectrometry (ETAAS). The existence of a matrix effect was observed and the use of SAM was required [21]. Additions to the test solution were made at 10 ppb regular intervals, from 0 to 80 ppb. Calibration solutions were replicated three times at each level. The least squares linear regression fit was statistically significant, without lack-of-fit (as measured by an analysis of variance), without outliers or trends in the residuals (as determined by visual inspection of plots of residuals). Homogeneity of the variances at the 9 concentration levels was tested by means of the Cochran, Levene and Bartlett statistical tests [19]. All them yielded not significant statistics (95% confidence level). The regression obtained this way will be called 'original or unmodified regression' throughout the text and its data is shown in Table 1.

Table 1. Standardization considered as reference for simulations.

Conc. (ppb Ni)	Absorbance	Conc. (ppb Ni)	Absorbance	Conc. (ppb Ni)	Absorbance
0	0.216	30	0.372	60	0.511
0	0.245	30	0.383	70	0.540
0	0.233	40	0.399	70	0.520
10	0.252	40	0.405	70	0.560
10	0.265	40	0.430	80	0.571
10	0.288	50	0.421	80	0.550
20	0.312	50	0.433	80	0.591
20	0.330	50	0.458		
20	0.341	60	0.468		
30	0.342	60	0.490		

Different scenarios where an addition suffers a slight error (e.g., during its preparation or at its measurement) and its signal is modified so that it becomes displaced slightly in the regression with respect to the original situation, were simulated. To systematize the study, the signals associated to three critically located calibrators were modified: the lowest addition, the solution in the middle of the calibration and the uppermost addition. The signals were both increased and reduced by 5, 10, 15 and 20% to simulate absorbance enhancements and depletions, respectively. In all cases it will be assumed that the researcher did not detect the modified points as anomalous and proceeded with the quantification.

The interpolated concentration of the unspiked test solution was predicted in accordance with Fig. 1 as ((*2 · signal of the unspiked sample − intercept)/slope*). Its variance and confidence interval were estimated using Eqs. (4) and (5), with y_0 *= 2 · signal of the unspiked test solution* and *N = 27*.

To extrapolate, $\hat{x}_0$ was calculated as usual (*intercept/slope*). Two equations were applied to derive the corresponding confidence intervals and compare them. One corresponds to the extrapolation treated correctly (Eq. (6), which is equivalent to Eq. (3)). The other corresponds to the usual situation observed in many occasions where despite an extrapolation was made the mathematical treatment corresponds (incorrectly) to a traditional interpolation (Eq. (5), which is equivalent to using Eq. (1) from Miller [5,12] and Miller and Miller [14–16], although including the term '*1*' within the parenthesis).

4. Results and discussions

The 24 standardization lines of the different scenarios were compared to the original regression by means of the joint confidence region for the slope and the intercept [17]. Fig. 2 reveals some interesting patterns that may be of help to interpret the results:

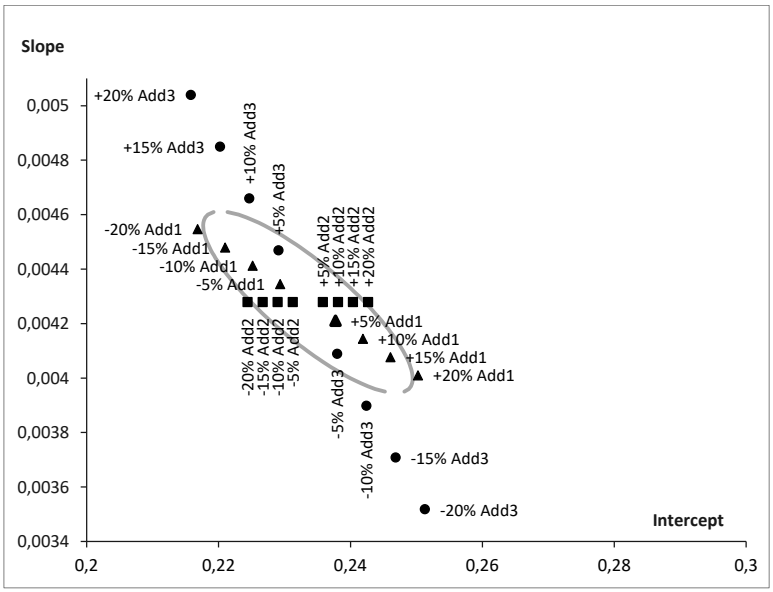

Figure 2. Joint confidence ellipse for the ordinate and intercept of the original regression, along with the pairs (intercept, slope) obtained for each of the 24 simulated calibration lines. The triangles, squares and circles correspond to modifications in the lowest (Add1), intermediate (Add2) and highest addition (Add3), respectively. Only data pairs out of the boundary

1. The translational effect produced by alterations in a central addition (*Add2*) does not involve serious consequences, even when as large variations as 20% in the original absorbance occurred. In all cases the straight lines are statistically indistinguishable from the unmodified one.
2. Errors in the lowest addition, *Add1*, yield straight lines statistically undistinguishable from the original one, unless the variations in the signal are higher than ca. ±18%. A clear trend exists on the intercept and slope depending on whether an enhancement or a depletion of the signal occurred on the lowest addition. Signal enhancements (due to, e.g., concomitants) increase the intercept and decrease the slope. The opposite situation occurs for signal depletion. The effect is simple to visualize if the physical law of the lever is recalled.
3. The uppermost addition (*Add3*) revealed critical to define the standardization function, as expected, although low errors (lower than ca. 7%) still yielded a line not different from the unmodified one. However, the ordinate and intercept degrade dramatically with almost

any other signal variation. The huge rotational effect caused by *Add3* on the regression line can be explained by its remote location to the intercept, which magnifies any slight deviation of the calibrator. This justifies also that *Add1* yields only moderate adverse effects as its closeness to the extrapolation/interpolation point mitigates its harmful effect. However, one must be very cautious with this because 'closeness' here depends on the slope, the intercept, and the concentration of the test solution. One must study always the calibration graph and avoid unrealistic extrapolations (the IUPAC approach [1] to distribute the calibrators would be a good guide).

4. Finally, it is worth noting that the two extremes of the straight line hold a logical opposite behavior when their signals become modified. In case the signal in *Add1* becomes depleted, the slope increases and, accordingly, the intercept decreases; whereas a depletion in the *Add3* signal reduces the slope and increases the intercept. In case an enhancement in the signal occurs, the complementary situation occurs (e.g., for *Add1* the slope decreases and the intercept increases, with respect to the original regression line).

The predictions and confidence intervals, C.I. (given as $\pm\, t \cdot s_{\hat{x}_0}$) for all scenarios are presented in Table 2. The percentual increments on the concentrations were calculated as $100 \cdot [(\hat{x}_{0,\text{modified signal}} - \hat{x}_{0,\text{unmodified}})/(\hat{x}_{0,\text{unmodified}})]$; with analogous calculations for the confidence intervals.

Table 2. Predictions and confidence intervals (C.I., given as $\pm t \cdot s_{\hat{x}_0}$) calculated by interpolation and extrapolation. Signal variations (*first column*) are presented as percentage of enhancements or depletions in the signal of the atomic peak for the first (Add1, 10 ppb), intermediate (Add2, 40 ppb) and last (Add3, 80 ppb) additions. The rows denoted as "original" correspond to the unaltered calibration.

		Interpolation		**Extrapolation**		
		$\hat{x}_0$	***C.I.*** *Eq. (5)*	$\hat{x}_0$	***C.I.*** *Eq. (6)*	***C.I.*** *Eq. 5 (Eq.1)*
Add1	Original	53.56	8.48	54.58	10.26	8.48
	+5%	53.43	8.51	56.44	10.37	8.53
	-5%	53.70	8.87	52.78	10.67	8.87
	+10%	53.28	9.02	58.37	11.07	9.06
	-10%	53.83	9.62	51.03	11.50	9.60
	+15%	53.14	9.97	60.35	12.32	10.04
	-15%	53.95	10.61	49.33	12.61	10.58
	+20%	52.99	11.29	62.40	14.05	11.39
	-20%	54.08	11.76	47.69	13.90	11.72
Add 2	Original	53.56	8.48	54.58	10.26	8.48
	+5%	53.03	9.55	55.12	11.58	9.56
	-5%	54.10	8.63	54.05	10.42	8.63
	+10%	52.50	11.51	55.65	13.99	11.53
	-10%	54.63	9.95	53.51	11.99	9.94
	+15%	51.96	13.98	56.18	17.03	14.02
	-15%	55.17	12.06	52.98	14.50	12.04
	+20%	51.43	16.74	56.72	20.44	16.80
	-20%	55.70	14.63	52.45	17.55	14.60
Add 3	Original	53.56	8.48	54.58	10.26	8.48
	+5%	52.28	8.49	51.27	10.17	8.49
	-5%	54.97	10.18	58.21	12.46	10.21
	+10%	51.10	9.85	48.22	11.68	9.83
	-10%	56.52	13.32	62.19	16.51	13.39
	+15%	50.01	11.86	45.41	13.95	11.84
	-15%	58.22	17.50	66.57	22.00	17.67
	+20%	49.00	14.09	42.82	16.44	14.07
	-20%	60.10	22.53	71.44	28.77	22.88

4.1. Effects on the predictions

With respect to interpolation, Table 2 shows that the predictions obtained when the lowest addition (*Add1*) suffers from some signal modification differ only in 0.5 ppb (<1%) and that signal enhancements yield lower concentrations than the unaltered regression line. In addition, the departures of the predictions from the con-centration derived from the unaltered calibration (i.e., biases) are slightly larger for signal enhancements than for signal depletions. A translational effect (variations in the central addition, *Add2*) caused more serious differences, reaching 2.2 ppb (4%) for the ±20% increment (again, signal enhancements caused slightly smaller biases than signal depletions). The effect induced by *Add3* leads, as expected, to the worst situation because results differ in more than 6 ppb (12%). It was observed also that signal depletions are more cumbersome than signal enhancements in *Add3*, as they decrease the slope and increase the intercept.

To study the extrapolation results, several ways to analyze the results in Table 2 are possible, providing slightly different views:

(i) comparing all the extrapolation predictions to the extrapolation with the unmodified regression line (*1st row* for each addition, 'extrapolation' column in Table 2), to assess how extrapolation becomes affected by a problem in an addition (regardless of the unmodified extrapolation quantitation being biased or not), Fig. 3a;

(ii) comparing an extrapolation prediction against its corresponding interpolation one (i.e., a *row-wise* comparison), Fig. 3b, to assess differences between both methods;

(iii) comparing the extrapolation predictions to the original interpolation, to observe how different the predictions will be with respect to interpolating in an unaltered regression line, Fig. 3c.

An immediate conclusion from Table 2 is that extrapolation an interpolation predictions do not agree, not even for the unmodified scenario (i.e., no calibrator departs from the line). This occurs regardless of the calibration solution and the magnitude of the enhancement/depletion of its signal. The same can be observed for the confidence intervals. It is noticed that variations in the predictions when *Add2* suffers an alteration are lower than for *Add 1* and *Add3*. The quantitations obtained by extrapolation when *Add2* is

modified differ at most in 2.2 ppb, <4%, with respect to the extrapolation of the original regression. Variations in *Add1* and *Add3* modified the quantitations up to 8 ppb (14%) and 17 ppb (31%), respectively; see Fig. 3a.

Signal enhancements in *Add1* and *Add2*, along with signal depletions in *Add3*, lead to similar biased behaviors (positive increments on the predicted concentrations). Analogously, signal depletions in *Add1* and *Add2*, along with signal enhancements in *Add3* lead to biased low concentrations. Nevertheless, the most important effects are produced by depleted signals in *Add3*, as expected because it is located furthest from the extrapolation region and it causes a large change in both the intercept and slope. Recall that some regression lines obtained from *Add3* alterations were statistically different from the unmodified one (Fig. 2).

Fig. 3b compares the predictions for the test solution by the extrapolation and interpolation methods (row-wise comparison of Table 2). It is observed that extrapolation and interpolation yield very different quantifications. Even without signal modification there are differences of 1 ppb, 2%, among them (*black bar* in Fig. 3b). Then, the larger the increment in the signal of the calibration solution is, the larger the difference in the concentration estimated by SAM becomes. As noted in the previous paragraph the effect is more pronounced for *Add1* and *Add3* than for *Add2*. Further, signal enhancements and signal depletions yield opposite behaviors in the predictions, with the former originating largest predictions than the latter for *Add1* and *Add2*. The opposite is seen for *Add3*.

Fig. 3c compares extrapolation to the original unmodified interpolation. The pattern is similar to Fig. 3b, with the most important changes on the predictions being caused by depletions on the signal of *Add3*, as high as 20–30%. Despite the fact that this corresponds to a regression line significantly different from the original one it is really useful to visualize how relevant the degradation of the quality of the predictions can be when extrapolating. In addition, the bias on the predictions resulting from signal modifications in *Add1* and *Add2* cannot be neglected at all. They differ in up to 8.8 ppb for *Add1* (17%), and up to 3.2 ppb for *Add2* (6%), for the largest (±20%) signal increments.

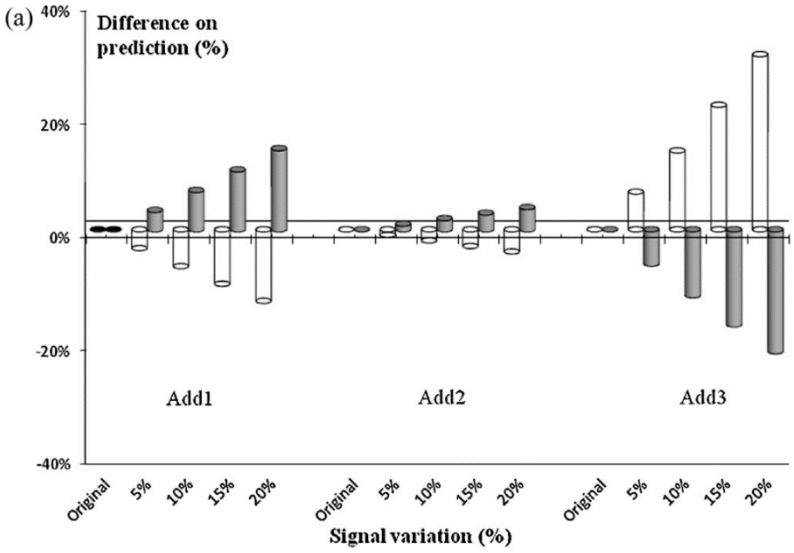
(a)
Difference on prediction (%)
40%
20%
0%
-20%
-40%
Add1
Add2
Add3
Original
5%
10%
15%
20%
Signal variation (%)

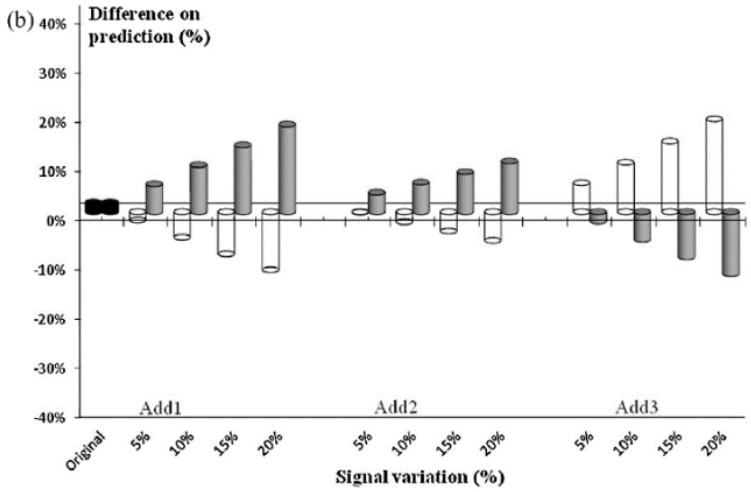
(b)
Difference on prediction (%)
40%
30%
20%
10%
0%
-10%
-20%
-30%
-40%
Add1
Add2
Add3
Original
5%
10%
15%
20%
Signal variation (%)

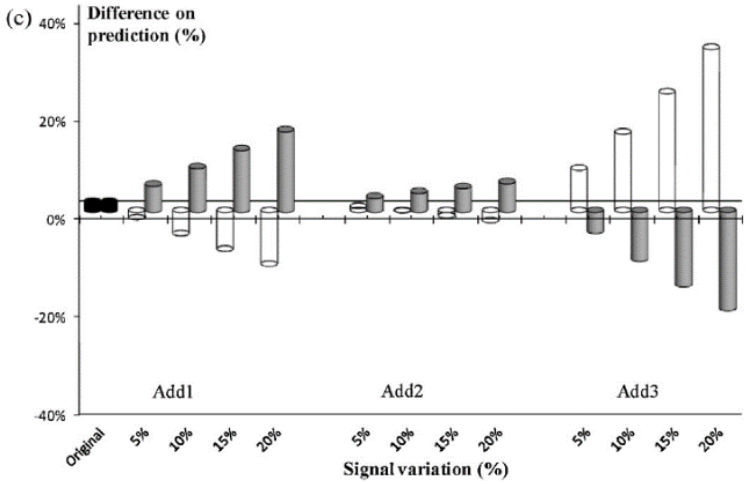

Figure 3. Comparing the predictions obtained by extrapolation when errors are simulated on the calibration solutions. Percentages of variation referred to: (a) the unmodified extrapolation, (b) the corresponding interpolation (row-wise comparison of Table 2), (c) the unmodified interpolation. White and grey bars correspond to depletions and enhancements of the signals, respectively.

4.2. Effects on the confidence intervals

The half-confidence intervals shown in Table 2 can be compared also in the three different ways shown above. However, as the conclusions and the plots are very similar, we will restrict the discussion to some particular situations which should clarify the importance of the risks assumed when extrapolation is used instead of interpolation. In general, all confidence intervals estimated by both extrapolation and interpolation were modified when the signal of a calibrator increased or decreased and they too behaved similarly.

When interpolation is considered, Table 2 shows that the maximum difference on the C.I. when the lowest addition (*Add1*) is modified amounts 39% (in our example, less than 3.3 ppb) with respect to the original interpolation. Signal variations in *Add2* enlarge the C.I. up to 8.2 ppb (98%). As expected, the worst situation occurs for variations in the *Add3* signal which increased the C.I. up to 166% (14 ppb, for signal depletions up to 20%). These extreme situations

coincide with those largest signal variations in *Add2* and *Add3* which produced regression lines different to the unmodified one (Fig. 2). This of course stresses the huge importance of carefully studying the calibration model (in particular, the lack-of-fit and the various residuals plots).

When extrapolation is studied, the first conclusion is that extrapolation leads to higher C.I. than interpolation when the correct equation is used (column labeled as Eq. (6) in Table 2). Considering the C.I. of the concentrations predicted by extrapolation the influence of the signal variation on the additions is very similar to that observed for interpolation (Fig. 4a). Variations in *Add1* caused the lowest disturbances on the C.I. (up to 3.8 ppb, 37% increment with respect to the unmodified extrapolation). Signal variations in *Add2* led to an intermediate situation, with largest C.I. derived from the highest signal modifications: ±15% (66% increment with respect to the unmodified extrapolation) and ±20% (99% increment in the C.I.). It is clear that *Add3* produced the most obvious changes in the C.I. (mainly when the signal was depleted); up to 18.5 ppb (180% increase; i.e., 37 ppb the whole range of the C.I.); see Fig. 4a.

Fig. 4b compares the C.I. obtained by extrapolation (using Eq. (6)) to the C.I. of the original unmodified interpolation. The *black bar* on the figure shows that even when no signal modification is considered on any calibration solution the confidence interval obtained by extrapolation is wider than that from interpolation by 21% (1.8 ppb, see Table 2). Again, the C.I. estimated by SAM increases with the level of signal alteration. Considering the worst situation, the C.I. increases by 5.5 ppb (66%) and by 12 ppb (141%) for ±20% signal enhancements in *Add1* and *Add2* respectively. It increases up to 20.3 ppb (239%) for signal depletions in *Add3*. Again, the situation for *Add3* stems from a poor regression function that should not be accepted in normal work.

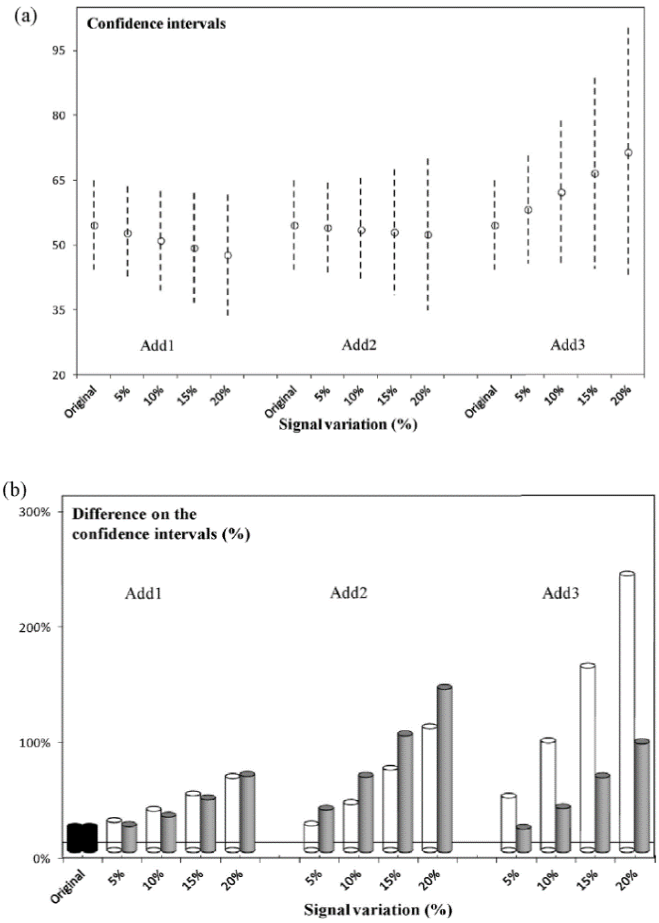

Figure 4. Confidence intervals (calculated using Eq. (6)) associated to extrapolation predictions when the signal of a calibration solution gets modified: (a) graphical comparison when the signals get depleted; (b) percentual differences when the C.I. are compared against the original unmodified interpolation. White and grey bars correspond to depletions and enhancements of the signals respectively.

A final discussion has to be devoted on the application of Eq. (5) (or Eq. (1), after completing the terms within the parenthesis) when extrapolation is carried out. The classical equation given by Miller [12,14] corresponds formally to an interpolation despite its use has been usual in connection with extrapolation. We show, however, that correct equations linked to extrapolation were Eqs. (3) and (6). When Eq. (5) is applied to predict the C.I. associated to the extrapolation the outcome is much lower than that yielded by

the correct equation (see Table 2). However, to be consistent with the working procedure and to provide appropriate results, this procedure should be avoided because the equations of two different approaches are interchanged. Table 2 reveals that the C.I. for an extrapolated concentration clearly underestimates the correct one when the incoherent equation is used.

Furthermore, we must bear in mind that the predicted extrapolations themselves seem not totally correct. Hence, we discourage the use of the extrapolation mode with the standard additions method and propose interpolating the signals instead. We cannot recommend either the combination of extrapolation practices with the use of equations related to interpolation.

5. Conclusions

The use of extrapolation in the standard additions method is a high-risk practice because it can yield biased predictions and confidence intervals substantially different from interpolation. In particular, the confidence intervals derived from extrapolation are always higher than those from interpolation. In addition, the biases on the predictions and the deterioration of the confidence intervals are exacerbated whenever a calibration solution suffers from some unnoticed error.

When interpolation is considered, alterations on the signal measured for an initial and central addition cause only moderate effects in the associated C.I. (with respect to the original unmodified interpolation) whereas changes on the signal of the highest addition yields differences in results as large as 166%, for signal depletions of 20%.

When extrapolation is studied, predicted concentrations are biased with respect to interpolation. Even when any calibration solution has wrong signals differences of 2%, with respect to interpolation, were obtained. Signal enhancements or depletions of the first, the central and the highest additions lead to biases on the predictions of 17%, 6% and 30%, respectively (when compared to the original interpolation). With regard to the confidence intervals, they widened in proportion to the alteration of the signal (in case no signal suffered alterations, the interval increased by 21%). Considering the worst scenarios (±20% modification of the signal of a calibration solution), the confidence interval increases by 66%, 141% and 239%, for the first, central and highest additions, respectively.

Finally, it is inappropriate to calculate a concentration by extrapolation and to calculate confidence intervals using equations associated with interpolation because the equations of two different approaches are being confused. In contrast, interpolating twice the signal of the unspiked sample in the calibration line yields predictions in the central part of the calibration function and thus minimize both the risk for bias and the variance (and confidence intervals) associated with the interpolated value. Therefore, interpolation is strongly recommended.

References

[1] Danzer, K.; Currie, L.A. Guideline for calibration in analytical chemistry. Part 1. Fundamentals and single component calibration. Pure Appl.Chem. 1998, 70:993–1014.

[2] ISO 11843-1, Capability of Detection, Part 1: Terms and Definitions, International Organization for Standardization, Geneva, 1997.

[3] van Nevel, L.; Taylor, P.; Örnemarkand, U.; De Bievre, P. International measurement evaluation programme: trace elements in water. Report to participants, European Commission, 1996.

[4] Mulholland, M.; Hibbert, D.B. Linearity and the limitations of least squares calibration. J.Chromatogr.A, 1997, 762:73–82.

[5] Miller, J.N. Why are calibration methods useful in Spectroscopy? Spectrosc. Int. 1991, 3:42–44.

[6] Ortiz, M.C.; Sánchez, S.; Sarabia, L. *Quality of analytical measurements: univariate regression*, in: Comprehensive Chemometrics: Chemical and Biochemical Data Analysis, eds. Brown, S.D; Tauler, R; Walczak, B. Elsevier, Amsterdam, 2009.

[7] Boqué, R.; Ferré, J. LC–GC Eur. 2004, 16:402–407.

[8] Ellison, S.L.R.; Thompson, M. Standard additions: myth and reality. Analyst, 2008, 133:992–997.

[9] Brown, R.J.C.; Roberts, M.R.; Milton, M.J.T. Systematic error arising from "Sequential" Standard Addition Calibrations: Quantification and correction. Anal.Chim.Acta, 2007, 587:158–163.

[10] Cal-Prieto, M.J.; Carlosena, A.; Andrade, J.M.; Muniategui, S.; López-Mahía, P.; Fernández, E.; Prada, D. Development of an analytical scheme for the direct determination of antimony in geological materials by automated ultrasonic slurry sampling. J.Anal.At.Spectrom. 1999, 14:703–710.

[11] Perkin-Elmer, Atomic Absorption Laboratory Benchtop. User's Guide, Überlingen, Perkin-Elmer, 1991.

[12] Miller, J.N. The method of standard additions. Spectrosc.Eur. 1992, 4:26–27.

[13] Meier, P.C.; Zünd, R.E. Statistical Methods in Analytical Chemistry. Wiley Inter-science, New York, 1993.

[14] Miller, J.N. Basic statistical methods for analytical chemistry. Part 2: Calibration and regression methods. A Review. Analyst, 1991, 116:3–13.

[15] Miller, J.C.; Miller, J.N. Estadística para química analítica. Addison-Wesley, Iberoamericana, Delaware, USA, 2002.

[16] Miller, J.N.; Miller, J.C. Estadística y Quimiometría para Química Analítica. Prentice Hall, Madrid, 2002.

[17] Massart, D.L.; Vandeginste, B.G.M.; Buydens, L.M.C.; De Jong, S.; Lewi, P.J.; Smeyers-Verbeke, J. Chemometrics: A Textbook. Elsevier, Amsterdam, 1988.

[18] Cuadros Rodríguez, L.; García Campaña, A.M.; Jiménez Linares, C.; Román Ceba, M. Estimation of performance characteristics of an analytical methods using the data set of the calibration experiment. Anal.Lett. 1993, 26:1243–1258.

[19] Sayago, A.; Asuero, A.G. Fitting straight line with replicated observations by linear regression: Part II. Testing for homogeneity of variances. Crit.Rev.Anal.Chem. 2004, 34:133–146.

[20] Draper, N.R.; Smith, H. Applied Regression Analysis. John Wiley & Sons, New York, 1998.

[21] Terán-Baamonde, J.; Carballo-Paradelo, S.; Soto-Ferreiro, R.M.; Carlosena-Zubieta, A.; Fernández-Fernández, E.; Muniategui-Lorenzo, S.; López-Mahía, P.; Prada-Rodríguez, D. XVII Conference Encontro Galego Portugués de Química, Pontevedra, Spain, 2011.

CHAPTER

IV

BIOACCESSIBLE METALLIC FRACTION IN MARINE SEDIMENTS

FAST ASSESSMENT OF BIOACCESSIBLE METALLIC CONTAMINATION IN MARINE SEDIMENTS

1. Abstract

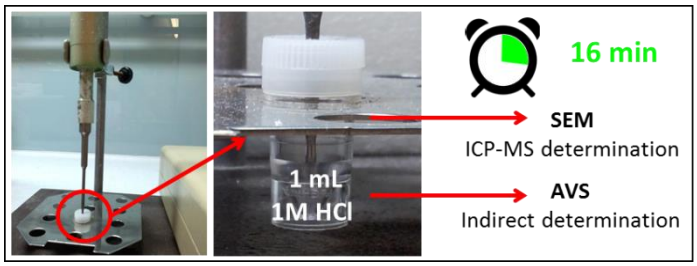

A fast (16 min) procedure to assess the bioaccessible metallic fraction of Cd, Cr, Cu, Ni, Pb and Zn simultaneously extracted (SEM) from marine sediments plus an indirect approach to determine acid volatile sulfides (AVS) are presented. The SEM procedure uses an ultrasonic probe and only 1 mL of 1 mol L^{-1} HCl. It dramatically minimizes the turnaround time and the residues. The fraction of metals extracted correlated well with the sum of the 3-step sequential fractions of the BCR 701 certified sediment. AVS were evaluated by subtracting the amount of sulphur in the extraction residues to total sulphur in the original samples. These procedures are fast, easy to implement and cost-effective to assess the potential risk posed by metals in marine sediments. As a practical application, sediments from two Galician Rias (NW of Spain) were analysed and their SEM-AVS values indicated no biological risk.

The results discussed in this chapter are summarized in the scientific publication:

Fast assessment of bioaccessible metallic contamination in marine sediments.

J. Terán-Baamonde, J.M. Andrade, R.M. Soto-Ferreiro, A. Carlosena and D. Prada.

Marine Pollution Bulletin (under revision), 2016.

2. Introduction

The total content of metals in sediments should not be the unique criterion to set their potential risks to the aquatic ecosystems as the levels of toxicity and bioavailability might not coincide with it. Quantifying the available (or labile) metal fraction in sediments is a better indication on their quality [1]. In the last years, there were attempts to clarify the terminology related to the study of the bioavailability of a compound in soils and sediments. Many different viewpoints created a "semantic stumbling block" that difficult the use of this term across disciplines [2]. Recently, IUPAC gave general definitions for bioaccessibility (i.e., the potential for a substance to come in contact with a living organism and then interact with it) and for bioavailability (i.e., the extent of absorption of a substance by a living organism compared to a standard system). In some cases, bioaccessibility will determine whether a substance is or it is not toxic. This is particularly important in relation to substances present in soils, sediments, aerosols, and other particulate matter to which humans may be exposed. Moreover, both terms are a function of both chemical fractionation and biological properties [3].

So far, there is not a uniform, broadly accepted methodology to measure the quantity of metals implied in such definitions despite relevant institutions, such as USEPA or ICMM [4-6], tried to establish guidance and sediment quality guidelines (SQGs) [7]. Moreover, the level of harmonization across the European Union on the metals to be monitored by different regional marine frameworks is rather low [8].

Several sediment analysis procedures, including sequential and partial (single) extractions, are performed to evaluate the available metallic fraction [9]. The first sequential extraction procedure proposed by Tessier [10] is still used [11]. Nevertheless, a lot of modifications have been proposed and sequential extraction schemes vary widely in number of steps, reagents and extraction conditions [12]. For this reason, it is very difficult to establish meaningful comparisons between results obtained in different laboratories. Worst, a detailed interpretation of the data generated in the studies is not usually provided and only the amount of metal associated with a certain phase is given [13].

In response to the need for standardization, the Standards, Measurements and Testing Programme, SM&T (formerly BCR) of the European Commission developed a harmonized, three-stage, sediment sequential extraction protocol [14] which was revised and modified later [15]. This is a four-step procedure which fractionate metals into weak acid extractable, reducible, oxidisable and residual fractions using three reagents of increasing reactivity: acetic acid, hydroxylamine hydrochloride and hydrogen peroxide. The overall sequential extraction protocols are labor-demanding and time-consuming, usually about 50 h are required to extract three or four individual phases, being its application to a large number of samples lengthy and costly [16]. Further, many issues are still under debate because the reagents are unspecific to dissolve target phases, metals can redistribute (by readsorption) among phases [1, 17], and the understanding of the fractionation of trace elements in solid samples is rather unsatisfactory because the analytical techniques are only defined operationally [18].

Partial (single) extractions constitute a simple and cost-effective approach to determine the labile metals in sediments, which make them suitable for incorporation into routine assessment programs. A wide range of reagents were reported although they can be classified into three groups: dilute solutions of strong mineral acids, weak acids and solutions of complexing agents or reducing agents [19, 20]. Diluted HCl has been used frequently to solubilize the metallic available fraction (strictly, potentially accessible) from the more resistant phases in sediments, as it can attack key labile phases in the sediments. Its reducing properties help liberating metals from Fe and Mn oxides, which are the major sink for trace metals in oxic sediments. It also decomposes efficiently the labile organic phase and amorphous sulfides that control metal bioavailability in anoxic and partially oxidized sediments [21]. Several acid concentrations, agitation modes and times were proposed. Validation of these methods is cumbersome because no reference material exists with certified values for such a procedure and, so, several strategies were undertaken.

Sutherland et al. [17] compared first time the BCR sequential extraction and single HCl-extraction. They concluded that there was no quantitative advantage in using the 3-step BCR sequential extraction procedure and that the results, particularly for Cu, Pb and Zn, were strongly related with those extracted by the sum of the 3-step BCR sequential procedure. They set that HCl-extraction

was useful as a first assessment technique to monitor these elements in disturbed environments [19]. Similar results were reported by Larner et al. [20] when analyzing the NIST 2711 Montana soil certified reference material; they highlighted its applicability to large sample sets [1]. However, when HCl single extraction was applied to urban soils, Madrid et al. [16] did not find an accurate estimation of the available metallic fraction.

Several authors considered that the extraction efficiencies of the HCl single extraction depend on the matrix composition of the samples and also on the nature of the elements [22]. Townsend et al. [23] applied a HCl single extraction (1 mol L^{-1}, 4 h) to two reference marine sediments (PACS-2 and MESS-3) concluding that the different composition of the materials determined the amount of metals extracted.

Diluted HCl was proposed to generate the acid volatile sulfides (AVS) and to lixiviate the so-called simultaneously extractable metals (SEM) in order to evaluate the bioaccessibility of some divalent metals in aquatic sediments. The AVS is defined as the sulfide that evolved from a sediment after its treatment with diluted HCl, being an operationally defined concept. A large variety of SEM-AVS extraction techniques have been developed employing cold [24, 25] and hot HCl [26], at different concentrations [27]. Nowadays, the U.S. Environmental Protection Agency (US-EPA) and the European Union established sediment quality guidelines in accordance to the SEM-AVS relationship [4, 28], based on the method described by Allen et al. (1991). Sediment samples are covered with 1 mol L^{-1} HCl and heated until all H_2S is expelled by boiling, which is collected as ZnS in a Zn acetate trap and analyzed by re-acidification of the ZnS. SEM are determined in the sediment suspension after the generation of the sulfides (after filtration through a 0.2 µm membrane filter).

Metal concentrations can be determined by atomic absorption spectrometry, inductively coupled plasma spectrometry, or other approved method. Besides, different methods for sulfide determination have been suggested; namely, gravimetric [29], ion-specific electrochemistry [30] and spectrophotometric [31]. Hammerschmidt and Burton [32] verified the irreproducibility of the results among laboratories for both parameters using an interlaboratory study, highlighting the need for improved quality control and standarization of the methods to determine SEM and AVS in sediments.

The SEM-AVS criterion for the assessment of the ecological risk associated with trace metals in sediments is based on the fact that the dissolved metal concentration in sediment pore water is controlled by the molar ratio between the fraction of reactive metals (SEM) and the sulfide (measured as AVS) [4]. If the AVS concentration in sediments exceeds that of the SEM, no adverse biological effects are expected. Conversely, a molar ratio greater than 1 means that unbound metals have more potential to be much more available than those bound to sulfides [33]. It is worth noting that not all sediments with a *SEM/AVS* ratio > 1 can cause toxicity because other metal-binding phases (particulate organic matter and amorphous Fe/Mn oxohydroxides) are present in sediments.

The aim of this study is twofold. First, to propose a fast and reliable procedure to assess the bioaccessible SEM fraction of Cd, Cu, Cr, Ni, Pb and Zn leached by diluted HCl (1 mol L^{-1}) in marine sediments. Second, to show that AVS can be evaluated fast by comparing the sulphur contents in both the solid residue and the original sample. To account for the first objective, magnetic agitation was compared with ultrasonic stirring (using both a bath and a probe). The metals were quantified by inductively coupled plasma-mass spectrometry (ICP-MS). The fraction leached was correlated with the sum of the 3-step sequential extraction procedure of the SM&T using the BCR 701 sediment (encompassing the exchangeable, reducible and oxidisable fractions) to validate the method. In addition, two reference sediments whose total metallic content were certified were also employed. As a practical case study, sediments from two economically relevant Galician Rias (Rias of Arousa and Vigo, NW of Spain), were analysed and toxicologically evaluated using the SEM-AVS criterion.

3. Materials and methods

3.1. Instruments

Magnetic stirring was performed using a Multipoint Magnetic Stirrer system model ANM-10112, 50 Hz frequency (Science Basic Solution, Barcelona, Spain) allowing the treatment of twelve 50 mL glass beakers simultaneously. A 3000513 Selecta ultrasounds bath, 360 W and 50/60 Hz (Selecta, Barcelona, Spain) and a VC 50-1 sonicator probe, 50 W and 20 KHz, equipped with a CV 18 titanium probe (Sonic Materials, Newtown, CT, USA) were utilized. The leachates were filtered through 0.45 µm, 30 mm diameter nylon syringe filters

(Thermo Scientific, Tennessee, USA). A XSERIES 2 Quadrupole ICP-MS (Thermo Scientific, Bremen, Germany) was employed for metal determination. It was equipped with a collision/kinetic energy discrimination cell (CC/KED), an ASX-520 autosampler (CETAC Technologies, USA), standard Ni-cones, Meinhard nebuliser and a Scout double pass spray chamber refrigerated at 4 °C. An EA 1112 Thermo Finnigan Flash analyser was employed for elemental sulphur measurements.

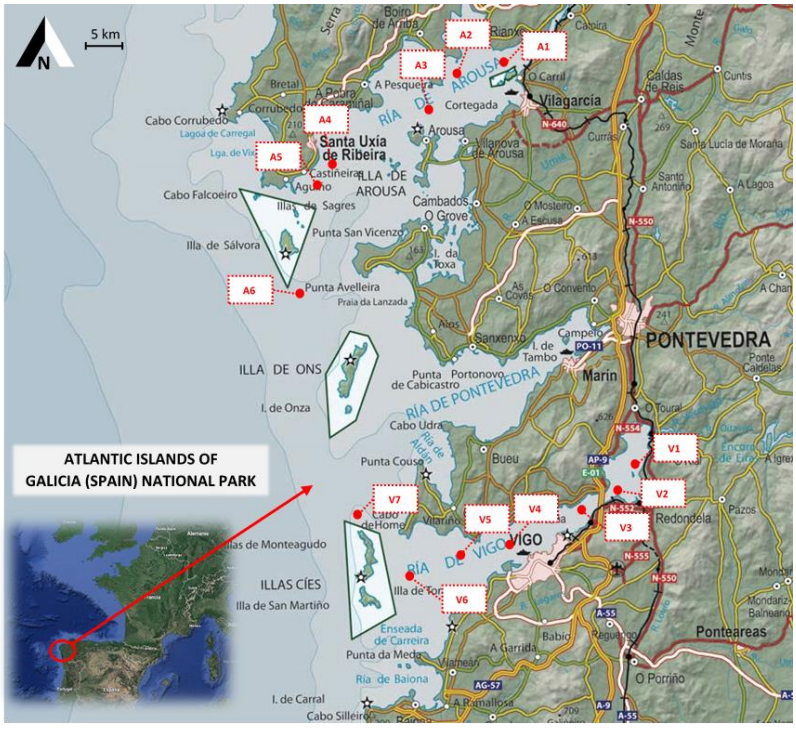

Figure 1. Location map showing the sediment sampling points at the Arousa (A1-A6) and Vigo (V1-V7) Rias (Galicia, Northwest of Spain).

3.2. Reagents and samples

All chemicals were of reagent grade and high-purity water of 18 MΩ · cm resistivity, obtained from a Milli-Q purification device (Millipore Co., Bedford, MA, USA) was used throughout. Suprapur quality hydrochloric acid (37 %) was employed (J.T. Baker, Phillipsburg, NJ, USA). Standard solutions (1000 g L^{-1}) for ICP analysis of Cd, Cu, Cr, Ni, Pb and Zn (SCP Science, Courtaboeuf,

France) were utilized; working standard solutions were prepared daily by diluting appropriate aliquots of the commercial solutions and acidified with HCl. Certified reference sediments were: Lake sediment BCR 701 (Institute for Reference Materials and Measurements, Belgium); New York/New Jersey waterway sediment SRM 1944 (National Institute of Standards & Technology, USA); harbour sediment PACS-2 and marine sediment BCSS-1 (both from National Research Council of Canada). All glassware and plasticware were soaked in 10 % (v/v) nitric acid for 24 h and rinsed with high-purity water at least three times before use.

The samples from the Rias of Arousa and Vigo were provided by the Spanish Institute of Oceanography (IEO). They were sampled in 2011 at the locations shown in Figure 1.

3.3. Single-step lixiviation procedures

Three methods based on HCl-single lixiviation were assayed using magnetic stirring and ultrasonic agitation (a bath and a probe). For the first, "magnetic stirring-assisted extraction" procedure (MSEP), 0.250 g aliquots of sediment were accurately weighed directly in a glass beaker (50 mL) and, then, 10 mL of 1 mol L^{-1} HCl were added. Agitation times varied from 20 min to 4 hours. Up to twelve samples were treated simultaneously. For the second, "ultrasound bath assisted extraction" procedure (UBEP), 0.250 g of sediment were weighted into glass test tubes (20 mL), 10 mL of 1 mol L^{-1} HCl were added and, then, a rack with 12 tubes was introduced into the ultrasound bath (refrigerated with tap water), for 5 to 20 min. After that, the suspensions were filtered and stored in polyethylene bottles at 4 °C until their analysis. Blanks were obtained following the whole procedure.

For the third, the "ultrasound probe assisted extraction" procedure (UPEP), 0.025 g aliquots of sediments were weighted directly into polyethylene cups (1.2 mL) and 1 mL of 1 mol L^{-1} HCl was added. The cups were closed, the Ti probe was introduced through a cap hole and the suspensions were sonicated at 40 % power (maximum 50 W) for 0.5 to 20 min. The supernatant was filtered and the extracts were stored in polyethylene cups at 4 °C until analysis. Blanks were prepared in the same manner.

All procedures were tested with the 3-step BCR-701 certified reference sediment. The method selected finally was applied also to analyze two additional reference marine sediments (with certified total metal contents): SRM-1944 and PACS-2. In addition, the 3052 USEPA method [34] was used to determine the total metal contents of the BCR-701 sediment, which had not been reported in the certificate.

3.4. Acid Volatile Sulfides procedure

The content of acid volatile sulfides in sediment samples was indirectly estimated as the difference between total sulphur and non-volatile sulphur. Total sulphur was measured directly in an aliquot of lyophilized sediments whereas non-volatile sulphur was determined using the solid residue obtained after the HCl-lixiviation, drying it at 40 °C during 48 h. Both sulphur determinations were performed on a EA 1112 Thermo Finnigan Flash analyser (2 mg aliquots). The method was validated using certified reference sediments (BCSS-1, PACS-1 and PACS-2 from NRCC).

3.5. ICP-MS measurements

The following atomic masses were selected for quantification by ICP-MS: ^{52}Cr, ^{60}Ni, 65Cu, ^{66}Zn, ^{111}Cd and ^{208}Pb. Aqueous standards were prepared in the 0 - 2000 µg L^{-1} range, except for Cd and Ni which ranged from 0 to 200 µg L^{-1}. The internal standards were: ^{45}Sc for Cr, Cu and Zn; ^{72}Ge for Ni; ^{103}Rh for Cd; and ^{209}Bi for Pb. Under these conditions, straight linear relationships were obtained throughout the working range of concentrations. The operating conditions of the ICP-MS spectrometer are given in Table 1. The extracts of the samples were diluted (to 4 mL) for analysis.

Table 1. Instrumental parameters used for metal determination in sediments by ICP-MS after 1 mol L^{-1} HCl acid extraction.

ICP source settings	
Power	1.35 kW
Nebulizer gas flow	0.75 L min^{-1}
Auxiliary gas flow	1.00 L min^{-1}
Cooling gas flow	14 L min^{-1}
Pneumatic nebulization	Meinhard 1 mL min^{-1}
Spray chamber	Scout double pass, refrigerated at 4°C
ICP measurements	
Measurement mode	Scan
Detection mode	Dual
Measurement time	3s/isotope

4. Results and discussion

4.1. Single-step extraction procedure

Agitation of the slurry (sediment plus diluted acid) favors the lixiviation of the available metals, reducing the extraction time. Here, magnetic and ultrasonic agitation (bath and probe) were compared. For magnetic and ultrasonic bath, the times assayed were 20 min, 1 h, 2 h, 3 h and 4 h; and for ultrasonic probe agitation they were 0.5, 2, 4, 8 and 12 min. All assays were quadruplicated. The results were evaluated as recoveries, referred to the sum of the 3-step SM&T sequential extraction procedure, as the latter may represent the so-called mobilizable fraction of the metals [17, 35].

The effects of the type and time of agitation on the extraction efficiency were evaluated by two-way ANOVA. The results revealed (comparing the experimental F-value to $F_{95\%,6,6} = 4.28$) that both factors and their interactions were significant, except for the type of agitation for Cu. Both MSEP and UBEP methods leaded to quantitative recoveries after 1 h and 4 h, respectively, for Cd (92-97 %), Cu (96-98 %), Pb (97-98 %) and Zn (79-80 %). However, both methods

yielded low recoveries for Cr (50 %) and moderate ones for Ni and Zn (80 %) at the longest time (4 h). On the contrary, UPEP provided recoveries around 70 % for Cr, 103 % for Ni and 85 % for Zn, after only 12 min and around 100 % for Cu and Pb. For Cd a slightly low 80 % was obtained, although similar to other reports [20, 32]. In all cases, good precisions were obtained (< 8 % RSD).

Following, the ultrasound probe assisted extraction procedure (UPEP) was selected because it provided the best recoveries for the studied metals, approaching to the sum of the SM&T 3-step sequential procedure, and allowed for a significant reduction of the extraction time (from 4 h to 12 min). The ultrasonic energy entails particle size reduction, accelerates chemical reactions and increases the interface between the sample matrix and the extraction reagent [36]. Furthermore, the amount of reagents is minimized because only 1 mL of diluted HCl is required. To improve the recoveries for Cd, Cr and Zn the agitation time and the sample mass were optimized univariately. Agitation was studied submitting four 0.025 g aliquots of the BCR 701 sediment to each time level. For Cu, Ni and Pb extraction reached almost 100 % when agitating for 12 min. Zn required 16 min to get a 90 % recovery and Cr reached an 80 % almost constant value from 16 min. For Cd, an approximately 80 % constant recovery was obtained. Finally, a 16 min agitation time was selected seeking for a compromise for all studied metals.

Weights from 0.010 to 0.100 g were assayed to ascertain the applicability of the UPEP procedure to different metal concentration levels. Each level was tested four times. It was concluded that masses in the 0.025 – 0.10 g range yielded best recoveries, but for Cr, which showed better results for 0.025 g. Hence, this value was selected.

4.2. Suitability of the UPEP method to assess metal bioaccessibility

Diluted HCl has been widely used to determine the available or mobilizable metallic fraction in sediments but its validation is cumbersome because no certified reference materials exist for this purpose [23]. In this work an indirect strategy using the BCR 701 sediment (certified for the SM&T 3-step sequential extraction procedure) was undertaken. It consists on comparing the metallic content determined by the UPEP method with the sum of the exchangeable, reducible and oxidisable SM&T fractions, as they can represent

the so-called bioaccessible fraction of these elements, as proposed elsewhere [17, 35]. Thus, Table 2 presents the results obtained for the analysis of six aliquots of the BCR 701 reference sediment, measured by triplicate. The recoveries were calculated as the ratio between the bioaccessible content obtained using the UPEP method and the sum of the 3-step sequential BCR fractions. They were within acceptable limits for all elements (81-113 %). The lowest value (81 %) occurred for Cr; probably because it is strongly retained in the siliceous matrix of the sediment.

Table 2. Bioaccessible metallic contents obtained by UPEP method for the BCR 701 certified sediment. The recoveries were calculated as the ratio between the bioaccessible content and the sum of the certified 3-step sequential BCR fractions.

Element	Sum 3-steps BCR Certified content	Bioaccessible content	Recovery (%)
	($\mu g\ g^{-1}$ dry weight, ± *U**)		
Cd	11.34 ± 0.45	9.3 ± 0.4	82
Cr	191 ± 7	155 ± 15	81
Cu	228 ± 5	232 ± 8	101
Ni	57.3 ± 1.8	63 ± 7	110
Pb	138 ± 4	156 ± 9	113
Zn	365 ± 9	327 ± 15	90

**U*, expanded uncertainty. The coverage factor, *k*, is the Student's t-value for a 95 % confidence interval with 6 degrees of freedom.

Previous works evaluated also the effectiveness of the HCl partial extraction, although without using a reference sediment with the labile fractions certificated [20, 23]. Previous studies suggested that the application of weak acid extractions to reference sediments (with certified total metal contents) should be a routine quality control measurement for any laboratory analyzing marine sediments [23]. For comparison, in this work SRM 1944 and PACS-2 sediments were submitted to the UPEP method. Table 3 and Figure 2 summarize the extraction efficiencies, expressed as a percentage of the total certified metal concentration. Results for sediment BCR 701 are also included (total content

obtained by the USEPA 3052 method, microwave assisted digestion of siliceous matrices). For the three CRMs, similar extraction efficiencies were got for Cd (80 %) and Zn (74 %). Regarding Cr and Ni, very similar values were registered for SRM 1944 and BCR 701, 48% and 97% respectively; while for PACS-2 very low recoveries (< 25 %) were obtained. Different recoveries were achieved for Cu (65-99 %) and Pb (51-77 %). This variability can be attributed to the different parent material of the sediments and it can be stated that the metals typically related to anthropogenic sources (Cd, Pb, Cu and Zn) showed extraction efficiencies >50 %, even reaching 100 % in some cases. The most refractory metal among the studied ones, Cr, presented the lowest recoveries, with large variability as well, from 15 % to 49 %. From these results, the relevance of considering the nature of the sediment plus their origin is clear when it comes to studying the bioavailability of a metal in marine ecosystems [22, 23].

In order to screen further the UPEP method, the results obtained for PACS-2 and SRM 1644 were compared with those reported in literature (Figure 2). UPEP yielded similar results to those presented by Townsend et al. [23] and Larner et al. [20] for PACS-2. Recoveries for Cd, Pb and Zn were practically the same than for those references. Slightly low values were attained for Cd, Pb and Zn using UPEP. In those previous works, a 1 mol L^{-1} HCl partial extraction was accomplished during 4 h on an orbital shaker at room temperature. In addition, Larner et al. [20] found a strong correlation between the partial extraction and the sum of the three labile steps of the modified BCR sequential extraction procedure, although they did not analyze a sediment with these fracctions certified, like the BCR 701. Choi et al. [22] used the same approach as Townsend et al. [23] for PACS-2, although their results were not included in Figure 2 because the way in which the extraction efficiency was calculated was not indicated and they reported too high extraction efficiencies for all elements.

Regarding sediment SRM 1644, Figure 2 shows the same relative extractability for Townsend et al. [23] and UPEP (Cd ~ Pb > Zn ~ Cu > Ni > Cr), although the values reported for the metals (but for Cd) are slightly lower for Duzgoren-Aydin et al. [37], likely because they used a more diluted acid than UPEP (0.5 mol L^{-1} HCl at room temperature agitating with a shaking-table for 1 h). For Cd they obtained a 107 % recovery, although with low reproducibility because they reported 74 % recovery for the SRM 2702 marine sediment.

Therefore, the results presented in Tables 2 and 3 and Figure 2 indicate that the BCR-701 sediment seems an optimum candidate for method validation of bioaccessibility studies because its metallic concentrations are certificated for the three fractions corresponding to the modified BCR sequential extraction procedure. To the best of our knowledge no previous papers considered this CRM to validate HCl extraction methods.

Table 3. Bioaccessible metallic fractions in PACS-2, SRM-1944 and BCR 701 certified sediments obtained by UPEP (μg g^{-1} dry weight, ± U*). Extraction efficiency values are presented for each CRM (referred to the certified content; for BCR 701 to the total content of each metal obtained by the 3052 EPA method).

Metal	PACS-2			SRM-1944			BCR-701		
	Certified	Bioaccessible	Extraction (%)	Certified	Bioaccessible	Extraction (%)	3052 EPA method	Bioaccessible	Extraction (%)
Cd	2.1 ± 0.1	1.6 ± 0.1	77	8.8 ± 1.4	7.3 ± 0.4	82	11.3 ± 0.3	9.3 ± 0.4	82
Cr	91 ± 5	14 ± 1	15	266 ± 24	131 ± 8	49	329 ± 17	155 ± 15	47
Cu	312 ± 12	201 ± 8	65	380 ± 40	287 ± 20	76	235 ± 10	232 ± 8	99
Ni	39 ± 2	9.6 ± 0.7	24	76.1 ± 5.6	39 ± 3	51	97 ± 3	63 ± 7	65
Pb	183 ± 8	141 ± 7	77	330 ± 48	303 ± 28	92	153 ± 3	156 ± 9	102
Zn	364 ± 23	255 ± 13	70	(656 ± 75)	538 ± 48	82	469 ± 19	327± 15	70

*U, expanded uncertainty. The coverage factor, k, is the Student's t-value for a 95 % confidence interval with 6 degrees of freedom.

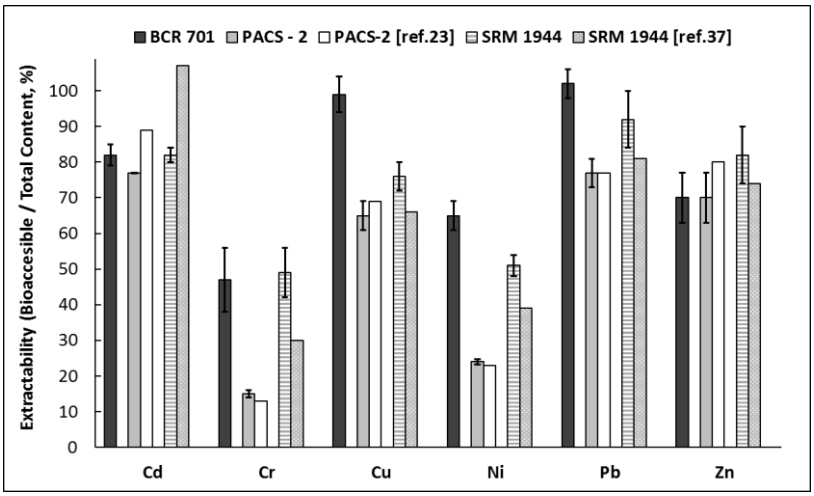

Figure 2. Extractability of the bioaccessible metallic fraction (dilute-cold HCl) for several certified reference sediments, expressed as recoveries of their total certified contents (for BCR 701, the total content was obtained by the 3052 EPA method). The error bars correspond to uncertainty. See text for details.

4.3. Performance characteristics

Once the extraction of the metallic labile fraction was validated, the quantitation methodology has to be evaluated as well. For ICP-MS, the linearity (straight line behavior) of the response was evaluated for each metal. For Cd and Ni good linearity was achieved up to 200 ng mL^{-1} while for Cr, Cu and Pb that extended up to 2000 ng mL^{-1}. The direct calibration and the standard addition methods were evaluated. In all cases, the slopes did not differ at a 95 % confidence level, allowing for the direct aqueous calibration quantitation.

The classical instrumental limits of detection (LOD = 3SD/m) and quantitation (LOQ = 10SD/m) were determined from 10 replicates of reagent blanks in different days. The average slope of at least six calibration curves was used. The method-LOD and method-LOQ were calculated from 10 procedural blanks, prepared and analysed in different days. Good performance characteristics were obtained (Table 4) thanks to the scarce dilution of the samples required by the UPEP method. These limits are more sensitive than others reported (e.g., [37]).

Table 4. Instrumental and method limits of detection (LOD) and quantitation (LOQ) (n = 10).

Element	Instrumental (µg L^{-1})		Method (µg g^{-1})	
	LOD	**LOQ**	**LOD**	**LOQ**
Cd	0.01	0.03	0.008	0.02
Cr	0.20	0.68	0.05	0.16
Cu	0.04	0.15	0.01	0.03
Ni	0.04	0.12	0.01	0.03
Pb	0.08	0.26	0.02	0.07
Zn	0.22	0.73	0.05	0.18

Good repeatability (< 2.5 %, RSD) was achieved when aqueous standard solutions were analysed six times at two concentration levels (100 and 1000 µg L^{-1} for Zn, Cr, Cu and Pb; 10 and 100 µg L^{-1} for Cd and Ni). Satisfactory precision was also attained for extracts of BCR 701 analysed the same day (< 5.7 % RSD, n = 6). The overall procedural precision was obtained by extracting BCR 701 aliquots in different days and analyzing them in triplicate (n = 6x3). The intra- and inter-day variations were in the range 3.6 % - 5.6 % for Zn, Cd, Cu and Pb and around 10 % for Cr and Ni. Such values compare satisfactorily with literature, as they are similar [37] or lower than previous reports with analogous methodologies [17]. Therefore, the proposed UPEP method provides highly reproducible results.

4.4. Indirect method for Acid Volatile Sulfides

Our second objective was to establish a simple procedure to assess AVS without the need for generating volatile sulphur, and taking advantage of the fact that the method to study the bioaccessible metallic fraction developed previously involves an acid treatment of the sediment. Two reference sediments with different certified total sulphur contents, BCSS-1 (0.36 ± 0.05) % S and PACS-2 (1.29 ± 0.13) % S, were employed. First, six aliquots of each CRM were analysed to determine their total sulphur content. The results obtained, expressed as mean value plus their expanded uncertainty (applying as coverage factor the Student's *t-value* for a 95 % confidence level), were (0.32 ± 0.01) % S for BCSS-1 and (1.19 ± 0.06) % S for PACS-2. Good agreement between the certified contents and the experimental values was achieved. Satisfactory repeatability (RSD < 3 %) and reproducibility were also attained (RSD < 5%). Next, six aliquots of each CRM were analysed by the UPEP procedure and the residue remaining after extraction was analysed to determine its sulphur content. The non-volatile sulphur fractions were (0.16 ± 0.02) % S for BCSS-1 and (0.89 ± 0.01) % S for PACS-2.

In general, large variability among laboratories is found for this parameter because there are neither certified aqueous standards for sulfides nor reference materials for *AVS/SEM* in sediments [32]. RSDs lower than 10 % were reported for AVS [26]. In our study, the reproducibility was very different

for the two CRMs: 12 % and 1 % for BCSS-1 and PACS- 2, likely because the amount of non-volatile sulfides of BCSS-1 is six times lower than for PACS-2.

Now, to estimate the volatile sulphur fraction in the sediments, the difference between the total sulphur and that present in the residue is calculated. The values (mean value plus expanded uncertainty) were (0.16 ± 0.02) % S for BCSS-1 and (0.40 ± 0.06) % S for PACS-2.

4.5. Application to a case-study

The ultrasonic probe extraction procedure (UPEP) was applied to determine the potentially bioaccessible fraction of Cd, Cr, Cu, Ni, Pb and Zn in several sediments collected in two economically relevant Galician estuaries (Northwest Spain), namely the Rias of Arousa and Vigo (Figure 1). The Galician Rias were defined [38] as incised valleys where the estuarine zone can fluctuate according to climatic changes. These sites are particularly suitable for evaluation of coastal contamination because they are being subjected to increasingly dense population as well as industrial and aquaculture activities [39].

Table 5 summarizes the results obtained. The sediments from the inner part of both rias showed higher metallic contents than those sampled at the mouth of the estuary. Very few historical data on HCl extracted metals in these two rias were found. Thus, Real et al. [40] found abnormally high extractable concentrations for Cr and Cu in the upper area of the Ria of Arousa, likely derived from effluent discharges to the Ulla River (mainly, a tanning factory effluent and an old copper mine). They reported high values of Cr (from 84 μg g^{-1} to 252 μg g^{-1}) in the lower estuary. We found out that the bioaccessible fraction of Cr was much lower for this area (3 μg g^{-1} to 52 μg g^{-1}). This is explained by the time elapsed between both studies, about 20 years, during which the main contamination sources ceased their activities and the enforcement of environmental protection regulations.

Table 5. Bioaccessible metallic fractions in sediments of the Rias of Arousa (A1-A6) and Vigo (V1-V7) obtained by UPEP method (μg g^{-1} dry weight, ± 1SD; *n*=3).

Sample	Cd	Cr	Cu	Ni	Pb	Zn
A1	0.23 ± 0.01	19.2 ± 1.9	11.5 ± 0.2	6.0 ± 0.5	38.9 ± 1.4	30.9 ± 1.2
A2	0.09 ± 0.01	52.2 ± 2.9	19.9 ± 0.5	9.8 ± 1.0	36.0 ± 1.7	42.0 ± 2.4
A3	< LOQ	22.6 ± 1.8	7.1 ± 0.7	8.4 ± 0.6	31.1 ± 2.3	29.6 ± 3.2
A4	< LOQ	15.7 ± 0.4	5.6 ± 0.1	7.2 ± 0.2	32.3 ± 1.4	25.7 ± 9.8
A5	< LOQ	10.7 ± 0.8	4.8 ± 0.2	5.9 ± 0.3	27.9 ± 1.0	21.1 ± 1.6
A6	< LOQ	3.3 ± 0.4	< LOQ	1.2 ± 0.1	9.3 ± 0.4	7.7 ± 1.0
V1	0.23 ± 0.02	6.7 ± 0.1	13.7 ± 0.3	3.97 ± 0.01	68.8 ± 0.9	48.0 ± 2.3
V2	0.15 ± 0.02	9.3 ± 0.3	16.4 ± 0.3	4.5 ± 0.1	62.8 ± 1.3	111 ± 16
V3	0.14 ± 0.01	12.3 ± 0.7	20.4 ± 1.3	5.7 ± 0.4	75.3 ± 1.0	103 ± 17
V4	0.09 ± 0.03	9.4 ± 1.1	13.4 ± 0.5	6.03 ± 0.5	63.6 ± 0.7	53.9 ± 4.5
V5	0.10 ± 0.04	9.7 ± 0.6	14.6 ± 0.6	4.8 ± 0.2	58.8 ± 5.8	51.1 ± 4.8
V6	< LOQ	8.6 ± 0.6	4.0 ± 0.1	5.7 ± 0.4	23.2 ± 2.4	28.3 ± 1.1
V7	< LOQ	9.3 ± 1.5	7.0 ± 0.4	5.9 ± 1.4	36.9 ± 1.0	32.2 ± 1.7

**LOQ: 0.008 μg g^{-1} for Cd; 0.03 μg g^{-1} for Cu.*

Regarding the Ria of Vigo, the distribution pattern of the metals reflects the anthropogenic discharges it receives. The highest values were found for Pb and Zn (75 and 111 μg g^{-1}, respectively) in the vicinity of the harbour of Vigo and the brigde of Rande. This is in accordance with the list of contaminating metals proposed by Prego and Cobelo-Garcia (2003) for this ria for the total fraction [39]. The labile fraction corresponding only to the first step of the 3-step SM&T protocol (fraction exchangeable and carbonates phases, determined by 0.11 mol L^{-1} acetic acid) had been reported for Cd, Cu, Ni, Fe, V and Zn [41]. Surprisingly, they presented values for Zn (50 μg g^{-1} - 929 μg g^{-1}) higher than those found in the present work (30 μg g^{-1} - 111 μg g^{-1}). Their highest values correspond to locations near the shipyards and docks which may explain their values because Zn is widely used to prevent corrosion of the ship hulls. All sampling sites considered here were far from direct contamination focus (i.e., sewers, harbours) that could affect the results. With respect to copper, they

obtained a much lower extractability than that corresponding to the first fraction of the BCR 701 certificated sediment (21 %).

Rubio et al [42] stressed the difficulty in assessing the degree of metal contamination in estuarine and marine sediments due to variations in analytical procedures and the unknown natural background. Different solutions have been proposed to circumvent this. In particular, when a simultaneous extraction of metals is applied as an indirect estimate of metal toxicity to aquatic life, the *SEM-AVS* criterion should be considered. US-EPA presented two alternatives depending on the availability or the absence of organic carbon data [4]. The latter is used here, which establishes three levels of toxicity depending on whether SEM is lower or higher than AVS. Tier 1 is declared when the subtraction *SEM-AVS* > 5, likely risk of toxicity to aquatic life; Tier 2 corresponds to values between 0 and 5, possible adverse effects on aquatic life, and Tier 3 is considered when the subtraction < 0, no indication of adverse effects.

Figure 3 shows the results obtained for SEM, calculated as the sum of the acid extractable fractions for Cd, Cu, Pb, Ni and Zn, and for AVS, both expressed in μmol g^{-1} [32]. The SEM content is higher in the Vigo estuary than in the ria of Arousa, which agrees with the higher industrial activity around the harbour of Vigo. In both rias, inner sediments exhibited higher SEM values than outer ones, as expected [43]. When examining the individual contributions of each metal to SEMs, different conclusions were derived for each ria. Cr, Pb and Zn represented the main contribution (around 30 %) in the ria of Arousa, whereas Cu and Ni contributed less than 10 %, each. For Vigo, Pb and Zn accounted for 40-50 % of the SEMs, whereas Cr, Cu and Ni participated less than 10 %. These results are in accordance with the pollution patterns associated to each ria [39, 43, 44].

The AVS values showed the same behaviour than the SEM ones (Figure 3). For both parameters, a positive correlation with organic matter was observed, whose values decreased from the inner to outer zones. For both rias, the maximum values of organic matter were reported in the central axis and in the internal parts, linked to important build-ups of muddy sediments (10-14%). Towards the outer areas, the organic matter values do not exceed 4% [45].

When the SEM-AVS subtraction was calculated, values lower than 0 were obtained, indicating that there is little or no risk to aquatic life derived from the studied metals in these sediments.

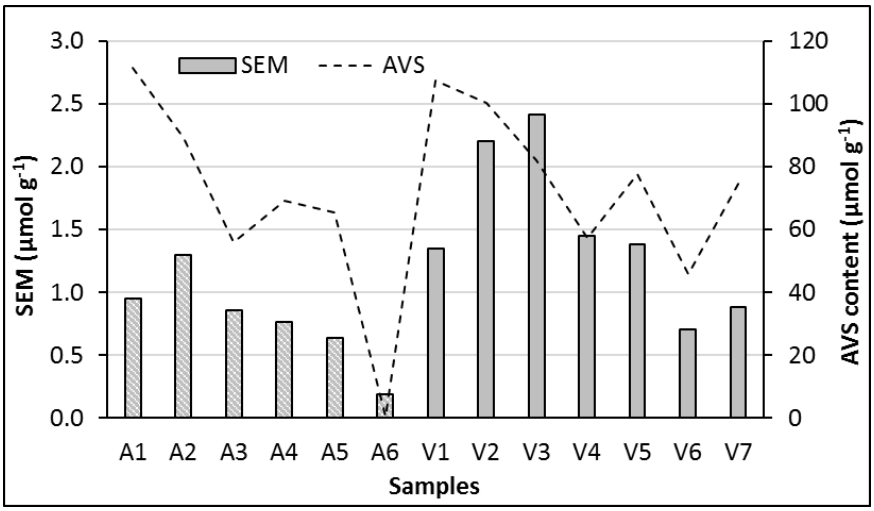

Figure 3. SEM and AVS values obtained for the sediments of the Rias of Arousa (A) and Vigo (V).

The total metal contents were determined latter. The levels obtained for Cr, Cu, Pb and Zn in some samples from the inner part of the rias exceeded the background levels reported for Galician Rias [46], whereas the samples from the outer and middle parts of the rias showed values comparable to those backgrounds. In general, the concentrations obtained in our study were similar or even lower than those compiled by Prego and Cobelo-García (2003) for total metal contents in surface sediments of Galician Rias [39]. However, these authors highlighted the necessity to treat every Galician ria separately to establish their background levels due to their different lithological characteristics.

Figure 4 shows the percentage of bioaccessible metallic fraction of the samples (with respect to their total content). A similar behavior was observed in all sediments for Cd, Cu and Pb, with 80 % - 100 % recoveries, and for Ni (25 % recovery). For Cd, this term could not be calculated for samples with contents lower than its LOQ. For Zn, a higher extractability of the labile fraction was

obtained for Vigo (40 % - 95 %) compared to Arousa (25 % – 45 %), although in both rias these values increase close to anthropogenic sources of metallic discharges (harbor, Rande Bridge, etc.). Regarding Cr, sediments from the inner part of the Ria of Arousa presented the highest extractability, 45 %, whereas the sediments of the outer zone have values around 30 %. Extractability was only 20 % for almost all sediments of the ria of Vigo, all of them with low Cr concentrations.

All these facts allow us to conclude that the metallic bioaccessible fraction depends on the characteristics of the element, the nature of the sediments as well as on the proximity to pollution spots, and their kind. In addition, this fraction will be high when the anthropogenic contribution to the total metal content in the sediment is significant because metals from anthropogenic sources are more easily extractable for the aquatic environment than those embedded in the very matrix of the sediments. Therefore, it can be affirmed that the total content of metals in sediments is not enough to evaluate whether metals are indeed contaminating these ecosystems, and their potential risks.

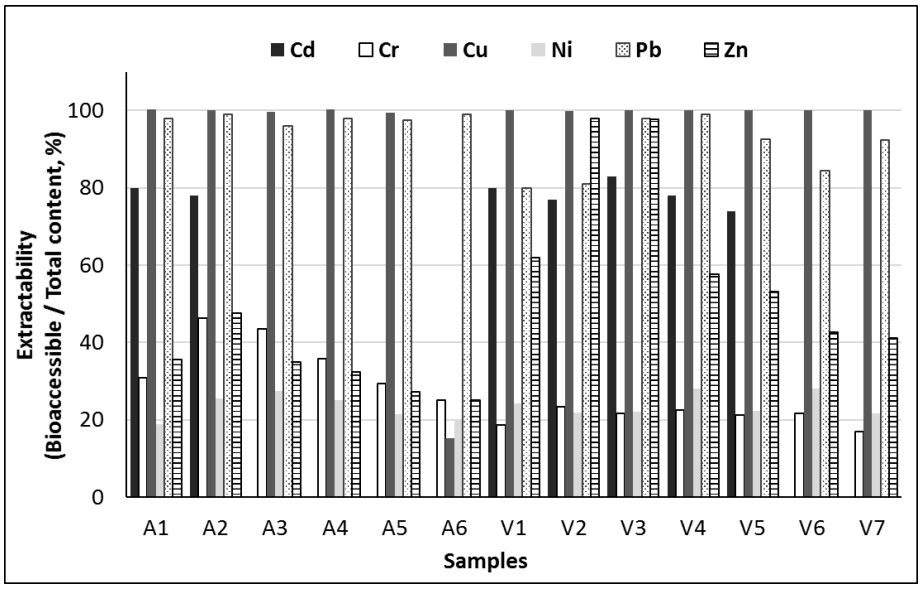

Figure 4. Extractability of the bioaccessible metallic fraction (dilute-cold HCl) for the sediments of the Rias of Arousa (A) and Vigo (V), expressed as recoveries of their total content (obtained by the 3052 EPA method).

5. Conclusions

This work presents a one-step, simple and quick method to estimate the bioaccessible metallic fraction in sediments. In addition, an indirect method to estimate the content of AVS was proposed. Both procedures follow the green analytical chemistry philosophy, minimizing time, reagents consumption, wastes and avoiding risks. The performance characteristics indicate that this methodology can be applied as a screening approach in environmental studies to calculate the SEM-AVS relation as a reliable criterion to evaluate if further investigations are required. The sum of the contents of the 3-steps of the SM&T procedure for the BCR 701 certified sediment revealed as an adequate validation approach for the proposed procedure. For the practical case study considered, sediment samples from the Rias of Arousa and Vigo (NW Spain), the *SEM-AVS* values were < 0 in all cases, suggesting that there is little or no risk to aquatic life in the sampled area. A direct association was observed between the highest bioaccessible fractions of Cr and Zn with the anthropogenic inputs in the studied areas.

References

[1] Larner, B.L.; Palmer, A.S.; Seen, A.J.; Townsend, A.T. A comparison of an optimised sequential extraction procedure and dilute acid leaching of elements in anoxic sediments, including the effects of oxidation on sediment metal partitioning. Anal.Chim.Acta, 2008, 608:147-157.

[2] Semple, K.T.; Doick, K.J.; Jones, K.C.; Burauel, P.; Craven, A.; Harms, H. Defining Bioavailability and Bioaccessibility of contaminated Soils and Sediments is Complicated. Environ.Sci.Technol. 2004, 38:228A-231A.

[3] Nordberg, M.; Duffus, J.; Templeton, D.M. Explanatory dictionary of key terms in toxicology: Part II (IUPAC Recommendations 2010). Pure Appl.Chem. 2010, 82:679-751.

[4] Environmental Protection Agency US. Procedures for the derivation of equilibrium partitioning sediment benchmarks (ESBs) for the protection of benthic organisms: metal mixtures (cadmium, copper, lead, nickel, silver and zinc). 2005, Washington (USA), EPA-600-R-02-011.

[5] Parkman, H. Critical reviews of Metals Environmental Risk Assessment Guidance for metals (MERAG). Nordic Council of Ministers, 2007, Copenhagen (Norway).

[6] Tarazona, J.V.; Versonnen, B.; Janssen, C.; De Laender, F.; Vangheluwe, M.; Knight, D. Principles for Environmental Risk Assessment of the Sediment Compartment: Proceeding of the Topical Scientific Workshop. European Chemical Agency, 2014, Helsinki (Finland).

[7] MacDonald, D.D.; Ingersoll, G.C.; Berger, T.A. (2000) Development and Evaluation of Consensus-Based Sediment Quality Guidelines for Freshwater Ecosystems. Arch.Environ.Contam Toxicol. 2000, 39:20-31.

[8] Tornero, V.; Hanke, G. Chemical contaminants entering the marine environment from sea-based sources: A review with a focus on European seas. Mar.Pollut.Bull. 2016, 112:17-38.

[9] Villanueva, U.; Raposo, J.C.; Madariaga, J.M. A new methodological approach to assess the mobility of As, Cd, Co, Cr, Cu, Fe, Ni and Pb in river sediments. Microchem.J. 2013, 106:107-120.

[10] Tessier, A.; Campbell, P.G.C.; Bisson, M. Sequential Extraction Procedure for the Speciation of Particulate Trace-Metals. Anal.Chem. 1979, 51:844-851.

[11] Anju, M.; Banerjee, D.K. Comparison of two sequential extraction procedures for heavy metal partitioning in mine tailings. Chemosphere, 2010, 78:1393-1402.

[12] Rao, C.R.M.; Sahuquillo, A.; López Sánchez, J.F. A review of the different methods applied in environmental geochemistry for single and sequential extraction of trace elements in soils and related materials. Water Air Soil Poll. 2008, 189:291-333.

[13] Bacon, J.; Jeffrey, R.; Davidson, C.M. Is there a future for sequential chemical extraction? Analyst, 2008, 133:25-46.

[14] Quevauviller, P.; Rauret, G.; Muntau, H.; Ure, A.M.; Rubio, R.; López-Sánchez, J.F.; Fielder, H.D.; Griepink, B. Evaluation of a sequential extraction procedure for the determination of extractable trace metal contents in sediments. Fresenius J.Anal.Chem.1994, 349:808-814.

[15] Rauret, G.; López-Sánchez, J.F.; Sahuquillo, A.; Rubio, R.; Davidson, C.M.; Ure, A.M.; Quevauviller, P. Improvement of the BCR three step sequential extraction procedure prior to the certification of new sediment and soil reference materials. J.Environ.Monit. 1999, 1:57-61.

[16] Madrid, F.; Reinoso, R.; Florido, M.C.; Días Barrientos, E.; Ajmone-Marsan, F.; Davidson, C.M.; Madrid, L. Estimating the extractability of potentially toxic metals in urban soils: a comparison of several extracting solutions. Environ.Pollut.2007, 147:713-722.

[17] Sutherland, R.A. Comparison between non-residual Al, Co, Cu, Fe, Mn, Ni, Pb and Zn released by a three-step sequential extraction procedure and a dilute hydrochloric acid leach for soil and road deposited sediment. Appl.Geochem. 2002, 17:353-365.

[18] Hlavay, J.; Prohaska, T.; Weisz, M.; Wenzel, W.W.; Stingeder, G.J. Determination of trace elements bound to soils and sediment fractions (IUPAC technical report). Pure Appl.Chem. 2004, 76:415-442.

[19] Sutherland, R.A.; Tack, F.M.G. Extraction of labile metal from solid media by dilute hydrocholoric acid. Environ.Monit.Assess. 2008, 138:119-130.

[20] Larner, B.L.; Seen, A.J.; Townsend, A.T. Comparative study of optimised BCR sequential extraction scheme and acid leaching of elements in the certified reference material NIST 2711. Anal.Chim.Acta, 2006, 556:444-449.

[21] Snape, I.; Scouller, R.C.; Stark, S.C.; Stark, J.; Riddle, M.J.; Gore, D.B. Characterisation of the dilute HCl extraction method for the identification of metal contamination in Antartic marine sediments. Chemosphere, 2004, 57:491-504.

[22] Choi, K.Y.; Kim, S.H.; Chon, H.T. Relationship between total concentration and dilute HCl extraction of heavy metals in sediments of Korea. Environ.Geochem.Health, 2012, 34:243-250.

[23] Townsend, A.T.; Palmer, A.S.; Stark, S.C.; Samson, C.; Scouller, R.C.; Snape, I. Trace metal characterisation of marine sediment reference material MESS-3 and PACS-2 in dilute HCl extracts. Mar.Pollut.Bull. 2007, 54:236-239.

[24] Brumbaugh, W.G.; Arms, J.W. (1996) Quality control considerations for the determination of acid-volatile sulfide and simultaneously extracted metals in sediments. Environ.Toxicol.Chem. 1996, 15:282-285.

[25] Machado, W.; Carvalho, M.F.; Santelli, R.E.; Maddock, J.E.L. Reactive sulfides relationship with metals in sediments from a eutrophicated estuary in Southeast Brazil. Mar.Pollut.Bull. 2004, 49:89-92.

[26] Zhuang, W.; Gao, X.L. Acid-volatile sulfide and simultaneously extracted metals in surface sediments of the southwestern coastal Laizhou Bay, Bohai Sea: Concentrations, spatial distributions and the indication of heavy metal pollution status. Mar.Pollut.Bull. 2013, 76:128-138.

[27] Rickard, D.; Morse, J.W. Acid volatile sulfide (AVS). Mar.Chem. 2005, 97:141-197.

[28] Environmental Protection Agency US. Analytical method for determination of acid volatile sulfide in sediments. 1991, Washington (USA), EPA-821R-91-100.

[29] Di Toro, D.M.; Mahony, J.H.; Hansen, D.J.; Scott, K.J.; Hicks, M.B.; Mayr, S.M.; Redmond, M. Toxicity of Cadmium in Sediments: The Role of Acid Volatile Sulfides. Environ.Toxicol.Chem. 1990, 9:1487-1502.

[30] Leonard, E.N.; Cotter, A.M.; Ankley, G.T. Modified diffusion method for analysis of acid volatile sulfides and simultaneously extracted metals in freshwater sediments. Environ.Toxicol.Chem. 1996, 15:1479-1481.

[31] Silva, M.S.P.; da Silva, I.S.; Abate, G.; Masini, J.C. Spectrophotometric determination of acid volatile sulfide in river sediments by sequential injection analysis exploiting the methylene blue reaction. Talanta, 2001, 53:843-850.

[32] Hammerschmidt, C.R.; Burton Jr., G.A. Measurements of acid volatile sulfide and simultaneously extracted metals are irreproducible among laboratories. Environ.Toxicol.Chem. 2010, 29:1453-1456.

[33] Berry, W.J.; Hansen, D.J.; Mahony, J.D.; Robson, D.L.; Di Toro, D.M.; Shipley, B.P.; Rogers, B.; Corbin, J.M.; Boothman, W.S. Predicting the toxicity of metal-spiked laboratory sediments using acid-volatile sulfide and interstitial water normalizations. Environ.Toxicol.Chem. 1996, 15:2067-2079.

[34] Environmental Protection Agency US. Test methods for evaluating solid waste: Physical/Chemical methods (3rd ed.). 1999, Washington (USA), EPASW-846.3-3a.

[35] Kubová, J.; Matús, P.; Bujdos, M.; Hagarová, I.; Medved, J. Utilization of optimized BCR three-step sequential and dilute HCl single extraction procedures foir soil-plant metal transfer predictions in contaminated lands. Talanta, 2008, 75:1110-1122.

[36] Remeteiová, D.; Ruzicková, S.; Rusnák, R. Ultrasound-assisted extraction in the fractionation analysis of gravitation dust sediments. Microchim.Acta, 2008, 163:257-261.

[37] Duzgoren-Aydin, N.S.; Avula, B.; Willet, K.L.; Khan, I.A. Determination of total and partially extractable solid-bound element concentrations using collision/reaction cell inductively coupled plasma-mass spectrometry and their significance in environmental studies. Environ.Monit.Assess. 2011, 172:51-66.

[38] Evans, G.; Prego, R. Rias, estuaries and incised valleys: is a ria an estuary? Mar.Geol. 2003, 196:171-175.

[39] Prego, R.; Cobelo-García, A. (2003) Twentieth century overview of heavy metals in the Galician Rias (NW Iberian Peninsula). Environ.Pollut. 2003, 121:425-452.

[40] Real, C.; Barreiro, R.; Carballeira, A. Heavy metal mixing behaviour in estuarine sediments in the Ria de Arousa (NW Spain). Differences between metals. Sci.Total Environ. 1993, 128:51-67.

[41] Prego, R.; Filgueiras, A.V.; Santos-Echeandía, J. Temporal and spatial changes of total and labile metal concentration in the surface sediments of the Vigo Ria (NW Iberian Peninsula): Influence of anthropogenic sources. Mar.Pollut.Bull. 2008, 56:1031-1042.

[42] Rubio, B.; Nombela, M.A.; Vilas, F. Geochemistry of major and trace elements in sediments of the Ria de Vigo (NW Spain): an assessment of metal pollution. Mar.Pollut.Bull. 2000, 40:968-980.

[43] Quelle, C.; Besada, V.; Andrade, J.M.; Gutiérrez, N.; Schultze, F.; Gago, J.; González, J.J. Chemometric tools to evaluate the spatial distribution of trace metals in surface sediments of two Spanish rías. Talanta, 2011, 87:197-209.

[44] Besada, V.; Quelle, C.; Andrade, J.M.; Gómez-Carracedo, M.P.; Schultze, F. A 10-year survey of trace metals in sediments using self-organizing maps. J.Chemom. 2014, 28:558-566.

[45] Vilas, F.; Bernabeu, A.M.; Ménde,z G. Sediment distribution pattern in the Rias Baixas (NW Spain): main facies and hydrodynamic dependence. J.Mar.Syst. 2005, 54:261-276.

[46] Carballeira, A.; Carral, E.; Puente, X.; Villares, R. Regional scale monitoring of coastal contamination. Nutrients and heavy metals in estuarine sediments and organisms on the coast of Galicia (Norwest Spain). Intern.J.Environ.Poll. 2000, 13:534-572.

CHAPTER

V

ISOTOPE DILUTION ANALYSIS FOR METAL QUANTIFICATION BY ICP-MS

V.1.

A SIMPLE PROCEDURE TO SELECT A MODEL FOR MASS DISCRIMIANTION CORRECTION IN ISOTOPE DILUTION INDUCTIVELY COUPLED PLASMA MASS SPECTROMETRY

1. Abstract

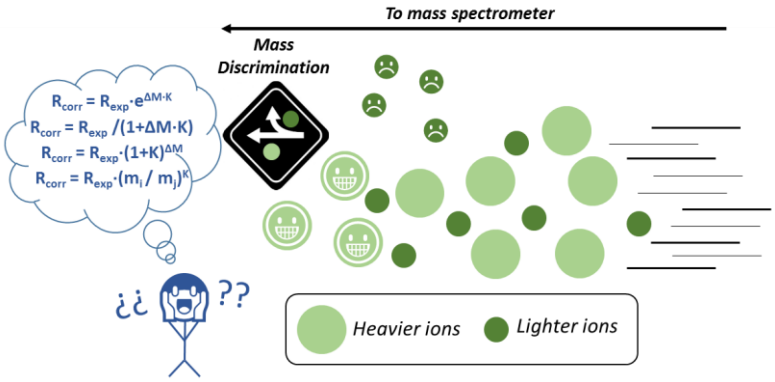

A fast, simple and straightforward procedure to decide on the best model to calculate the mass discrimination factor in Isotope Dilution Inductively Coupled Plasma Mass Spectrometry (ID-ICP-MS) is proposed. It is based on the study of the residuals of the different models that are proposed commonly, *viz.*, the linear, the exponential, the power and Russell's models. However, it can be generalized to evaluate any model proposed to linearize the relationship between the *theoretical/measured* isotope ratios and the mass. The procedure does not involve laboratory extra work, it is rooted on basic statistics associated with the least squares fit, and can be applied easily by the analysts so that decision making is fast and reliable. The procedure was exemplified with four different examples where Cd, Cr, Nd and Sm were determined by ID-ICP-MS.

The results discussed in this chapter are summarized in the scientific publication:

A simple procedure to select a model for mass discrimination correction in isotope dilution inductively coupled plasma mass spectrometry.

J. Terán-Baamonde, J.M. Andrade, R.M. Soto-Ferreiro, A. Carlosena and D. Prada.

Journal of Analytical Atomic Spectrometry, 2015, 30, 1197-1206.

2. Introduction

Isotope dilution inductively coupled plasma mass spectrometry (ID-ICP-MS) has become a work horse technique to quantify metals at trace and ultratrace levels, study their species and, more recently, determine proteins (using either unspecific and species-specific methods) [1-3]. This can be explained, amongst other considerations, because isotope dilution mass spectrometry (ID-MS) was recognized as a definite primary method, meeting the highest metrological standards, by the "Comité Consultative pour la Quantité de Matière (CCQM)" and so its results are directly traceable to SI units [4].

Further, in most ID-MS applications the typical working calibration graphs based on the use of calibration solutions of different quantities of the analyte may be avoided. This saves costly instrument time and makes ID-MS applications much more robust than conventional methodologies so less-careful sample preparation is required. Also, ID-MS procedures are more accurate than conventional methodologies, so that fewer quality-control failures are to be expected [5].

However, adequate training of laboratory staff is required as ID-ICP-MS needs a careful and laborious optimization in order to look for the best measuring conditions that yield a reliable and traceable working chain. A relevant issue here is to recall that a mass discrimination occurs in ICP-MS when ions of different mass are transmitted through the spectrometer, leading to different efficiencies in the transport of ions which results in non-uniform sensitivity across the mass range and inaccurate isotope ratio measurements [6].

Following, ICP-MS devices may yield biased isotope amount ratios [7] and, therefore, mass discrimination must be corrected for using a correction factor, termed mass discrimination factor, *K* (it is often presented, simply, as the "mass bias" or "mass bias factor", or "mass bias factor per unit mass"). This is defined as the quotient between the true and the measured mass ratios for a pair of given isotopes and so it underlines that the instrumental system may yield a systematic error regarding the correct mass ratio [8-10].

It is worth noting that *K* is defined and determined locally for a specific isotope pair. This raises a further potential difficulty as *K* may incorporate contributions from unsuspected spectral interferences which could vary from

sample to sample and, thus, make it unrepresentative of the bias obtained for adjacent masses [6].

In general, two approaches exist to correct for mass discrimination, measured by *K* [11]. First, external standardisation, where the isotope ratio of interest is measured in a standard solution of exactly known composition of the analyte to be analyzed, and the experimental bias is used to correct the same ratio in the unknown sample. This allows the mass discrimination factor to be measured at the same masses as the analyte, and approximately at the same abundances. Second, internal standardisation determines the mass discrimination factor of the isotope ratio of interest in the unknown sample solution by means of either a known isotope ratio of an element added to the sample for that purpose, or using a pair of invariant isotopes of the analyte element [6]. Another relevant issue is that K can drift throughout the experiment time and, thus, it must be determined periodically. A standard bracketing sequence is adopted usually, yielding low throughput [10].

The relative magnitude of mass discrimination can be ascertained using multielemental molar-response curves by which the response observed in the detector is measured as a function of the ion transmission efficiency through the system [5]. In general, these curves have to span through a range of mass/charge values, and are complex and depend on the instrument at hand. To make them useful it is necessary to model them functionally. All models calculate a corrected isotope ratio (R_{corr}) from an experimentally measured one (R_{exp}), the absolute masses of the isotopes (m_i and m_j), or the mass difference between the isotopes (ΔM), and K (the mass bias factor, which must be determined empirically).

Three functions are of general use; *viz.* the linear, the exponential and the power ones. They were criticized somehow by Ingle et al. [6] because they predicted that the bias was dependent on the mass difference and not on the absolute mass. Besides, they have a common origin and the former two may be considered as approximations to the power model [6, 12]. Further, in these functions K should be considered as the mass bias per unit mass and it is assumed to be constant across the mass range and proportional, which is not totally correct [6]. This explains why Russell's model became popular because it avoids these problems as it uses the mass of the two isotopes.

Even though the models might yield similar mass bias factors, inaccuracy may arise from the use of an inappropriate one [13]. Accordingly, the selection of the most suitable functional model is not trivial. Indeed, calculating the mass bias factor is far from a standardized procedure and is demonstrated by the existence of several approaches. Some can be mentioned here (a complete review is out of the scope of this technical note). *K* was determined as the ratio between the theoretical, or true, isotope ratio and the same ratio measured experimentally [8]. Then, *K* can be applied using either a bracketing approach or a mathematical model [4, 6, 14]. The use of several internal reference isotope pairs was compared against the classical approaches mentioned above [11]. This implied the use of a polynomial function and the so-called "common analyte internal standardization". The results emphasized the importance of a proper mass discrimination correction (along with the need for a selection of an adequate internal standard).

To complicate things further, the reasons why a model was selected have not always been clarified [15-17].

Following, this paper aims at presenting a fast and simple procedure to select the best model to calculate the mass discrimination factor in ID-ICP-MS. The key idea is to study and compare the residuals of the different linearized models. Here we will consider the most common ones; *viz.*, the exponential, the linear, the power and Russell's models, although the procedure can be generalized to any other. Four examples will be considered where Cd, Cr, Sm and Nd were determined.

2.1. Evaluation of the mass bias factor per unit mass

From a pragmatic viewpoint, the most convenient way to model the instrumental mass discrimination is to relate a suite of theoretical isotope ratios (R_{theo}) to their corresponding empirical values (R_{exp}), calculate *K* and, then, use it (along with R_{exp}) to calculate a corrected ratio (R_{corr}) for the unknown. In general, *K* is involved in an algebraic equation describing a curve but it can be calculated straightforwardly whenever a linear model is used instead [6, 8].

As discussed in the previous section, the empirical relationship between R_{theo}, R_{exp} and the two isotope masses can be described in different ways, among

which four stand out in the literature: the linear (straight line), the exponential, the power and Russell's models. They are depicted in the second column of Table 1. As their direct use is not trivial, the common practice is to linearize them to get simpler and more straightforward equations (see the third column of Table 1). To select the best model for a particular problem it was proposed to fit the four linearized models and to study the straight lines obtained by plotting the R_{theo}/R_{exp} *ratio* (or a logarithmic form) against the mass difference (or logarithm of the masses, in Russell's model) [5]. However, this approach is subjective and prone to errors because the significance of those plots is not immediate and a sound decision making is not possible.

Table 1. Models to determine the mass bias factor (*K*) in ID-ICP-MS. R_{corr} is the corrected isotope ratio, R_{exp} is the measured isotope ratio, R_{theo} is the theoretical isotope ratio, m_i and m_j are the absolute masses of the selected isotopes and ΔM is the mass difference between them.

Model	Instrumental relationship	Functional linearized form	Dependent variable
Exponential	$R_{corr} = R_{exp} \cdot e^{\Delta M \cdot K}$	$y = \Delta M \cdot K$	$y = \ln(R_{theo}/R_{exp})$
Straight line (linear)	$R_{corr} = R_{exp} /(1+\Delta M \cdot K)$	$y = \Delta M \cdot K$	$y = (R_{exp} - R_{theo})/R_{theo}$
Power	$R_{corr} = R_{exp} \cdot (1+K)^{\Delta M}$	$y = \Delta M \cdot \log_{10}(1+K)$	$y = \log_{10}(R_{theo}/R_{exp})$
Russell	$R_{corr} = R_{exp} \cdot (m_i/m_j)^K$	$y = K \cdot \log_{10}(m_i/m_j)$	$y = \log_{10}(R_{theo}/R_{exp})$

Fortunately, basic statistics associated with the straight line (or first-order) least squares fit yield very simple and reliable criteria to judge on the adequacy of each linearized model [18–20]. Note that the expression “straight line fit” will be used throughout the text to denote that the models are converted to a straight line function. The term “linear fit” and the like are not of sufficient quality to assure the traceability of the calculations because, after all, any mathematical relationship is “a line”. Analogously, the term “linearization” is used to denote an algebraic transformation from a (usually) complex mathematical expression to a straight line equation, whose parameters are of interest (here, *the slope K*).

Although the conceptual idea is really simple, it is worth remembering some basic statistics. More details and extensive explanations can be found in the references given herein.

2.2. Review of some concepts associated with the straight line fit

In a typical model, two variables are related as $y = f(x) + \varepsilon$, where $f(x)$ is a mathematical function that relates y to x (it is a common practice to select a straight line function but other possibilities exist, and the choice is under the analyst's responsibility based on his/her experience and/or experimental data). Note that the model is a mere working hypothesis, which must be modified if the experimental data are against it. Finally, ε is the random error, or information not modelled by the calibration function, which is associated with the variable response and denotes how closely the model resembles the measured signals. It is reasonable to accept that the smaller the random errors are, the better the model is. Therefore, how can we fit the best model through a swarm of points? A quite intuitive solution is to look for a model that adheres as much as possible to each and every experimental point so that it minimizes the average difference between the experimental signals and those predicted by the model. Hence, the common criterion by which the sum of the squared differences between the measured signal (y_{exp}) and that predicted by the model (y_{pred}) is minimal was accepted as a natural fitting criterion [18–20]. The differences ($y_{pred} - y_{exp}$) are referred to as "residuals". This is the (ordinary) least squares criterion (OLS or LS). Despite its widespread and ubiquitous usage, the OLS criterion has three basic mathematical assumptions that are less broadly known [18-22]:

(i) the experimental errors occur only in the direction of the signal to be measured, y.

(ii) The errors in the y-direction are normally distributed. This means that the resulting errors associated with the analytical signals should follow a normal distribution.

(iii) The errors in the y-direction are independent and of the same magnitude regardless of the x values. This property is referred to as 'homoscedasticity' (the opposite situation is called

'heteroscedasticity'). Its presence simplifies the calculations and gives rise to the usual unweighted least-squares line.

Statements (ii) and (iii) above constitute two cornerstones to assure whether a model fit is acceptable. Since the OLS criterion is a universal procedure to fit functions, it does not guarantee by itself that the model under scrutiny is correct. In order to accept it, we must assess that these two requisites hold on. There are different statistical tests to evaluate the models but most of them should not be used due to the usual low number of data points employed to fit the model [23] (this will be considered later). Therefore, a suitable alternative consists of a graphical visualization and evaluation of the residuals associated with our (temptative) model.

Homoscedasticity of the fit must be assured and, fortunately, can be visualized easily. First, the absence of outlying points must be checked as they may strongly bias any model in different ways, [24] see Fig. 1a and b for a general, conceptual idea on how strongly an outlier will influence the regression. In general, outliers situated in extreme positions affect more the fit (rotational effects) [22]. Check that all points do follow a unique trend; in case a point behaves anomalously, consider rejecting it and recalculating the model. Sometimes, decisions are not immediate and plotting the residuals will help. This can be done straightforwardly in any spreadsheet, less than a minute, and it may yield enormous benefits. Any data point with a too high residual is suspicious (more formally, a point whose standardized residual is around 3, or higher, should be considered as an outlier [23]). Next, check for the absence of visual trends in the residuals (Fig. 1c and d). In particular, parabolic trends are frequent (Fig. 1d) and they mean that a straight line does not fit the experimental data properly. If a clear trend is not visualized, all residuals are more or less randomly distributed, and are of the same magnitude (Fig. 1c), it can be reasonably assured that they are normally distributed and that they have common variance (another requisite of the OLS methodology) [20]. Normality can be studied more formally using statistical tests, as those described in the next section, where more details are presented.

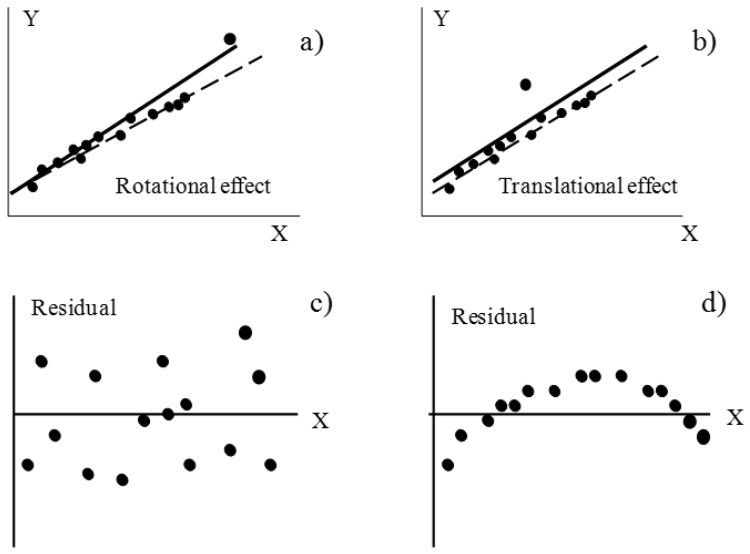

Figure 1. Effect on the regression lines calculated by the ordinary least squares criterion when outliers are present in the dataset (the rotational and translational denominations stem from ref. 24 (a and b) and a graphical example of homoscedasticity (c) and heteroscedasticity (d) in the residuals.

It may surprise that so much emphasis is put on graphical decision-making but this can be explained quoting NIST: “Numerical methods for model validation are useful, but usually to a lesser degree than graphical methods. The latter have an advantage […] because they readily illustrate a broad range of complex aspects of the relationship between the model and the data” [25].

3. Experimental

3.1. Datasets

Four case studies will exemplify the working methodology proposed here. Two of them deal with the determination of Sm and Nd and were used as tutorials in a recent textbook [5]. They present a situation where the replicates of the experimental ratios are not considered explicitly to set the model. The other two examples are about determining Cd and Cr by ID-ICP-MS, using a

quadrupole analyzer equipped with a kinetic energy discrimination cell. They correspond to an ongoing study in our laboratory to measure some environmentally relevant metals in sediments. Replicates of the mass isotopes are presented and, therefore, will be applied to illustrate the use of the lack-of-fit test (LOF). In addition, Cr was selected because of the low number of isotopes and their low mass (compared to the other elements in the present work).

The experimental isotope ratios were obtained from measurements carried out on Cd and Cr standard solutions of natural isotope composition for ICP analysis (Sigma Aldrich) whose theoretical isotope abundances were obtained from IUPAC [26]. Table 2 shows the compiled experimental results.

Table 2. Original data for the four case studies considered here. The isotopes selected for each element are shown under the heading "Isotopes", along with their theoretical (derived from IUPAC [26]) and experimentally measured ratios. The mass difference is denoted as $\Delta M^{a,b.}$

Isotopes	Theoretical ratio	Experimental ratio	ΔM	Isotopes	Theoretical ratio	Experimental ratio	ΔM	Isotopes	Theoretical ratio	Experimental ratio	ΔM
Case study 1: Cd											
106/114	0.043508528	0.031349113	8	111/114	0.445527323	0.391757742	3	113/114	0.425339367	0.406410177	1
		0.031121068	8			0.391053577	3			0.405081916	1
		0.030958661	8			0.394968971	3			0.406683127	1
		0.030647223	8			0.392116797	3			0.406479036	1
		0.030951996	8			0.393185914	3			0.405911499	1
108/114	0.030978072	0.023971763	6	112/114	0.839888618	0.772383915	2	116/114	0.260703098	0.279916302	−2
		0.023763753	6			0.768285734	2			0.278555226	−2
		0.0247017*	6			0.775911501	2			0.279184221	−2
		0.024381751	6			0.774078028	2			0.281141181	−2
		0.02392011	6			0.772314239	2			0.279164297	−2
110/114	0.434737208	0.365326652	4								
		0.365379831	4								
		0.370625246	4								
		0.3654346 5	4								
		0.366794537	4								
Case study 2: Cr											
50/52	0.051456543	0.04146233	2	53/52	0.114016237	0.126390065	−1	54/52	0.028414518	0.035143948	−2
		0.039952749*	2			0.125910941	−1			0.03487478	−2
		0.041939234	2			0.125490294	−1			0.034398109	−2
		0.042557359	2			0.126713427	−1			0.036049048	−2
		0.042027005	2			0.127015489	−1			0.035308014	−2
		0.042005136	2			0.125975986	−1			0.03475144	−2
		0.041460437	2			0.126565896	−1			0.035736555	−2
		0.040932561	2			0.125553057	−1			0.034422643	−2
Case study 3: Nd (**)								**Case study 4: Sm (**)**			
142/146	1.57961487	1.491953	4					144/147	0.2048032	0.197872	3
143/146	0.70824364	0.679507	3					148/147	0.74983322	0.758822	−1
144/146	1.38449008	1.345698	2					149/147	0.92194797	0.943961	−2
145/146	0.48245971	0.475716	1					150/147	0.49232822	0.510151	−3
148/146	0.33486532	0.34442	−2					152/147	1.78452302	1.891842	−5
150/146	0.32800047	0.346675	−4					154/147	1.51767845	1.647119	−7

[a] (*) Outliers excluded from the studies. [b] (**) Case studies 3 and 4 stem from ref. 5.

3.2. Working methodology

In the following, the different candidate models will be considered in their functional linearized straight line forms and the unweighted OLS fit obtained for each one. The first step in selecting a model is to inspect visually the residuals (potential outliers, relative magnitudes of the residuals and the absence of clear trends) and to study the statistics associated with the regression line (the standard error of the fit, or residual standard deviation, $S_{y/x}$). A careful inspection and a bit of experience are usually enough to make sound decisions, as it will be shown next.

Note that as a referee pointed out, the units of $S_{y/x}$ depend on the particular transformation undergone by the data. Hence, to compare them it is necessary to get rid of the scales. A natural way would be to divide $S_{y/x}$ by an average value (like the classical relative standard deviation, RSD). However, this is not possible here because the average value of the residuals is zero. To circumvent this problem, the average absolute error (i.e., the average of the absolute values of the residuals), $|\overline{y_{res}}|$,is proposed here to get a sort of "relative standard deviation of the fit", RSDF as: RSDF = 100*(($S_{y/x}$)/ $|\overline{y_{res}}|$). As classical RSD, it shows the extent of the variability of the residuals in relation to the average value (of the absolute residuals).

In addition, two traditional scale-independent statistics were also considered: the coefficient of determination (R^2) and the lack-of-fit test (which must be derived from an Analysis of Variance – ANOVA – study when replicates are available) [27]. Both are used to evaluate the adequacy of the model to the experimental data. In simple linear regression, the former equals the squared correlation coefficient (given in percentage), but this cannot be generalized to other situations and it is a rough approach to evaluate goodness-of-fit. The lack-of-fit test is an F-test which determines whether the residual information can be associated with the experimental random errors or with "something" else (i.e., the model has not been able to capture all the relevant variance in the data points and therefore causes a "lack-of-fit"). Though both tests can be used to compare among different regression models, they should be used in conjunction with the residual plots because they are not powerful enough to assure by themselves that the model is suitable [28,29] (a typical problem is that even curvilinear models can exhibit very good figures in both parameters).

Then, statistical tests can be applied to check the normality of the residuals. A normal probability curve (available in most common software) will also simplify decision making. However, as mentioned above, usual calibrations in analytical chemistry do not imply many experimental points due to work, time and resources constraints. As a consequence, it is difficult (sometimes impossible) to rely on sound statistics for decision making due to the low power of the tests (very few degrees of freedom). Non parametric statistics might constitute a powerful alternative but, again, they are not good enough when very few data are available. A clear example here was the impossible application of the non parametric Wald–Wolfowitz's runs test (to check for a random distribution of the residuals) to the Nd and Sm examples due to a lack of tabulated values for such a small number of runs (because of the few data points).

Here, the standardized Kurtosis and Skewness were calculated as a way to describe whether the distribution of the residuals is symmetric and without tails. Then, the non para-metric sign test and the Wilcoxon's signed rank test were used to check whether the residuals are distributed randomly. Finally, the Kolmogorov–Smirnov's and the Shapiro–Wilk's tests (the latter is more powerful than the Kolmogorov–Smirnov's one when few data are available) were used to check whether the distribution of the experimental residuals is compatible with a Gaussian one [22]

Fig. 2 shows the working procedure conceptually.

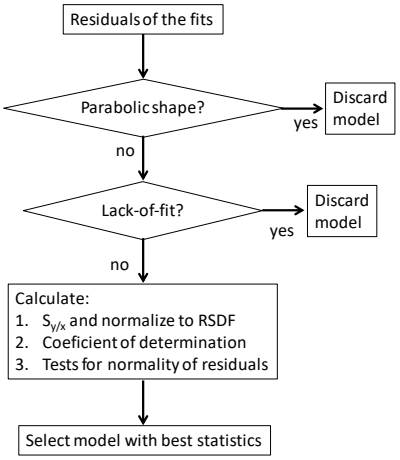

Figure 2. Conceptual description of the approach proposed to select the most suitable model to calculate the mass discrimination factor, *K*.

3.3. Software

The statistical studies were performed using Excel® and Stat-graphics (StatPoint Technologies, Inc., Warrenton, VA, USA).

4. Results and discussion

4.1. Case study 1 and 2: selection of the model when determining Cd and Cr

Table 3 shows the results of several statistical tests calculated on the residuals of the different models whereas Fig. 3 and 4 depict the residuals associated with each model and each example, along with the standard error of the calibration ($S_{y/x}$), the relative standard deviation of the fit (RSDF), the coefficient of determination (R^2) and the lack-of-fit test (LOF).

Table 3. Statistics associated to the residuals of the models developed to calculate the mass bias factor in each case study. See text for details.

Case study		Exponential	Straight line	Power	Russell
Cd	Skewness	0.14	1.41	0.14	-0.48
	Kurtosis	0.01	-0.46	0.01	-0.44
	Sign test	*p*-value=1.00	*p*-value=0.39	*p*-value=1.00	*p*-value=0.61
	Wilcoxon's test	*p*-value=1.00	*p*-value=0.78	*p*-value=1.00	*p*-value=0.76
	Chi-square test	*p*-value=0.00	*p*-value=0.00	*p*-value=0.00	*p*-value=0.00
	Shapiro-Wilk`s test	*p*-value=0.99	*p*-value=0.16	*p*-value=0.99	*p*-value=0.54
	Kolmogorov-Smirnov`s test	*p*-value=0.99	*p*-value=0.65	*p*-value=0.99	*p*-value=0.89
Cr	Skewness	-1.26	2.13	-1.26	-1.61
	Kurtosis	0.53	0.80	0.53	0.57
	Sign test	*p*-value=1.00	*p*-value=0.40	*p*-value=1.00	*p*-value=0.40
	Wilcoxon's test	*p*-value=0.75	*p*-value=0.57	*p*-value=0.75	*p*-value=0.70
	Chi-square test	*p*-value=0.00	*p*-value=0.01	*p*-value=0.00	*p*-value=0.00
	Shapiro-Wilk test	*p*-value=0.30	*p*-value=0.03	*p*-value=0.29	*p*-value=0.21
	Kolmogorov-Smirnov's test	*p*-value=0.93	*p*-value=0.71	*p*-value=0.93	*p*-value=0.88
Nd	Skewness	-0.05	0.75	-0.05	-1.52
	Kurtosis	-0.22	0.13	-0.22	1.24
	Sign test	*p*-value=1.00	*p*-value=0.68	*p*-value=1.00	*p*-value=0.68
	Wilcoxon's test	*p*-value=1.00	*p*-value=0.83	*p*-value=1.04	*p*-value=0.68
	Chi-square test	*p*-value=0.00	*p*-value=0.00	*p*-value=0.00	*p*-value=0.00
	Shapiro-Wilk test	*p*-value=0.99	*p*-value=0.53	*p*-value=0.99	*p*-value=0.19
	Kolmogorov-Smirnov's test	*p*-value=1.00	*p*-value=0.99	*p*-value=1.00	*p*-value=0.93
Sm	Skewness	-1.12	0.71	-1.12	-0.56
	Kurtosis	0.57	-0.94	0.57	-0.94
	Sign test	*p*-value=1.00	*p*-value=0.68	*p*-value=1.00	*p*-value=0.68
	Wilcoxon's test	*p*-value=1.00	*p*-value=1.00	*p*-value=1.04	*p*-value=1.00
	Chi-square test	*p*-value=0.00	*p*-value=0.00	*p*-value=0.00	*p*-value=0.00
	Shapiro-Wilk's test	*p*-value=0.34	*p*-value=0.07	*p*-value=0.34	*p*-value=0.14
	Kolmogorov-Smirnov's test	*p*-value=0.94	*p*-value=0.75	*p*-value=0.94	*p*-value=0.89

With respect to Cd, a replicate was rejected because it had an outlying behaviour throughout the studies (see Table 2). The linear (straight-line) fit presents a rather clear parabolic pattern (Fig. 3) and, so, it has to be discarded. This model shows also a significant lack-of-fit (95% confidence) and, accordingly, it is not suitable for our purposes. The other models do not exhibit a clear trend and, thus, are considered further. The exponential and power models (whose behaviour is almost equal) present a borderline lack-of-fit (LOF). Although, strictly speaking, the test is not significant as the experimental p-value associated with the F test is too close to the critical one (0.05, 95% confidence). Finally, the residuals for Russell's method do not have a definite pattern, the LOF test is clearly not significant, the RSDF is comparable to the other models and the R^2 statistic is marginally better. Therefore, the latter model should be selected.

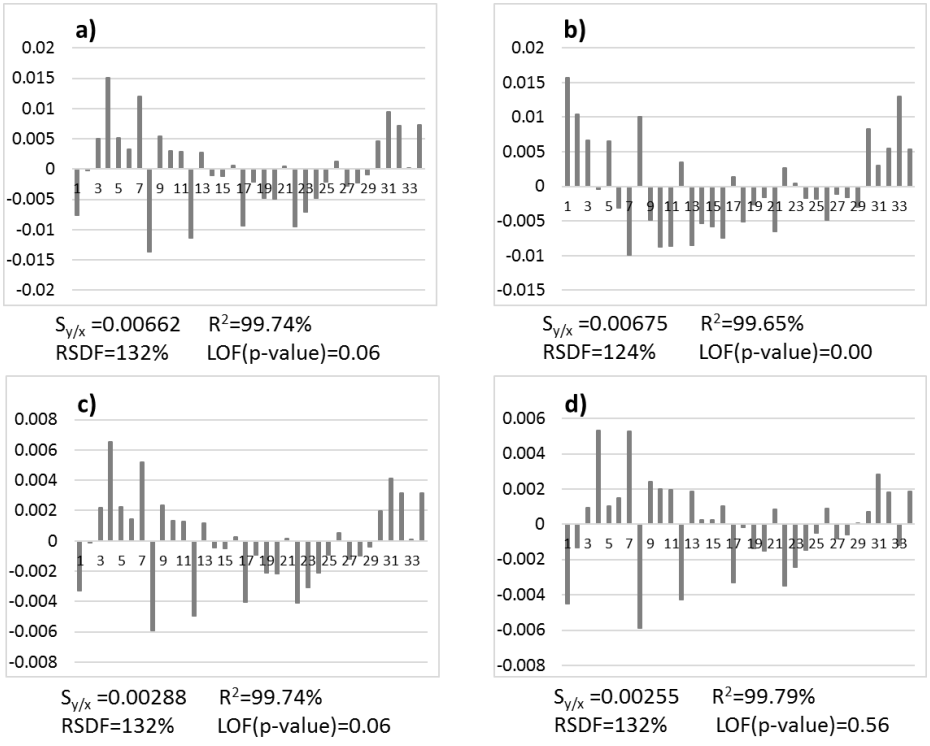

Figure 3. Case study 1 (Cd): statistics associated with the calibration and graphical representation of the residuals. Models to calculate the *K* factor: a) exponential, b) straight-line, c) power, and d) Russell.

This conclusion was assured by studying the residuals of the models deeper and calculating the statistics mentioned above. Table 3 reveals that no model had either a skewed distribution or a tailed shape (standardized skewness and kurtosis lower than ±2). Thus, these statistics do not help in deciding on the best model.

The null hypotheses of the sign test and of the Wilcoxon's signed rank test (in both cases, H_0: the data derive from a population with a median value of zero) cannot be rejected for any model, hereby revealing that the sets of residuals are compatible with a symmetric distribution whose median is zero. However, this does not guarantee that they are normally distributed [22].

The other tests are intended to check whether the distribution of the residuals is Gaussian (H_0: the distribution of residuals follows a normal distribution); namely, the Shapiro–Wilk's and the Kolmogorov–Smirnov's tests. In Table 3 no rejection can be made so all models are compatible with the normal distribution of the residuals. The other tests yielded the same conclusion (but for a borderline situation of the straight line model when the Shapiro–Wilk's test was used).

Finally, Russell's method led to the lowest dispersion of the residuals (Fig. 5). Therefore, there is not additional evidence against the selection of Russell's model for Cd.

With respect to Cr, the low number of isotopes yields only three different calibration levels, which complicates decision making. However, the linear model shows a clear trend (Fig. 4) which makes it unsuitable (Fig. 2). This was confirmed by the high skewness of the residuals (Table 3), a bad normal probability plot (figure not shown) and a high dispersion of its residuals (Fig. 5). Further, the R^2 and LOF revealed that it is the model that fits the experimental data worst. Hence, it should be discarded definitely.

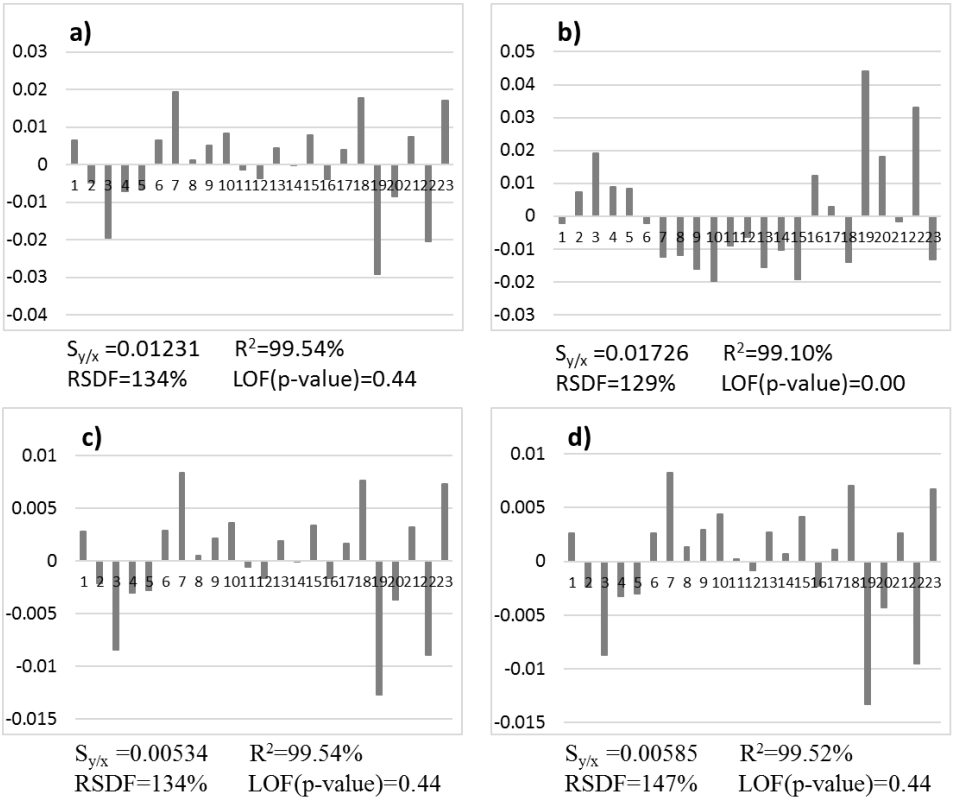

Figure 4. Case study 2 (Cr): Statistics associated with the calibration and graphical representation of the residuals. Models to calculate the *K* factor: a) exponential, b) straight-line, c) power, and d) Russell.

The other three models performed very similar, with good statistics for the residuals (Table 3). The R^2 and LOF tests were almost equal and only marginal best RSDF values were obtained for the exponential and power models. The LOF test was not significant for any of these three models (95% confidence) although it was better for the power and exponential models than for Russells' one. As the dispersion of the residuals (Fig. 5) was slightly better for the power than for the exponential method, the former was selected for Cr.

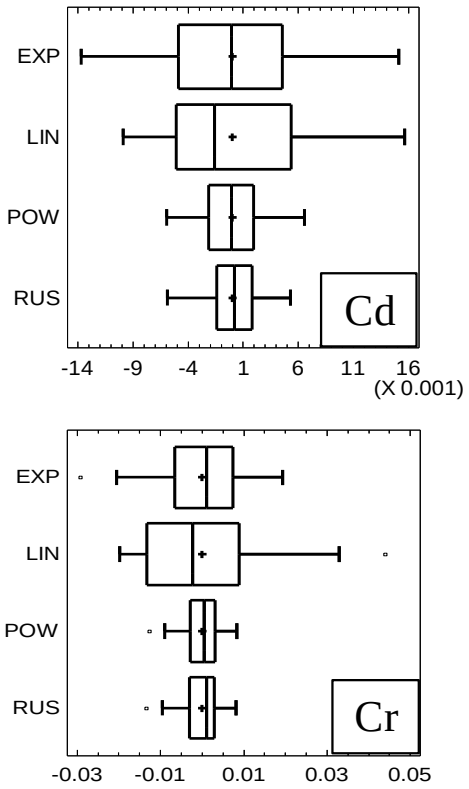

Figure 5. Box and Whiskers plot of the residuals for each model (Exp= exponential, Lin= straight line, Pow= power, Rus= Russell). The cross in the middle of the box represents the average value whereas the vertical line within the box represents the median.

4.2. Case study 3 and 4: selection of the model when determining Nd and Sm

Analogous studies were carried out to select the best model to determine *K* when studying Nd and Sm. These examples do not include replicates for the isotope ratios and, so, the lack-of-fit test cannot be calculated. Previous studies concluded that all models, but the straight-line one, may be

acceptable and the exponential method was preferred (although there was a somehow marginal best performance of Russell's method when determining Nd) [5].

When the residual plots were considered for Nd (Fig. 6) it was concluded that any one showed a particularly cumbersome behavior as all models had a quite random distribution. The model with the best RSDF was the exponential one, which agreed with the conclusion obtained elsewhere, although following a more elaborate procedure [5]. The R^2 statistic was almost the same for all models and it did not allow drawing sound conclusions.

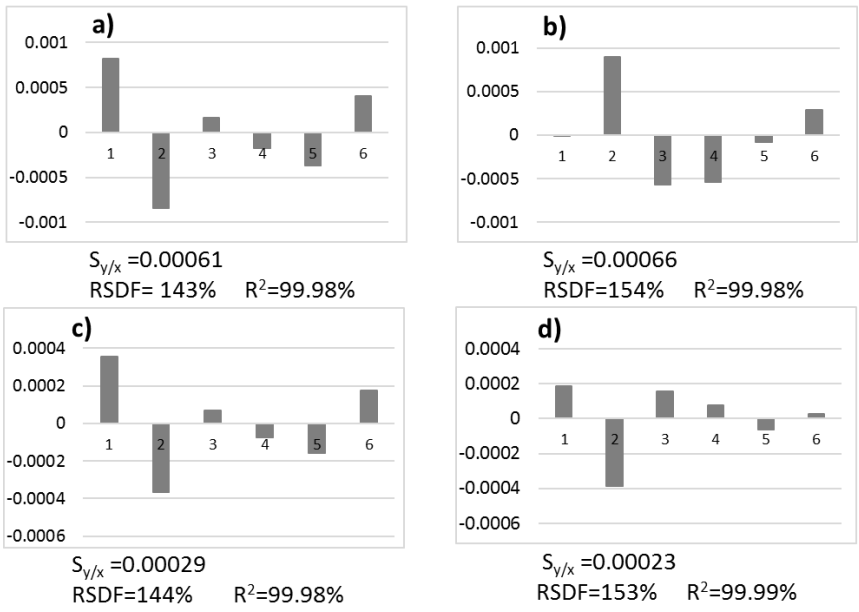

Figure 6. Case study 3 (Nd): Standard error of the fit (*Sy/x*) and graphical representation of the residuals. Models to calculate the *K* factor: a) exponential, b) straight-line, c) power, and d) Russell.

The statistics associated with the residuals, Table 3, revealed that Russell's method yielded a somehow worst distribution (skewness and kurtosis, although not statistically significant), whereas the exponential and the power methods performed the best. The latter one was selected finally for Nd because of the lowest dispersion of the residuals (Fig. 8).

When Sm was considered (Fig. 7) Russell's and the straight-line methods were not acceptable as they showed a parabolic residual pattern and, therefore,

the models do not fit the data properly. Hence, they are discarded at the first step of Fig. 2. It is noteworthy that the approach presented here allows an immediate and clear rejection of Russell's model, which was not so simple when calculating relative errors [5]. The exponential and power models behave totally similar (as noticed previously) [5] although with a marginal better RSDF for the power method. With regards to the residual statistics (Table 3) they reinforce the graphical conclusions. Note that it is not possible to select between the methods (once Russell's and straight-line ones were discarded) considering the statistics alone (as for most models in the previous section, the null hypotheses of the statistical tests could not be rejected and they were of little value to select a model). The power model was selected owing to the smallest scattering of the residuals (Fig. 8).

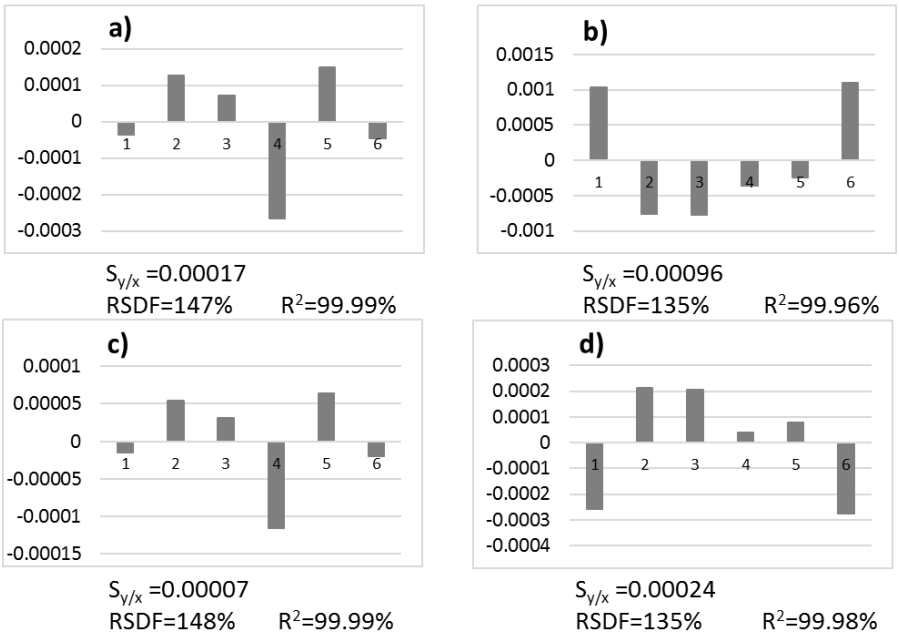

Figure 7. Case study 4 (Sm): Standard error of the fit ($S_{y/x}$) and graphical representation of the residuals. Models to calculate the *K* factor: a) exponential, b) straight-line, c) power, and d) Russell.

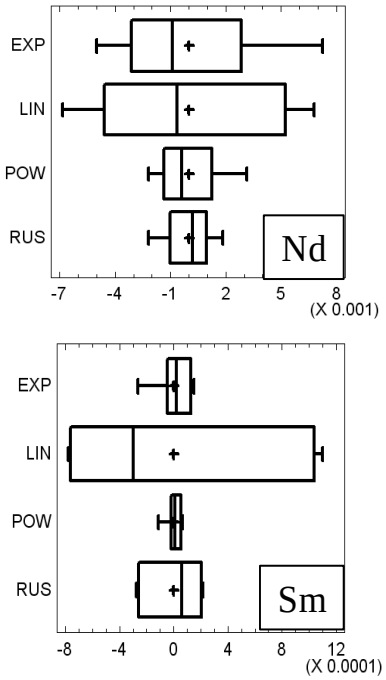

Figure 8. Box and Whiskers plot of the residuals for each model (Exp= exponential, Lin= straight line, Pow= power, Rus= Russell). The cross in the middle of the box represents the average value whereas the vertical line within the box represents the median.

Two final notes can be given. First, most statistics shown in Table 3 can be visualized in a common box and whiskers plot (Fig. 5 and 8). Although – strictly speaking – such a plot is not a graphical representation of the tests, the symmetry of the residuals, their distribution and the closeness of the mean and the median can be observed easily. So, for a reduced dataset (as is usually the case), it is possible to take advantage of this plot for decision making:

(i) the smaller the box and the whiskers are, the lower the standard error of the regression is;

(ii) the closer the mean (in the plot this is shown by a cross) and the median (the bar within the box) are, the less likely the existence of outliers will be;

(iii) the more symmetrical the box and the whiskers are, the less skewed the distribution will be and, likely, the more Gaussian the distribution of the residuals will become. Second, the RSDF was always greater than 100 % because it is derived from the residuals. These, in turn, follow essentially a random distribution and, therefore, their variability is expected to be large when compared to the average (of the absolute values, because the arithmetic average is zero). The relevant issue here is to look for models with the lowest RSDF values.

5. Conclusions

It was shown that simple plots derived from the residuals of the least squares fit provide a powerful, simple and rather objective criterion to decide on the suitability of a model to calculate the mass discrimination factor (*K*) in ID-ICP-MS. Visualization of the residuals of the fit for the different models allows deciding on the existence of both outliers and non random (typically, parabolic) patterns.

Then, the lack-of-fit test (if replicates are available) will further test the adequacy of the model. In the examples studied in this paper, the classical coefficient of determination (R^2) and the relative standard error of the fit (RSDF) were not critical to select among different candidate models. However, their calculation is straightforward and it is recommended to keep them in order to gather additional information on the models. Further, a box and whiskers plot yields good clues on the symmetry (likely, on the Gaussian distribution) and scattering of the residuals, which can help selecting amongst two very similar candidate models.

It was also observed that on some occasions non parametric statistics were not conclusive enough for decision making. Thus, the graphical study of the residuals and the lack-of-fit test constitute the cornerstones to differentiate among several models to calculate the mass discrimination factor and to select a suitable one.

References

[1] Blanco González, E.; Sanz Medel, A. *Liquid chromatographic techniques for trace element speciation analysis*, in: Elemental Speciation: new approaches for trace element analysis, eds. Caruso, J.A.; Sutton, K.L.; Ackley, K.L. Elsevier, Amsterdam (Netherlands), 2000.

[2] Gómez Espina, J.; Blanco González, E.; Montes Bayón, M.; Sanz Medel, A. Elemental mass spectrometry for Se-dependent glutathione peroxidase determination in red blood cells as oxidative stress biomarker. J.Anal.At. Spectrom. 2012, 27:1949–1954.

[3] Nuevo Ordoñez, Y.; Montes-Bayón, M.; Blanco-González, E.; Sanz-Medel, A. Quantitative analysis and simultaneous activity measurements of Cu, Zn-superoxide dismutase in red blood cells by HPLC-ICPMS, Anal.Chem. 2010, 82:2387–2394.

[4] Yip, Y.; Chu, H.; Chan, K.; Chan, K.; Cheung, P.; Sham, W. Determination of cadmium in oyster tissue using isotope dilution inductively coupled plasma mass spectrometry: comparison of results obtained in the standard and He/H_2 cell modes. Anal.Bioanal.Chem. 2006, 386:1475–1487.

[5] García Alonso, J.I.; Rodríguez González, P. Isotope dilution mass spectrometry, Royal Society of Chemistry, Cambridge (United Kingdom), 2013.

[6] Ingle, C.P.; Sharp, B.L.; Hortswood, M.S.A.; Parrish, R.R.; Lewis, D.J. Instrument response functions, mass bias and matrix effects in isotope ratio measurements and semi-quantitative analysis by single and multi-collector ICP-MS. J.Anal.At.Spectrom. 2003, 18:219–229.

[7] Ruiz Encinar, J.; García Alonso, J.I.; Sanz-Medel, A.; Main, S.; Turner, P.J. A comparison between quadrupole, double focusing and multicollector ICP-MS. Part II: Evaluation of total combined uncertainty in the determination of lead in biological matrices by isotope dilution. J.Anal.At.Spectrom. 2001, 16:322–326.

[8] Heumann, K.G.; Gallus, S.M.; Rädlinger, G.; Vogl, J. Precision and accuracy in isotope ratio measurements by plasma source mass spectrometry. J.Anal.At.Spectrom. 1998, 13:1001–1008.

[9] US Environmental Protection Agency, Method 6800: Elemental and speciated isotope dilution mass spectrometry, Washington (USA), 2007.

[10] Ciceri, E.; Recchia, S.; Dossi, C.; Yang, L.; Sturgeon, R.E. Validation of an isotope dilution, ICP-MS method based on internal mass bias correction for the determination of trace concentrations of Hg in sediment cores. Talanta, 2008, 74:642–647.

[11] Yang, L.; Sturgeon, R.E. Comparison of mass bias correction models for the examination of isotopic composition of mercury using sector field ICP-MS. J.Anal.At.Spectrom. 2003, 18:1452–1457.

[12] Mejia, J.; Yang, L.; Mester, Z.; Sturgeon, R.E. *Instrumental mass discrimination for isotope ratio determination with multicollector Inductively Coupled Plasma Mass Spectrometry*, in: Isotopic Analysis. Fundamentals and Applications using ICP-MS, eds. Vanhaecke, F.; Degryse, P. Wiley-VCH, Weingeim (Germany), 2012.

[13] Begley, I.S.; Sharp, B.L. Characterization and correction of instrumental bias in inductively coupled plasma quadrupole mass spectrometry for accurate measurement of lead isotope ratios. J.Anal.At.Spectrom. 1997, 12:395–402.

[14] García-Ruiz, S.; Petrov, I.; Vassileva, E.; Quétel, C.R. Cadmium determination in natural waters at the limit imposed by European legislation by isotope dilution and TiO_2 solid-phase extraction. Anal.Bioanal.Chem. 2011, 401:2785–2792.

[15] Murphy, K.E.; Vetter, T.W. Recognizing and overcoming analytical error in the used of ICP-MS for the determination of cadmium in breakfast cereal and dietary supplements. Anal.Bioanal.Chem. 2013, 405:4579–4588.

[16] Liu, H.; You, C.; Cai, W.; Chung, C.; Huang, K.; Chen, B.; Li, Y. Precise determination of seawater calcium using isotope dilution inductively coupled plasma mass spectrometry. Analyst, 2014, 139:734–741.

[17] Lee, J.; Boyle, E.A.; Echegoyen-Sanz, Y.; Fitzsimmons, J.N.; Zhang, R.; Kayser, R.A. Analysis of trace metals (Cu, Cd, Pb, and Fe) in seawater using single batch nitrilotriacetate resin extraction and isotope dilution inductively coupled plasma mass spectrometry. Anal.Chim.Acta, 2011, 686:93-101.

[18] Ortiz, M.C.; Sánchez, S.; Sarabia, L. *Quality of analytical measurements: univariate regression*, in: Comprehensive Chemometrics: chemical and biochemical data analysis, eds. Brown, S.D.; Tauler, R.; Walczack, B. Elsevier, Amsterdam (Netherlands), 2009.

[19] Draper, N.R.; Smith, H. Applied Regression Analysis, John Wiley & Sons, New York (USA), 1998.

[20] Andrade-Garda, J.M.; Carlosena-Zubieta, A.; Soto-Ferreiro, R.M.; Terán-Baamonde, J.; Thompson, M. *Classical linear regression by the least squares method*, in: Basic Chemometric Techniques in Atomic Spectroscopy, ed. Andrade-Garda, J.M. RSC Publishing, Cambridge (United Kingdom), 2013, pp. 52–122.

[21] Miller, J.N. Int.J.Spectrosc. 1991, 3:43–46.

[22] Miller, J.N.; Miller, J.C. Statistics and chemometrics for analytical chemistry, Prentice Hall, Harlow (United Kingdom), 2010.

[23] Thompson, M.; Lowthian, P.J. Notes on statistics and data quality for analytical chemists, ICP, London (United Kingdom), 2011.

[24] Thompson, M.; Ellison, S.L.R. A review of interference effects and thir correction in chemical analysis with special reference to uncertainty. Accredit.Qual.Assur.2005, 10:82–97.

[25] NIST/SEMATECH e-Handbooks of Statistical Methods, http://www.itl.nist.go.v/div898/handbook/.

[26] Rosman, K.I.R.; Taylor, P.D.P. Isotopic compositions of the elements. Pure Appl.Chem. 1999, 71:1593–1607.

[27] Massart, D.L. Chemometrics a textbook, Elsevier, Amsterdam (Netherlands), 1988.

[28] StatPoint Technologies, User's manual. Statgraphics v15.2, StatPoint Technologies Inc., Warrenton, USA.

[29] Otto, M. Chemometrics, Wiley-VCH, Weingeim (Germany),2007.

V.2.

A FAST APPROACH TO EVALUATE THE BIOACCESSIBLE FRACTION OF CADMIUM IN SEDIMENTS USING ISOTOPE DILUTION INDUCTIVELY COUPLED PLASMA MASS SPECTROMETRY (ID-ICP-MS)

1. Abstract

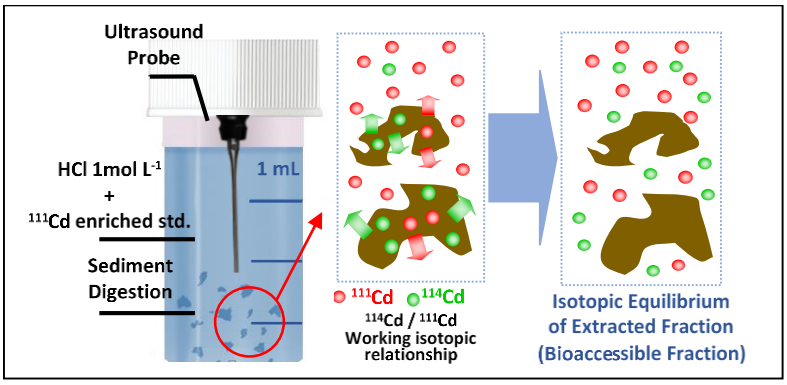

Isotope dilution analysis is proposed first time to determine the bioaccessible fraction of Cd by ICP-MS in marine sediments. The ^{111}Cd isotopically enriched isotope was added before the extraction to equilibrate it with native Cd solubilized from the sample. A relevant advantage of the methodology is that a fast and simple extraction procedure based on ultrasonic probe agitation and diluted HCl is required. The parameters affecting trueness and precision were evaluated carefully in order to minimize the sources of errors; namely: spectral interferences, detector dead time, mass discrimination factor and selection of the optimum sample/spike ratio. The fraction leached was correlated with the sum of the 3-step sequential extraction procedure of the Standards, Measurements and Testing Programme (SM&T) using the BCR 701 sediment to validate the method. The certified and measured values agreed statistically, giving a recovery of 105%. Further, the extraction procedure itself was studied by spiking the enriched isotope before and after the extraction step, resulting mandatory the addition of the enriched spike from the beginning of

the process. Two additional reference sediments with certified total cadmium content were also analysed. The method provided good reproducibility (0.9 %, RSD) and a low detection limit, 1.80 ng g^{-1}. It was applied to determine bioaccessible Cd in sediments from two environmentally and economically important areas of Galicia (rias of Arousa and Vigo, NW of Spain).

The results discussed in this chapter are summarized in the scientific publication:

A fast approach to evaluate the bioaccessible fraction of cadmium in sediments by ID-ICP-MS.

J. Terán-Baamonde, A. Carlosena, R.M. Soto-Ferreiro, J.M. Andrade and D. Prada.

Analytica Chimica Acta (under revision), 2017.

2. Introduction

The environmental consequences of the presence of trace metals in the environment cannot be understood fully considering only their total concentration in related matrices. Mobility and, hence, accessibility to these elements is determined by the fraction that can be liberated easily and, so, affect the environment [1]. Bioaccessibility (defined by IUPAC as the potential for a substance to come in contact with a living organism and, then, interact with it) must be differentiated from bioavailability (the extent of absorption of a substance by a living organism compared to a standard system). The former is the main factor that poses potential threats to human health when metals are transferred to the aquatic media and enter the food chain [2]. Therefore, an accurate and fast determination of the bioaccessible metal fraction in different environmental compartments is mandatory. In particular, cadmium is a non-essential metal with recognized high toxicity at very low exposure levels. Its persistence leads to bioaccumulation and, further, shows an important mobility between environmental matrices, such as soils and sediments, where it tends to accumulate, in particular in seabed sediments close to industrial and urban zones [3].

To quantify the accessible or labile metal fraction in sediments several single and sequential extraction procedures were proposed [4]. The importance (and complexity) of this topic is shown by the many comparisons between extraction procedures, extractants and stages. A major issue is that currently the extraction procedures cause analyte losses, contamination and/or inefficient extraction, although it is usually being very difficult to quantify those problems. In this context, isotope dilution analysis can be of most help because an isotope equilibration between the fraction of the element that is released by a procedure and an enriched spike added to the sample will take place at the beginning of the extraction.

Isotope dilution mass spectrometry (ID-MS) is a primary method of measurement whose operation can be completely described and understood, for which a complete uncertainty statement can be written in terms of SI units [5, 6], and where operation is completely described by a measurement equation [7]. ID-MS measurements are much more robust than conventional methodologies so sample preparation is less critical and a calibration step is not

mandatory, saving expensive instrumental and manpower time. In addition, the accuracy of ID-MS is higher than that of conventional methodologies [8]. Combined with inductively coupled plasma (ID-ICP-MS) a powerful methodology based on the measurement of isotope ratios arises, which makes it independent from other sources of uncertainty, such as analyte loss during the sample treatment and possible matrix effects [6]. Indeed, the use of ID-MS by national metrology institutes is well-known [9]. In particular, Cd has been certified in a variety of standard reference materials, including sediments, [10-14], herbal materials [15] and cosmetic baby powder samples [16]. Several international interlaboratory exercises have been put in force using this technique; for instance, the European Union National Reference Laboratories for total and extractable fractions of Cd and Pb in mineral feed [6], and that from NIST to assign the Cd mass fraction in a vitamin matrix [17].

The situation is more complex for environmental samples because determining Cd by ICP-MS at trace and ultratrace levels is subject to several interferences, including oxides and hydroxides of Mo and Zr, a number of double oxide molecular ions of major matrix elements, and isobaric interferences at masses 112 and 114 from Sn [18]. Early literature on this topic focused on the development of matrix separation procedures to resolve those interferences. Despite the large advances in instrumentation, such approaches are still under development. For instance, Cd co-precipitation separation techniques reported reliable quantifications in presence of high concentrations of Mo, Sn and/or Zn in sediments [19], cereals and dietary supplements [20], etc. Electrochemical separation and manual chromatographic separations were proposed to determine Cd in certified reference soils [21]. Anion exchange chromatography proved effective in reducing interferences on the Cd isotopes when analysing soils, dust, sediments and sludge, although for the latter two Sn remained in the solutions and additional corrections were required [12]. Chemical vapor generation using an on-line system was developed to analyze sediments as slurries, introducing the vapor directly into the plasma (FI-CVG-ICP-MS). They found that isotope equilibration for Cd was attained in the slurries after 6 h of resting [22]. A novel four-step separation method combined thiourea solid phase extraction (SPE), co-precipitation and strong anion exchange chromatography, yielding interference-free measurement of Cd in sediments

[23]. In general, all these recent alternatives are labor-demanding and time-consuming.

Another way to approach ID-ICP-MS implies mathematical corrections for isobaric interferences using instrumental software. Thus, Valles-Mota et al. [11] corrected a severe interference of Sn on ^{114}Cd by measuring the ^{118}Sn isotope (free of isobaric interference) when analysing sediments and other matrices. Park et al. [24] stressed that the software correction did not take into account the mass bias of the $^{112}Sn/^{117}Sn$ ratio, resulting in overcorrection. They corrected the isobaric interference of Sn on Cd determination in sediments by ID-ICP-MS using a mass bias corrected $^{112}Sn/^{117}Sn$ ratio to estimate the interfering ^{112}Sn intensity. More recently, instrumental advances such as ultrasonic nebulization, membrane desolvation, collision/reaction cells, and high resolution sector-field mass analysis eliminated or minimized the polyatomic interferences. For Cd, these derived mainly from the formation of molybdenum and zirconium oxides and hydroxides during measurement (such as $^{95}Mo^{16}O^{+}$, $^{96}Mo^{16}O^{+}$ and $^{96}Zr^{16}O^{+}$) [18]. Wysocka and Vassileva [14] assayed different analytical strategies and ID-ICP-techniques to solve the spectral interferences on Cd isotopes when analyzing a candidate reference sediment (IAEA-458), acid digested. They achieved satisfactory results considering both chemical matrix separation or collision cell, using a quadrupole ICP-MS, and a sector-field-ICP-MS device.

Most reports on the determination of Cd in sediments by ID-ICP-MS involve a total digestion of the sample. This is intended to guarantee the total equilibration between the added spike and the endogenous analyte in the sample [25]. It is generally performed in a closed microwave system and takes several hours. In some cases, the enriched isotope is spiked to the acid digest obtained after the sample treatment [26], squandering the capabilities of isotopic dilution to evaluate possible loss of analyte during extraction [10, 24].

Gardolinski et al. [26] applied ID-ICP-MS to determine trace concentrations of Cd, Cu, Pb and Zn in four different sediment fractions extracted in sequence, according to the “BCR 3-step protocol”. This is a four-step procedure which fractionates metals into weak acid extractable, reducible, oxidisable and residual fractions using three reagents of increasing reactivity: acetic acid, hydroxylamine hydrochloride and hydrogen peroxide. The overall

sequential extraction protocols are labor-demanding and time-consuming, usually about 50 h are required to extract three or four individual phases, being its application to a large number of samples lengthy and costly [27]. An accurate determination of Cd (plus Cu, Pb and Zn) at the extracts obtained from a sequential extraction procedure using ID-ICP-MS was proposed [26]. The BCR-701 sediment, which is certified for the SM&T 3-step sequential extraction procedure, was not used there.

In the present work, ID was applied to determine the bioaccessible fraction of Cd by ICP-MS in marine sediments, for which no references in literature were found. The ^{111}Cd enriched isotope was added before the extraction process for its equilibration with native Cd solubilized from the sample. A fast and simple extraction procedure based on ultrasonic probe agitation and diluted HCl is presented. The parameters affecting accuracy of the ID-ICPMS measurements were carefully evaluated in order to minimize spectral interferences, detector dead time, mass discrimination factor and selection of the optimum sample/spike. The fraction leached in this methodology was correlated with the sum of the 3-step sequential extraction procedure of the SM&T using the BCR-701 sediment (encompassing the exchangeable, reducible and oxidisable fractions) to validate the method. In order to study the performance of the extraction procedure and exploit the advantages of isotope dilution analysis, additional assays adding the enriched spike to the acid extract obtained after the extraction step were also accomplished. In addition, two reference sediments with certified total cadmium contents were considered. As a practical case study, sediments from two economically relevant Galician Rias (Rias of Arousa and Vigo, NW of Spain) were analysed.

3. Experimental

3.1. Instrumentation

A VC50-1 ultrasonic probe (50 W, 20 KHz) equipped with a CV18 titanium probe (Sonic Materials, Newtown, CT, USA) was utilized to perform the extractions. A microwave oven (Anton Paar Multiwave, Graz, Austria) equipped with a built-in magnetic stirrer, a fibre-optic temperature sensor, a pressure

sensor and a basic six-position extraction rotor as well as high pressure Teflon vessels were used for the digestions.

Isotope ratio measurements were performed on a XSERIES 2 Quadrupole ICP-MS (Thermo Scientific, Bremen, Germany) in collision cell/kinetic energy discrimination (CC/KED) mode. The instrument was equipped with standard Ni-cones, a Meinhard nebuliser and a Scout double pass spray chamber refrigerated at 4 °C. An ASX-520 autosampler (CETAC Technologies, USA) was employed. The instrumental settings of the ICP-MS are summarised in Table 1. The nebulizer gas flow rate, torch position and ion lens settings were optimised for high sensitivity and minimum values of CeO^+/Ce (< 1.5 %), monitoring a 10 μg L^{-1} standard solution of Be, In and U in 1% (v/v) HNO_3.

Table 1. Instrumental operating conditions and acquisition parameters used in ICP-MS.

ICP operation conditions	
Rf power	1.35 kW
Nebulizer gas flow	0.75 L min^{-1}
Auxiliary gas flow	1.00 L min^{-1}
Cooling gas flow	14 L min^{-1}
He-KED	4.00 L min^{-1}
Acquisition parameters	
Acquisition mode	Pulse counting
Measurement mode	Scan
Number of sweeps	100
Dwell time (ms)	10
Isotope masses	$^{106, 108, 110, 111, 112, 113, 114, 116}Cd$ - ^{118}Sn

3.2. Chemicals and materials

High-purity water, 18.2 MΩ·cm resistivity, obtained from a Milli-Q®Direct purification device (Millipore Co., Bedford, MA, USA) was used. Hydrochloric (37 %) and nitric (65 %) acids were of suprapur quality (J.T. Baker, Phillipsburg, NJ, USA). Stock standard solutions of Cd and Sn (1000 mg L^{-1}) for ICP analysis (SCP Science) were used to prepare working solutions for the studies on dead time detector, mass discrimination factor (referred to as “K factor”) and

spectral interferences. Natural isotopic compositions were assumed to agree with IUPAC [28] in all samples and solutions.

The enriched ^{111}Cd isotope solid spike in the form of chloride (95.5 %) was purchased from Cambridge Isotope Laboratories (USA). Enriched stock solutions were prepared by dissolution of the appropriate amount of the solid with 2 % (v/v) HNO_3, and working spike solutions were obtained by subsequent gravimetric dilution of the enriched stock solution with 2 % (v/v) HNO_3.

The validation scheme applied in this work involved different reference materials: Lake sediment BCR-701, supplied by the Institute for Reference Materials and Measurements (IRMM); New York/New Jersey waterway sediment SRM 1944, from the National Institute of Standards & Technology (NIST) and harbour sediment PACS-2, from the National Research Council of Canada (NRCC). The samples from the Rias of Arousa and Vigo were collected by the Spanish Institute of Oceanography (IEO), in 2011. They had been lyophilized and kept in dark bottles until analysis.

All glassware and plastic ware were soaked in 10 % (v/v) HNO_3 for 24 h and rinsed with high-purity water at least three times before use. Nylon syringe filters 0.45 µm, 30 mm diameter (Thermo Scientific, Tennessee, USA) were used to filter the extracts.

3.3. Sample preparation

The extraction procedure described elsewhere (in review) was employed; in brief, it consists of weighing 0.0250 g of the sample in polyethylene cups (1.2 mL capacity) and adding 1.0000 g of 1 mol L^{-1} HCl. Agitation was performed with an ultrasonic probe introduced into the cup through a cap hole during 16 min. The extracts were filtered and stored in polyethylene cups at 4°C until their analysis. Procedural blanks were prepared in the same manner.

The ID analysis was performed adding the enriched ^{111}Cd spike directly to the aliquot of sediment sample to be analyzed. For this, the extractant (1 mol L^{-1} HCl) was spiked with an adequate amount of the enriched standard, as explained in the following sections. In order to study the performance of the extraction procedure, additional assays adding the enriched spike to the acid extract obtained after the extraction step were accomplished.

Sediment samples and the BCR-701 CRM were submitted to the microwave-based digestion procedure (USEPA Method 3052) to determine their total cadmium content [29]. The digests so obtained were analysed by ICP-MS (conditions presented in Table 1), using conventional calibration and ^{103}Rh as internal standard.

3.4. Isotope dilution analysis

The ID method is based on adding a known amount of an enriched isotope to a sample. The altered isotope ratio of the mixture solution is measured by ICP-MS after equilibration of the spiked isotope with the analyte in the sample. Therefore, the analyte isotope to be used must be adequately selected. Cd has eight stable isotopes but only one, ^{111}Cd, is free from isobaric interferences. In general, either ^{112}Cd or ^{114}Cd are used as major isotopes with the interference-free ^{111}Cd isotope as spiked isotope [24]. In the present work ^{111}Cd and ^{114}Cd were employed for ID analysis.

The isotopic ratio measurements were performed by ICP-MS using the conditions indicated in Table 1, after adequate dilution of the sediment extracts. All measurements were done by triplicate and the concentration of Cd in the samples (C_s) was calculated with the well-known equation for isotope dilution [8], measuring the ^{114}Cd/^{111}Cd ratio.

The enriched ^{111}Cd working solutions were characterized determining the abundances of seven Cd isotopes by ICP-MS. The spike solutions were prepared by triplicate, measured five times and calculating the ratio $A^i = \frac{R^i}{\sum_{i=1}^{n} R^i}$; where A^i is the abundance of the isotope *i* in the enriched spike and R^i the isotope ratios measured for all isotopes (*i* takes values of 106, 108, 110, 112, 113, 114 and 116) with respect to a given reference isotope *k*, here isotope ^{111}Cd [8]. The concentration of the spike solutions was calculated by reverse isotope dilution using the equation derived from the isotope dilution equation referred to above.

4. Results and discussion

4.1. Quantification by isotope dilution ICP-MS

The parameters affecting ID-ICP-MS accuracy measurements were carefully evaluated in order to minimize their sources of errors. These were: spectral interferences, detector dead time, mass discrimination factor and the sample/spike ratio [30].

4.1.1. Spectral interferences

^{111}Cd and ^{114}Cd were used as spike and major isotopes, respectively, throughout this study. The major interferences that affect isotopic Cd measurements (highlighted in the introductory section) were addressed in order to minimize or eliminate them. The polyatomic interferences (due to the plasma gas, solvent, matrix and/or entrained air) were eliminated using a collision kinetic energy discrimination cell with a He gas flow containing 7 % H_2, resulting essentially in an energy discrimination process.

Meanwhile, isobaric interferences were corrected mathematically measuring an alternative isotope of the interfering element. Here, Sn overlaps with isotopes 112, 114 and 116 of Cd, so ^{118}Sn was measured. For this, the following equations were applied, using the intensities obtained from aqueous solutions with natural isotopic composition: I_{corr} (^{11x}Cd) = I_{exp} (^{11x}Cd) – (f_{Sn} x I_{exp} (^{118}Sn)); where f_{Sn} = I (^{11x}Sn) / I (^{118}Sn).

4.1.2. Dead time of the detector

Electron multipliers suffer from non-linearity effects at high counting rates [8]. This leads to the detector dead time, which can be defined as the time necessary to detect one ion including the multiplication effect itself and the electronics handling the pulse. The detector dead time was determined using Cd itself as it may vary with the mass number [31]. The common Russ approach was applied [32, 33], and the determination was repeated periodically as it is affected by the aging of the detector. For this, eight Cd standard solutions of natural isotopic composition in the 25 - 200 µg L^{-1} range were measured using a

dead time of 0 ns. The intensities were corrected for different dead time values (τ) ranging from 0 to 100 ns, using $I_{corr} = I_{exp} / (1- I_{exp} \cdot \tau(s))$.

Then, the $^{111}Cd/^{114}Cd$ ratios were calculated and the normalized isotope ratios (R_{exp}/R_{theo}) were represented versus the assumed dead time values (Figure 1). The experimental value corresponds to the intersection of the lines obtained for the different analyte concentration level, where the isotope ratio does not change with the concentration of the element; that was 35 ± 5 ns.

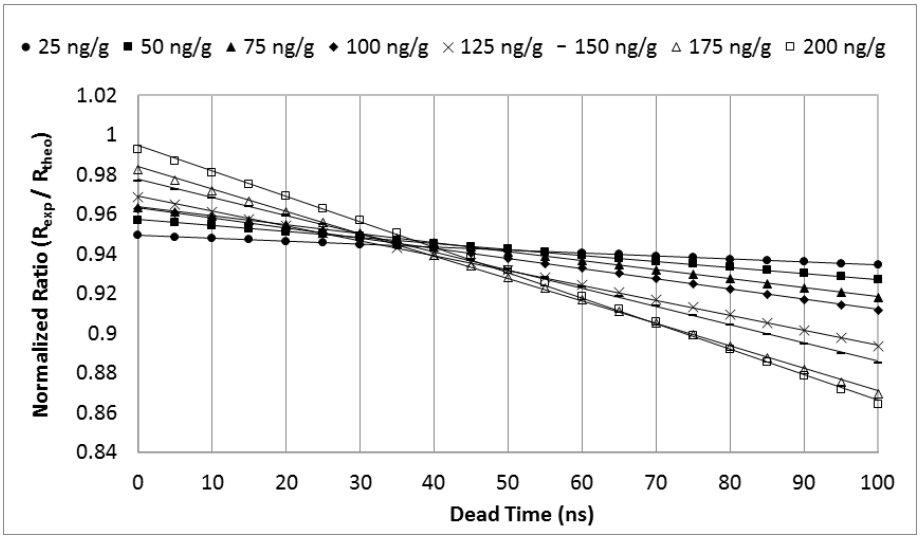

Figure 1. Determination of detector dead time for the $^{111}Cd/^{114}Cd$ isotope ratio at different Cd concentrations.

4.1.3. Mass discrimination factor

Heavy isotopes are transmitted more efficiently than light isotopes in ICP-MS. This effect is called mass discrimination and leads to a mass bias in the isotope ratios that has to be corrected for. In general, two approaches can be applied: (i) an external standardization where the isotope of interest is measured in a standard solution of the analyte, and (ii) an internal standardization which determines *K* in the unknown samples by means of either a known isotope ratio of an element added to the samples, or using a pair of invariant isotopes of the analyte [8].

Here, the first approach was applied. Specifically, the multielemental molar-response curve was adjusted to a Russell´s function, which demonstrated to be the more adequate model when measuring Cd [34]. The isotope ratios (ratioted against the 111 reference mass) were obtained from measurements carried out on a Cd natural standard solution. Figure 2 shows a straight line whose slope is the discrimination factor (*K*). This factor was calculated in each working session as the mean of the values obtained at the beginning and at the end of the measurement sequence.

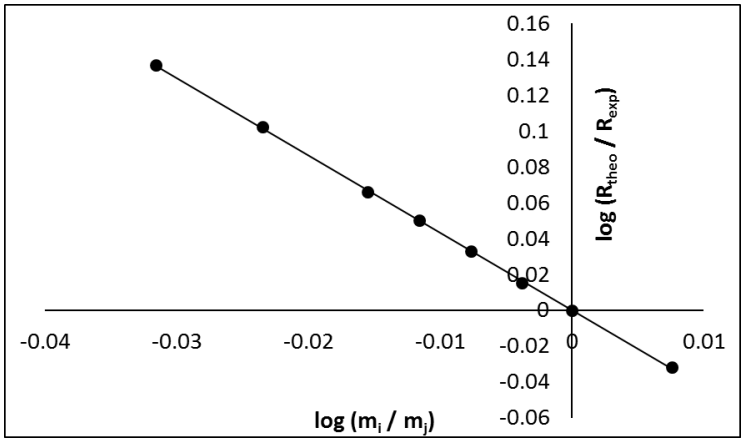

Figure 2. Graphical representation of the linearized Russell´s function for the determination of the K factor as the slope of the straight line.

4.1.4. Sample/spike ratio

An optimum sample/spike ratio is critical for achieving a highly precise isotope ratio by ID-ICP-MS. Indeed, the uncertainty associated to the concentration calculated by ID is a function of the uncertainty in the measured isotope ratio in the mixture (R_m) [35]. The amount of spike solution is a compromise between several factors including results from preliminary measurements, the characteristics of the spiking materials, the final uncertainty, a sufficiently high counting rate and reduced dead time effects [36]. The representation of the so-called error magnification factor f(R) versus the theoretical isotope ratio (R_m) provides a U-shapped error curve, where a theoretical Rm value can be selected in order to obtain the minimum value of

f(R). Then, knowing the approximate content of analyte in the sample, the amount of spike to be added to fulfil the theoretical R_m can be calculated [37].

Figure 3 shows the error curve obtained for the $^{114}Cd/^{111}Cd$ ratio, with the flat zone (providing the lowest f(R) values) ranging approximately from 0.034-0.700. The R_m value will be selected within this interval to add a minimum amount of spike (which, besides helps reducing costs) without increasing the error significantly. Here, the R_m value was 0.16, with a corresponding error magnification factor f(R) of 1.15, which minimized the amount of spike required and is in accordance with others (e.g., [17]). Thus, following the extraction procedure described above and considering the fraction of Cd extracted, 1.0000g of 1 mol L^{-1} HCl containing 200 µg kg^{-1} of spike was added to 0.0250 g of each sediment sample.

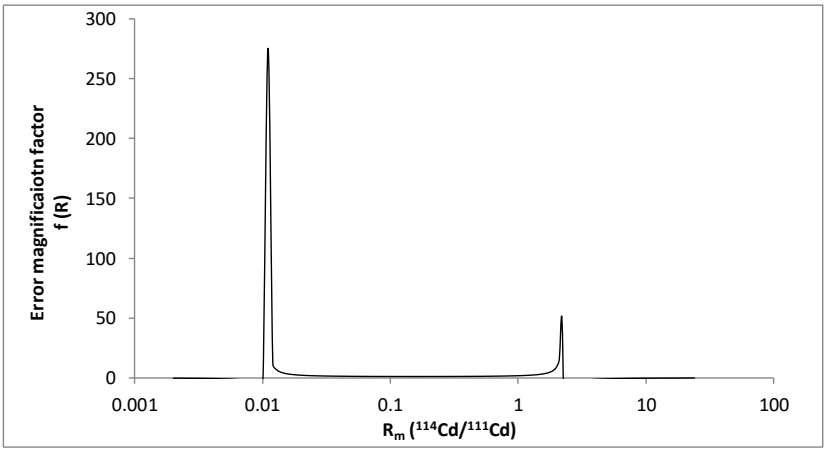

Figure 3. Error magnification factor curve for the ^{114}Cd / ^{111}Cd isotope ratio.

4.2. Assessment of the extraction method

Three CRMs were analysed (BCR-701, PACS-2 and SRM-1944) in two parallel assays. In the first, the ^{111}Cd-spike was added before the extraction process; in the second, the ^{111}Cd-spike was added to the acid extracts. In both approaches, the ratio between the metal in the extracted fraction (here, bioaccessible-Cd) and its total content was calculated. Some authors recommend this evaluation as a routine quality control when analysing marine

sediments [38]. Since BCR-701 does not report total Cd, it was obtained experimentally with external calibration by ICP-MS applying the USEPA 3052 method (microwave-assisted digestion of siliceous matrices).

Table 2 summarizes the results obtained. For all CRMs, when the isotope was added after the extraction step low extraction efficiencies (expressed as percentages) were attained, 64-69 %. They notably increased, up to 101-107 %, when the sediment was spiked before the extraction procedure. Therefore, it has to be concluded that the bioaccessible content of Cd got reduced somehow during the extraction process, likely due to evaporation or reabsorption processes [38, 39]. In effect, when the ultrasonic probe is applied to a so small volume it can excessively heat and, even, project some liquid out of the cup, despite its cap has a small hole to insert the probe. This is a problem encountered in literature and different extraction efficiencies for Cd in sediments using diluted HCl-based extraction methods have been reported (without ID quantitation), 74 % for SRM 2702 marine sediment [40], 89 % for PACS-2 [38] and 107 % for SRM 1944 [40].

Table 2. Bioaccesible-Cd contents (μg g^{-1} dry weight, ± *U**) obtained for three reference sediments using the proposed one-step ID extraction procedure, adding the isotope spike before and after extraction step. Extraction efficiencies were calculated referred to the total content.

		Spike added after extraction		**Spike added before extraction**	
CRM	Total Certified content	Bioaccessible content	Extraction (%)	Bioaccessible content	Extraction (%)
BCR-701	11.31±0.34(**)	7.50 ± 0.12	66	11.89 ± 0.07	105
PACS-2	2.11 ± 0.10	1.34 ± 0.06	64	2.12 ± 0.01	101
SRM-1944	8.80 ± 1.40	6.04 ± 0.35	69	9.43 ± 0.24	107

(*) U, expanded uncertainty. The coverage factor, k, is the Student´s t-value for a 95% confidence interval with 6 degrees freedom.

(**) Not certified, obtained applying USEPA method 3052.

These results demonstrate that the use of ID is a real, critical advantage to cope with situations involving analyte losses during extraction, providing the enriched isotope is added at the beginning of the process and isotopic equilibration of the isotope ratios is assured (with, e.g., a proper time contact).

Taking into account the extraction figures shown in Table 2, it can be stated that the bioaccessible-Cd fraction extracted applying the partial digestion proposed in this report is comparable to the total content of this metal in the certified sediments. Analogous results have been reported [41, 42] and this should be attributed to the high lability of this metal, even in so refractory matrices as sediments.

4.3. Analytical performance

The limits of detection (LOD) and quantitation (LOQ) of the overall procedure were determined from 10 procedural blanks, prepared and analysed in different days, in a traditional way; LOD = 3SD and LOQ = 10SD. Very satisfactory low limits (LOD = 1.8 ng g^{-1} and LOQ = 6.1 ng g^{-1}) were obtained. They are about 10-fold lower than those obtained in our laboratory applying classical calibration for USEPA method 3052, which in turn is in accordance with reported values for Cd in soils and sediments by ICP-MS after microwave-assisted digestion [43]. They are even 50 times lower than those obtained with an on-line flow injection (FI) system for slurry sampling chemical vapor generation (CVG) using DI-ICP-MS (0.15 µg g^{-1}) [22]. Further improvements can be obtained for food samples (LOD = 0.23 ng g^{-1}) using solid phase extraction (SPE) with chelating resins before microwave-acid total digestion [44].

As an attempt to validate the extraction method for the bioaccessible-Cd fraction based on diluted-HCl and analysis by ID-ICPMS, the BCR-701 CRM sediment, certified for the SM&T 3-step sequential extraction procedure, was analysed and the results compared with the sum of the three certified extractable fractions. That content was considered as an adequate equivalent to the bioaccessible metallic fraction [45].

Six aliquots of the BCR-701 CRM were submitted to the ID one-step extraction procedure, measured by triplicate by ICP-MS. The concentration of Cd was 11.89 ± 0.07 µg g^{-1} (mean value ± U, expanded uncertainty), which

overlapped with the sum of the certified contents of the 3-steps sequential extraction (11.34 ± 0.49 μg g^{-1}), 105 % recovery. The repeatability, expressed as the relative standard deviation (n = 6), was good: 0.9 %. Therefore, the proposed methodology can be considered accurate to assess the bioaccessible fraction of Cd in sediments, with the additional advantages of reducing significantly the amount of reagents and manpower time of the procedure, not only in the extraction step but in the instrumental measurement (recall that the method proposed here is an absolute method of quantification).

4.4. Application to a case-study

The one-step ID extraction procedure was applied to evaluate the potentially bioaccessible fraction of Cd in sediment samples from two Galician Rias (NW Spain). The evaluation of the coastal metal contamination in these sites is of great concern because they are exposed to an important population, industrial activities and aquaculture [3]. For these reasons, should a metal contamination occur, the environment and the local economy would have a major impact.

The ria of Arousa is the largest one of Galicia, characterised by important marine resources and it is one of the largest producers of mussels in the world. The ria of Vigo has important touristic and industrial activities and houses the National Park of the Atlantic Islands (a Spanish protected natural area).

The bioaccessible-Cd fractions observed for Arousa ranged from 0.10 to 0.58 μg g^{-1} (Figure 4). Highest values corresponded to the inner part of the ria (samples A1 and A2), as it seems logical because they are the zones affected most by anthropogenic contributions, such as industrial and small shipyard activities or sewage contributions. The ria of Vigo showed higher values than the Arousa one (Figure 4), because it supports more population and heavier industrial activities, in addition to a major harbour. The same trend for the extractable contents was observed for both rias: highest values corresponded to the inner and middle part of the rias, which decreased to their mouths, i.e., to open sea. A particular situation was encountered for sample V1, which showed the highest Cd-bioaccessible content, owing to its location in the estuarine zone of the ria of Vigo (near the San Simón inlet), which is a zone with

important periodic disturbances of the sediments owing to the cultivation of clam and cockles [46].

Total Cd concentrations found in the target samples (determined with the USEPA method 3052 and external calibration) are also shown in Figure 4. These results were used to calculate the extraction efficiencies, as the ratio of the bioaccessible/total contents (Figure 4), and values from 53 % to 97 % were achieved. This wide variation can be explained by considering that the metallic fraction associated to an anthropogenic origin is not fixed to the siliceous matrix of the sediments, and therefore it will be easily removed. Thus, the most contaminated sediments showed also the highest extractable fractions of Cd, as it was reported elsewhere [47].

A range between 0.01 μg g^{-1} to 0.20 μg g^{-1} is reported as background levels of Cd in sediments [3]. Accordingly, the concentration of Cd in the outer parts of both rias are similar or slightly superior to it. The sediments located at the inner part of the rias (as well as the middle part of the ria of Vigo, the main shipyard zone) exhibited contents two- to four-fold higher because of the anthropogenic inputs that these areas suffer. The same pattern was found by Quelle et al. [46] and no differences between the Cd contents in the sediments of both rias were reported. The obtained total-Cd values in this work were similar or lower than those reported for both rias (from not detected to 6.6 μg g^{-1} [3]).

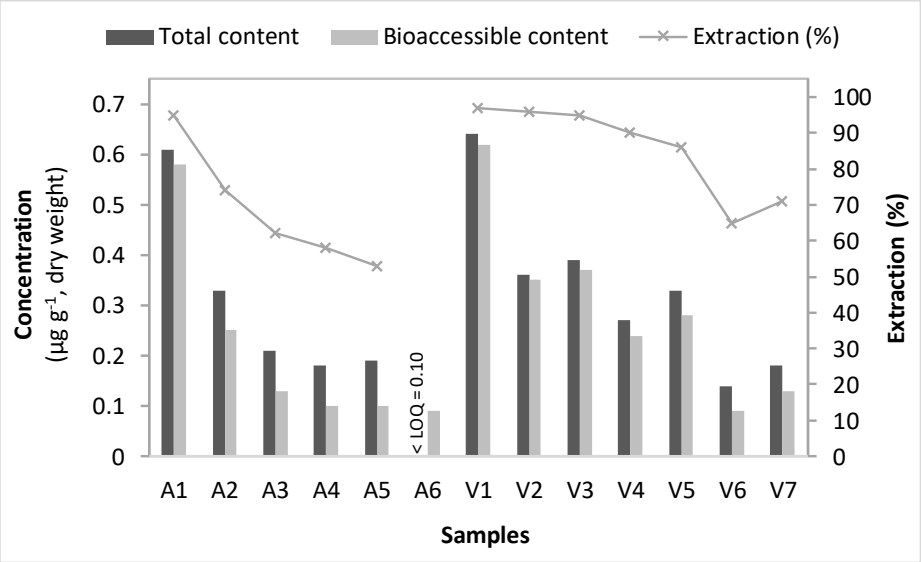

Figure 4. Bioaccessible-Cd fractions in sediments of the Rias of Arousa (A1-A6) and Vigo (V1-V7) obtained using the proposed one-step ID extraction procedure and their total content of Cd (estimating using the 3052 USEPA method). Extraction efficiencies were calculated referred to the total content.

5. Conclusions

The application of isotope dilution analysis to estimate the bioaccessible fraction of Cd in sediments was probed to be a satisfactory approach. ICP-MS with a collision cell as well adequate mathematical corrections allowed for free-interference Cd measurements.

On one hand, losses that may occur during extraction are overcome providing that the spike isotope is added before the extraction and that the isotopic equilibrium is achieved. On the other hand, the method is accurate and it shows that the bioaccessible-Cd fraction extracted by diluted-HCl equals the sum of the three extractable fractions certified for sediment BCR-701 (105 % recovery; 0.6 % RSD).

The time for the overall measurement is significantly reduced due to the efficiency of the ultrasound probe agitation and the use of an absolute quantitation method, avoiding external calibration. The method attained a very satisfactory detection limit, 1.8 ng g^{-1}. The consumption of reagents was reduced to a minimum, yielding reduced wastes and avoiding highly toxic solvents. Therefore, the method follows the Green Analytical Chemistry philosophy.

The applicability of this methodology was demonstrated analysing sediment samples from two coastal zones of Galicia (Northwest of Spain), namely, ria of Arousa and ria of Vigo. The results showed that the extractable fractions of Cd are higher for samples with important anthropogenic contributions, which coincide with high extraction efficiencies, because the anthropogenic fractions are not linked to the siliceous matrix of the sediments.

References

[1] Gäbler, H.E.; Bahr, A.; Mieke, B. Determination of the interchangeable heavy-metal fraction in soils by isotope dilution mass spectrometry. Fresenius J.Anal.Chem. 1999, 365:409.414.

[2] Nordberg, M.; Duffus, J.H.; Templeton, D.M. Explanatory dictionary of key terms in toxicology: Part II (IUPAC Recommendations 2010). Pure Appl.Chem. 2010, 82:679-751.

[3] Prego, R.; Cobelo-García, A. Twentieth century overview of heavy metals in the Galician Rias (NW Iberian Peninsula). Environ.Pollut. 2003, 121:425-452.

[4] Rao, C.R.M.; Sahuquillo, A.; López Sánchez, J.F. A review of the different methods applied in environmental geochemistry for single and sequential extraction of trace elements in soils and related materials. Water Air Soil Poll. 2008, 189:291-333.

[5] Comité Consultatif pour la Quantité de Matière (CCQM), Rapport de la 1er session, BIMP, Sèvres (France), 1995.

[6] Vassileva, E.; Hoenig, M. Determination of the total and extractable mass fraction of cadmium and lead in mineral feed by using isotope dilution inductively coupled plasma mass spectrometry. Anal.Chim.Acta, 2011, 701:37-44.

[7] Yu, L.L.; Davis, W.C.; Nuevo Ordonez, Y.; Long, S.E. Fast and accurate determination of K, Ca, and Mg in human serum by sector field ICP-MS. Anal.Bioanal.Chem. 2013, 405:8761-8768.

[8] García-Alonso, J.I.; Rodríguez-González, P. Isotope dilution mass spectrometry. RSC Publishing, Cambridge (UK), 2013.

[9] Vogl, J. Characterisation of reference materials by isotope dilution mass spectrometry. J.Anal.At.Spectrom. 2007, 22:475-492.

[10] McLaren, J.W.; Beauchemin, D.; Berman, S.S. Application of isotope dilution inductively coupled plasma mass spectrometry to the analysis of marine sediments. Anal.Chem. 1987, 59:610-613.

[11] Valles Mota, J.P.; Ruiz Encinar, J.; Fernández de la Campa, R.; García Alonso, J.I.; Sanz-Medel, A. Determination of cadmium in environmental and biological

reference materials using isotope dilution analysis with double focusing ICP-MS: a comparison with quadrupole ICP-MS. J.Anal.At.Spectrom. 1999, 14:1467-1473.

[12] Murphy, K.E.; Beary, E.S.; Rearick, M.S.; Vocke, R.D. Isotope dilution inductively coupled plasma mass spectrometry (ID ICP-MS) for the certification of lead and cadmium in environmental standard reference materials. Fresenius J.Anal.Chem. 2000, 368:362-370.

[13] Inagaki, K.; Takatsu, A.; Kuroiwa, T.; Nakama, A.; Eyama, S.; Chiba, K.; Okamoto, K. Certified sediment reference materials for trace element analysis from the National Metrology Institute of Japan (NMIJ). Anal.Bioanal.Chem. 2004, 378:1271-1276.

[14] Wysocka, I.; Vassileva, E. Determination of cadmium, copper, mercury, lead and zinc mass fractions in marine sediment by isotope dilution inductively coupled plasma mass spectrometry applied as a reference method. Microchem.J. 2016, 128:198-207.

[15] Hon, P.Y.T.; Chan, P.; Cheung, S.T.C.; Wong, Y. Evaluation of a proficiency test on cadmium and lead in herbal material using assigned reference values. Microchem.J. 2011, 98:44-50.

[16] Kim, S.H.; Lim, Y.; Hwang, E.; Yim, Y-H. Development of an ID ICP-MS reference method for the determination of Cd, Hg and Pb in a cosmetic powder certified reference material. Anal.Methods, 2016, 8:796-804.

[17] Christopher, S.J.; Thompson, R.Q. Determination of trace level cadmium in SRM 3280 multivitamin/multielement tablets via isotope dilution inductively coupled plasma mass spectrometry. Talanta, 2013, 116:18-25.

[18] Makishima, A.; Kitagawa, H.; Nakamura, E. Simultaneous determination of Cd, In, Tl and Bi by isotope dilution-internal standardization ICP-QMS with corrections using externally measured MoO^+/Mo^+ ratios. Geostand.Geoanal.Res. 2011, 35:57-67.

[19] Inagaki, K.; Takatsu, A.; Uchiumi, A.; Nakama, A.; Okamoto, K. Determination of cadmium in sediment by isotope dilution inductively coupled plasma mass spectrometry using a co-precipitation separation technique. J.Anal.At.Spectrom. 2001, 16:1370-1374.

[20] Murphy, K.E.; Vetter, T.W. Recognizing and overcoming analytical error in the use of ICP-MS for the determination of cadmium in breakfast cereal and dietary supplements. Anal.Bioanal.Chem. 2013, 405:4579-4588.

[21] Beary, E.S.; Paulsen, P.J. Selective application of chemical separations to isotope dilution inductively coupled plasma mass spectrometric analyses of standard reference materials. Anal.Chem. 1993, 65:1602-1608.

[22] Vieira, M.A.; Schwingel Ribeiro, A.; Felicidade Dias, L.; José Curtius, A. Determination of Cd, Hg, Pb and Se in sediments slurries by isotopic dilution calibration ICP-MS after chemical vapor generation using an on-line system or retention in an electrothermal vaporizer treated with iridium. Spectrochim.Acta Part B, 2005, 60:643-652.

[23] Thompson, R.Q.; Christopher, S.J. Novel separation for the determination of cadmium by isotope dilution ICP-MS samples containing high concentrations of molybdenum and tin. Anal.Methods, 2013, 5:1346-1351.

[24] Park, C.J.; Cho, K.H.; Suh, J.K.; Han, M.S. Determination of cadmium in sediment reference materials by isotope dilution inductively coupled plasma mass spectrometry with correction of tin isobaric interference using mass bias equations. J.Anal.At.Spectrom. 2000, 15:567-570.

[25] Gao, Y.; Shi, Z.; Zong, Q.; Wu, P.; Su, J.; Liu, R. Direct determination of mercury in cosmetic samples by isotope dilution inductively coupled plasma mass spectrometry after dissolution with formic acid. Anal.Chim.Acta, 2014, 812:6-11.

[26] Gardolinski, P.C.F.C.; Packer, A.P.; de Almeida, C.R.; Giné, M.F. Determination of Cd, Pb, Zn and Cu in sediment compartments by sequential Extraction and isotope dilution inductively coupled plasma mass spectrometry (ID-ICP MS). J.Braz.Chem.Soc. 2002, 13:375-381.

[27] Madrid, F.; Reinoso, R.; Florido, M.C.; Días Barrientos, E.; Ajmone-Marsan, F.; Davidson, C.M.; Madrid, L. Estimating the extractability of potentially toxic metals in urban soils: a comparison of several extracting solutions. Environ.Pollut. 2007, 147:713-722.

[28] Rosman, K.J.R.; Taylor, P.D.P. Isotopic composition of the elements (Technical Report). Pure Appl.Chem. 1998, 70:217-235.

[29] U.S. EPA (United States Environmental Protection Agency) Method 3052. Microwave assisted acid digestion of siliceous and organically based matrices. Washington (USA), 1996.

[30] García-Ruiz, S.; Petrov, I.; Vassileva, E.; Quétel, C.R. Cadmium determination in natural waters at the limit imposed by European legislation by isotope dilution and TiO_2 solid-phase extraction. Anal.Bioanal.Chem. 2011, 401:2785-2792.

[31] Vanhaecke, F.; de Wannermacker, G.; Moens, L.; Damns, R.; Latkoczy, C.; Prohaska, T.; Stingeder, G. Dependence of detector dead time on analyte mass number in inductively coupled plasma mass spectrometry. J.Anal.At.Spectrom. 1998, 13:567:571.

[32] Russ, G.P. Isotope ratio measurements using ICP-MS, in applications of inductively coupled plasma mass spectrometry. Champan and Hall, London (UK), 1987.

[33] Nelms, S.M.; Quétel, C.R.; Prohaska, T.; Vogl, J.; Taylor, P.D.P. Evaluation of detector dead time calculations models for ICP.MS. J.Anal.At.Spectrom. 2001, 16:333-338.

[34] Terán-Baamonde, J.; Andrade, J.M.; Soto-Ferreiro, R.M.; Carlosena, A.; Prada D. A simple procedure to select a model for mass discrimination correction in isotope dilution inductively coupled plasma mass spectrometry. J.Anal.At.Spectrom. 2015, 30:1197-1206.

[35] García Alonso, J.I. Determination of fission products and actinides by inductively coupled plasma-mass spectrometry using isotope dilution analysis: a study of random and systemic error. Anal.Chim.Acta, 1995, 312:57-78.

[36] Liu, H-C.; You, C.F.; Cai, W.J.; Chung, C-H.; Huang, K-F.; Chen, B-S.; Li, Y. Precise determination of seawater calcium using isotope dilution inductively coupled plasma mass spectrometry. Analyst, 2014, 139:734-741.

[37] Rodríguez-González, P.; Marchante Gayón, J.M.; García Alonso, J.I.; Sanz Medel, A. Isotope dilution analysis for elemental speciation: a tutorial review. Spectrochim.Acta Part B, 2005, 60:151-207.

[38] Townsend, A.T.; Palmer, A.S.; Stark, S.C.; Samson, C.; Scouller, R.C.; Snape, I. Trace metal characterization of marine sediment reference material MESS-3 and PACS-2 in dilute HCl extracts. Mar.Pollut.Bull. 2007, 54:226-246.

[39] Larner, B.L.; Palmer, A.S.; Seen, A.J.; Townsend, A.T. A comparison of an optimized sequential extraction procedure and dilute acid leaching of elements in anoxic sediments, including the effects of oxidation on sediment metal partitioning. Anal.Chim.Acta, 2008, 608:147-157.

[40] Duzgoren-Aydin, N.S.; Ayula, B.; Willet, K.L.; Khan, I.A. Determination of total and partially extractable solid-bound element concentrations using collision/reaction cell inductively coupled plasma-mass spectrometry and their significance in environmental studies. Environ.Monit.Assess. 2011, 172:51-66.

[41] Pueyo, M.; Mateu, J.; Rigol, A.; Vidal, M.; López-Sánchez, J.F.; Rauret, G. Use of the modified BCR three-step sequential extraction procedure for the study of trace element dynamics in contaminated soils. Environ.P. 2008, 152:330-341.

[42] Kubová, J.; Matús, P.; Bujdos, M.; Hagarová, I.; Medved, J. Utilization of optimized BCR three-step sequential and dilute HCl single extraction procedures for soil-plant metal transfer predictions in contaminated lands. Talanta, 2008, 75:1110-1122.

[43] Falciani, R.; Novaro, E.; Marchesini, M.; Gucciardi, M. Multi-element analysis of soil and sediment by ICP-MS after a microwave assisted digestion method. J.Anal.At.Spectrom. 2000, 15:561-565.

[44] Zhu, Y.; Chiba, K. Determination of cadmium in food samples by ID-ICP-MS solid phase extraction for eliminating spectral-interferences. Talanta, 2012, 90:57-62.

[45] Sutherland, R.A. Comparison between non-residual Al, Co, Cu, Fe, Mn, Ni, Pb and Zn released by a three-step sequential extraction procedure and a dilute hydrochloric acid leach for soil and road deposited sediment. Appl.Geochem. 2002, 17:353-365.

[46] Quelle, C.; Besada, V.; Andrade, J.M.; Gutiérrez, N.; Schultze, F.; Gago, J.; González, J.J. Chemometric tools to evaluate the spatial distribution of trace metals in surface sediments of two Spanish rías. Talanta, 2011, 87:197-209.

[47] Prego, R.; Filgueiras, A.V.; Santos-Echeandía, J. Temporal and spatial changes of total and labile metal concentration in the surface sediments of the Vigo Ria (NW Iberian Peninsula): influence of anthropogenic sources. Mar.Pollut.Bull., 2008, 56:1022-1042.

V.3.

AN ISOTOPE DILUTION INDUCTIVELY COUPLED PLASMA MASS SPECTROMETRY (ID-ICP-MS) PROCEDURE TO ASSESS THE BIOACCESSIBLE FRACTION OF CHROMIUM IN SEDIMENTS

1. Abstract

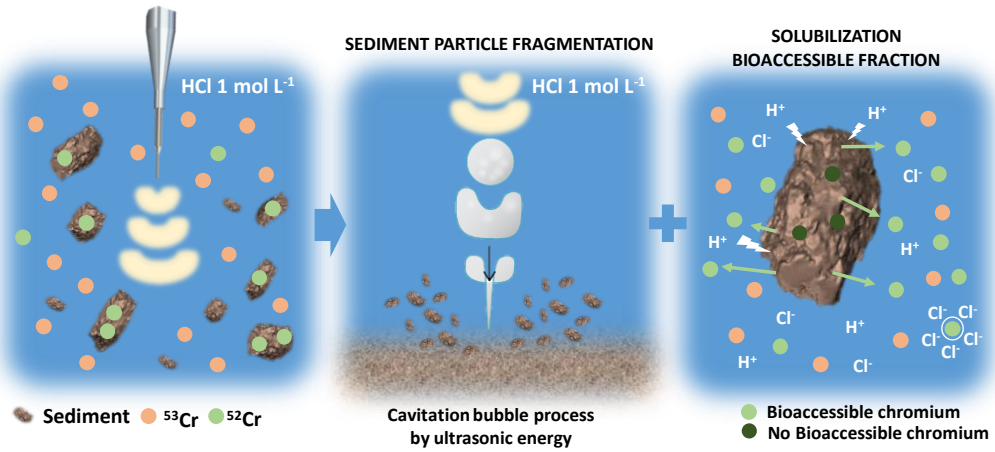

The bioaccessible fraction of chromium in marine sediments is determined first time using isotope dilution ICP-MS. For this, the ^{53}Cr enriched isotope was equilibrated before extraction with native Cr. The parameters affecting trueness and precision were evaluated to minimize the errors; namely: spectral interferences, detector dead time, mass discrimination factor and selection of the optimum sample/spike ratio. The leached fraction obtained after a one-step-dilution with hydrochloric acid correlated fine with the sum of the 3-step sequential extraction procedure of the Standards, Measurements and Testing Programme (SM&T), as verified using the BCR-701 sediment to validate the method. A satisfactory 100 % recovery was attained. The extraction procedure itself was studied spiking the enriched isotope before and after the extraction step, where from it was deduced that only the first option was acceptable. Three additional reference sediments whose total chromium

content are certified were also analysed. The method provided good reproducibility (2.7 %, RSD) and low detection limit, 16.7 ng g^{-1}. The bioaccessible fractions of Cr in sediments from two environmentally and economically important areas of Galicia (rias of Arousa and Vigo, NW of Spain) were studied using the method developed here.

The results discussed in this chapter are summarized in the scientific publication:

An isotope dilution inductively coupled plasma mass spectrometry (ID-ICP-MS) procedure to assess the bioaccessible fraction of chromium in sediments.

J. Terán-Baamonde, A. Carlosena, R.M. Soto-Ferreiro, J.M. Andrade and D. Prada.

Journal of Analytical Atomic Spectrometry (under revision), 2017.

2. Introduction

Metals are stable and persistent contaminants that tend to accumulate in the environmental compartments because they cannot be degraded easily. They are transported through the aquatic systems where they quickly adsorb on the solid material. Hence, they incorporate into the sediments, which become a relevant sink for metals, whose concentrations there are much higher than in adjacent water [1].

From an analytical viewpoint, the different forms in which metals can be presented into the environment and the fractions where they can accumulate gave rise to a large list of extraction procedures, extractants, number of steps and operational conditions [2, 3]. One of the most popular working schemes is the 3-step sequential extraction procedure developed by the SM&T (Standards, Measurements and Testing Programme of the European Commission), which determines three metal fractions as acid-extractable, reducible and adsorbed, according to the extractant employed [4]. The main disadvantages of the sequential extraction protocols are their high workload, time-consumption and the possibility of a metal redistribution (by readsorption) among phases. These drawbacks led to the use of partial (single) extraction protocols, which provide less specific information but allow the study of the metallic fraction that is easily released from the sediment and, therefore, bioaccessible to the surrounding environment [5, 6].

A common selection is to use diluted HCl as extractant agent, due to its ability to extract environmentally relevant geochemical fractions [5], and its acidic and reducing properties that dissolve calcareous materials, attack Fe and Mn oxides (the major sink of metals in oxic sediments) [7] and decompose organic phases and amorphous sulphides (control metal bioaccessibility in anoxic sediments) [8]; combined to the chelatant property of Cl^-, which is a strong ligand [9]. Several authors claimed that results obtained by diluted HCl extraction can be related to the sum of the 3-step SM&T sequential extraction procedure [5, 6, 10]. This fraction may be assimilated to what IUPAC defined as bioaccessible, “the potential for a substance to come in contact with a living organism and then interact with it”, as opposed to bioavailability, “the extent of the absorption of a substance by a living organism compared to a standard system” [11]. In particular, chromium is a toxic and persistent metal that is often

found in contaminated sediments, and that is usually associated to smelters and plating activities [12]. With regard to the subject of this study, the bioaccessible fractions of chromium have been evaluated using single [13 – 17] and sequential [18, 19] procedures, a comparison of which can be found elsewhere [20].

Despite isotope dilution analysis (IDA) is frequently applied to determine the total content of chromium in sediments [21, 22]; no report was found in literature applying it to determine its bioaccessible content in such a matrix.

IDA is a time-efficient alternative to classic quantitation approaches as it avoids external calibration (i.e. the preparation of a series of calibration solutions) and compensates for matrix interferences. In this sense, it can be considered a one-point internal-calibration method, providing far superior data quality than traditional procedures that do not use isotopic information [23]. IDA is based on modifying the elemental isotope composition in the sample by adding an isotopically enriched form of the element and the subsequent measurement of the isotope ratio of the mixture (R_m) by elemental mass spectrometry, frequently inductively coupled plasma mass spectrometry (ICP-MS). Once the equilibrium between the additioned enriched spike and the endogenous element is reached, any source of uncertainty (e.g. matrix effects or losses) in subsequent working steps does not affect the isotope ratios, resulting in greater accuracy in analytical measurements [24 ,25]. Therefore, isotope dilution applications are much more robust than conventional methodologies so less-careful sample preparation can be acceptable.

ID-ICP-MS was employed to determine chromium and their species in a wide range of matrices, as polycarbonate [26], plastics [27], drinking water [28, 29], seawater [30], silicate materials [31, 32] or soil [33]. Recently, a new strategy to effectively quantitate hexavalent, soluble trivalent and insoluble chromium species in soil [34] was presented. However, only scarce references were found dealing with sediment analysis. Thus, McLaren et al. [22] applied first time isotope dilution to determine 11 trace elements, including chromium, improving significantly the precision of the analysis. A reference sediment candidate was certified for chromium by ID-ICP-MS [21]. In both cases, a complete dissolution of the sediments was performed by a laborious and lengthy digestion process (4 -24 h). However, depending on the acids employed,

Cr can evaporate as CrO_2Cl_2 (b.p. 117 °C) when is heated with $HClO_4$ [21], or get incorporated into fluorides before the decomposition of chromite when HF is used [35], leading to an isotopic disequilibrium between the sample and the spike.

Noteworthy, an accurate determination of Cr by ID-ICP-MS requires avoiding or minimizing the isobaric and polyatomic interferences that affect it. Chromium has four naturally occurring isotopes - ^{50}Cr, ^{52}Cr, ^{53}Cr and ^{54}Cr – being free of any isobaric interference the 52 and 53 isotopes. ^{50}Cr and ^{54}Cr are interferred by ^{50}Ti, ^{50}V and ^{54}Fe, which requires either a mathematical correction or instrumental solutions [32]. Polyatomic ion interferences from carbon, chloride or oxide (e.g. $^{36}Ar^{16}O^+$, $^{37}Cl^{16}O^+$, $^{35}Cl^{16}O^1H^+$, $^{40}Ar^{12}C^+$, etc.) can enhance significantly the signals of ^{52}Cr and ^{53}Cr. In these cases, traditional mathematical corrections [36] have been replaced by the use of high resolution ICP-MS modes or collision/reaction cells, as demonstrated when determining chromium in honeys [37], seawater [30] or silicates [35]. Other alternatives are based on allowing an effective matrix separation, e.g. for water [30, 38, 39].

In the present work, ID was applied to determine the bioaccessible fraction of Cr in marine sediments by ICP-MS, for which no references in literature were found. The ^{53}Cr enriched isotope was added before the extraction process for its equilibration with native Cr solubilized from the sample, using ultrasonic probe agitation and diluted HCl. The parameters affecting accuracy were evaluated in order to minimize spectral interferences, detector dead time, mass discrimination factor and selection of the optimum sample/spike. The fraction obtained using this methodology will be correlated with the sum of the 3-step sequential extraction procedure of the SM&T using the BCR-701 sediment (encompassing the exchangeable, reducible and oxidisable fractions) to validate the method. Furthermore, to study the performance of the extraction procedure and exploit the advantages of isotope dilution analysis, additional assays adding the enriched spike to the acid extract obtained after the extraction step were also performed. Three reference sediments with certified total chromium contents were considered as well. As a practical case study, sediments from two Rias of Galicia (Arousa and Vigo, NW of Spain) were analysed.

3. Experimental

3.1. Instrumentation

A VC50-1 ultrasonic probe (50 W, 20 KHz) equipped with a CV18 titanium probe (Sonic Materials, Newtown, CT, USA) was utilized to perform the extractions. A microwave oven (Anton Paar Multiwave, Graz, Austria) equipped with a built-in magnetic stirrer, a fibre-optic temperature sensor and a pressure sensor and a basic six-position extraction rotor as well as high pressure Teflon vessels were used for the digestions.

Isotope ratio measurements were performed on a XSERIES 2 Quadrupole ICP-MS (Thermo Scientific, Bremen, Germany) which included a collision/kinetic energy discrimination cell. The instrument was equipped with standard Ni-cones, a Meinhard nebuliser and a Scout double pass spray chamber refrigerated at 4 °C. An ASX-520 autosampler (CETAC Technologies, USA) was employed. The instrumental settings on the ICP-MS are summarised in Table 1. The nebulizer gas flow rate, torch position and ion lens settings were optimised for higher sensitivity and minimal signals for CeO^+/Ce (< 1.5%), monitoring a 10 µg L^{-1} standard solution of Be, In and U in 1% (v/v) HNO_3.

Table 1. Instrumental operating conditions and acquisition parameters used in ICP-MS.

ICP operation conditions	
Rf power	1.35 kW
Nebulizer gas flow	0.75 L min^{-1}
Auxiliary gas flow	1.00 L min^{-1}
Cooling gas flow	14 L min^{-1}
He-KED	4.00 L min^{-1}
Acquisition parameters	
Acquisition mode	Pulse counting
Measurement mode	Scan
Number of sweeps	100
Dwell time (ms)	10
Isotope masses	$^{50, 52, 53, 54}Cr$ – ^{50}Ti – ^{56}Fe

3.2. Chemicals and materials

High-purity water, 18.2 MΩ·cm resistivity, obtained from a Milli-Q®Direct purification device (Millipore Co., Bedford, MA, USA) was used. Hydrochloric (37 %) and nitric (65 %) acids were of suprapur quality (J.T. Baker, Phillipsburg, NJ, USA). Stock standard solutions of Cr, Fe and Ti (1000 mg L^{-1}) for ICP analysis (SCP Science) were used to prepare working solutions for studying the detector dead time, the mass discrimination factor (referred to as "K factor") and spectral interferences. Natural isotopic compositions for Cr were assumed to agree with IUPAC data [40] in all samples and solutions.

The enriched ^{53}Cr isotopic standard (as oxide, 97.7 %) was from Cambridge Isotope Laboratories (USA). Enriched stock solutions were prepared following the 6800 EPA method [41], by dissolving the appropriate amount of the solid with 8 mL of concentrated perchloric acid, heating on a hot plate until complete dissolution and evaporating to 2 mL. Working spike solutions were prepared by subsequent gravimetric dilution of the enriched stock solution with 2 % (v/v) HNO_3.

Different reference materials were used for the validation scheme applied in this work: Lake sediment BCR-701, supplied by the Institute for Reference Materials and Measurements (IRMM); New York/New Jersey waterway sediment SRM-1944, from the National Institute of Standards & Technology (NIST) and harbour sediments PACS-2 and PACS-3 from the National Research Council of Canada (NRCC). The samples from the Rias of Arousa and Vigo, that constitute the case study, were collected by the Spanish Institute of Oceanography (IEO), in 2011. They had been lyophilized and kept in dark bottles until analysis.

All glassware and plasticware were soaked in 10 % (v/v) HNO_3 for 24 h and rinsed with high-purity water at least three times before use. Nylon syringe filters, 0.45 μm, 30 mm diameter (Thermo Scientific, Tennessee, USA) were used to filter the extracts.

3.3. Sample preparation

The extraction procedure consists of weighing 0.0250 g of the sample in polyethylene cups (1.2 mL capacity) and adding 1.0000 g of 1 mol L^{-1} HCl.

Agitation is performed during 16 min with an ultrasonic probe introduced through a cap hole. The extracts were filtered and stored in polyethylene cups at 4 °C until their analysis. Procedural blanks were prepared in the same manner.

The ID analysis was performed adding the enriched ^{53}Cr spike directly to the aliquot of the sediment sample to be analyzed. For this, the extractant (1 mol L^{-1} HCl) was spiked with the adequate amount of the enriched standard (as detailed in the following sections). In order to study the performance of the extraction procedure, additional assays adding the enriched spike to the acid extract obtained after the extraction step were carried out.

The sediment samples from the rias and the BCR-701 sediment were submitted to the microwave-based digestion procedure (USEPA Method 3052) to determine their total content on Cr [42]. The digests so obtained were analysed by ICP-MS, using conventional calibration and ^{45}Sc as internal standard. For quality control purposes, the SRM-1944, PACS-2 and PACS-3 CRMs were also analysed in this way. The confidence intervals of both the certified contents and the experimental values overlapped largely, which validated the procedure employed for total Cr in these samples.

3.4. Isotope dilution analysis

The ID method is based on adding a known amount of an enriched isotope of the element of interest to a sample. The altered isotope ratio of the mixture is measured by ICP-MS after equilibration of the spiked isotope with the native analyte. In the present work ^{52}Cr was used as the natural most abundant isotope and ^{53}Cr as the spiking one. Both isotopes are free from isobaric interferences.

All ICP-MS measurements (see setup in Table 1) were done by triplicate and the concentration of Cr in the samples (C_s) was calculated using the well-known equation for isotope dilution [23], measuring the $^{52}Cr/^{53}Cr$ ratio. Previously a 5-fold dilution of the sediment extracts was carried out.

Note that the enriched ^{53}Cr working solutions were characterized determining the abundances of the four Cr isotopes by ICP-MS. The spike solutions were prepared by triplicate, measuring five times each, and calculating

the $A^i = \frac{R^i}{\sum_{i=1}^{n} R^i}$ ratio; where A^i is the abundance of isotope *i* in the enriched spike and R^i represents each of the isotope ratios calculated (for Cr, *i* takes values of 50, 52 and 54) with respect to a given reference isotope, here ^{53}Cr [43]. The concentration of the spike solutions was calculated by reverse isotope dilution using the equation derived from the isotope dilution equation [23].

4. Results and discussion

4.1. Quantification by isotope dilution ICP-MS

The parameters affecting accuracy of the ID-ICP-MS measurements were carefully evaluated in order to minimize their sources of errors. These were: spectral interferences, detector dead time, mass discrimination factor and the sample/spike ratio [23].

4.1.1. Spectral interferences

The polyatomic interferences due to the plasma gas, solvent, matrix and/or entrained air were eliminated using a collision kinetic energy discrimination cell with a He gas flow containing 7 % H_2, which yielded an energy discrimination process.

The isobaric interferences were corrected mathematically measuring an alternative isotope of the interfering element. Throughout this study, ^{53}Cr and ^{52}Cr were used as spike and major isotopes, respectively, because they are not affected by these effects under the experimental conditions. Ti and Fe overlap with isotopes 50 and 54 of Cr, respectively, so ^{48}Ti and ^{56}Fe were also measured. The ^{50}V interference was considered negligible thanks to its very low natural abundance [32]. Despite masses 50 and 54 of Cr were not used for quantitation purposes, they must be corrected for isobaric interferences in order to characterize the spike. The following equations were applied, using the intensities provided by aqueous solutions with natural isotopic composition:

I_{corr} (^{50}Cr) = I_{exp} (^{50}Cr) – (f_{Ti} x I_{exp} (^{48}Ti)); I_{corr} (^{54}Cr) = I_{exp} (^{54}Cr) – (f_{Fe} x I_{exp} (^{56}Fe)); where f_{Ti} = I (^{50}Ti) / I (^{48}Ti) and f_{Fe} = I (^{54}Fe) / I (^{56}Fe).

4.1.2. Dead time of the detector

Nonlinearity of ion-counting detectors, as electron multipliers, occurs at high counting rates, due to the time required for the electronics to register and count a single ion (a few nanoseconds). A second ion arriving at the detector during this time interval will not be counted, leading to the so-called detector dead time [23]. Since the dead time may vary as a function of the element mass number, it is experimentally determined using the target element itself. The Russ approach, widely used for this purpose, was applied in this work and the dead time determination was repeated periodically as it may be affected by the aging of the detector [44].

Eight Cr standard solutions of natural isotopic composition in the 50 - 200 µg L^{-1} range were measured five times using a dead time of 0 ns. The average intensities were corrected for different dead time (τ) values, ranging from 0 to $1 \cdot 10^{-4}$ s, using $I_{corr} = I_{exp}/(1- I_{exp} . \tau(s))$.

Then, the $^{53}Cr/^{52}Cr$ isotope ratio was calculated and the normalized isotope ratios (R_{exp}/R_{theo}) were plotted *versus* the assumed dead times values, in ns (Figure 1). The correct dead time corresponds to the intersection of the lines obtained for the different analyte concentration levels; at this point the measured isotope ratio is independent on the concentration of the element. This value (here 35 ± 5 ns,) was introduced in the software of the instrument for automatic correction of all measured intensities.

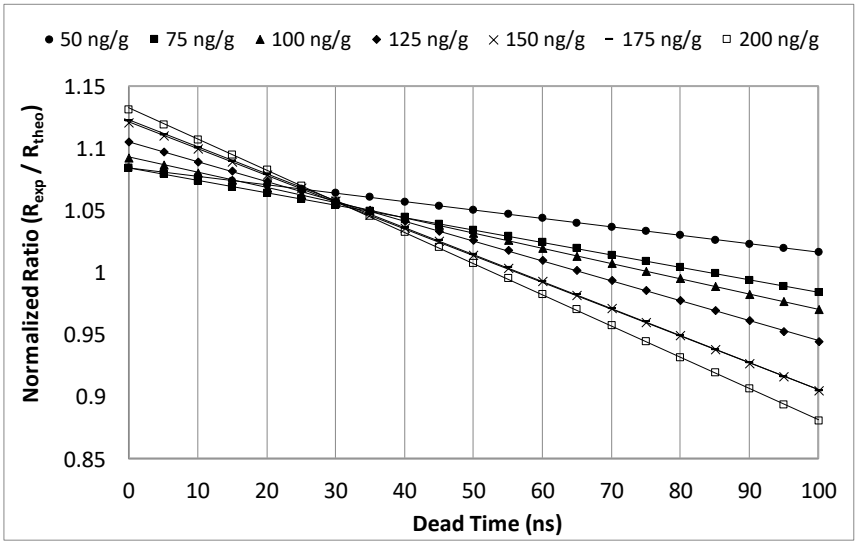

Figure 1. Determination of detector dead time for the $^{53}Cr/^{52}Cr$ isotope ratio at different Cr concentrations.

4.1.3. Mass discrimination factor

Mass discrimination occurs in ICP-MS because heavier isotopes are transmitted more efficiently than lighter isotopes in the mass spectrometer. This effect leads to a measurable mass bias in the experimental isotope ratios that has to be corrected for. In general, two approaches can be applied: an external standardization where the isotope of interest is measured in a standard solution of the analyte, and an internal standardization which determines *K* in the unknown samples by means of either a known isotope ratio of an element added to the samples, or using a pair of invariant isotopes of the analyte [23].

In this work, an external standardization approach is used. Specifically, the molar-response curve was adjusted to a power function, which demonstrated to be the more adequate model when measuring Cr [45]. The isotope ratios (ratioted against the 53 reference mass) were obtained from measurements made on a Cr natural standard solution. Figure 2 shows a straight line, whose slope is the discrimination factor (*K*). This factor was calculated in each working session as the mean of the values obtained at the beginning and at the end of the measurement sequence.

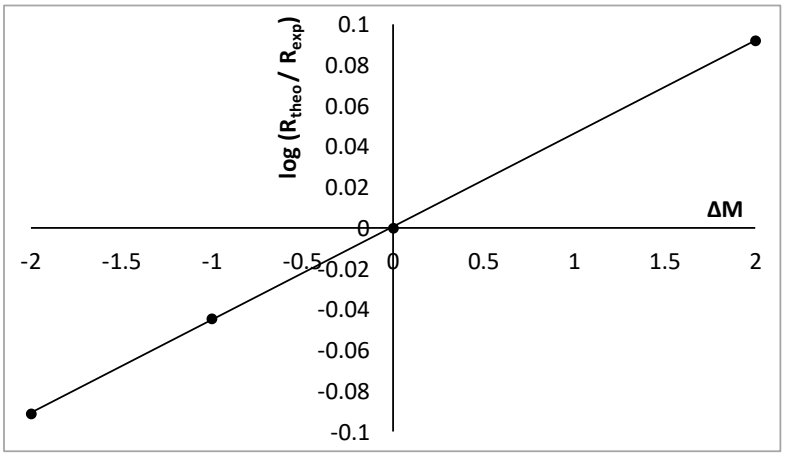

Figure 2. Graphical representation of the linearized power function for the determination of the K factor as the slope of the straight line.

4.1.4. Sample/spike ratio

An optimum sample/spike ratio is critical for achieving high precision in the isotope ratio calculated by ID-ICP-MS. In this sense, selecting the amount of reference solution added as spike is a trade off among several factors, including results from preliminary measurements, the characteristics of the spiking materials, the required final uncertainty, a sufficiently high counting rate and dead time effects [46]. Thus, it is possible to state that the uncertainty associated to the concentration calculated by isotope dilution is a function of the uncertainty in the measured isotope ratio in the mixture (R_m), therefore the optimum value of R_m should be studied.

The representation of the so-called error magnification factor f(R) versus the theoretical isotope ratio (R_m) provides a U-shapped error curve, where a theoretical R_m value can be selected in order to obtain the minimum value of f(R). Then, considering the approximate content of analyte in the sample, the amount of spike to be added is calculated to fulfil the theoretical value of R_m [47]. The curve obtained for the $^{52}Cr/^{53}Cr$ ratio is shown in Figure 3, with the flat zone (providing the lowest f(R) values) ranging approximately from 0.03 to 7.00. The R_m value will be selected within this interval to add a minimum amount of spike (which, besides helps reducing costs) without increasing the error significantly. Here, the R_m value was 1.0, with a corresponding error magnification factor f(R) = 1.15, which agrees with other reports (e.g. [35, 46]).

Therefore, considering the extraction procedure described above and accounting for the fraction of Cr extracted, 1.0000 g of 1 mol L^{-1} HCl containing 3.00 µg kg^{-1} of spike was added to 0.0250 g of sediment sample.

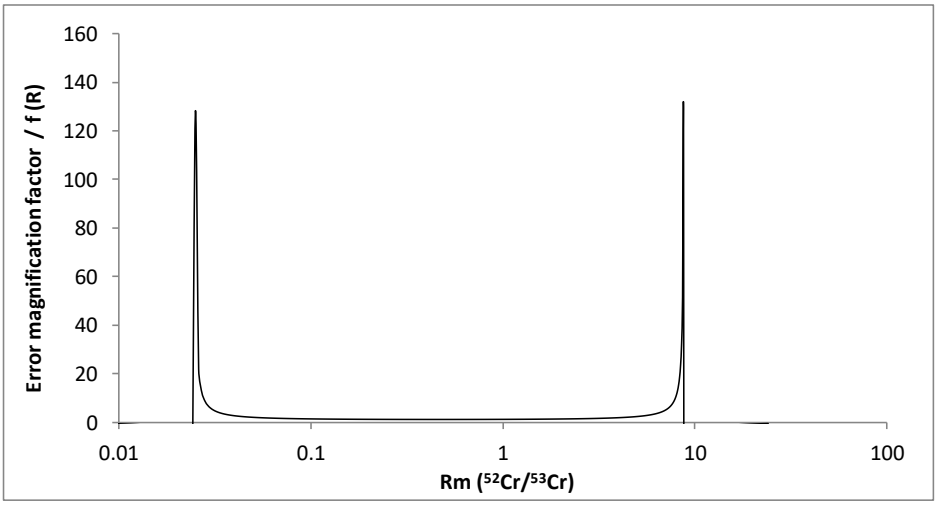

Figure 3. Error magnification factor curve for the ^{52}Cr / ^{53}Cr isotope ratio.

4.2. Assessment of the extraction method

Four CRMs were analysed (BCR-701, PACS-2, PACS-3 and SRM-1944) in two parallel assays where the ^{53}Cr-spike was added before and after the extraction process (in the second case, the ^{53}Cr-spike was added to the acid extracts). In both approaches, the ratio between the metal in the extracted fraction (here, bioaccessible-Cr) and its total content was calculated. Some authors recommend this evaluation as a routine quality control when analysing marine sediments [13]. Since BCR-701 does not report total Cr, it was obtained experimentally with external calibration by ICP-MS applying the USEPA 3052 method (microwave-assisted digestion of siliceous matrices).

Table 2 summarizes the results obtained, which allow drawing several conclusions. First, it is seen that the extraction efficiencies (expressed as percentages) increase for all CRMs when the isotope is added before the extraction step: from 12-49 % (after the extraction) to 16-58 % (before the extraction). Recall that dissolved-Cr may form easily volatile species. Therefore,

adding the enriched isotope before the extraction guarantees that ID can overcome any possible analyte loss during extraction.

Second, the low extraction efficiencies can be justified considering that Cr is associated to chromite in silicate-based materials, which is very difficult to dissolve [35]. Thus, as it was expected, a large fraction of this metal remains in the sediment, being no-bioaccessible. Townsend et al. [13] and Larner et al. [6] showed almost the same recovery (13 %) as that obtained here for PACS-2 (in these cases, Cr was measured after a 1 mol L^{-1} HCl partial extraction during 4 h on an orbital shaker at room temperature). Besides, Larner et al. [6] found a strong correlation between the partial extraction and the sum of the three labile steps of the modified SM&T sequential extraction procedure, although they did not analyze a sediment with these fractions certified, like the BCR-701 one. Choi et al. [15] used the same approach as Townsend et al. [23] for PACS-2, although their results do not agree at all (87 %), likely because the way in which the extraction efficiency was calculated by the former was not indicated and they reported too high extraction efficiencies for all elements.

Third, the extraction percentages shown in Table 2 are different for each sample, which is a positive fact because they reveal that the method is indeed extracting the bioaccessible fraction of chromium associated to each sample. Contrary to complete acid digestions where all the metal is solubilized, the method proposed here releases only Cr associated to labile fractions and do not break the silicate lattice of the sediments. It is clear that such fraction will depend on both the sources of Cr in the environmental compartment and the sample matrix.

Table 2. Bioaccessible-Cr contents (μg g^{-1} dry weight, ± *U**) obtained for four reference sediments using the proposed one-step ID extraction procedure, adding the isotope spike before and after extraction step. Extraction efficiencies were calculated referred to the total content.

		Spike added after extraction		**Spike added before extraction**	
CRM	Total Certified content	Bioaccessible content	Extraction (%)	Bioaccessible content	Extraction (%)
BCR-701	328.7±8.38(**)	138.11 ± 0.82	42	191.18 ± 2.59	58
PACS-2	90.7 ± 4.6	10.95 ± 0.39	12	14.93 ± 0.54	16
PACS-3	91.6 ± 4.0	13.03 ± 1.39	14	16.93 ± 1.52	18
SRM-1944	266 ± 24	131.17 ± 6.66	49	141.52 ± 3.22	53

(*) U, expanded uncertainty. The coverage factor, k, is the Student´s t-value for a 95% confidence interval with 6 degrees freedom.

(**) Not certified, obtained applying USEPA method 3052.

4.3. Analytical performance

The limits of detection (LOD) and quantitation (LOQ) of the overall procedure were calculated in a traditional way from 10 procedural blanks, prepared and analysed in different days: LOD = 3SD and LOQ = 10SD (SD = standard deviation). Very satisfactory low limits (LOD = 16.7 ng g^{-1} and LOQ = 55.8 ng g^{-1}) were obtained. They are about 3-fold lower than those obtained in our laboratory applying classical calibration, which in turn is in accordance with reported values for Cr in soils or sediments by ICP-MS after microwave-assisted digestion [48]. For silicate materials some improvements were reported (LOD = 7 ng g^{-1}) using high resolution ID-ICP-MS [35].

To validate the extraction method for the bioaccessible-Cr fraction in sediments based on the use of diluted-HCl and its subsequent analysis by ID-ICP-MS, the BCR-701 CRM sediment was analysed and the results were compared with the sum of the three certified extractable fractions. That sum was considered as an adequate equivalent to the bioaccessible metallic fraction [10].

Six aliquots of the BCR-701 CRM were submitted to the ID one-step extraction procedure, measured by triplicate by ICP-MS. The concentration of Cr was 191.2 ± 2.6 μg g-1 (mean value ± U, expanded uncertainty), which overlapped with the sum of the certified contents of the 3-steps sequential extraction (191.0 ± 7.3 μg g^{-1}), 100 % recovery. The repeatability, expressed as the relative standard deviation (n = 6), was good: 2.7 %. Therefore, the proposed methodology can be considered as a reliable approach to assess the bioaccessible fraction of Cr in sediments, with the additional advantages of reducing significantly the amount of reagents and manpower time of the procedure, not only in the extraction step but in the instrumental measurement (recall that the method proposed here is an absolute method of quantification).

4.4. Application to a case-study

The one-step ID extraction procedure was applied to evaluate the potentially bioaccessible fraction of Cr in sediment samples from two Galician Rias (NW Spain). The assessment of the coastal metallic pollution in these sites is of importance because they hold an important population, with industrial activities and aquaculture areas [49]. For these reasons, should a metal contamination occur, the environment and the local economy would suffer a major impact.

The ria of Arousa is the Galician (NW Spain) largest estuary, characterised by relevant marine resources and being one of the most important harvesting areas of mussels in the world. The ria of Vigo has important touristic and industrial activities and houses the National Park of the Atlantic Islands (a Spanish protected natural area).

Figure 4 summarizes the results obtained using ID-ICP-MS. The bioaccessible-Cr fractions observed for Arousa (samples denoted by "A") ranged from 4.16 μg g^{-1} to 61.63 μg g^{-1}. Very few historical data on metals extracted by HCl in these two rias were found for comparison. Real et al. [50] reported very high extractable concentrations for Cr (and Cu) in the upper part of the Ria of Arousa, likely derived from effluent discharges to the Ulla River (mainly, a tanning factory effluent and an old copper mine). They reported high values of Cr (from 84 μg g^{-1} to 252 μg g^{-1}) in the lower estuary. We found out that the bioaccessible fraction of Cr was much lower for this area (26.35 μg g^{-1} to 61.63

μg g^{-1}). This difference was attributed to the time elapsed between both studies, about 20 years, during which the main contamination sources ceased their activities and some environmental protection regulations were enforced.

No relevant differences were found between the bioaccessible-Cr concentrations of the sediments withdrawn from the ria of Vigo (from 9.41 μg g^{-1} to 15.22 μg g^{-1}). These values are low and suggest that the ria of Vigo is not polluted significantly by chromium (or, at least, that Cr is not bioaccessible easily), despite it suffers anthropogenic activities derived from a dense population, inputs from food factories and holds several shipyards and many activities related with mussel rafts and farming of clams and cockles.

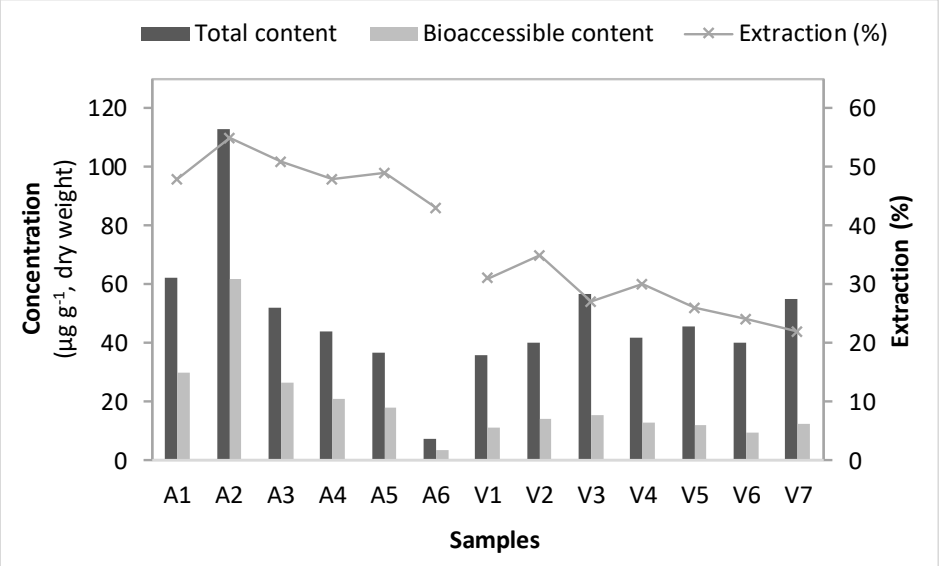

Figure 4. Bioaccessible-Cr fractions in sediments of the Rias of Arousa (A1-A6) and Vigo (V1-V7) obtained using the proposed one-step ID extraction procedure and their total content of Cr (estimating using the 3052 USEPA method). Extraction efficiencies were calculated referred to the total content.

The total Cr concentrations found in the sediment samples, determined with the 3052 USEPA method and validated with 3 CRMs used as quality controls within the analyses batches, are also shown in Figure 4. Previous publications on total-Cr in these two Galician rias reported values from 30 μg g^{-1} to 54 μg g^{-1}

and they were considered as background levels [51]. In our study here, the concentrations for the ria of Arousa varied in a wider range (7.10 μg g^{-1} - 112.72 μg g^{-1}); while those for the ria of Vigo were more similar (35.93 μg g^{-1} - 56.56 μg g^{-1}).

All those results were used to calculate the so-called "extraction efficiencies", as the ratio between the bioaccessible and the total contents (Figure 4), which yielded values from 22 % to 62 %. Comparing the two rias, the ria of Arousa showed the highest extractions (48 % - 62 %), whilst the yields for the ria of Vigo were around 22 % - 35%. This relevant difference can be explained by considering that the metallic fraction associated to an anthropogenic origin is not fixed to the siliceous lattice of the sediments, and therefore it will be removed more easily than from the parent material. Thus, it appears that the sediments from the ria of Arousa support more anthropogenic inputs containing Cr than the ria of Vigo, which leads to highest extractable fractions of Cr, as it was reported elsewhere [49,51].

5. Conclusions

The application of a partial extraction with diluted HCl to estimate the bioaccessible fraction of Cr in sediments was probed to be a satisfactory approach, because the fraction extracted equal the sum of the three extractable fractions certified for sediment BCR-701 (100 % recovery; 2.7 % RSD).

The losses that may occur during the extraction process are overcome by spiking the samples with an enriched isotope before the extraction. The subsequent isotope dilution ICP-MS analysis is free from interferences thanks to the use of a collision cell and adequate mathematical corrections.

The overall method is accurate, constitutes an absolute quantitation method, avoids external calibration and yields very satisfactory detection and quantification limits, 16.7 ng g^{-1} and 55.8 ng g^{-1}, respectively. In addition, the analysis time is reduced significantly due to the efficiency of the ultrasound probe agitation, and the consumption of reagents was reduced to a minimum, leading to reduced wastes and avoiding the use of toxic solvents. Therefore, it can be affirmed that the method follows the Green Analytical Chemistry philosophy.

The applicability of this methodology was demonstrated analysing sediment samples from two coastal zones of Galicia (Northwest of Spain), namely, ria of Arousa and ria of Vigo. The results showed that the extractable fractions of Cr are higher for samples associated to anthropogenic inputs, which in turn yields high extraction efficiencies, because the anthropogenic inputs are not linked to the siliceous matrix of the sediments.

References

[1] Tessier, A.; Campbell, P.G.C. Partitioning of trace metals in sediments, in: Metal Speciation: Theory, Analysis and Application, eds. Kramer, J.R.; Allen, H.E. Lewis Publishers Inc., Chelsea (UK) 1988.

[2] Rao, C.R.M.; Sahuquillo, A.; López Sánchez, J.F. A review of the different methods applied in environmental geochemistry for single and sequential extraction of trace elements in soils and related materials. Water Air Soil Poll. 2008, 189:291-333.

[3] Filgueiras, A.V.; Lavilla, I.; Bendicho, C. Chemical sequential extraction for metal partitioning in environmental solid samples. J.Environ.Monit. 2002, 4:823-857.

[4] Oluwabukola Oyeyiola, A.; Olayinka, K.O.; Alo, B.I. Comparison of three sequential extraction protocols for the fractionation of potentially toxic metals in coastal sediments. Environ.Monit.Assess. 2011, 172:319-327.

[5] Sutherland, R.A.; Tack, F.M.G. Extraction of labile metal from solid media by dilute hydrochloric acid. Environ.Monit.Assess. 2008, 138:119-130.

[6] Larner, B.L.; Seen, A.J.; Townsend, A.T. Comparative study of optimized BCR sequential extraction scheme and acid leaching of elements in the certified reference material NIST 2711. Anal.Chim.Acta, 2006, 556:444-449.

[7] Warren, L.A.; Haack, E.A. Biogeochemical controls on metal behaviour in freshwaters environments. Earth Sci.Rev. 2000, 54:261-320.

[8] Hall, G.E.M. Determination of trace elements in sediments, in: Manual of physico-chemical analysis of aquatic sediments, eds. Mudroch, A.; Azcue, J.M.; Mudroch, P. Lewis Publishers, Boca Raton (USA), 1997.

[9] Leleyter, L.; Rousseau, C.; Biree, L.; Baraud, F. Comparison of EDTA, HCl and sequential extraction procedures, for selected metals (Cu, Mn, Pb, Zn), in soils, riverine and marine sediments. J.Geochem.Exploration, 2012, 116-117:51-59.

[10] Sutherland, R.A. Comparative between non-residual Al, Co, Cu, Fe, Mn, Ni, Pb and Zn released by a three-step sequential extraction procedure and a dilute hydrochloric acid leach for soil and road deposited sediment. Appl.Geochem., 2002, 17:353-365.

[11] Nordberg, M.; Duffus, J.; Templeton, D.M. Explanatory dictionary of key terms in toxicology: Part II (IUPAC Recommendations 2010). Pure Appl.Chem., 2010, 82:679-751.

[12] Berry, W.J.; Boothman, W.S.; Serbst, J.R.; Edwards, P.A. Predicting the toxicity of chromium in sediment. Environ.Toxicol.Chem. 2004, 23:2981-2992.

[13] Townsend, A.T.; Palmer, A.S.; Stark, S.C.; Samson, C.; Scouller R.C.; Snape, I. Trace metals characterization of marine sediment reference material MESS-3 and PACS-2 in dilute HCl extracts. Mar.Pollut.Bull. 2007, 54:236-239.

[14] Snape, I.; Scouller, R.C.; Stark, S.C.; Stark, J.; Riddle, M.J.; Gore, D.B. Characterisation of the dilute HCl extraction method for the identification of metal contamination in Antarctic marine sediments. Chemosphere, 2004, 57:491-504.

[15] Choi, K.Y.; Kim, S.H.; Chon, H.T. Relationship between total concentration and dilute HCl extraction of heavy metals in sediments of harbors and coastal area of Korea. Environ.Geochem.Health, 2012, 34:243-250.

[16] Ashley, K.; Andrews, R.N.; Cavazos, L.; Demange, M. Ultrasonic extraction as a sample preparation technique for elemental analysis by atomic spectrometry. J.Anal.At.Spectrom. 2001, 16:1147-1153.

[17] de la Calle, I.; Cabaleiro, N.; Lavilla, I.; Bendicho, C. Analytical evaluation of a cup-horn sonoreactor used for ultrasound-assisted Extraction of trace Metals from troublesome matrices. Spectrochim.Acta Part B, 2009, 64:874-883.

[18] Sharmin, S.; Zakir, H.M.; Shikazono, N. Fractionation profile and mobility pattern of trace metals in sediment of Nomi River, Tokyo, Japan. J.Soil Sci.Environ.Manag. 2010, 1:1-14.

[19] Oygard, J.K.; Gjengedal, E.; Mobbs, H.J. Trace element exposure in the environment from MSW landfill leachate sediments measured by a sequential extraction technique. J.Hazard.Mat. 2008, 153:751-758.

[20] Larner, B.L.; Palmer, A.S.; Seen, A.J.; Townsend, A.T. A Comparison of an optimized sequential extraction procedure and dilute acid leaching of elements in anoxic sediments, including the effects of oxidation on sediment metal partitioning. Anal.Chim.Acta, 2008, 608:147-157.

[21] Inagaki, K.; Takatsu, A.; Kuroiwa, T.; Nakama, A.; Eyama, S.; Chiba, K.; Okamoto, K. Certified sediment reference materials for trace element analysis from the National Metrology Institute of Japan (NMIJ). Anal.Bioanal.Chem. 2004, 378:1271-1276.

[22] McLaren, J.W.; Beauchemin, D.; Berman, S.S. Application of isotope dilution inductively coupled plasma mass spectromertry to the analysis of marine sediments. Anal.Chem. 1987, 59:610-613.

[23] García-Alonso, J.I.; Rodríguez-González, P. Isotope dilution mass spectrometry. RSC Publishing, Cambridge (United Kingdom), 2013.

[24] Ugarte, A.; Abrego, Z.; Unceta, N.; Aranzazu Goicolea, M.; Barrio, R.J. Evaluation of the bioaccumulation of trace elements in tune species by correlation analysis between their concentrations in muscle and first dorsal spone using microwave-assisted digestion and ICP-MS. Inter.J.Environ.Anal.Chem. 2012, 92:1761-1775.

[25] Vassileva, E.; Hoenig, M. Determination of the total and extractable mass fraction of cadmium and lead in mineral feed by using isotope dilution inductively coupled plasma mass spectrometry. Anal.Chim.Acta, 2011, 701:37-44.

[26] Lee, K.J.; Lee, Y.J.; Choi, Y.R.; Kim, J.S.; Kim, Y.S.; Heo, S.B. Development of new reference materials for the determination of cadmium, chromium, mercury and lead in polycarbonate. Anal.Chim.Acta, 2013, 758:19-27.

[27] Vogl, J.; Maren, K.; Pritzkow, W.; Riebe, G. Development of reference procedures for the quantification of metals and S in plastics. J.Anal.At.Spectrom. 2010, 25:1633-1642.

[28] Rientiz, O.; Schiel, D.; Güttler, B.; Koch, M.; Borchers, U. A convenient and economic approach to achieve SI-traceable reference values to be used in drinking-water interlaboratory comparisons. Accred.Qual.Assur. 2007, 12:615-622.

[29] Markiewicz, B.; Komorowicz, I.; Baralkiewicz, D. Accurate quantification of total chromium and its speciation from Cr (VI) in water by ICP-DRC-IDMS and HPLC/ICP-DRC-IDMS. Talanta, 2016, 152:489-497.

[30] Yang, L.; Willie, S.; Sturgeon, R.E. Determination of total chromium in seawater with isotope dilution sector field ICP-MS following on-line matrix separation. J.Anal.At.Spectrom. 2009, 24:958-963.

[31] Makishima, A.; Yamakawa, A.; Yamashita, K.; Nakamura, E. Precise determination of Cr, Mn, Fe, Co and Ni concentration by an isotope dilution-internal standardization method employing. Chem.Geo. 2010, 274:82-86.

[32] Schiller, M.; Van Kooten, E.; Holst, J.C.; Olsen, M.B.; Bizarro, M. Precise measurement of chromium isotopes by MC-ICPMS. J.Anal.At.Spectrom. 2014, 29:1406-1416.

[33] Nagourney, J.S.; Wilson, S.A.; Buckley, B.; Kingston, H.M.S.; Yang, S-Y.; Long, S.E. Development of a standard reference material for Cr (VI) in contaminated soil. J.Anal.At.Spectrom. 2008, 23:1550-1554.

[34] Wolle, M.M.; Rahman, G.M.M.; Kingstona, H.M.S.; Pamukub, M. Optimization and validation of strategies for quantifying chromium species in soil based on speciated isotope dilution mass spectrometry with mass balance. J.Anal.At.Spectrom. 2014, 29:1640-1647.

[35] Makishima, A.; Kobayashi, K.; Nakamura, E. Determination of chromium, nickel, copper and zinc in milligram samples of geological materials using isotope dilution high resolution inductively coupled plasma-mass spectrometry. J.Geostand.Geoanal. 2002, 26:41-51.

[36] Krushevska, A.; Waheed, S.; Nobrega, J.; Amarisiriwardena, D.; Barnes, R.M. Reducing polyatomic interferences in the ICP-MS determination of chromium and vanadium in biofluids and tissues. Appl.Spectros. 1998, 52:205-211.

[37] Li, Y-T.; Jiang, S-J.; Sabayam, A.C. Electrothermal vaporization inductively coupled plasma mass spectrometry for the determination of Cr, Cd, Hg and Pb in honeys. Food Anal.Chem. 2017, 10:434-441.

[38] Yi, Y-Z.; Wu, S-Y.; Jiang, S-J.; Sahayam, A.C. Cloud point extraction of Cr, Cu, Cd and Pb from water samples and determination by electrothermal vaporization inductively coupled plasma mass spectrometry with isotope dilution. At.Spectroc. 2013, 34:39-47.

[39] Mädler, S.; Todd, A.; Kingston, H.M.; Pamuku, M.; Sun, F.; Tat, C.; Tooley, R.J.; Switzer, T.A.; Furdui, V.I. Ultra-trace level speciated isotope dilution

measurement of Cr(VI) using ion chromatography tandem mass spectrometry in environmental water. Talanta, 2016, 156-157:104-111.

[40] Rosman, K.J.R.; Taylor, P.D.P. Isotopic composition of the elements 1997 (Technical Report). Pure Appl.Chem. 1998, 70:217-235.

[41] EPA Method 6800. Elemental and speciated isotope dilution mass spectrometry, 2007.

[42] EPA Mehotd 3052, Microwave assisted acid digestion of siliceous and organically based matrices, 1996.

[43] Lam, J.W.H.; McLaren, J.W.; Methven, B.A.J. Determination of chromium in biological tissues by inductively coupled plasma mass spectrometry. J.Anal.At.Spectorm., 1995, 10:551-554.

[44] Nelms, S.M.; Quétel, C.R.; Prohaska, T.; Vogl, J.; Taylor, P.D.P. Evaluation of detector dead time calculations models for ICP.MS. J.Anal.At.Spectrom. 2001,16:333-338.

[45] Terán-Baamonde, J.; Andrade, J.M.; Soto-Ferreiro, R.M.; Carlosena, A.; Prada, D. A simple procedure to select a model for mass discrimination correction in isotope dilution inductively coupled plasma mass spectrometry. J.Anal.At.Spectrom. 2015, 30:1197-1206.

[46] Wysocka, I.; Vassileva, E. Determination of cadmium, copper, mercury, lead and zinc mass fractions in marine sediment by isotope dilution inductively coupled plasma mass spectrometry applied as a reference method. Microchem.J. 2016, 128:198-207.

[47] Rodríguez-González, P.; Marchante-Gayón, J.M.; García Alonso, J.I.; Sanz-Medel, A. Isotope dilution analysis for elemental speciation: a tutorial review. Spectrochim.Acta Part B, 2005, 60:151-207.

[48] Falciani, R.; Novaro, E.; Marchesini, M.; Gucciardi, M. Multi-element analysis of soil and sediment by ICP-S after a microwave assisted digestion method. J.Anal.At.Spectrom. 2000, 15:561-565.

[49] Prego, R.; Cobelo-García, A. Twentieth century overview of heavy metals in the Galician Rias (NW Iberian Peninsula). Environ. Pollut. 2003, 121:425-452.

[50] Real, C.; Barreiro, R.; Carballeira, A. Heavy metal mixing behaviour in estuarine sediments in the Ria de Arousa (NW Spain). Differences between metals. Sci.Total Environ. 1993, 128:51-67.

[51] Carballeira, A.; Carral, E.; Puente, X.; Villares, R. Regional scale monitoring of coastal contamination. Nutrients and heavy metals in estuarine sediments and organisms on the coast of Galicia (Norwest Spain). Intern.J.Environ.Poll. 2000, 13:534-572.

V.4.

DIRECT AND SIMULTANEOUS DETERMINATION OF CADMIUM AND CHROMIUM IN SEDIMENTS BY SOLID-SPIKING MATRIX MATCHED ISOTOPE DILUTION LASER ABLATION ICP-MS

1. Abstract

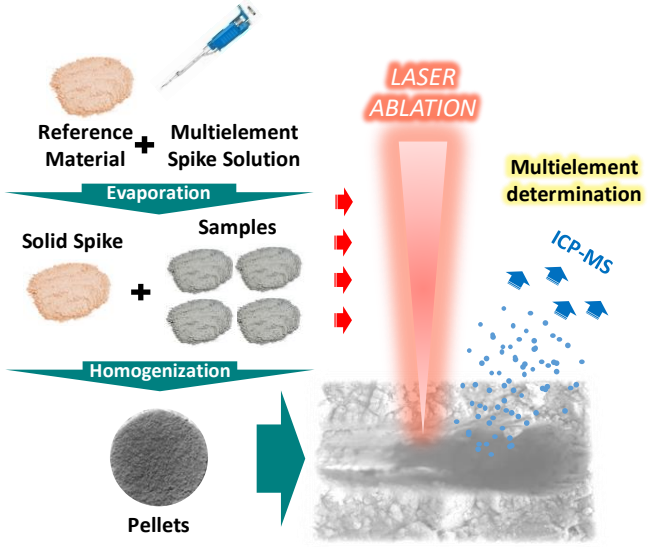

Cadmium and chromium have been determined simultaneously and directly in sediments employing laser ablation inductively coupled plasma isotope dilution mass spectrometry (LA-ICP-IDMS with a conventional nanosecond laser ablation system). A simplified protocol for sample preparation by solid spiking was developed. It reduces considerably the sample preparation and manpower times, when compared to other common alternatives. The pellets prepared from the sediments showed a homogeneous distribution of the metals, according to the satisfactory precision figures recorded (< 5 % for Cd, < 10 % for Cr). A unique sequence to measure Cd (low mass resolution) and Cr (medium mass resolution) isotopes, was implemented in the same ablation line. The effect variables affecting the laser ablation were optimized considering a Plackett–Burman experimental design. The overall procedure was assessed

analyzing three sediments with certified contents of Cr and Cd, with almost a perfect agreement between the certified and the experimental values. Results can be considered of high quality for direct solid analysis by LA-ICP-IDMS. The LODs were 0.40 μg g^{-1} and 0.10 μg g^{-1} for Cr and Cd respectively. The method was applied to a set of samples collected in the NW Spanish coast.

The results discussed in this chapter will be included in a future scientific publication:

Direct and simultaneous determination of cadmium and chromium in sediments by solid-spiking matrix matched isotope dilution laser ablation ICP-MS.

J. Terán-Baamonde, A. Carlosena, R.M. Soto-Ferreiro, J.M. Andrade and D. Prada.

In preparation.

2. Introduction

General environmental awareness and, specifically, environmental protection rules require a sound knowledge on the total content of harmful trace metals in environmental compartments. In particular, sediments pose a real challenge because of the difficulties arising when analyzing them. Hence, very many approaches were applied to evaluate the contents of metals in marine and aquatic ecosystems, set their background levels, initial geochemistry studies, etc. Traditionally, sediments are treated by acid digestion before their measurement by spectrometric techniques, whether flame absorption spectrometry (FAAS) [1], electrothermal atomic absorption spectrometry (ETAAS) [2], inductively coupled plasma atomic emission spectrometry (ICP-AES) [3] or ICP-mass spectrometry (ICP-MS) [1, 4]. The main drawbacks of these methodologies are their high consumption of reagents, and hence generation of wastes, a very long time for sample preparation and the risk of analyte losses or contamination. Besides, a high diversity of digestion procedures has been reported, making it difficult to select the most appropriate one for the ongoing investigation.

The direct analysis of sediments offers important advantages that overcome most of the limitations of above referred conventional methods. In this sense, laser ablation inductively coupled plasma mass spectrometry (LA-ICP-MS) is one of the most powerful tools for elemental analysis in solid materials. It enables the analysis of compact and powdered samples, allows multi-elemental determination, and provides the possibility to perform microanalysis and depth profiling with an excellent lateral and in-depth resolution [5, 6]. However, it shows several limitations that complicate its implementation in routine quantitative analysis. The most important ones are the occurrence of non-stoichiometric effects in the transient signals, defined as elemental fractionation; matrix effects; non-linear calibrations, and the lack of certified reference materials for the majority of samples of interest [7].

In the last years, attempts were made to address these disadvantages by improving the instrumental parameters related to aerosol formation (wavelength of the laser radiation and pulse duration) but their complete elimination is still not possible. Therefore, ongoing research in LA-ICP-MS is devoted to methodological developments that permit a correct quantification

with the current available instrumentation. Most of them involve novel concepts for preparing matrix-matched standards [8].

Isotope dilution mass spectrometry (IDMS) is internationally regarded as a reference or primary method of analysis, providing that a complete mixing of the isotopically-enriched spike and the native element (isotope equilibration) is achieved [9-11]. In this sense, the combination of isotope dilution (ID) with LA-ICP-MS has the potential ability to compensate for fractionation effects; automatically correct for matrix effects, instrument instability and signal drift; and provide excellent accuracy [12]. Different strategies were proposed to get the complete mixing of the isotopically-enriched spike and the native element (isotope equilibration) when they are ablated. Some are based on the on-line introduction of an aerosol of a nebulized isotopically-enriched spike solution into the ablation chamber, where such an aerosol will mix with the sample ablation plasma [13, 14]. However, only drifts occurring during the measurement step will be corrected for, but not those derived from the ablation process itself.

Other approaches are based on matrix-matching. A liquid spike is added directly to the powdered samples, which then are mixed, dried and pressed into pellets. Hence, the errors derived from the ablation processes would be compensated. In particular, sediments have been analyzed in this way and satisfactory results were reported for Cd, but not for Cr, probably due to an inhomogeneous distribution of the spike isotope after drying [15]. Lee et al. [16] used 10 % (v/v) Triton X-100 to prepare a spike solution to determine Cr, Zn, Cu, Cd and Pb in isotopically enriched blend soil samples. They pointed out that this modifier increased significantly the signals of the elements since it could act as a chromophore during the interaction of the laser and the pelleted soil powder. Further, it acts as a binder to get a compact pellet. Boulyga et al. [17] mixed coal samples with methanol in the isotope dilution step to allow a better wetting of the coal particles by the aqueous spike solution and used high-purity graphite powder as binder. They achieved an accurate determination of chlorine, sulfur and trace metals by applying a high-ablation rate laser system and a sector field ICP-MS. One of the biggest problems of this approach is that the entire process of preparation of the enriched blend sample (pellet) should be repeated for each sample to be analyzed. This makes the procedure slow and tedious, mainly when

the number of samples is high, and it also increases the risk for inhomogeneous blends and leads to low precision.

To improve the homogeneity of the isotope-diluted blends (and so the precision), and circumvent the difficulties when pelletizing certain materials, Malherbe et al. [18] proposed a glass fusion approach. Lithium borate was used as fusing matrix when determining several metals (including Cr) in soil and sediments. Main advantages of this approach include homogenized spike and analytes, possible automation of the sample preparation, completely digested refractory phases and easier sample dilution. Drawback are that drying and fusion are time-consuming and have to be repeated for each sample.

As an alternative to adding spike solutions to powdered samples, Fernández et al. [19] synthetized a unique isotopically enriched solid spike. For this, a spike solution is added to a certified reference material which is then homogenized and dried. This solid spike can then be mixed easily by a simple and rapid procedure with every sample to be analyzed to get pellets. They found satisfactory results for Cu, Pb, Sn and Zn. An in-cell isotope dilution method based on the quasi-simultaneous ablation of the sample and an isotopically enriched solid spike was also developed [20], which leaded to good results for Cu, Pb, Sn and Zn in soils and sediments thanks to the use of a femtosecond laser ablation system.

The objective of the present work is to develop a simplified protocol for the solid spiking of sediment intended to determine simultaneously the total contents of Cd and Cr using direct analysis on a conventional (ns) LA-ICP-IDMS. Two drying systems were tested for preparing the isotopically enriched solid spike: rotary evaporation and lyophilization. A unique measurement sequence will be searched to measure Cd (with low mass resolution, LR) and Cr (medium mass resolution, MR) isotopes, in the same ablation line. The effect of the variables affecting the laser ablation system was studied using a Plackett–Burman experimental design. The homogeneity of the pellets prepared from each sediment was assessed through precision figures. The overall procedure was tested analyzing three CRMs (BCR-701, PACS-3 and SRM-1944) for total Cr and Cd. The applicability of this approach was demonstrated by the analysis of thirteen marine sediments collected in the NW coast of Spain.

3. Experimental

3.1. Samples, standards and reagents

Three CRMs were used to assess the solid-spiking LA-ICP-IDMS procedure: lake sediment BCR-701, supplied by the Institute for Reference Materials and Measurements (IRMM); New York/New Jersey waterway sediment SRM-1944, from the National Institute of Standards & Technology (NIST) and harbour sediment PACS-3, from the National Research Council of Canada.

Stock standard solutions of Cd, Cr, Fe, Ti, and Sn (1 000 g L^{-1}) for ICP analysis (SCP Science) were used to prepare 2 % (v/v) HNO_3 working solutions to determine the detector dead time, the mass discrimination factor (K factor) and for spectral interferences corrections. Natural isotopic composition, using IUPAC data as reference values, was assumed for Cr and Cd in all samples and solutions used [21].

The enriched ^{111}Cd and ^{53}Cr isotopic standards were from Cambridge Isotope Laboratories (USA). A 1 000 g L^{-1} enriched stock solutions of ^{111}Cd was prepared by dissolving the solid (in the form of chloride 95.5 %) with 2 % (v/v) HNO_3; working spike solutions were obtained by subsequent gravimetric dilution with 2 % (v/v) HNO_3. A 1 000 g L^{-1} enriched stock solutions of ^{53}Cr was prepared, by dissolving 3 mg of the ^{53}Cr-enriched solid (as oxide, 97.7 %) with 8 mL of concentrated perchloric acid, heating on a hot plate until complete dissolution and evaporating to 2 mL [22]. Next, adequate amounts of both solutions were mixed to prepare a solution containing both target elements (diluted with 2 % (v/v) HNO_3). This was used to prepare the isotopically-enriched solid spike. The isotopic abundances of the spike solutions used in this work were determined by ICP-MS. The elemental concentrations were calculated by reverse isotope dilution using the corresponding standards of natural composition.

High-purity water, 18.2 MΩ·cm resistivity, obtained from a Milli-Q®Direct purification device (Millipore Co., Bedford, MA, USA) was used. Hydrochloric (37 %) and nitric (65 %) acids were of suprapur quality (J.T. Baker, Phillipsburg, NJ, USA). All glassware and plasticware were soaked in 10 % (v/v) HNO_3 for 24 h and rinsed with high-purity water at least three times before use.

3.2. Sample preparation

3.2.1. Isotopically-enriched solid spike

The matrix-matched approach implies adding the isotope-enriched spike solution to each powdered solid sample to be analyzed, requiring subsequent homogenization and dryness steps. It is possible to synthetize only an isotopically-enriched solid spike for all solid samples [19].

Here, the PACS-3 CRM was used as solid matrix due to its low concentrations of Cd and Cr (in compared to other CRMs) which allows to significantly reduce the amount of spike solutions needed. A 2.5 g aliquot of PACS-3 was mixed with 5 g of the isotope-enriched spike solution (containing 1.5 µg mL^{-1} and 25 µg mL^{-1} of ^{111}Cd and ^{53}Cr, respectively) giving rise to a slurry. The amount of spike solution was selected following the error propagation theory in order to obtain an optimum analyte/spike ratio which does not affect the precision of the ICP-IDMS results [23, 24]. The slurry was homogenized by Vortex agitation during 5 min. Then, water was evaporated with a R-210 rotary evaporator, equipped with a V-700 vacuum pump, a F-108 chiller and a V-855 interface to control vacuum (Buchi, New Castle, US). A pressure gradient program at 40 °C was set: (i) from 1000 mbar to 75 mbar in 2 min, (ii) from 75 mbar to 30 mbar in 30 min, (iii) 30 mbar during 1 min; and finally (iv) 25 mbar during 5 min increasing the temperature to 45 °C. After drying, the isotopically-enriched solid was homogenized in an agate mortar until a fine and homogeneous powder was achieved (Figure 1a). This constituted the “isotope-enriched solid spike” used to analyze three CRMs (PACS-3, SRM-1944 and BCR-701) and thirteen marine sediments. So we had to add the amount of spike solution that guarantee an optimum analyte/spike ratio for all of them.

3.2.2. Isotope-diluted blend samples

Around 0.2 g - 0.5 g of each sediment were accurately weighed and mixed with the adequate amount of the isotopically-enriched solid spike (0.2 g - 0.05 g). In this case, the amount of solid spike was also selected following the error propagation theory. The mixtures were homogenized in an agate mortar for 5 min to obtain the “isotope-diluted blend samples”, which will be referred to as “blend sample” hereinafter. The powdered blend samples are pressed to

pellets as schematized in Figure 1b. In brief, a 10 mm Silicone/PTFE septum was drilled (5 mm i.d.) and filled with blend samples. The model and sample are sandwiched between two polyethylene layers, and this mold is pressed in a hydraulic press (2 tons, 1 min). The pellets thus obtained are removed easily and fixed directly to a glass holder (by a double-side tape) for its introduction in the ablation chamber.

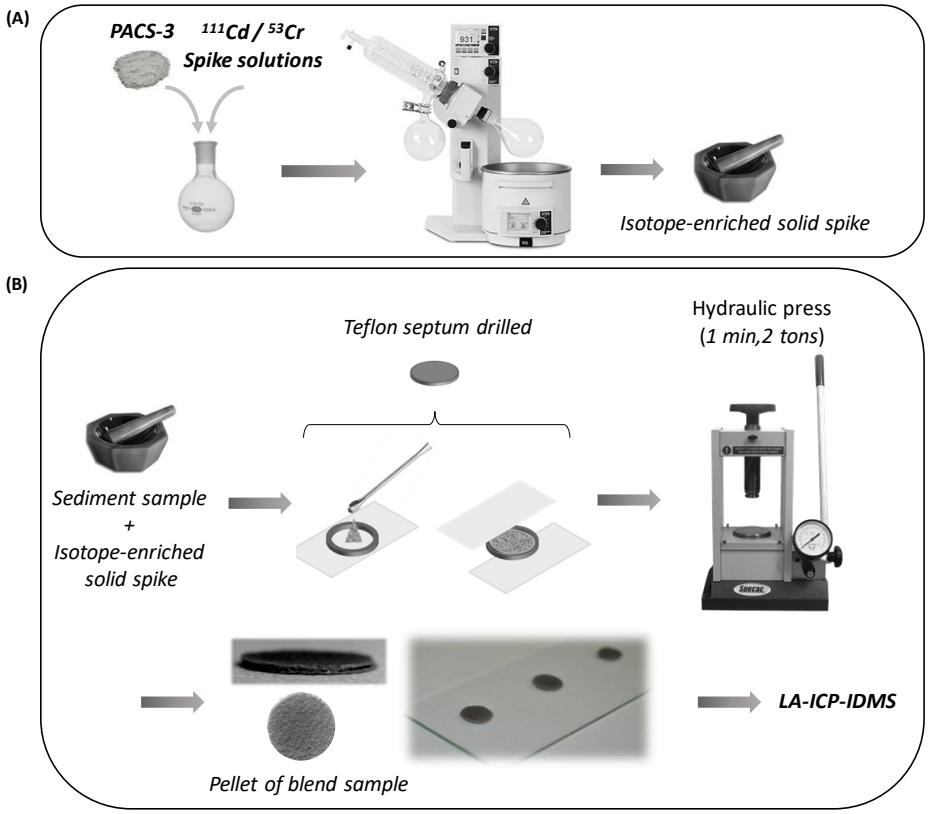

Figure 1. Operational steps for the preparation of: (A) the isotopically-enriched solid spike, (B) the isotope-diluted blend samples and their corresponding pellets.

3.2.3. MW assisted digestion of the isotopically-enriched solids and samples

The isotopically-enriched solid spike was digested following the 3052 EPA Method with a mixture of HNO_3 and HF (3:1) in a microwave oven (Anton Paar Multiwave, Graz, Austria). Its elemental concentration was determined by

reverse isotope dilution analysis adding the adequate amount of natural abundance standards before digestion. The isotopic abundances were calculated by ICP-MS considering three digested aliquots of the solid spike. The CRMs and sediment samples were also submitted to the same digestion procedure to determine their total content on Cd and Cr. The digests obtained were analysed by ICP-MS, using conventional calibration and ^{45}Sc and ^{103}Rh as internal standards.

3.3. LA-ICP-MS instrument and procedure

The measurement were carried out using a double-focusing sector-field ICP-MS (Element XR, Thermo Fisher Scientific, Bremen, Germany) coupled to a high-performance Nd:YAG deep UV (213 nm) laser system UP 213 (New Wave Research Co. Ltd, Huntingdon, UK). The ICP-MS operated under the so-called "dry plasma" configuration, which alleviated oxide ion interferences [16]. The laser-produced aerosol was transported through a polyurethane tube by a helium gas stream (1 L min^{-1}) which is mixed with an argon flow (1 mL min^{-1}) using a T-connection before being conected to the torch of the ICP-MS spectrometer. Helium was selected as carrier gas due to its satisfactory characteristics as an ablation medium and to transport the ablated material [25 - 26]. The instrumental settings of the ICP-MS device were optimized using a CRM (NIST SRM 612, trace elements in glass), so that maximum sensitivity, low oxide formation ($^{232}Th^{16}O^{+}/^{232}Th^{+}$ ratios less than 0.3 %) and minimum fractionation effects (Th/U ratio close to one) are obtained. The latter issue can be achieved rather easily as this material has similar U and Th concentrations, both elements have also similar ionization energies and masses, and the abundance of the major isotopes are > 99 %, for both metals. A 4000 medium mass resolution was selected to resolve polyatomic interferences ($^{35}ClOH^{+}$, $^{37}Cl^{16}O^{+}$, $^{40}Ar^{12}CH^{+}$, $^{40}Ar^{12}C^{+}$) [27] affecting the Cr isotopes, while low mass resolution was used for Cd isotopes in order to obtain sufficiently high counting rates, owing to its low contents in the sediments. The $^{114}Cd/^{111}Cd$ and $^{52}Cr/^{53}Cr$ ratios were considered. In addition, ^{27}Si, ^{47}Ti, ^{51}V, ^{56}Fe, ^{105}Pd, ^{115}In and ^{118}Sn were measured to mathematically correct for isobaric interferences. The operating conditions for LA-ICP-MS measurements are summarised in Table 1.

Table 1. Operating conditions of the ICP-MS and laser ablation systems.

ICP operation conditions	
Rf power	1.45 kW
Auxiliary gas flow	1.00 L min^{-1}
Cooling gas flow	15 L min^{-1}
Acquisition parameters	
Mass resolution	300 (Low) / 4000 (Medium)*
Mass window (%)	60 / 70
Samples per peak	35 / 35
Runs	50 / 50
Number of passes	1 / 1
Isotope masses	^{27}Si, ^{47}Ti, $^{50\text{-}52\text{-}53\text{-}54}Cr$, ^{51}V, ^{56}Fe, ^{105}Pd, $^{110\text{-}111\text{-}112\text{-}113\text{-}114\text{-}116}Cd$, ^{115}In and ^{118}Sn
Laser parameters	
Energy	65 %
Spot diameter	80 µm
Repetition rate	13 Hz
Scan velocity	5 µm s^{-1}
Cleaning time	55 s
Laser warm up time	20 s
Ablation time	172 s
Length of the ablated line	860 µm

* for Cd and Cr, respectively.

Signal registration was programmed to record 50 runs per line, which were processed in an Excell spreadsheet. Figure 2 shows the ablation profile obtained by LA-ICP-MS for an ablation line over a PACS-3 sediment pellet. Note that the background signal was recorded in LR mode at the beginning of the sequence and in MR mode at its end (over 10 runs). Signal intensities were measured at 40 runs/line and were corrected for detector dead time and background. The isotope ratios for each element were corrected for mass bias and the bracketing approach, using non-spiked pellets of PACS-3 sediment that were prepared and ablated for this purpose.

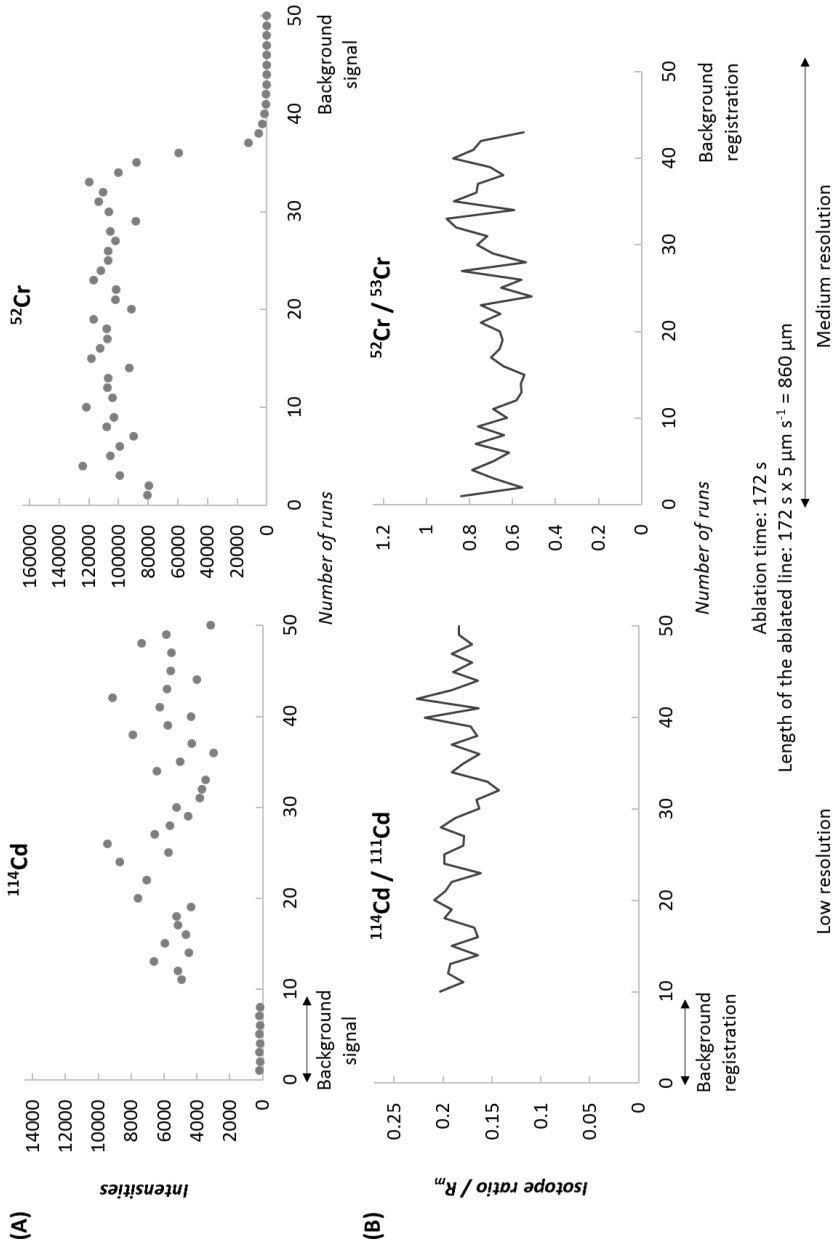

Figure 2. Ablation profile obtained by LA-ICP-IDMS for an ablation line (PACS-3 sediment pellet) programmed to simultaneously measure Cd (low resolution) and Cr (medium resolution): (A) ion signals intensities, (B) isotope ratios.

4. Results and discussion

4.1. Homogeneity of the pelletized CRM sediments

The homogeneity of the pelletized natural composition materials was studied considering the PACS-3, SRM-1944 and BCR-701 CRM was studied. For this, a pellet of each reference material was ablated programming 50 ablation lines across the whole pellet, and 50 runs per line (Figure 3).

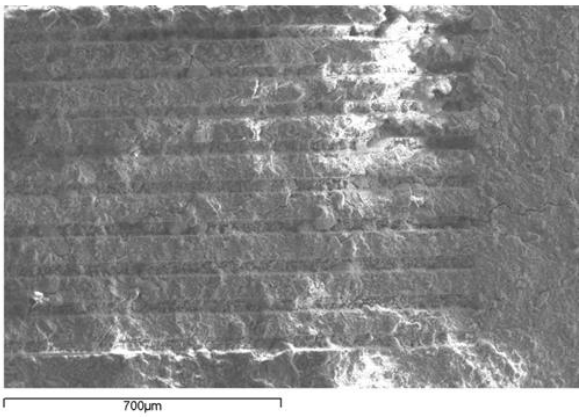

Figure 3. Scanning electron microscopy (SEM) image of the ablated sediment pellet for the homogeneity study.

The intensity data for isotopes ^{52}Cr and ^{114}Cd were acquired and normalized, after subtracting the mean background signal, against ^{27}Si (selected for Si being a major component of sediments). Table 2 summarizes the precision figures obtained for the individual lines, 50 runs ("within" RSD) and between lines, 50 lines ("between" RSD). Within-line precision was lower than 20 %. Only Cd exhibited a RSD higher than 30 % for PACS-3. These values improved for the between-lines precision, 8 % to 10 % for Cr, and 13 % to 16 % for Cd.

Table 2. Precision (measured as % RSD) ranges obtained for the ablation of pellets of three CRMs. Within-line corresponds to 50 runs per line, whereas between-lines consider 50 ablation lines through the whole pellet.

	Precision (% RSD)					
	PACS-3		**SRM-1944**		**BCR-701**	
	within	*between*	*within*	*between*	*within*	*between*
^{52}Cr	9 - 20	10	11 - 16	10	9 - 14	8
^{114}Cd	14 - 37	13	14 - 21	16	12 - 23	14

According to these results, the native analytes present in the sediments were considered to be distributed homogeneously in the pellets. This is a relevant issue for the following studies as they will consider pellets of the blend samples.

4.2. Multivariate study of the laser ablation

The main variables affecting the laser ablation efficiency, the signal stability, the sensitivity and the occurrence of elemental fractionation will be studied. A multivariate approach consisting of a 8-trial Plackett–Burman experimental design was applied to evaluate the effect of the variables determining the ablation process, by analysing a pellet of the PACS-3 CRM. The variables studied were: (A) laser energy (50 – 80 %), (C) spot diameter (40 – 110 µm), (E) repetition rate (5 – 20 Hz) and (F) scan velocity (1 – 10 µm s^{-1}). Three dummy variables (B, D, G) were also included to make the number of variables equal to 7 (Table 3).

For each trial five lines were ablated and the experimental response was the mean of the signal intensities (cps) registered per line for ^{52}Cr and ^{114}Cd, after subtracting the mean background signal. The signal of isotope ^{27}Si was also registered for isotope intensities normalization. Figure 4 shows a SEM image of the pellet used to perform the experimental design, where different appearances (length, thickness and depth profiles) can be observed, as a result of the different laser conditions applied in each trial.

Table 3. Experimental design matrix for the variables studied in the ablation process (A, laser energy; C, spot diameter; E, repetition rate; F, scan velocity; B, D, G dummies). Results expressed as isotope intensities (mean background signal subtracted and normalized to ^{27}Si).

	Variables							Normalized signal	
Experiment	**A**	**B**	**C**	**D**	**E**	**F**	**G**	**Cr**	**Cd**
1	80	+	110	-	20	1	-	$5.03 \cdot 10^{-4}$	$5.58 \cdot 10^{-6}$
2	50	+	110	+	5	10	-	$9.95 \cdot 10^{-4}$	$8.89 \cdot 10^{-6}$
3	50	-	110	+	20	1	+	$5.66 \cdot 10^{-4}$	$6.25 \cdot 10^{-6}$
4	80	-	40	+	20	10	-	$7.14 \cdot 10^{-4}$	$8.60 \cdot 10^{-6}$
5	50	+	40	-	20	10	+	$9.38 \cdot 10^{-4}$	$7.85 \cdot 10^{-6}$
6	80	-	110	-	5	10	+	$8.51 \cdot 10^{-4}$	$8.57 \cdot 10^{-6}$
7	80	+	40	+	5	1	+	$6.20 \cdot 10^{-4}$	$7.13 \cdot 10^{-6}$
8	50	-	40	-	5	1	-	$9.45 \cdot 10^{-4}$	$8.08 \cdot 10^{-6}$

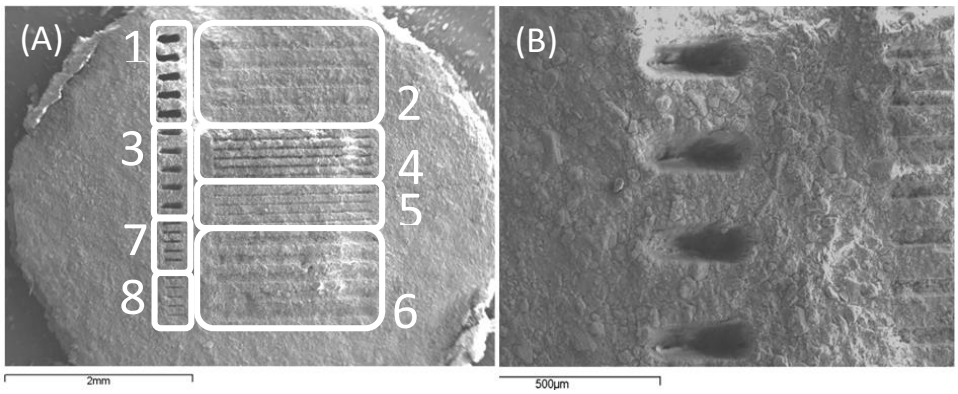

Figure 4. Scanning electron microscopy (SEM) images of: (A) the whole pellet submitted to the conditions of the experimental design (numbers correspond to the trials); (B) detail of the ablation produced in experiment #1.

The experimental t value (t_{exp}) was calculated as usual in these studies for each variable, for both metals. Table 4 shows that in all cases t_{exp} was lower than the tabulated one (t_{tab} (95% confidence level) ≈ 2). Therefore, when the variables considered in this study are modified within the ranges set above, they do not alter statistically (95 % confidence) the measured isotope intensities. Accordingly, the intermediate values of the ranges were selected to develop the laser ablation procedure (figures reported in Table 1).

Table 4. Experimental values calculated for statistic t (t_{exp}).

Variable	t_{exp} Cr	t_{exp} Cd
A	0.4826	0.5721
B	0.6041	0.5581
C	0.5575	0.5530
D	0.5507	0.6042
E	0.4935	0.5204
F	0.7499	0.7030
G	0.5771	0.5696

4.3. Drying step for the isotopically-enriched solid spike preparation

The drying step required to prepare the isotopically-enriched solid spike represents a keystone to achieve the equilibrium between the spike and the native isotopes and, besides, to obtain homogeneous pellets of blend samples. In the present work, two drying systems were tested, namely freeze-drying (FD) and rotary evaporator (RE). The PACS-3 sediment was used for the assays. As detailed above, a slurry was prepared by mixing an aliquot of the isotope-spike solution with the sediment. This was left overnight in the freeze-drying system. On the other hand, another slurry was prepared and introduced into a flask to evaporate the solvent in a rotary evaporator, applying the gradient program described above. These studies were performed in triplicate (three independent solid spikes) and three pellets were prepared from each solid spike (9 pellets in total per procedure).

Firstly, a previous study was made to assess whether the synthetized solid spike yields homogeneous pellets. This is analogous to the study of the pelletized CRMs above. In fact, the same general protocol will be followed here (50 ablation lines and 50 runs per line). The intensities of ^{52}Cr, ^{53}Cr, ^{114}Cd and ^{111}Cd isotopes were registered and their RSDs calculated within the same line and between the lines (Table 5).

Table 5. Precision (measured as % RSD) for ablated pellets to assess the homogeneity of the isotopically-enriched solid spike synthetized by two evaporation methods. Within-line and between-lines precision correspond to the precision values calculated to 50 runs/line and to 50 ablation lines, respectively.

	Precision (% RSD)			
	Rotary evaporator		**Freeze-drying**	
	within	*between*	*within*	*between*
^{52}Cr	8 - 21	9	12 - 20	10
^{53}Cr	11 - 20	11	12 - 27	13
^{114}Cd	17 - 30	13	23 - 53	18
^{111}Cd	14 - 29	12	22 - 50	16

The within-lines precision for Cr ranged from 8 % to 21 % for rotary system and from 12 % to 27 % for freeze-drying. Both drying systems led to satisfactory between-lines precision (9 % - 13 %). Regarding Cd, high values for the within-lines RSD were found for both systems, although for freeze-drying they were almost two fold. A notorious improvement was attained between-lines, slightly better for the rotary system (12 % - 13 %) than for the freeze-drying (16 % - 18 %) one.

The poorer results for Cd may be due to the low mass fraction of this element in the CRM, which lead to low isotope intensities and, therefore, to a higher dispersion. In the literature, RSDs lower than 10 % were found for Cd and Cr using a liquid isotope spike added to sediments [15] and around 6 % - 21 % for pressed pellets of sediments when Pb, Sr and Rb were determined [28].

After confirming that each synthetized spike yields homogeneous pellets, it is possible to compare both drying systems. The $^{52}Cr/^{53}Cr$ and $^{114}Cd/^{111}Cd$ isotope ratios were measured on five ablation lines over each pellet (50 runs/line).

For Cr, the precision of the isotope ratios was lower than 6 % when only a pellet was dried by the RE; and < 10 % for FD. When precision was calculated from the three pellets of an independent solid precision figures improved (< 3 % for RE and < 7 % for FD) (Figure 5a). Finally, when all three solid spikes and their three pellets were considered a very satisfactory 1 % RSD was obtained for RE.

For Cd (Figure 5b), the precision for only a pellet was < 10% (RE), while values highly variable for FD (8 % - 28 %). Considering the three pellets of a solid spike RSD values were 1 % – 7 % for RE, and 16 % - 25 % for FD. The overall nine pellets yielded 13 % RSD (RE) and 26 % (FD), which denoted a less homogeneous distribution of Cd isotopes in the isotopically-enriched solid spike synthetized by FD.

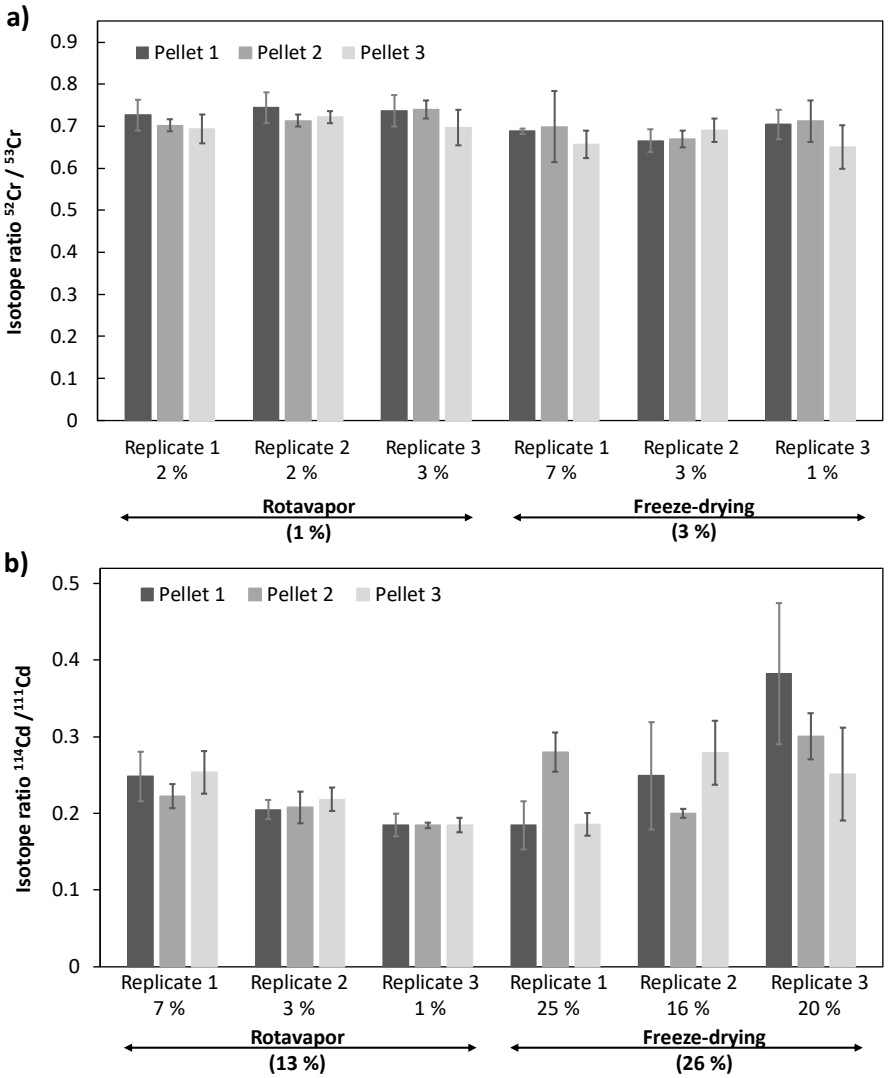

Figure 5. Precision of the isotope ratio measurements for (a) Cr and (b) Cd, as a function of the drying process applied to synthetize the isotopically-enriched solid spike (rotary evaporator and freeze-drying), and number of pellets.

Comparing both drying procedures rotary evaporator seems better than freeze-drying. Likely because the rotation of the round bottom flask contributes to a better mixing of the spike solution and the solid sample, favouring the isotope equilibration and, given rise to a more homogeneous synthetic product. In addition, freeze-drying caused partial sputtering an inhomogeneous deposition of the spike powder. Hence, rotary evaporation seems an adequate procedure to prepare the isotopically-enriched solid spike. Further, this procedure is less time-consuming (38 min) than freeze-drying (24 h). Previous protocols to dry the isotope-enriched solid spike heated the mixture at 90 °C for 6 h in a laminar flow clean bench using a DigiPREP Classic System [19], with the subsequent risk of analyte losses and we think this problem is avoided using rotary evaporation.

4.4. Method validation

Two reference sediments, PACS-3 and SRM-1944, with certified total Cd and Cr contents were analysed following the proposed solid-spiking LA-ICP-IDMS procedure. Reference sediment BCR-701, certified for the SM&T 3-step sequential extraction procedure, was also analysed. Three pellets were prepared from each blend sediment, after adding the adequate amount of the solid spike to obtain an optimum analyte/spike ratio for all of them (c.a. 1). Five ablation lines (50 runs per line) were programmed over each pellet. The $^{52}Cr/^{53}Cr$ and $^{114}Cd/^{111}Cd$ ratios were measured following the experimental protocol described above and the concentrations of Cr and Cd in the reference sediments were calculated using the isotope dilution equation. As shown in Table 6, the mass fractions of Cr and Cd calculated for the three CRMs agree very well with the certified values, with ratios (experimental/certified values) around unity. Regarding precision, the RSDs were calculated using three pellets. Values between 7 % and 10 % were obtained for Cr, and from 2 % to 4 % for Cd. Malherbe et al. [18] obtained slightly better precision for Cr in SRM-1944 (< 10 %) although the experimental/certified ratio was higher (1.11). It is worth nothing that these authors used a glass fusion procedure which implies the preparation of an isotope-diluted blend for each sample to be analyzed. That significantly increased the analysis time in comparison with the method proposed here. Moreover, as they stated, possible reagent impurities and

sample contamination during preparation can compromise the analysis of low mass fraction elements, and the repeated analysis of lithium borate glasses may contaminate the ICP-MS with Li due to memory effects.

For comparison, the CRMs were analysed by ICP-MS after their microwave acid digestion, using conventional calibration. Table 6 summarizes the results, which compare very well with those of the LA-ICP-IDMS procedure, in terms of accuracy.

Table 6. Determination of Cr and Cd concentrations (μg g^{-1}) in sediment reference materials by solid-spiking LA-ICP-IDMS (95% confidence intervals calculated from the mean of five ablated lines -50 runs per line- in three independent blend pellets).

	Solid-spiking LA-ICP-IDMS	**Certified value**	**Acid digestion***	**Ratio****
Chromium				
PACS-3	91.67 ± 5.81	91.6 ± 4.0	90.70 ± 2.03	1.00
SRM-1944	265.9 ± 12.2	266 ± 24	250.4 ± 16.2	1.00
BCR-701	331. 4 ± 14.4	-	328.7 ± 10.4	-
Cadmium				
PACS-3	2.28 ± 0.05	2.23 ± 0.13	2.12 ± 0.03	1.02
SRM-1944	9.47 ± 0.20	8.80 ± 1.40	9.11 ± 0.31	1.08
BCR-701	12.13 ± 0.16	-	11.31 ± 0.21	-

(*) 3052 USEPA method.

(**) Referred to (experimental LA-ICP-IDMS results / certified values).

The limits of detection (LOD) of the LA-ICP-IDMS procedure for Cr and Cd were calculated using the *3σ* criterion ($3\sigma_b$ / *S*). For this, five independent measurements of the blank gas were performed and its standard deviation (σ_b) was computed. *S* is the sensitivity for the corresponding analyte isotope, evaluated measuring the PACS-3 CRM. Values of 0.40 μg g^{-1} and 0.10 μg g^{-1} were obtained for Cr and Cd, respectively. These results are satisfactory because an almost three-fold higher limit was reported for Cd using a similar ablation system [29] and similar values were also declared when considering a superior equipment [17]. For Cr, reported limits were more widespread: 0.098 [18], 0.32 [29] and 3.3 [17] μg g^{-1}.

4.5. Application to a case-study

The applicability of a new methodology to analyze field samples is a challenge for scientists. Surprisingly, scarce references were found including this topic with LA-ICP-IDMS procedures. Major problems reported to tackle with this issue relate to the different matrix composition of the samples, the wide range of contents of the target analytes, and the absence of previous information about them.

In this work the simplified protocol developed to simultaneously determine total Cd and Cr content by direct analysis with solid-spiking conventional (ns) LA-ICP-IDMS was applied to analyze marine sediments collected in two estuaries at the NW coast of Spain. Before the analysis a preliminary test was made to assess whether the sample pellets were homogeneous, following the scheme depicted in Figure 1. The relative standard deviations were calculated both for the isotope ratios obtained within-line and between-lines (50 lines, 50 runs per line). As was observed for the CRMs, good precision figures were obtained when several lines where considered, for both elements (< 6 % and < 10 % for Cr and Cd, respectively), revealing that the sample pellets had a homogenous distribution of these elements.

Next, the blend samples were prepared according to the protocol above. The amount of solid spike added to the samples was selected so as to obtain an optimum analyte/spike ratio for each one, considering the previous information about the Cr and Cd contents in the samples provided by preliminary measurements performed in our laboratory.

Figure 6 shows the mass fractions obtained for six sediments from the ria of Arousa and seven from the ria of Vigo. It shows the concentrations calculated for the same samples by microwave-assisted acid digestion and conventional ICP-MS calibration. It can be observed that both procedures led to comparable results. Precision was also similar (< 10 %), but for four laser ablated samples with the lowest concentrations of Cd (RSD ca. 20 %). In addition, LA-ICP-IDMS allowed to determine low levels of Cd in some samples, no detected by the classical procedure (A6).

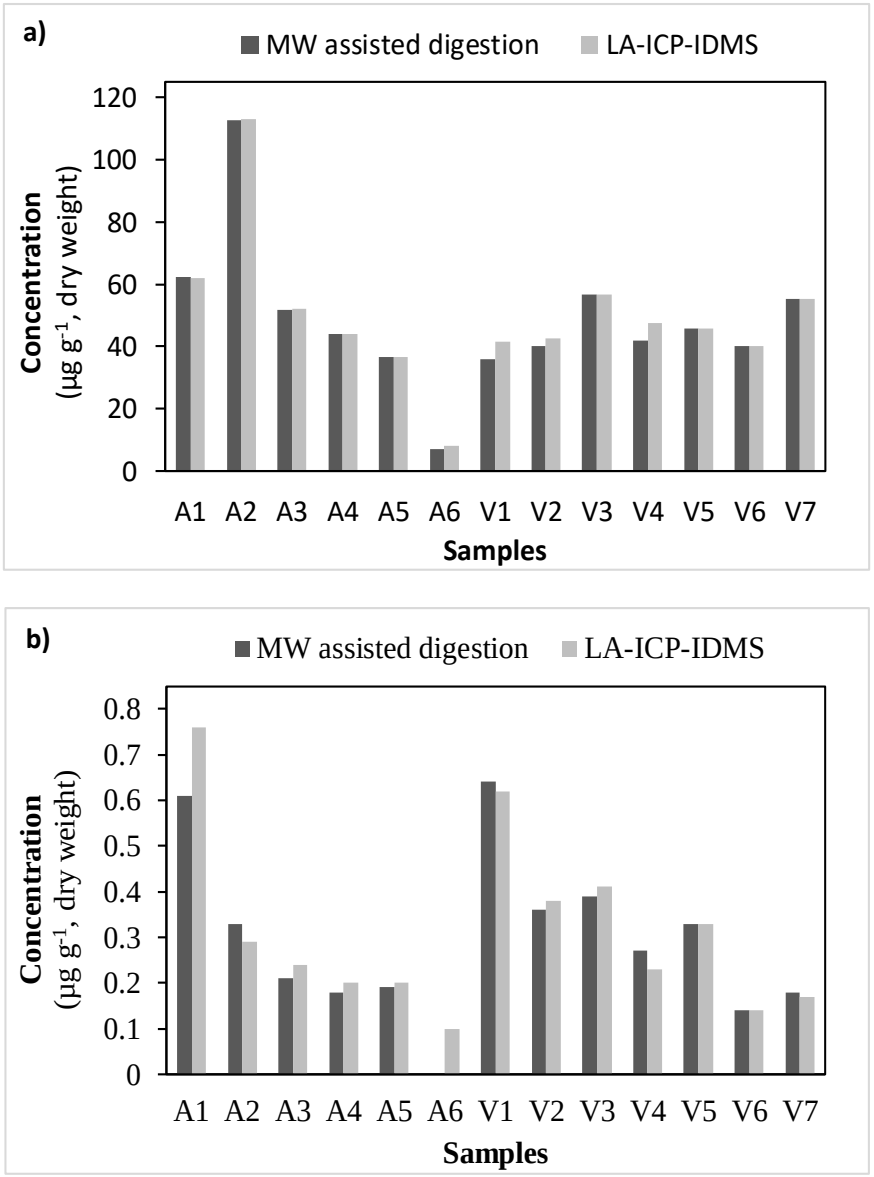

Figure 6. Cr (a) and Cd (b) mass fractions (µg g^{-1}) obtained by LA-ICP-IDMS for marine samples from the ria of Arousa (A1-A6) and from the ria of Vigo (V1-V7). Concentrations obtained by acid digestion and conventional calibration were included for comparison.

5. Conclusions

The solid-spiking LA-ICP-IDMS procedure enabled the simultaneous and accurate determination of Cr and Cd in sediments using a conventional nanosecond laser ablation system and a sector field ICP-MS. A time-efficient measurement step was programmed so that a unique measurement sequence measured Cd (with low mass resolution, LR) and Cr (medium mass resolution, MR) isotopes in the same ablation line.

The isotopically-enriched solid spike preparation method was optimized to be less time-consuming than others proposed elsewhere. It includes a drying step under controlled pressure in a rotary evaporator, which lasted only 38 min (vs. 6 h of previous approaches [19]). Indeed, the rotation during evaporation lead to a better mixing, favouring the isotope equilibration and providing a more homogeneous solid spike. The evaluation of the homogeneity of the pellets thus prepared from either CRMs and samples revealed a homogeneous distribution of the metals. Further, this yielded a homogeneous distribution of the studied metals in the pellets corresponding to the isotope-enriched solid spike and the isotope-diluted blend samples, as revealed by the very good precision figures.

A multivariate experimental study (8-trial Plackett–Burman experimental design) revealed that none of the variables that are usually critical for the ablation process significantly affected the isotope intensities of both Cr and Cd, likely because of a previous careful selection of the experimental values. This allowed setting the most convenient conditions according to operational criteria.

Validation was done using two CRMs with certified total contents of Cr and Cd. Good agreement with the certified values was achieved, with (experimental/certified) ratios in the 1.00 – 1.08 range. Precision was between 7 % and 10 % (RSD) for Cr, and 2 % - 4 % (RSD) for Cd, calculated from three analysis using independent pellets. These results can be considered of high quality for direct solid analysis by LA-ICP-MS using a conventional nanosecond laser ablation system.

The applicability of the proposed solid spike LA-ICP-IDMS procedure was demonstrated by analysing of thirteen marine sediments collected in NW Spain. The mass fractions of Cr and Cd agreed with those obtained by conventional ICP-MS with microwave-assisted digestion method and conventional calibration.

Also, the precision for both methods were comparable and the laser-based method attained LODs (0.40 μg g^{-1} and 0.10 μg g^{-1} for Cr and Cd respectively) that improved others from similar applications. Finally, it is worth noting that the proposed methodology meets the main requisites of the green analytical methods and it is relatively fast.

References

[1] Sastre, J.; Sahuquillo, A.; Vidal, M.; Rauret, G. Determination of Cd, Cu, Pb and Zn in environmental samples: microwave-assisted total digestion versus aqua regia and nitric acid extraction. Anal.Chim.Acta, 2002, 462:59-72.

[2] Álvarez, M.A.; Carrillo, G. Simultaneous determination of arsenic, cadmium, copper, chromium, nickel, lead and thallium in total digested sediment samples and available fractions by electrothermal atomization atomic absorption spectroscopy (ETAAS). Talanta, 2012, 97:505-512.

[3] Bettinelli, M.; Beone, G.M.; Spezia, S.; Baffi, C. Determination of heavy metals in soils and sediments by microwave-assited digestion and inductively coupled plasma optical emission spectrometry analysis. Anal.Chim.Acta, 2000, 424:289-296.

[4] Hassan, N.M.; Rasmussen, P.E.; Dabek-Zlotorzynska, E.; Celo, V.; Chen, H. Analysis of environmental samples sing microwave-assisted acid digestion and inductively coupled plasma mass spectrometry: maximizing total element recoveries. Water Air Soil Poll. 2007, 178:323-334.

[5] Pisionero, J.; Günther, D. Femtosecond laser ablation inductively coupled plasma mass spectrometry: fundamentals and capabilities for depth profiling analysis. Mass Spectrom.Rev. 2008, 27:609-623.

[6] Kock, J.; Günther, D. Reviewof the state-of-the-art of laser ablation inductively coupled plasma mass spectrometry. Appl.Spectrosc. 2011, 65:155A-162A.

[7] Fernández, B.; Claverie, F.; Pécheyran, C.; Donard, O.F.X. Direct analysis of solid samples by fs-LA-ICP-MS. Trends Anal.Chem. 2007, 26:951-966.

[8] Limbeck, A.; Galler, P.; Bonta, M.; Bauer, G.; Nischkauer, W.; Vanhaecke, F. Recent advances in quantitative LA-ICP-MS analysis: challenges and solutions in the life sciences and environmental chemistry. Anal.Bioanal.Chem. 2015, 407:6593-6617.

[9] Comité Consultatif pour la Quantité de Matière (CCQM), Rapport de la 1er sesión. BIMP, Sèvres (France), 1995.

[10] Heumann, K.G. Isotope-dilution ICP-MS for trace element determination and speciation: from a reference method to a routine method? Anal.Bioanal.Chem. 2004, 378:318-329.

[11] Rodríguez-González, P.; Marchante.Gayón, J.M.; García Alonso, J.I.; Sanz Medel, A. Isotope dilution analysis for elemental speciation: a tutorial review. Spectrochim.Acta Part B, 2005, 60:151-207.

[12] Compernolle, S.; Wambeke, D.; De Raedt, I.; Vanhaecke, F. Evaluation of a combination of isotope dilution and single standard addition as an alternative calibration method for the determination of precious metals in lead fire assay button by laser ablation-inductively coupled plasma-mass spectrometry. Spectromchim.Acta Part B, 2012, 67:50-56.

[13] Sela, H.; Karpas, Z.; Zoriy, M.; Pickhardt, C.; Becker, J.S. Biomonitoring of hair samples by laser ablation inductively coupled plasma mass spectrometry (LA-ICP-MS). Int.J.Mass Spectrom. 2007, 261:199-207.

[14] Pickhardt, C.; Izmer, A.V.; Zoriy, M.; Schaumlöffel, D.; Becker, J.S. On-line isotope dilution in laser ablation inductively coupled plasma mass spectrometry using a microflow nebulizer inserted in the laser ablation chamber. Int.J.Mass Spectrom. 2006, 248:136-141.

[15] Tibi, M.; Heumann, K.G. Isotope dilution mass spectrometry as a calibration method for the analysis of trace elements in powder samples by LA-ICP-MS. J.Anal.At.Spectrom. 2003, 18:1076-1081.

[16] Lee, Y-L.; Chang, C-C.; Jiang, S-J. Laser ablation inductively coupled plasma mass spectrometry for the determination of trace elements in soil. Spectrochim.Acta Part B, 2003, 58:523-530.

[17] Boulyga, S.F.; Heilmann, J.; Prohaska, T.; Heumann, K.G. Development of an accurate sensitive and robust isotope dilution laser ablation ICP-MS method for simultaneous multi-element analysis (chlorine, sulfur, and heavy metals) in coal samples. Anal.Bioanal.Chem. 2007, 389:697-706.

[18] Malherbe, J.; Claverie, F.; Alvarez, A.; Fernández, B.; Pereiro, R.; Molloy, J. Elemental analysis of soil and sediment fused with lithium borate using isotope dilution laser ablation-inductively coupled plasma-mass spectrometry. Anal.Chim.Acta, 2013, 793:72:78.

[19] Fernández, B.; Claverie, F.; Pécheyran, C.; Donard, O.F.X. Solid-spiking isotope dilution laser ablation ICP-MS for the direct and simultaneous determination of trace elements in soils and sediments. J.Anal.At.Spectrom. 2008, 23:367-377.

[20] Fernández, B.; Clavarie, F.; Pécheyran, C.; Alexis, J.; Donard, O.F.X. Direct determination of trace elements in powdered samples by in-cell isotope dilution femtosecond laser ablation ICPMS. Anal.Chem. 2008, 80:6981-6994.

[21] Rosman, K.J.R.; Taylor, P.D.P. Isotopic composition of the elements 1997 (Technical Report). Pure Appl.Chem. 1998, 70:217-235.

[22] EPA Method 6800. Elemental and speciated isotope dilution mass spectrometry, 2007.

[23] García Alonso, J.I. Determination of fission products and actinides by inductively coupled plasma-mass spectrometry using isotope dilution analysis: a study of random and systemic error. Anal.Chim.Acta, 1995, 312:57-78.

[24] García-Alonso, J.I.; Rodríguez-González, P. Isotope dilution mass spectrometry. RSC Publishing, Cambridge (UK), 2013.

[25] Horn, I., Günther, D. The influence of ablation carrier gases Ar, He and Ne on the particle size distribution and transport efficiencies of laser ablation-induced aerosols: implications for LA-ICP-MS. Appl. Surface Sci., 2003, 207:144-157.

[26] Bleiner, D., Günther, D. Theorical description and experimental observation of aerosol transport process in laser ablation inductively coupled plasma mass spectrometry. J.Anal.At.Spectrom., 2001, 16:449-456.

[27] Chang, Y-L.; Jiang, S-J.; Determination of chromium in water and urine by reaction cell inductively coupled plasma mass spectrometry. J.Anal.At.Spectrom. 2001, 16:134-1438.

[28] Fernández, B.; Rodríguez-González, P.; García Alonso, J.I.; Malherbe, J.; García-Fonseca, S.; Pereiro, R.; Sanz-Medel, A. On-line isotope dilution laser ablation inductively coupled plasma mass spectrometry for the quantitative analysis of solid materials. Anal.Chim.Acta, 2014, 851:64-71.

[29] Boulyga, S.F.; Heumann, K.G. Comparative LA-ICP-IDMS determinations of trace elements in powdered samples using laser ablation systems with low and high ablation rates. J.Anal.At.Spectrom. 2004, 19:1501-1503.

CHAPTER

VI

SIMULTANEOUS SPECIATION OF Hg, Sn AND Pb COMPOUNDS IN NATURAL WATERS BY ID AND PTV-GC-ICP/MS

SIMULTANEOUS SPECIATION OF MERCURY, TIN AND LEAD COMPOUNDS IN NATURAL WATERS BY ISOTOPIC DILUTION AND PROGRAMMED TEMPERATURE VAPORIZATION INJECTION-GAS CHROMATOGRAPHY HYPHENATED WITH INDUCTIVELY COUPLED PLASMA-MASS SPECTROMETRY

1. Abstract

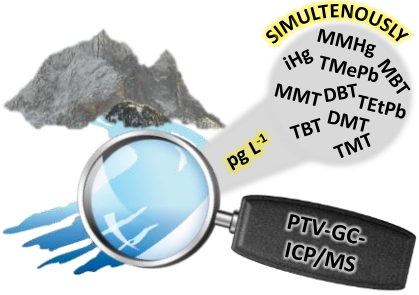

The current EU legislation lays down Environmental Quality Standards (EQS) for 45 priority substances in surface waters; among them levels for mercury, tin, lead and their (organo)compounds are set between ng L^{-1} (for Hg and Sn) and µg L^{-1} (for Pb). Therefore, comprehensive analytical methods able to analyze organometallic species down to these very restrictive limits are required. To date, only a few methods can reach these limits and determine background concentration levels in natural waters. The aim of this work is to develop an online automated pre-concentration method using large volume injections in a programmable temperature Vaporizer (PTV) inlet fitted with a sorbent packed liner coupled to GC-ICP/MS to further improve the detection limits associated to this well-established method. The influence of several analytical parameters such as the PTV transfer temperature and time, carrier gas flow rate and amount of packing material was investigated. Finally, the maximum volume injected through single or multiple injection modes was optimized to obtain the best compromise between chromatographic resolution and sensitivity. After optimization, very satisfactory results in terms of absolute method detection limits were achieved, in the level of pg L^{-1} for all species studied. The method was applied to determine the concentrations of organometallic compounds in unpolluted river waters samples from the Adour

river basin (SW France) and results were compared with regular (splitless) GC-ICP/MS. The strength of this analytical method lies in the low detection limits reached for the simultaneous analysis of a wide group of organometallic compounds, and the potential to transfer this method to other gas chromatographic applications with inherent lower sensitivity.

The results discussed in this chapter will be included in a future scientific publication:

Development of a large volume injection technique using programmed temperature vaporization injector with a packed liner for the simultaneous speciation of mercury, tin and lead species at ultra-trace levels by GC-ICP-MS.

J. Terán-Baamonde, S. Bouchet and D. Amouroux.

In preparation.

2. Introduction

Chemical forms under which elements are present in the environment play a critical role in their mobility, bioavailability and eventually toxicity. Nowadays, organometallic species of mercury, tin and lead are among the most problematic in the environment [1], since they present high toxicity even at trace levels but are also bioaccumulated and/or bioamplified along food webs. These compounds have therefore been included in the list of priority substances from the EU Water Framework Directive (WFD, Directive 2013/39/EU, amending Directives 2000/60/EC and 2008/105/EC) [2].

Mercury compounds are wide spread in aquatic ecosystems with both a natural and anthropogenic origin [3]. Maximum allowable concentrations have been set to 70 ng L^{-1} for Hg species by the EU WFD. Monomethylmercury (MMHg) and inorganic Hg (IHg) are the dominant dissolved species compared to ethyl or phenyl Hg and volatile species such as elemental Hg (Hg^0) and dimethylmercury (Me_2Hg) [4]. MMHg is formed from IHg through a biomethylation process [5] and then bioamplifies along food chains. It is a potent neurotoxic [6] while the toxicological role of IHg is still under discussion [7].

Organotin compounds were extensively used due to their powerful biocide properties in anti-fouling paints, pesticide formulations, wood preservatives and polymer additives [8] until their ban in 2008 [9] (except for warships, naval auxiliary and some other ships used by governmental services [10]). Their fates have been mainly investigated in marine and coastal ecosystems due to sediment legacy contamination and the risk of diffusion and resuspension during dredging operations of contaminated harbors [11, 12]. Triorganotin are the most toxic species, followed by di- and mono-compounds, as they present an endocrine disruption potential [13, 14] even at the low levels at which they are present in water [15]. However, only the tributyltin compounds are regulated by the EU directive with annual average concentrations set to 0.2 ng L^{-1} and maximum allowable concentrations to 1.5 ng L^{-1}. Triorganotins can be degraded by microorganisms or light (photolysis) into less toxic forms (di-, mono-, and inorganic Sn); but these process are very slow in sediments, where they persist long after their release [16].

The use of tetraethyllead as antiknocking additive for gasoline has been the major source of lead contamination until it was phased out in the mid-1970s even if there are still a few countries using leaded gasoline nowadays [17]. Organolead compounds are neurotoxic [18], and the toxicity is highest for monopositive cations (R_3Pb^+) resulting from the loss of one organic group from tetraalkyllead compounds [18]. The main sources of lead in urban environments are runoff waters from roadways, mineral extraction and processing, smelting and refining, power generation, battery plants and waste disposal/incinerator [19]. Triethylead (Et_3Pb) and its degradation product, diethyllead (Et_2Pb), are the two most frequent organolead species detected in water samples [20]. Annual average concentrations are set to 1.2 - 1.3 µg L^{-1} with maximum allowed up to 14 µg L^{-1}.

Considering both the Environmental Quality Standards (EQS) set by the EU WFD for these compounds and their ambient concentrations in natural waters, the development of accurate and sensitive analytical methods is required to implement monitoring and research programs [2]. Although liquid chromatography has been used for such analysis [21, 22], most techniques use gas chromatography given its excellent separation efficiency, coupled to different detectors [23]: atomic fluorescence spectrometry (GC-AFS) [24], flame photometry (GC-PFPD) [25], flame ionization detection (GC-FID) [26, 27], microwave-induced plasma atomic emission spectrometry (GC-MIP-AES) [28, 29] and mass spectrometry in single or tandem mode (GC-MS/MS) [30, 31]. However, many of these and other recognized methods like ISO 17353:2004 present detection and quantification limits far above the legal requirements [32]. The coupling of gas chromatography to inductively coupled plasma mass spectrometry (GC-ICP/MS) has been widely developed [33, 34] to cope with the sensitivity issue and because it allows multi-elemental and isotopic measurements and therefore species-specific isotope dilution analysis (SS-IDA) [35 - 40].

Still, detection limits can be closed to the EQS or ambient concentrations. Cavalheiro et al. [20] obtained TBT detection limits of 0.08 ng L^{-1} by regular GC-ICP/MS while the annual average is set to 0.2 ng L^{-1} by the legislation. Moreover 91 over 152 analyzed samples in this large scale study were found below the DLs for TBT and an additional pre-concentration step is therefore needed to improve the detection/quantification capacity. Among

various options, the large volume injection (LVI) technique using a programmed temperature vaporization (PTV) inlet is very convenient for GC analyses since it can be automated and carried out on-line [41]. The use of a packed liner is furthermore attractive in LVI given a larger solvent capacity and since it eliminates the need for liquid nitrogen required with regular liners. Besides, the packing not only retain the analytes but also prevent the transfer of high-boiling matrix constituents to the analytical column. However, the choice of the packing material is critical as it should (1) retain the analytes but also allow their transfer to the column without degradation; (2) be thermally stable (above the desorption/cleaning temperature) but also chemically stable to the solvent use and (3) not increase the blank levels.

To the best of our knowledge, an on-line pre-concentration method using a PTV inlet with a packed liner has never been optimized for the simultaneous determination of organometallic compounds of Hg, Sn and Pb by GC-ICP/MS. Therefore, it was the aim of this work to find a suitable packing for species retention and then to optimize the various PTV parameters in order to achieve the best solvent elimination, species transfer to the GC and their subsequent separation and detection. Finally, we demonstrated the applicability of the optimized technique through the analyses of natural water samples.

3. Experimental

All material and vessels used for sampling and standards/samples preparation were carefully cleaned with trace-metal protocol: first with a detergent and then in successive acid baths (10% nitric or hydrochloric acid) and rinsed with MQ water. Finally, they were dried under a laminar flow hood and stored in double sealed polyethylene bags.

3.1. Reagents and standards

Ultrapure water was obtained from a Milli-Q system (Quantum EX, Millipore, USA). Buffer solution of pH 5 was prepared by dissolving sodium acetate tryhidrate (NaAc, puriss p.a.; from Riedel-de-Haën, Seelze, Germany) in MQ water and adjusting to pH 5 with glacial acetic acid (HAc, Instra-analyzed;

from J.T. Baker, Phillisburg, NJ, USA). Hydrochloric acid (HCl, 33-36%, ULTREX II Ultrapure Reagent) and ammonium hydroxide (NH_4OH ≥ 25% in H_2O, TraceSELECT® Ultra, for ultratrace analysis) for pH value control were from J.T. Baker (Phillipsburg, NJ, USA) and Fluka (Steinheim, Germany), respectively. Analytical reagent-grade hexane was from Sigma-Aldrich (Belgium), and sodium tetrapropylborate ($NaBPr_4$, purity > 99%) was purchased from GALAB (Geesthacht, Germany). Methanol (MeOH, ≥ 99.9% Chromasolv) for the preparation of standards solutions was obtained from Sigma-Aldrich (Seelze, Germany). Inorganic thallium and antimony used for mass-bias were obtained from Spex Certiprep (USA).

Stock solutions of IHg and MMHg of natural isotopic composition were prepared dissolving mercury (II) chloride pure salt from Sigma-Aldrich and monomethylmercury chloride (98,4%) from Stream Chemicals (MA, USA). The isotopically enriched species were purchased from ISC Science (Oviedo, Spain): IHg enriched in ^{199}Hg (91%) at 10 µg g^{-1} and MeHg enriched in ^{201}Hg (96.5%) at 5 µg g^{-1}. Tributyltin (TBT) chloride (96%), dibutyltin (DBT) dichloride (97%), monobutyltin (MBT) trichloride (95%), were obtained from Sigma-Aldrich; whereas trimetyltin (TMT) chloride (98%), dimetyltin (DMT) dichloride (95%) and monometyltin (MMT) trichloride (98+%), were purchased from Strem Chemicals (MA, USA). A mixture of MBT, DBT and TBT enriched in ^{119}Sn (82.4%) at 0.110 ± 0.005, 0.691 ± 0.009 and 1.046 ± 0.020 µg g^{-1} respectively, was obtained from ISC Science (Oviedo, Spain). Triemethyllead chloride (Me_3PbCl, 85 %) and triethyllead chloride (Et_3PbCl, 82.3%) were purchased from Dr. Ehrenstorfer (LGC Standards, Molheim, France).

All stock solutions (1000 µg g^{-1} as Hg, Sn and Pb) were prepared by dissolving the corresponding salt either in a 3:1 mixture of acetic acid/methanol for tin compounds, methanol for MeHg and lead compounds, and 1% HCl in ultrapure water for IHg. Then, they were kept in the dark at 4 °C until use. Working standard solutions were prepared daily by appropriate dilution of the stock standard solutions with 1% HNO_3 in ultrapure water and stored under refrigeration. The exact concentration of each enriched solutions used were determined by reverse isotope-dilution mass spectrometry (RIDMS) at the same time as the sample preparation. Three independent isotope-dilution RIDMS analyses were carried out and each solution was injected three times.

3.2. Sampling, preservation and preparation of natural samples

Natural river waters were collected during October 2015 at different locations in a tributary of the Adour river (Aquitaine, SW France) using pre-cleaned Teflon bottles. The samples were stored for a few hours in a cooler and back in the lab, filtered through 0.45 µm PVDF filters, acidified to 1 % HCl (v/v) and stored in the dark at + 4 °C until analyses that were carried out within a few days.

The sample preparation was done in a similar way as previously described [20, 39]. Briefly, 50 mL of sample is accurately weighted in a flask containing 5 mL of an acetate buffer (0.1 mol L^{-1}, pH 5) and spiked with an appropriate amount of the isotopically enriched spiking solutions (1.5 µg Hg L^{-1} for ^{199}IHg, 0.1 µg Hg L^{-1} for ^{201}MeHg and 2.5 µg Sn L^{-1} for butyltin organometallic compounds). For aqueous samples, an equilibration step is less critical than for solid matrix, since samples are usually previously acidified allowing rapid equilibrium between species [39]. The amount of enriched standard added to samples is adjusted to reach a final spike to analyte isotope ratio close to one in order to minimize error in the final determination [42]. The pH was adjusted to 5 with ammonium hydroxide and hydrochloric acid pure solutions. Appropriate amount of hexane (500 µL) and $NaBPr_4$ (100 µL, 5%) were added and samples were then vigorously shaken for 15 min. Finally, the organic phase was separated and transferred to an injection vial (1.5 mL) kept at -18 °C until measurement. Note that the sample preparation procedure described above was done in duplicate for each sample, one replicate being analyzed by the method proposed here with PTV and the other without to compare them.

3.3. Instrumentation

A Trace Ultra GC (ThermoFisher, Whatham, MA, USA) was coupled to an inductively coupled plasma mass spectrometer (X7 Series 2, ThermoFisher Scientific, France) through a commercial heated interface (ThermoFisher Scientific, France). The GC was fitted with a fused silica column (30 m, 0.25 mm i.d., 0.25 µm thick coating, Restek Corporation, Bellefonte, PA, USA) and equipped with a TriPlus RSD autosampler. Microliter syringes of 10 or 100 µL were obtained from Hamilton (Bonaduz, Switzerland). The ICP-MS instrument

was operated under wet plasma conditions with a commercial dual inlet glass torch fitted with a shield bonnet, a concentric nebulizer and an impact ball spray chamber allowing the continuous aspiration of a solution containing Tl and Sb at 10 µg L^{-1} for mass bias corrections [39]. All sample aliquots and spike additions were weighted out using an analytical balance (Sartorius, model BP211D, Goettingen, Germany) to a precision of 10^{-5} g.

Straight liners (2 mm ID, 2.75 mm OD, 120 mm length, ThermoFisher Scientific, France) were filled with a solid phase (Bondesil-ENV, 125 µm, Agilent Technologies) made of a styrene-divinylbenzene polymeric resin and maintained with two tight glass wool plugs (about 0.5 cm each, ThermoFischer Scientific, France). Liners were pre-conditioned under an inert atmosphere (He, 20 ml min^{-1}) as follow before use: a first flushing step to eliminate O_2 (15 min), then a step by step incremental heating phase (50 °C per step for 15 min each) from room temperature to 245 °C and eventually several high-speed cycles from room temperature to the maximum temperature were performed to complete the process.

3.4. Data treatment

Peak areas and heights were determined with the Plasmalab software embedded in the instrument. Hg and butyl-Sn species concentrations were determined by isotope dilution while methyl-organotin and organolead compounds were quantified by external calibrations. Methodological detection limits (MDLs) were calculated as three times the standard deviation of procedural blank peak areas plus average and divided by the slope obtained from the calibration plot of peak areas versus standard concentrations. Absolute detection limits (ADLs) were similarly calculated, but taking into account the background signal variation values and the slope obtained from the calibration plot of peak heights versus mass injected. For comparison between results achieved by PTV-GC-ICP/MS and conventional GC-ICP/MS methods for the analysis of control samples (only for organometallic mercury compounds) or natural river waters, some statistical tests based on the calculations of confidence intervals and regression studies were applied.

4. Results and discussion

No certified reference materials are available for the speciation of our target compounds because of their instability [39]. To optimize the different factors and to test the accuracy and precision of the analytical procedure, the method was applied to standard solutions and real aqueous samples (river waters).

4.1. Optimization of the PTV injector parameters for large volume injections

The starting conditions for our optimization were based on previous studies dedicated to multi-elemental speciation analyses [20] and to the optimization of the PTV injector for Hg species alone (Bouchet et al. in prep). Compared to this latter, several parameters had to be adjusted to meet the best conditions for both the retention of the most volatile species (TMT and DMT) in the liner and the transfer of the least volatile ones, i.e. TBT and TEtPb, from the liner to the head of the column.

4.1.1. Optimization of species retention and transfer to the column

About 20 mg of sorbent (ca 1.8 cm length in the 2 mm ID liner used) was found to be the optimal amount between species retention and elution. With lower amounts the maximum volume injectable “at-once” or by multiple injections was limited while with higher amounts, species with the highest boiling points were not transferred to the column or presented bad peak shapes (data not shown). Table 1 presents the optimized parameters found for the operation of the PTV inlet and GC oven. The initial temperature of the PTV was set to 35 °C (the lowest reachable without cryo-cooling) to maximize the retention of volatile species whereas the injection duration and gas flow rate were set to 0.25 min and 50 mL min^{-1}, respectively during the venting phase to obtain an optimal elimination of the solvent. Under these conditions, the perturbation of the plasma by the solvent elution (assessed with the drop in the ^{205}Tl and ^{121}Sb signals) lasted 7 min (420 s) (Figure 1). To achieve the transfer of the least volatile species, the temperature of the PTV inlet was maintained at

260 °C for a duration of 6 min, respectively. Above 260 °C, the chromatograms were seriously deteriorated with noisy baseline and Sn species overlapped.

Table 1. Operating conditions for the GC-ICP/MS coupling systems.

GC conditions	
Column	Rxi-5ms 30 m
	i.d. 0.25 mm; d.f. 0.25 µm
PTV inlet initial conditions	
Temperature	35 °C
Split flow	45 mL min^{-1}
Splitless time	6 min
Injection phase	
Volume injected	25 µL
Duration	0.25 min
Gas flow rate	50 mL min^{-1}
Transfer temperature	260 °C
Transfer duration	6 min
Oven program	
Initial temperature	40 °C
Initial time	6.5 min
Ramp rate 1	35 °C
Final temperature 1	180 °C
Hold time 1	0 min
Ramp rate 2	50 °C
Final temperature 2	280 °C
Hold time 2	2 min
Carrier gas flow (He)	5 mL min^{-1}
ICP-MS parameters	
Forward power	1250 W
Plasma gas flow (Ar)	15 L min^{-1}
Auxiliary gas flow (Ar)	0.9 L min^{-1}
Nebulizer gas flow (Ar)	0.27 L min^{-1}
Make up gas flow (Ar)	300 mL min^{-1}
Isotopes/dwell times	Hg (199, 200, 201, 202) / 30 ms
	Sn (116, 117, 118, 119, 120) / 30 ms
	Pb (206, 208) / 30 ms
	Tl (203, 205) / 5 ms
	Sb (121, 123) / 5 ms

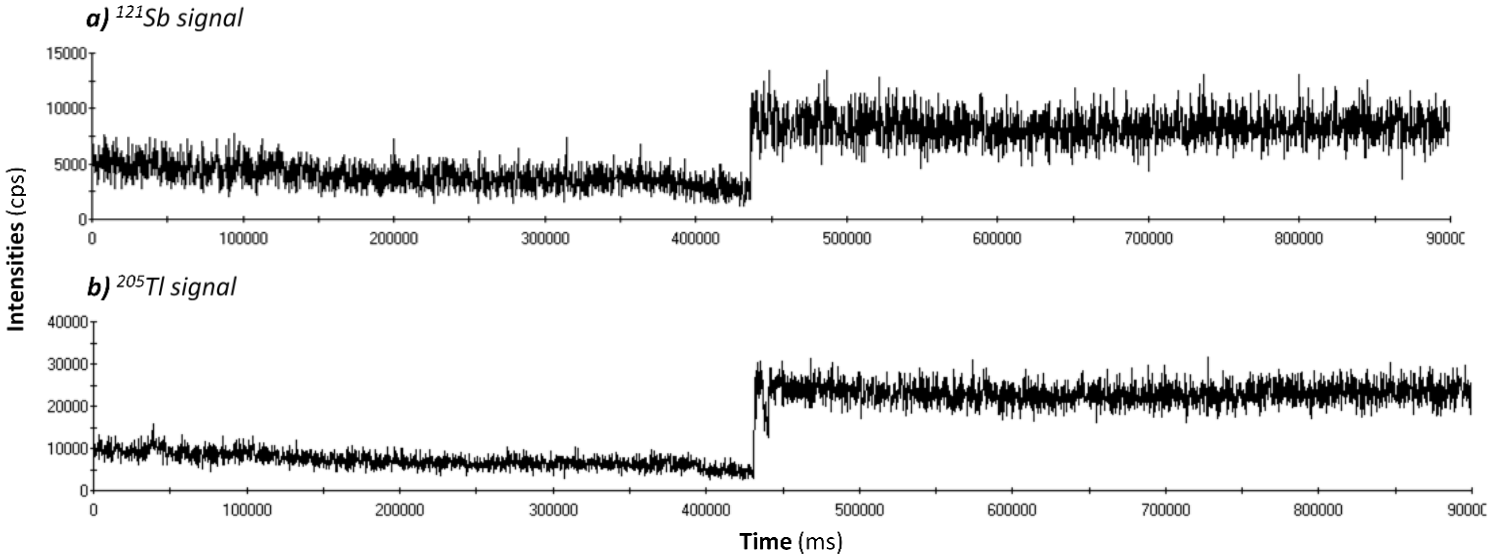

Figure 1. ^{121}Sb (a) and ^{205}Tl (b) signal representation
where it is possible to appreciate the plasma perturbation by the solvent elution.

Compared to regular GC conditions for multi-elemental speciation analysis without PTV [20], several changes were made: (1) the carrier gas (He) flow was increased to 5 mL min^{-1} instead of 2 mL min^{-1} to improve the species transfer and elution, (2) the initial oven temperature was lowered to 40 °C instead of 60 °C to better refocus the analytes at the head of the column, (3) the initial oven temperature was hold for 6.5 min instead of 0.5 min in order to accommodate the longer transfer time of the species from the inlet and (4) the temperature ramping rates were modified to improve the peak separation of organotin compounds with 2 stages of ramping at 35 °C min^{-1} until 180 °C and then 50 °C min^{-1} until 280 °C compared to 60 °C min^{-1} without PTV. Following those modifications, the duration for one analysis increased to 15 min compared to 11 min without PTV.

Figure 2 presents a comparison of typical chromatograms obtained with the regular GC program and under the optimized conditions with PTV. As can be seen, the chromatograms are fairly similar, except for the shifted retention times with the PTV, demonstrating the suitability of the trapping, release and separation steps. Retention times are consistent between the two methods and peak shapes remain very good with the use of PTV (elution duration times in Table 2). Besides, statistical Student´s t-tests were made to compare slopes of calibrations obtained by both methods, being the p-values higher than 0.05 in all cases (thus, the null hypothesis should not be rejected).

a)

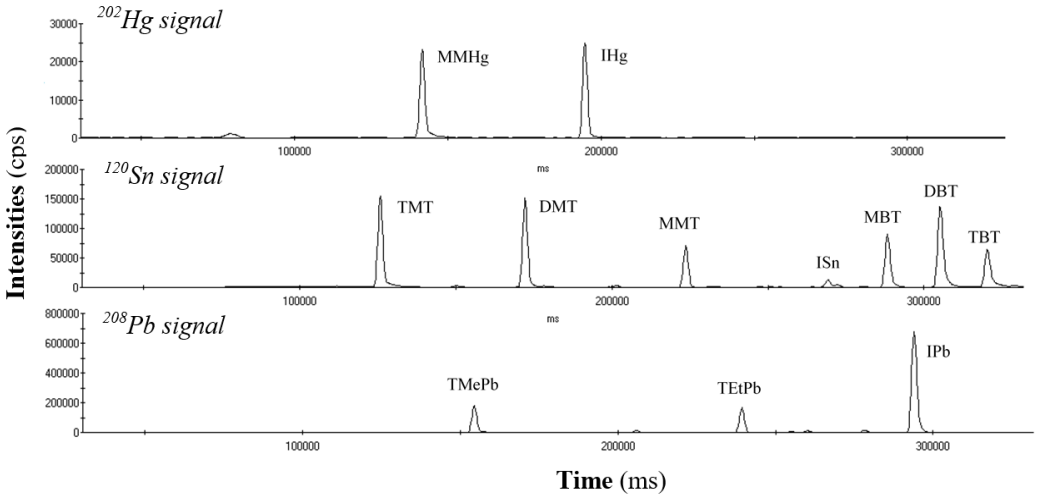

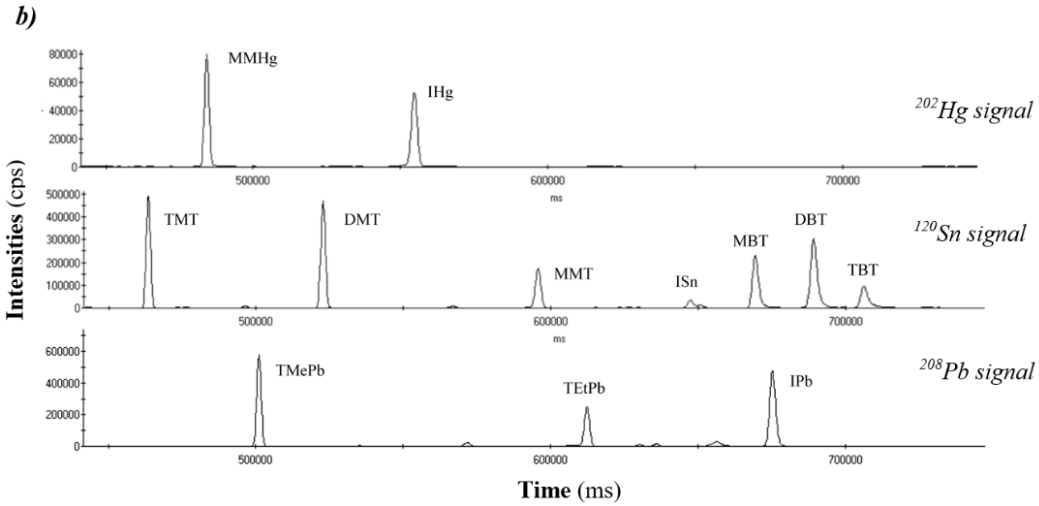

Figure 2. Comparison of chromatograms obtained under (a) regular GC conditions without PTV (Injection volume = 2 µL; standard concentration = 0.5 µg L^{-1}) and (b) the optimized conditions for PTV described in Table 1 (Injection volume = 25 µL; standard concentration = 0.1 µg L^{-1}).

Table 2. Elution duration times (ms) for organometallic Hg, Sn and Pb compounds by conventional GC-ICP/MS and PTV-GC-ICP/MS methods.

Compound	GC-ICP/MS	PTV-GC-ICP/MS
MMHg	9010	8011
IHg	9742	9093
TMT	6928	5412
DMT	6711	5196
MMT	4980	5629
MBT	8444	7794
DBT	9526	9309
TBT	9742	10392
TMePb	6278	5196
TEtPb	6062	5629

4.1.2. Maximum volume injectable at-once

After these first optimization steps, we investigated the maximum volume that can be injected at-once. Figure 3 presents the increase of peak areas for each species according to the volume of solvent injected. The species clearly grouped in two pools with: (i) the more volatile TMT, DMT, TMePb, MMHg and IHg showing a linear increase over the full range of injection; and (ii) the least volatile MMT, MBT, DBT, TBT and TEtPb (boiling points > 200 °C) that presented a plateau or a slight decrease over 30 µL. This was a surprising result as one would expect the heavier species to interact more easily with the solvent and we hypothesized that during the injection phase there could be a competition for adsorption sites between the solvent and the analytes or a kinetic effect preventing their adsorption to explain these observations.

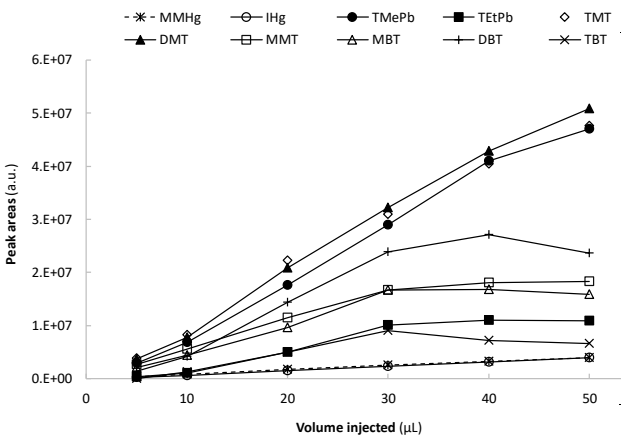

Compound	Specie propylated	Boiling point / °C
MMHg	$MeHgPr$	151
IHg	$HgPr_2$	193
TMT	Me_3SnPr	127
DMT	Me_2SnPr_2	171
MMT	$MeSnPr_3$	211
ISn	$SnPr4$	222
MBT	$BuSnPr_3$	266
DBT	Bu_2SnPr_2	282
TBT	Bu_3SnPr	297
TMePb	Me_3PbPr	159
TEtPb	Et_3PbPr	220

Figure 3. Peak areas for each species (with their boiling points) according to the volume injected.

In order to be able to increase the volume injected, various tests were conducted on the effect of increasing the gas flow rate or decreasing the speed of solvent delivery to the liner during the injection period (Figures 4, 5 and 6). Increasing the gas flow rate from 50 to 150 mL min^{-1} during the injection period led to slight improvements in peak areas for some heavy species but it also seriously deteriorated the peak shape for others. Most obvious were IHg and

TEtPb that suffered from severe fronting or even peak splitting under these conditions.

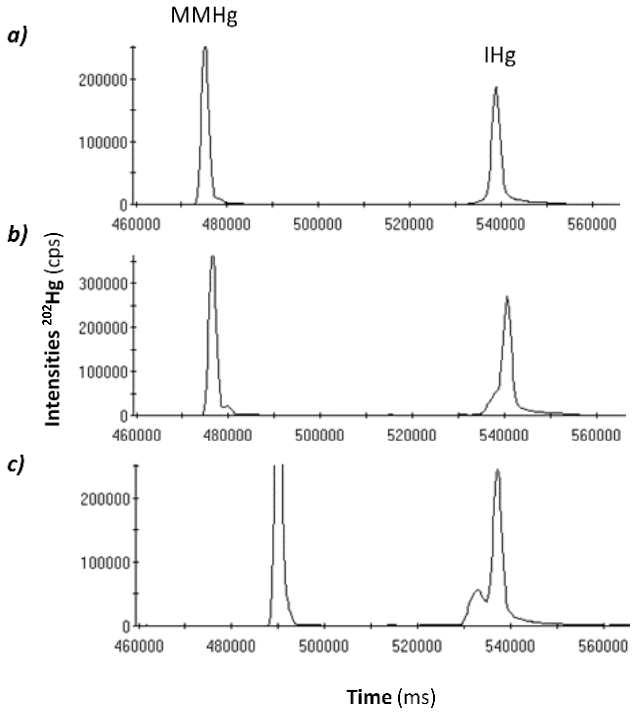

Figure 4. Effect of injection flow in speciation analysis of mercury organometallic compounds. (a) Injection flow 50 mL min^{-1} and 25 µL of volume injected, (b) Injection flow 50 mL min^{-1} and 40 µL of volume injected and (c) Injection flow 100 mL min^{-1} and 40 µL of volume injected.

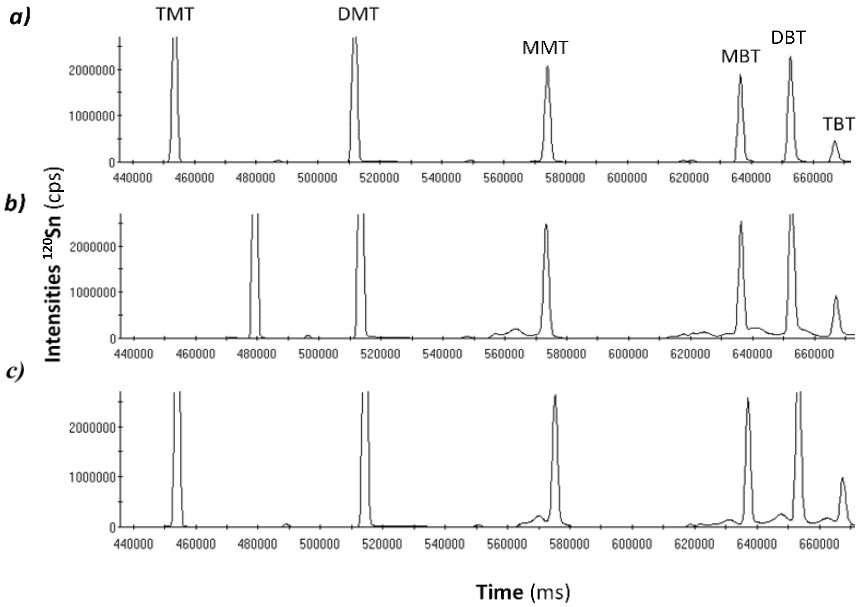

Figure 5. Effect of injection flow in speciation analysis of tin organometallic compounds. (a) Injection flow 50 mL min^{-1} and 25 µL of volume injected, (b) Injection flow 50 mL min^{-1} and 40 µL of volume injected and (c) Injection flow 100 mL min^{-1} and 40 µL of volume injected.

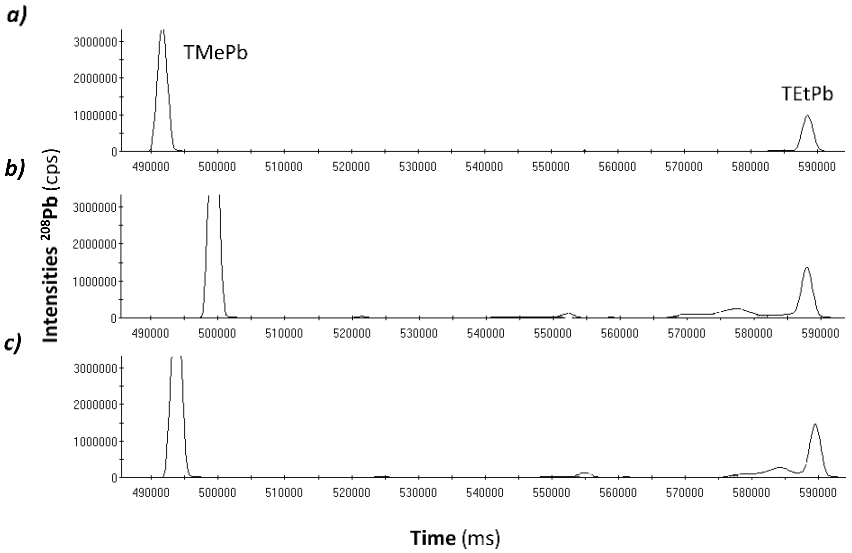

Figure 6. Effect of injection flow in speciation analysis of lead organometallic compounds. (a) Injection flow 50 mL min^{-1} and 25 µL of volume injected, (b) Injection flow 50 mL min^{-1} and 40 µL of volume injected and (c) Injection flow 100 mL min^{-1} and 40 µL of volume injected.

Similarly, decreasing the speed of solvent delivery (from 200 to 5 µL s^{-1}) did not lead to increased intensities and chromatograms were worse than those obtained with initial conditions (Figure 7). Given these results, 25 µL was eventually chosen as the optimal volume of injection together with a gas flow rate of 50 mL min^{-1} and a solvent delivery of 200 µL s^{-1}.

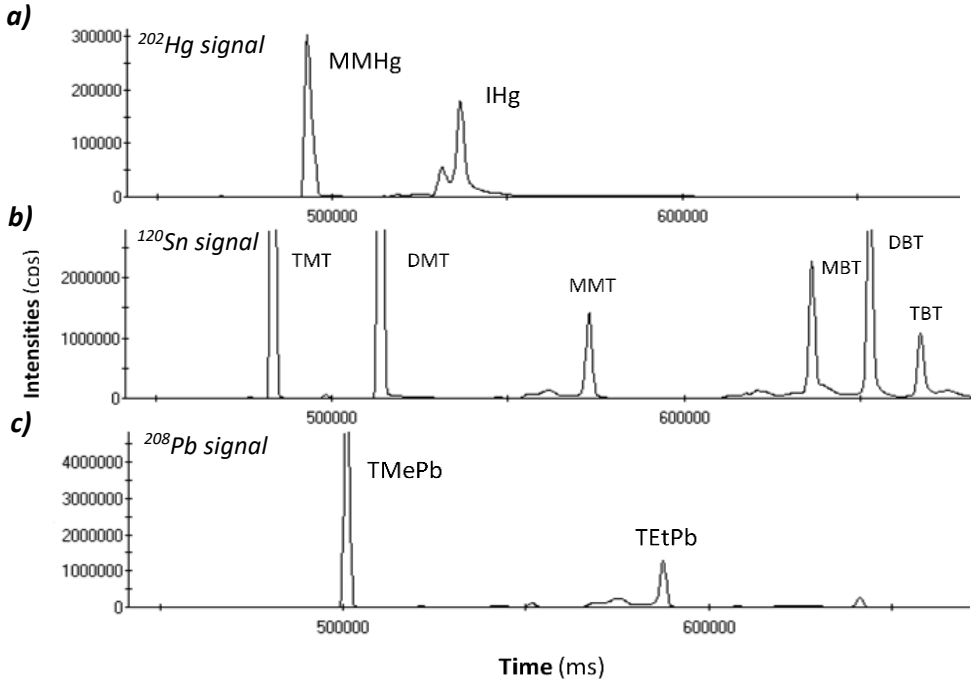

Figure 7. Chromatogram obtained for (a) Hg (b) Sn and (c) Pb speciation with syringe speed 10 µL s^{-1}.

4.1.3. Multiple injection mode

Based on the previous results, the maximum volume that can be injected through multiple injection of 25 µL was then evaluated. In this case, the time interval between injections is critical and should be optimized to allow the solvent to evaporate while avoiding species losses. For this, the time between two injections was checked (52 s) because it must be a little more of the time to vent the solvent. Figure 8 shows the increases in peak areas for each species according to the total volume injected. They all showed a linear increase up to the fourth repetition ($R^2 > 0.998$) except TMT ($R^2 > 0.992$), the most volatile

species, that clearly deviate between 75 and 100 µL. The repeatability was good (RSD < 6 %) over the injection range for all species while the peak shapes remain good/acceptable up to 75 µL (Figure 9) even if some peaks were slightly broader, e.g. IHg. However, they were strongly deteriorated at 100 µL (Figure 10) with severe fronting or even peak splitting for the late eluting compounds suggesting that the retention capacity of the packing material for solvent and/or analytes was exceeded in this latter case (elution duration times comparison in Table 3).

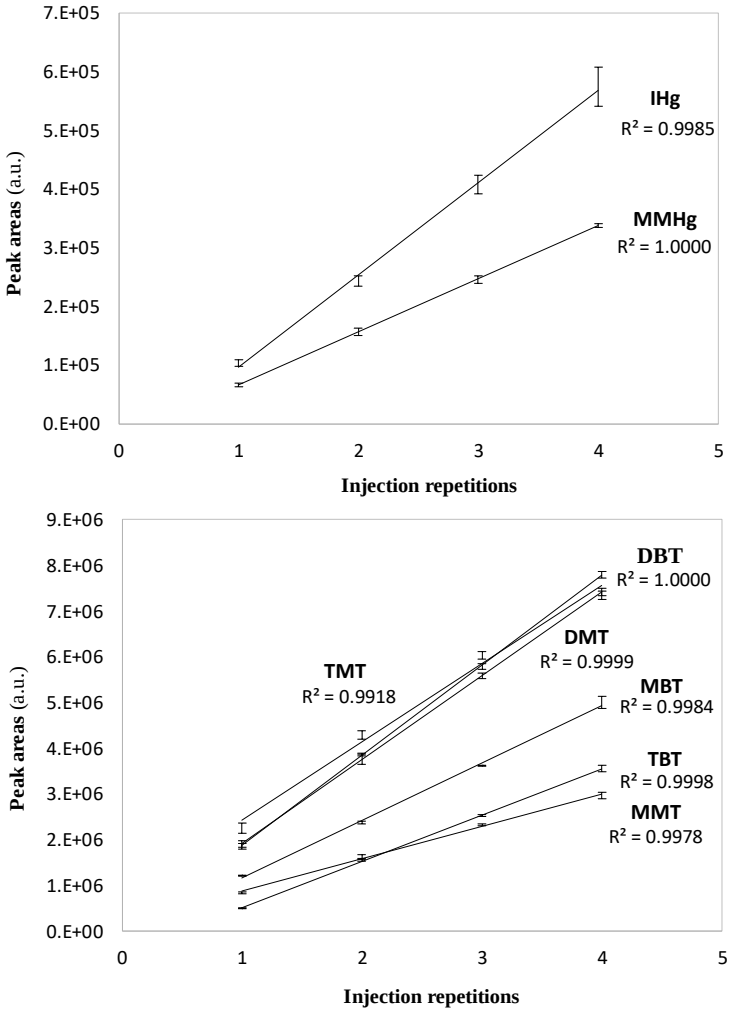

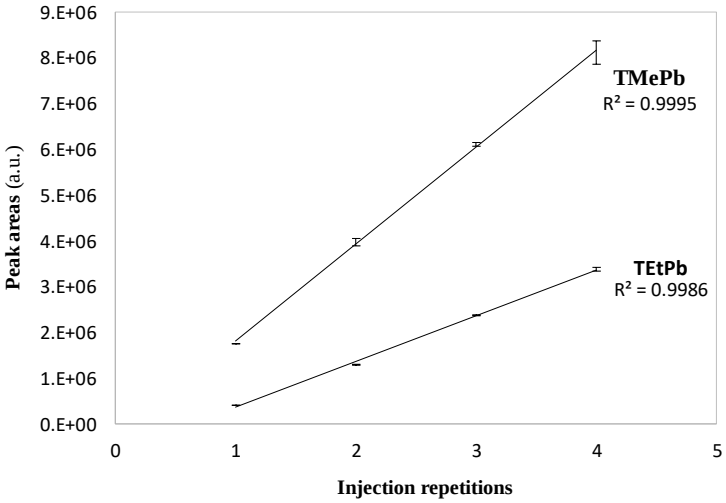

Figure 8. Peak areas for Hg, Sn and Pb species in multiple injection of 25 µL.

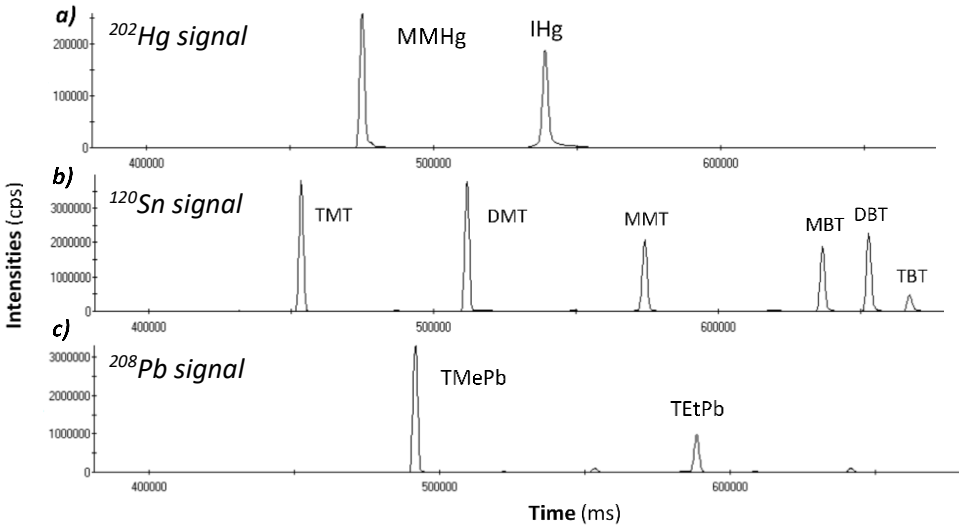

Figure 9. Chromatograms obtained for (a) Hg, (b) Sn and (c) Pb species with the optimized PTV-GC-ICP/MS conditions (Injection volume = 3 x 25 µL; standard concentration = 0.1 µg L^{-1}).

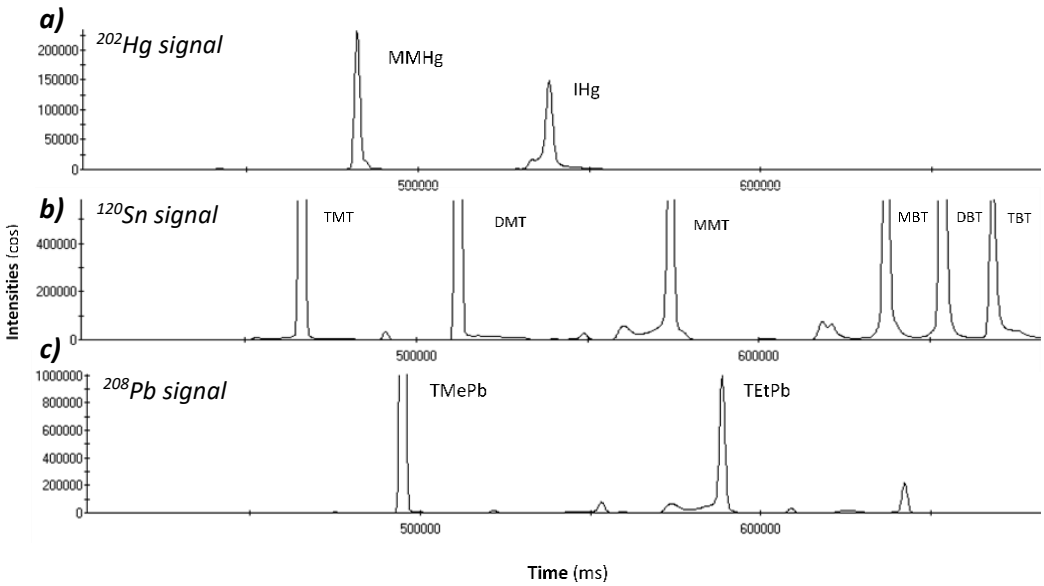

Figure 10. Chromatograms obtained for (a) Hg, (b) Sn and (c) Pb speciation with a multiple injection mode (4 x 25 µL).

Table 3. Elution duration times (ms) for organometallic Hg, Sn and Pb compounds for multiple injection study.

Compound	1 x 25 µL	2 x 25 µL	3 x 25 µL	4 x 25µL
MMHg	8794	8010	7578	11474
IHg	10557	10021	14464	25980
TMT	4980	5846	4979	15155
DMT	6495	5629	5412	7361
MMT	5412	6279	6928	15155
MBT	7928	7794	8227	12557
DBT	8660	8444	8876	14722
TBT	8928	9526	8227	16887
TMePb	6443	7361	8175	7361
TEtPb	6145	7289	7371	7887

4.2. Analytical Performances

4.2.1. Linearity, precision and stability

The performances, robustness and stability of the developed method was tested over one-month period with the same liner by three replicate analyses of standard solutions (0, 5, 10, 25, 50 and 100 pg L^{-1}) in multiple injection mode (3 x 25 µL). Over this low concentration range, the linearity was always excellent for all species with $R^2 \geq 0.992$ (Table 4). In all cases, the relative standard deviations of the peak areas for triplicate injections were below 5%). No significant differences were observed over this time period with respect to linearity, slopes and relative standards deviations demonstrating the stability of the method and especially of the packed liner.

4.2.2. Methodological and absolute detection limits

Table 4 presents methodological (MDLs) and absolute detection limits (ADLs) for the optimized method as well as those for regular GC-ICP/MS and various other methods from the literature. Overall, ADLs ranged from 1.1 for TMT to 19.7 fg to IHg and were the highest for Hg species due to the higher ionization potential of Hg while usually lower than 5 fg for Sn and Pb species. The ADLs obtained in this work are often one or several orders of magnitude lower to what has been previously reported [43 – 45], although it should be noted that such values are hardly reported. On the other hand, MDLs range from 0.1 to 12.6 pg L^{-1}, which is also lower than previous works in almost any case albeit to a different extent depending on the species. Unfortunately, no such detection limits could be found for methyltin species in the literature limiting our comparison. Monperrus et al. (2005) [39] developed a similar SSID-GC-ICP/MS method for the simultaneous determination of mercury and tin organometallic compounds, but only applied for butyltin compounds and they achieved detection limits 3-4 times higher. Only Sharif et al. [46] obtained similar sub pg L^{-1} MDLs for IHg and MMHg by using pre-cleaned reagents (buffer and derivatizing reagent) and a specific technique combining purge and trap with AFS detection (PT-GC-Pyr-AFS). Overall, our method offers MDLs that are better than any other multi-elemental speciation techniques and similar/comparable to the best mono-elemental techniques available up to date. It is noteworthy

that given our ADLs, the MDLs could be further improved by the use of cleaned reagents.

Table 4. Methodological and absolute detection limits. Comparison with limits for conventional GC-ICP/MS method (without PTV) and other bibliographic limits.

	PTV-GC-ICP/MS		GC-ICP/MS	Bibliographic limits		
Species	**ADL[a] (fg)**	**MDL[b] (pg L^{-1})**	**MDL (pg L^{-1})**	**ADL (pg)**	**MDL (pg L^{-1})**	**Coefficient R^2**
IHg	19.7	12.6	38.1	3[43], 13[44]	9-90[46], 60[39], 74[43], 130[44], 140[20]	0.9969
MMHg	8.3	3.7	16.9	3[43], 1[44]	1-6[46], 5[43], 10[39], 10[44], 40[20]	0.9982
MMT	5.4	7.0	73.9			0.9985
DMT	2.1	0.7	61.3			0.9986
TMT	1.1	3.3	26.2			1.0000
MBT	3.5	10.1	21.6	0.01-0.17[45]	33[39], 90[20], 250[47]	0.9923
DBT	2.3	6.5	19.9		27[39], 80[20], 180[47], 200[48]	0.9996
TBT	6.0	7.0	15.4		11[15], 13[32], 22[39], 25[50], 80[20], 210[47], 700[48]	0.9926
TMePb	1.2	0.1	9.3		400[49]	0.9996
TEtPb	4.1	0.7	12.1		200[49], 1000[20]	0.9997

[a] Calculated as (Average + 3SD) / Slope, where "SD" is referred to signal variation values and the slope is achieved from "Peak heighs vs. Mass injected" calibration plot.
[b] Calculated as (Average + 3SD) / Slope, where "SD" is referred to blank peak area values and the slope is achieved from "Peak areas vs. Concentration" calibration plot. Number of blanks = 10 and the volume of water required = 100 mL.

Another useful comparison is with respect to the species background levels found in ecosystems that were recently evaluated at the French national level using an extensive collection of samples [20]. In this work, background concentrations in waters were between <0.04 - 0.14, <0.14 - 2.1, 0.49 – 151, <0.08 - 3.04 and <0.08 – 0.25 ng L^{-1}, for MMHg, IHg, MBT, DBT and TBT respectively. From these values, they established the calculated threshold (upper limit which defines when action should be taken) at 0.10, 1.38, 79.0, 2.33 ng L^{-1}, for MMHg, IHg, MBT and DBT, respectively; and presented the

distribution of concentrations. For TBT, authors were not able to estimate the calculated threshold and the distribution of concentrations due the high amount of samples below the LOQ. Taking into account the improvement of the MDLs achieved (about 10 times lower for all compounds; see Table 4), it is possible to ensure that the proposed method here would allow to refine the distribution of the concentrations and to obtain more accurate results of the calculated thresholds.

Finally, it is also important to note that MDLs achieved comply with the WFD demands as they are lower than the established environmental quality standards (1.2 μg L^{-1} for Pb, 50 ng L^{-1} for Hg and 0.2 ng L^{-1} for Sn).

4.3. Methodological validation through comparison with natural water samples

No certified reference materials are available for the speciation of our target compounds in water due to their instability [39] but an intercomparison sample from the international program "Geotraces" could be analysed to test the accuracy of the developed method for the Hg species. We found concentrations of 199.0 ± 1.9 (RSD = 3 %) and 81.0 ± 0.6 (RSD = 2 %) pg L^{-1} for IHg and MMHg each, which compared well with 201.9 ± 1.4 (RSD = 2 %) and 79.9 ± 1.3 (RSD = 5 %) pg L^{-1}, respectively (obtained by a regular GC-ICP/MS method). Note that the previous intervals correspond to 95% confidence intervals.

To further demonstrate the applicability, accuracy and potential of the proposed method, the concentrations of organometallic compounds of Hg, Sn and Pb were analyzed in natural river water samples by GC-ICP/MS with and without PTV. Table 5 shows the results obtained by each method for water samples collected in different points of the Adour river basin (SW France). For the most abundant species that are present well above the detection limits of the regular GC-ICP-MS, the results from both methods are in excellent agreement as demonstrated by regression analyses (Figure 11). Indeed, for IHg, MMT, DMT and MBT, slopes and intercepts were equal to 1 and 0, respectively considering their confidence intervals at 95% while the correlation coefficients were equal or better than 0.993 in all cases. In the case of MMHg, TMT and DBT, results were satisfactory taking into account that all samples, or most of them, presented contents below the quantification of the conventional GC-ICP/MS

method: correlation coefficient for DBT was also good (0.998), because only two samples were below the detection limit and three below the quantification limit; but for MMHg and TMT (0.995 and 9.886) it is needed to take into account that all sample contents determined by the conventional way were below the quantification or detection limits, with the most remarkable differences between contents determined by both method at lowest levels. For TBT no results are presented because the majority of samples had concentrations below the detection capacity of the method.

In the case of precisions, both methods gave satisfactory results but the PTV one retain relative standard deviation below 5 % for all species in all samples studied, even for the samples that the conventional GC-ICP/MS method was not able to detect. Therefore, even if the precision of the conventional GC-ICP/MS method is very good, it is surpassed by the capacity of PTV-GC-ICP/MS method which is able to provide these excellent values at the very low concentration values for all organometallic compound analysed.

Finally, Figure 12 shows an example of chromatogram obtained with the developed PTV-GC-ICP/MS method to the study of a natural river water analyzed.

Table 5. Contents of Hg, Sn and Pb organometallic compounds in river water samples. Mean values (ng L^{-1}; for TMePb in pg L^{-1}) and relative standard deviation (n = 3). Comparison between PTV-GC-ICP/MS method (first line) and conventional GC-ICP/MS method (second line). Note that lead organometallic compounds were not analyzed with the conventional GC-ICP/MS methods.

	MMHg	IHg	MMT	DMT	TMT	MBT	DBT	TBT	TMePb	TEtPb
1	0.021±0.001 (2%)	0.233±0.007 (3%)	0.483±0.029 (6%)	2.268±0.068 (3%)	0.198±0.002 (1%)	0.032±0.001 (1%)	0.591±0.018 (3%)	0.031±0.001 (3%)	0.319±0.006 (2%)	0.174±0.003 (2%)
	<LOQ	0.250±0.005 (2%)	<LOQ	2.810±0.056 (2%)	<LOQ	0.045±0.003 (7%)	0.540 ±0.005 (1%)	<LOD	-	-
2	0.021±0.001 (1%)	0.224±0.005 (2%)	2.190±0.066 (3%)	4.969±0.050 (1%)	0.235±0.005 (2%)	0.394±0.020 (5%)	0.708±0.007 (1%)	0.034±0.001 (2%)	0.386±0.004 (1%)	0.488±0.010 (2%)
	<LOQ	0.300±0.006 (2%)	2.080±0.042 (2%)	4.201±0.084 (2%)	0.210±0.004 (2%)	0.384±0.008 (2%)	0.694±0.014 (2%)	<LOD	-	-
3	0.020±0.001 (2%)	0.535±0.016 (3%)	0.697±0.021 (3%)	5.072±0.051 (1%)	0.195±0.002 (1%)	0.564±0.006 (1%)	0.892±0.009 (1%)	0.038±0.001 (3%)	0.766±0.024 (3%)	0.338±0.014 (4%)
	<LOQ	0.55±0.033 (6%)	<LOQ	4.530±0.091 (2%)	<LOQ	0.534 ±0.011 (2%)	0.841±0.008 (1%)	<LOQ	-	-
4	0.040±0.001 (3%)	0.386±0.012 (3%)	8.322±0.166 (2%)	38.634±1.159 (3%)	0.302±0.006 (2%)	0.673±0.020 (3%)	1.087±0.033 (3%)	0.033±0.001 (1%)	0.457±0.018 (4%)	0.268±0.008 (3%)
	<LOQ	0.850±0.009 (1%)	2.550±0.076 (3%)	35.006±0.700 (2%)	<LOQ	0.720±0.014 (2%)	1.004±0.021 (2%)	<LOD	-	-
5	0.015±0.001 (2%)	0.274±0.008 (3%)	1.653±0.033 (2%)	8.920±0.089 (1%)	0.167±0.002 (1%)	0.739±0.022 (3%)	0.998±0.030 (3%)	0.040±0.001 (2%)	0.589±0.024 (4%)	0.202±0.008 (4%)
	<LOD	0.298±0.015 (5%)	1.780±0.071 (4%)	8.73±0.087 (1%)	<LOQ	0.730±0.015 (2%)	0.940±0.019 (2%)	<LOQ	-	-

5	0.015±0.001 (2%)	0.274±0.008 (3%)	1.653±0.033 (2%)	8.920±0.089 (1%)	0.167±0.002 (1%)	0.739±0.022 (3%)	0.998±0.030 (3%)	0.040±0.001 (2%)	0.589±0.024 (4%)	0.202±0.008 (4%)
	<LOD	0.298±0.015 (5%)	1.780±0.071 (4%)	8.73±0.087 (1%)	<LOQ	0.730±0.015 (2%)	0.940±0.019 (2%)	<LOQ	-	-
6	0.017±0.001 (1%)	0.403±0.012 (3%)	0.935±0.009 (1%)	4.533±0.136 (3%)	0.174±0.002 (1%)	0.119±0.001 (1%)	0.093±0.009 (1%)	0.035±0.001 (4%)	0.420±0.013 (3%)	0.741±0.007 (1%)
	<LOD	0.470±0.009 (2%)	0.900±0.018 (2%)	5.1±0.102 (2%)	0.160±0.003 (2%)	0.125±0.004 (3%)	0.107±0.002 (2%)	<LOD	-	-
7	0.014±0.001 (3%)	0.558±0.006 (1%)	0.780±0.031 (4%)	16.630±0.499 (3%)	0.336±0.011 (3%)	0.460±0.009 (2%)	0.228±0.002 (1%)	0.031±0.001 (3%)	0.595±0.018 (3%)	0.185±0.004 (2%)
	<LOD	0.595±0.006 (1%)	0.750±0.015 (2%)	15.71±0.314 (2%)	0.310±0.006 (2%)	0.397±0.016 (4%)	<LOD	<LOD	-	-
8	0.051±0.002 (3%)	0.957±0.029 (3%)	0.289±0.006 (2%)	1.954±0.059 (3%)	0.095±0.003 (3%)	0.173±0.009 (5%)	0.056±0.002 (3%)	0.033±0.001 (1%)	0.389±0.012 (3%)	0.250±0.010 (4%)
	<LOQ	0.913±0.064 (7%)	<LOQ	1.900±0.038 (2%)	<LOQ	0.130±0.005 (4%)	<LOQ	0.069±0.006 (9%)	-	-
9	0.021±0.001 (1%)	0.650±0.020 (3%)	0.675±0.007 (1%)	6.820±0.205 (3%)	0.123±0.004 (3%)	0.093±0.003 (3%)	0.045±0.002 (4%)	0.033±0.001 (1%)	0.398±0.020 (5%)	0.218±0.009 (4%)
	<LOQ	0.704±0.049 (7%)	0.650±0.013 (2%)	6.700±0.134 (2%)	<LOQ	0.091±0.004 (4%)	<LOQ	<LOD	-	-
10	0.013±0.001 (1%)	0.773±0.023 (3%)	0.858±0.017 (2%)	5.984±0.180 (3%)	0.136±0.001 (1%)	0.140±0.001 (1%)	0.040±0.001 (3%)	0.029±0.001 (2%)	0.389±0.027 (3%)	0.250±0.010 (4%)
	<LOD	0.790±0.008 (1%)	0.737±0.015 (2%)	4.280±0.086 (2%)	<LOQ	0.154±0.003 (2%)	<LOQ	0.063±0.006 (9%)	-	-
11	0.018±0.001 (2%)	0.239±0.003 (1%)	0.307±0.003 (1%)	3.563±0.071 (2%)	0.061±0.001 (2%)	0.103±0.002 (2%)	0.076±0.002 (2%)	0.037±0.001 (2%)	0.214±0.04 (2%)	0.185±0.009 (5%)
	<LOD	0.326±0.003 (1%)	<LOQ	2.970±0.060 (2%)	<LOQ	0.117±0.006 (5%)	<LOD	<LOD	-	-

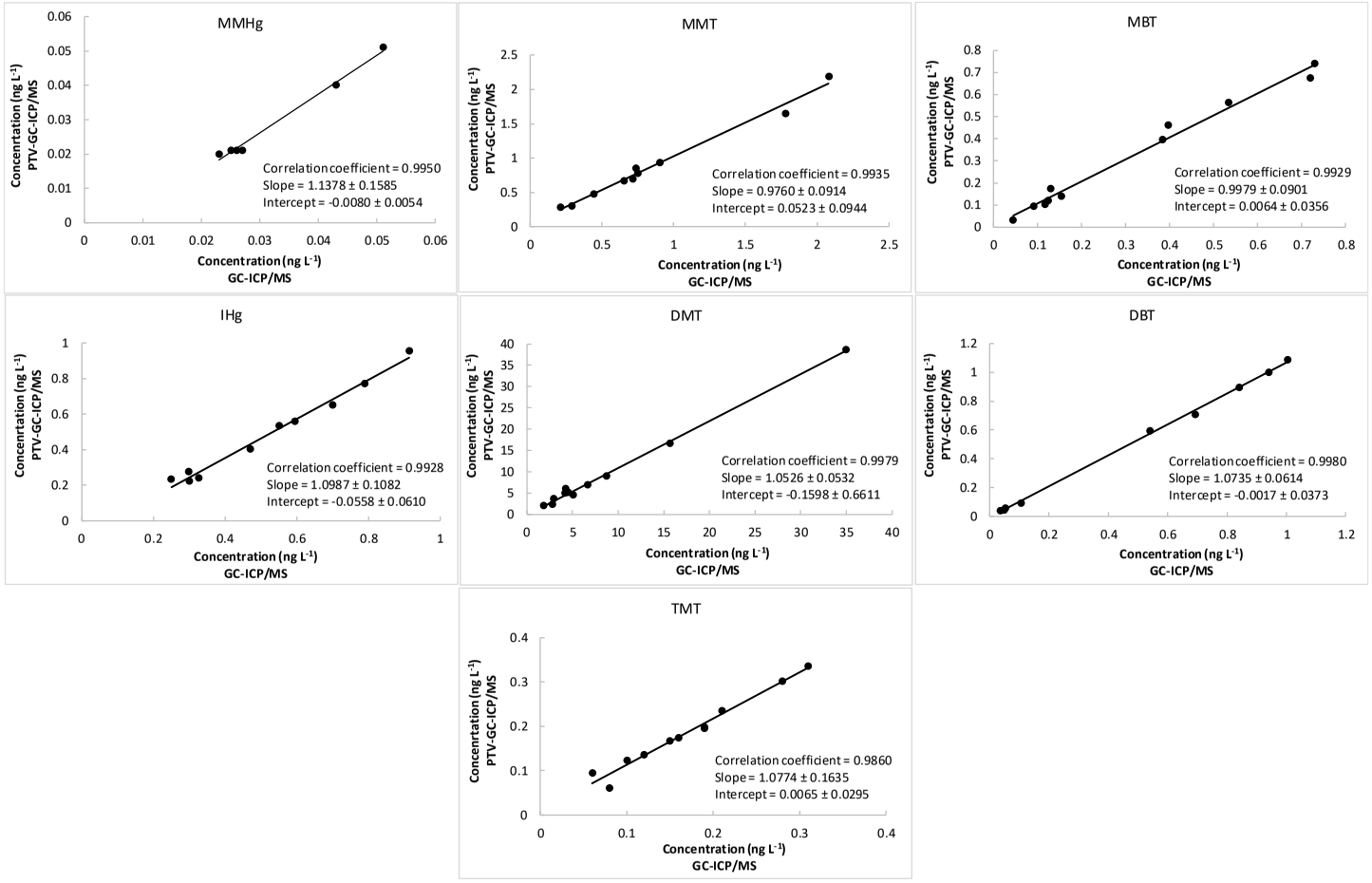

Figure 11. Regression lines for the comparison of PTV-GC-ICP/MS and conventional GC-ICP/MS methods. Regression lines were built taking into account only contents above the detection limits for both methods.

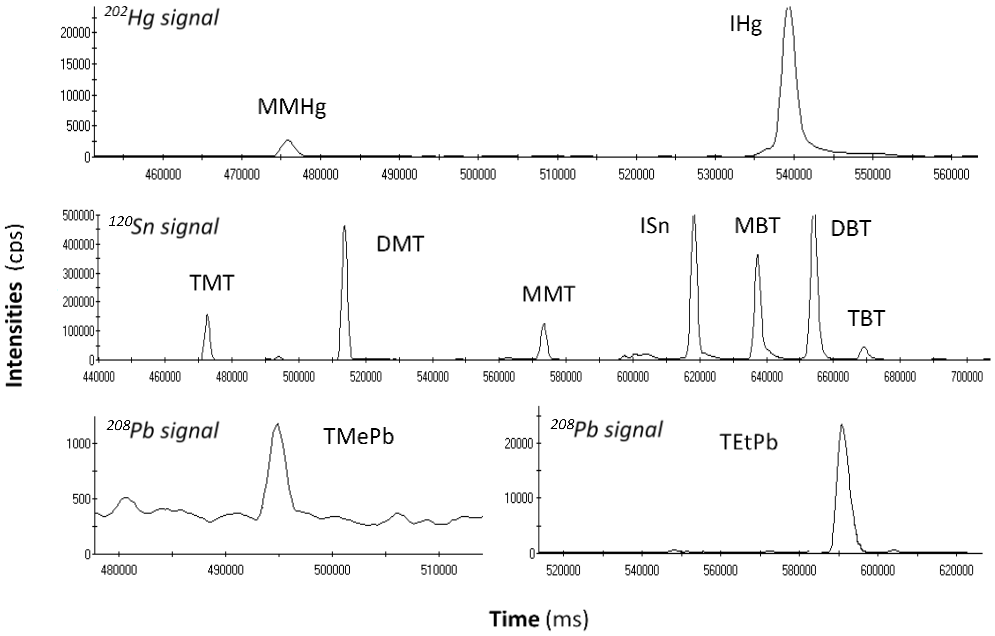

Figure 12. Chromatograms obtained for Hg and Sn and simultaneously speciation with final PTV-GC-ICP/MS conditions in a natural river sample analyzed.

5. Conclusions

An accurate and precise method was developed for simultaneous determination of organometallic compounds of mercury, tin and lead in natural waters by an online automated pre-concentration method using large volume injections in a programmable temperature Vaporizer (PTV) inlet fitted with a sorbent packed liner coupled to GC-ICP/MS. Besides, an optimization of various PTV parameters to achieve the best solvent elimination, species transfer to the GC and their subsequent separation and detection, was performed. Absolut and methodological detection limits achieved (in the level of pg L^{-1}) were well below the actual directive requirements and the majority of referenced values obtained in other works. The relevance of the method was tested by the analysis of a set of unpolluted river water samples, and comparing the contents achieved for all organometallic compounds analysed with an analogous conventional GC-ICP/MS from a statistical point of view. The new proposed method was able to reach the very low concentration levels with very good precisions for all samples analysed. On this way, this new methodology could be used as a reference method in control laboratories, ensuring compliance with regulations and normative over the short and medium term; and has the potential to transfer this method to other gas chromatographic applications with inherent lower sensitivity.

References

[1] Beceiro González, E.; Guimaraes, A.; M.F. Alpendurada, M.F. Optimisation of a headspace-spolid-phase micro-extraction method for simultaneously determination of organometallic compounds of mercury, lead and tin in water by gas chromatography-tandem mass spectrometry. J.Chromatogr.A, 2009, 1216:5563-5569.

[2] 2013/39/EU, Directive of the European Parlament and of the Council amending Directives 2000/60/EC as regards priority substances in the field of water policy, Off.J.Eur.Union I. 2013, 226:1-17.

[3] Hsu-Kim, H.; Kucharzyk, K.H.; Zhang, T.; Deshusses, M.A. Mechanisms regulating mercury bioavailability for methylating microorganism in the aquatic environment: A critical review. Environ.Sci.Technol. 2013, 47:2441-2456.

[4] Puk, R.; Weber, J.H. Critical review of analytical methods for determination of inorganic mercury and methylmercury compounds. Appl.Organomet.Chem. 1994, 8:293-302.

[5] Gilmour, C.C.; Henry, E.A.; Mitchell, R. Sulfate stimulation of mercury methylation in freshwater sediments. Environ.Sci.Technol. 1992, 26:2281-2287.

[6] Harrington, C.F. The speciation of mercury and organomercury compounds by using high-performance liquid chromatography. Trends Anal.Chem. 2000, 19:167-179.

[7] Clarkson, T.W. The three modern faces of mercury. Environ. Health Perspect. 2002, 110:11-23.

[8] Graceli, J.B.; Sena, G.C.; Lopes, P.F.I.; Zamprogno, G.C.; da Costa, M.R.B.; Godoi, A.F.L.; dos Santos, D.M.; de Marchi, M.R.R.; dos Santos Fernandez, M.A. Organotins: A review of their reproductive toxicity, biochemistry, and environmental fate. Reprod.Toxicol. 2013, 36:40-52.

[9] Dafforn, K.A.; Lewis, J.A.; Johmston, E.L. Antifouling strategies: History and regulation, ecological impacts and mitigation. Mar.Poll.Bull. 2011, 62:453-465.

[10] Regulation (EC) No 782/2003 of the European Parliament and of the Council on the prohibition of organotin compounds on ships. Official Journal of the European Union, 2003.

[11] Yi, A.X.; Leung, K.M.Y.; Lam, M.H.W.; Lee, J.S.; Giesy, J.P. Review of measured concentrations of triphenyltin compounds in marine ecosystems and meta-analysis of their risks to humans and the environment. Chemosphere, 2012, 89:1015-1025.

[12] Du, J.; Chadalavada, S.; Chen, Z.; Naidu, R. Environmental remediation techniques of tributyltin contamination in soil and water: A review. Chem.Eng.J. 2014, 235:141-150.

[13] Delgado Filho, V.S.; Mancini, C.N.; Silva, I.V.; Pedrosa, D.F.; Destefani, A.C.; Samoto, V.Y.; Takiya, C.M.; Graceli, J.B. Endocrine disruption induced by triorganotin (IV) compounds: impacts in the reproductive and genetic function. J.Med.Genet.Genomics, 2010, 2:29-37.

[14] Macejova, D.; Toporova, L.; Brtko, J. The role of retinoic acid receptors and their cognate ligands in reproduction in a context of triorganotin based endocrine disrupting chemical. Endocr.Regul. 2016, 50:154-164.

[15] Devos, C.; David, F.; Sandra, P. A new validated analytical method for the determination of tributyltin in water samples at the quantification level set by the European Union. J.Chromatogr.A, 2012, 1261:151-157.

[16] García Alonso, J.I.; Ruiz Encinar, J.; Rodríguez González, P.; Sanz-Medel, A. Determination of butyiltin compounds in environmental samples by isotope-dilution GC-ICP-MS. Anal.Bioanal.Chem. 2002, 373:432-440.

[17] UNEO 2015. Partnership for clean fuels and vehicles. http://www.unep.org/transport/new/pcfv/about.asp.

[18] Craig, P. Organometallic compounds in the environment, 2nd ed. John Wiley and Sons Ltd., West Sussex (UK), 2003.

[19] Duzgoren-Aydin, N.S. Sources and characteristics of lead pollution in the urban environment of Guangzhou. Sci.Total Environ. 2007, 385:182-195.

[20] Cavalheiro, J.; Sola, C.; Baldanza, J.; Tessier, E.; Lestremau, F.; Botta, F.; Preud'homme, H.; Monperrus, M.; Amouroux, D. Assessment of background concentrations of organometallic compounds (methylmercury, ethyllead and butyl- and phenyltin in French aquatic environments. Water Res. 2016, 94:32-41.

[21] Yin, Y.; Liu, J.; He, B.; Shi, J.; Jiang, G. Simple interface of high-performance liquid chromatography-atomic fluorescence spectrometry hyphenated system for speciation of mercury based on photo-induced chemical vapour generation with formic acid in mobile phase as reaction reagent. J. Chromatogr.A, 2008, 1181:77-82.

[22] Ugarte, A.; Unceta, N.; Sampedro, M.C.; Goicolea, M.A.; Gómez-Caballero, A.; Barrio, R.J. Solid phase microextraction coupled to liquid chromatography-inductively coupled plasma mass spectrometry for the speciation of organotin compounds in water samples. J.Anal.At.Spectrom. 2009, 24 :347-351.

[23] Amouroux, D.; Seby, F.; Monperrus, M.; Pannier, F.; Mendiguchia, C.; Benoit-Bonnemason, C.; Donard, O.F.X. Chemical species, in: Chemical Marine Monitoring: Policy Framework and Analytical Trends, eds. Quevauviller, P.; Roose, P.; Verreet, G. John Wiley & Sons, pp: 101-160, West Sussex (UK), 2011.

[24] Mao, Y.; Liu, G.; Meichel, G.; Cai, Y.; Jiang, G. Simultaneous speciation of monomethylmercury and monoethylmercury by aqueous phenylation and purge-and-trap preconcentration followed by atomic spectrometry detection. Anal.Chem. 2008, 80:7163-7168.

[25] Le Gac, M.; Lespes, G.; Potin-Gautier, M. Rapid determination of organotin compounds by headspace solid-phase microextraction. J.Chromatogr.A, 2003, 999:123-134.

[26] Millán, E.; Pawliszyn, J. Determination of butyltin species in water and sediment by solid-phase microextraction-gas chromatography-flame ionization detection. J.Chromatogr.A, 2000, 873:63-71.

[27] Yu, X.; Pawliszyn, J. Speciation of alkyllead and inorganic lead by derivatization with deuterium-labelled sodium tetraethylborate and SPME-GC/MS. Anal.Chem. 2000, 72:1788-1792.

[28] Slaets, S.; Adams, F.C. Determination of organomercury compounds with a miniaturized automated speciation analyser. Anal.Chim.Acta, 2000, 414:141-149.

[29] Carpintero Botana, J.; Rodil Rodríguez, R.; Carro Díaz, A.M.; Lorenzo Ferreira, R.A.; Cela Torrijos, R.; Rodríguez Pereiro, I. Fast and simultaneous

determination of tin and mercury species using SPME, multicapillary gas chromatography and MIP-AES detection. J.Anal.At.Spectrom. 2002, 17:904-907.

[30] Centineo, G.; Rodríguez-González, P.; Blanco-González, E.; García Alonso, J.I.; Sanz-Medel, A. Simultaneous determination of mono-, di- and tributyltin in environmental samples using isotope dilution gas chromatography mass spectrometry. J.Mass Spectrom. 2004, 39:485-494.

[31] Moscoso-Pérez, C.; Fernández-González, V.; Moreda-Piñeiro, J.; López-Mahía, P.; Muniategui-Lorenzo, S.; Prada-Rodríguez, D. Determination of organotin compounds in waters by headspace solid phase microextraction gas chromatography triple quadrupole tandem mass spectrometry under the European Water Framework Directive. J.Chromatogr.A, 2015, 1385:85-93.

[32] Rodríguez-Cea, A.; Rodríguez-González, P.; Font Cardona, N.; Aranda Mares, J.L.; Ballester Nebot, S.; García Alonso, J.I. Determination of ultratrace levels of tributyltin in waters by isotope dilution and gas chromatography coupled to tandem mass spectrometry. J.Chromatogr.A, 2015, 1425:265-272.

[33] Alasonati, E.; Fabbri, B.; Fettig, I.; Yardin, C.; Del Castillo Busto, M.E.; Richter, J.; Philipp, R.; Fisicaro, P. Experimental design for TBT quantification by isotope dilution SPE-GC-ICP-MS under the European water framework directive. Talanta, 2015, 134:576-586.

[34] Cavalheiro, J.; Preud´homme, H.; Amouroux, D.; Tessier, E.; Monperrus, M. Comparison between GC-MS and GC-ICPMS using isotope dilution for the simultaneous monitoring of inorganic and methyl mercury, butyl and phenyl tin compounds in biological tissues. Anal.Bioanal.Chem. 2014, 406:1253-1258.

[35] Rodriguez-Gonzalez, P.; Bouchet, S.; Monperrus, M.; Tessier, E.; Amouroux, D. In situ experiments for element species-specific environmental reactivity of tin and mercury compounds using isotopic tracers and multiple linear regression. Environ.Sci.Pollut.Res. 2013, 20:1269-1280.

[36] Clémens, S.; Monperrus, M.; Donard, O.F.X.; Amouroux, D.; Guérin, T. Mercury speciation in seafood using isotope dilution analysis: A review. Talanta, 2012, 89:12-20.

[37] Rodriguez Martin Doimeadios, R.C.; Monperrus, M.; Krupp, E.; Amouroux, D.; Donard, O.F.X. Using speciated isotope dilution with GC-inductively coupled

plasma MS to determine and unravel the artificial formation of monomethylmercury in certified reference sediments. Anal.Chem. 2003, 75:3202-3211.

[38] Monperrus, M.; Rodriguez Martin-Doimeadios, R.C.; Scancar, J.; Amouroux, D.; Donard, O.F.X. Simultaneous sample preparation and species-specific isotope dilution mass spectrometry analysis of monomethylmercury and tributyltin in a certified oyster tissue. Anal.Chem. 2003, 75:4095-4102.

[39] Monperrus, M.; Tessier, E.; Veschambre, S.; Amouroux, D.; Donard, O.F.X. Simultaneous speciation of mercury and bultyltin compounds in natural waters and snow by propylation and species-specific isotope dilution mass spectrometry analysis. Anal.Bioanal.Chem. 2005, 381:854-862.

[40] Monperrus, M.; Rodriguez Gonzalez, P.; Amouroux, D.; García Alonso, J.I.; Donard, O.F.X. Evaluating the potential and limitations of double-spiking species-specific isotope dilution analysis for the accurate quantification of mercury species in different environmental matrices. Anal.Bional.Chem. 2008, 390:655-666.

[41] Fernández-González, V.; Concha-Graña, E.; Muiategui-Lorenzo, S.; López-Mahía, P.; Prada-Rodriguez, D. A multivariate study of the programmed temperature vaporization injection-gas chromatographic-mass spectrometric determination of polycyclic aromatic hydrocarbons. Application to marine sediments analysis. Talanta, 2008, 74:1096-1103.

[42] García-Alonso, J.I.; Rodríguez-González, P. Isotope dilution mass spectrometry. RSC Publishing, Cambridge (UK), 2013.

[43] Jackson, B.; Taylor, V.; Baker, R.A.; Miller, E. Low level mercury speciation in freshwaters by isotope dilution GC-ICP-MS. Enivron.Sci.Technol. 2009, 43:2463-2469.

[44] Stoichev, T.; Rodriguez Martin-Doimeadios, R.C.; Tessier, E.; Amouroux, D.; Donard, O.F.X. Improvement of analytical performances for mercury speciation by on-line derivatization, cryofocussing and atomic fluorescence spectrometry. Talanta, 2004, 62:433-438.

[45] Cole, R.F.; Mills, G.A.; Parker, R.; Bolam, T.; Birchenough, A.; Kröger, S.; Fones, G.R. Trends in the analysis and monitoring of organotins in the aquatic environment. Trend in Environ.Anal.Chem. 2015, 8:1-11.

[46] Sharif, A.; Monperrus, M.; Tessier, E.; Amouroux, D. Determination of methyl mercury and inorganic mercury in natural waters at the pgL-1 level: Intercomparison between PT-GC-Pyr-AFS and GC-ICP-MS using Ethylation or Propylation derivatization. E3S Web of Conference, 2013, 1: 09001.

[47] Centineo, G.; Rodríguez-González, P.; Blanco-González, E.; García Alonso, J.I.; Sanz-Medel, A.; Font Cardona, N.; Aranda Mares, J.L.; Ballester Nebot, S. Isotope dilution GC-MS routine method for the determination of butyltin compounds in water. Anal.Bioanal.Chem. 2006, 384:908-914.

[48] Cole, R.F.; Mills, G.A.; Bakir, A.; Townsend, I.; Gravell, A.; Fones, G.R. A simple, low cost GC7MS method ofr the sub-nanogram per litre measurement of organotins in coastal water. MethodsX, 2016, 3:490-496.

[49] Centineo, G.; Blanco-González, E.; Sanz-Medel, A. Multielemental speciation analysis of organometallic compounds of mercury, lead and tin in natural water samples by headspace-solid phase microextraction followed by gas chromatography-mass spectrometry. J.Chromatogr.A, 2004, 1034:191-197.

[50] Segovia-Martínez, L.; Bouzas-Blanco, A.; Campíns-Falcó, P.; Seco-Torrecillas, A. Improving detection limits for organotin compounds in several matrix water samples by derivatization-headspace-solid-phase microextraction and GC-MS. Talanta, 2010, 80:1888-1893.

CHAPTER

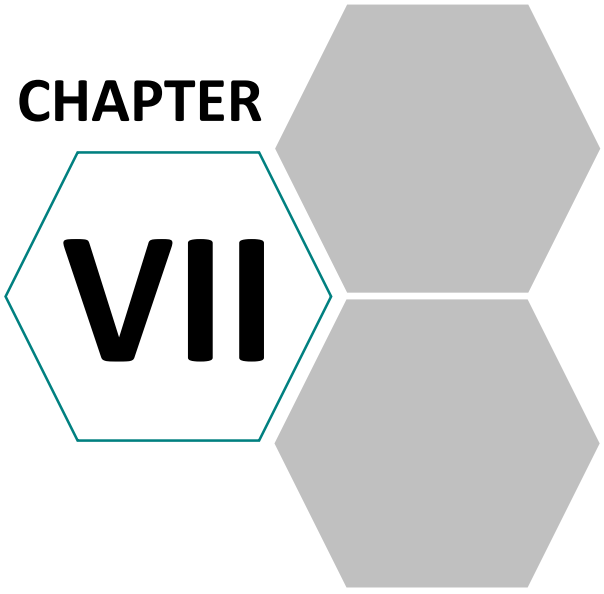

VII

GENERAL CONCLUSIONS

GENERAL CONCLUSIONS

As a general conclusion, it can be affirmed that the overall objective of this Doctoral Thesis was accomplished because new, simple and reliable analytical methods to determine metals and organometallics in sediments and river waters were developed, following the principles of Green Analytical Chemistry.

This assertion is derived from the collection of conclusions that was presented in each chapter. Some of the most important achievements are highlighted below:

- The in-depth mathematical study about the quantitation using the standard addition method (SAM) demonstrated that the use of extrapolation can yield biased predictions and confidence intervals substantially different from interpolation. Therefore, the last one is strongly recommended to guarantee accurate results, which are of relevance in quality assurance, method validation and error propagation.

- A new analytical method was developed for determination of metals in marine sediments, which aims contributing to the necessary simplification and harmonization of the analytical methodologies required to set and monitor worldwide “Sediment Quality Guidelines” (SQGs). The simple and fast method proposed here was validated to determine the simultaneously extracted metals (SEM) fraction, as well as to estimate the acid volatile sulfides (AVS), allowing for a new screening methodology to monitor metal pollution in marine sediments.

- The mass discrimination factor, affecting accuracy in ICP-IDMS, was set by means of a fast, simple and straightforward procedure based on the statistical study of the residuals of the least squares fit from several models. This approach does not involve laboratory extra work and can be applied easily by the analysts so that decision making is fast and reliable.

- The application of the isotope dilution (ID) analysis provided good accuracy and low LODs in the determination of the bioaccessible fractions of cadmium and chromium in sediments, avoiding the influence of possible losses of analytes during the extraction process. In addition, it reduces the total analysis time.

- The direct analysis of solid samples by LA-ICP-IDMS for cadmium and chromium determination in sediments, based on the synthesis of a unique solid spike to analyze all the samples, constitutes a promising way to implement direct and absolute analytical procedures that can be applied by monitoring laboratories. This would allow them to perform fast, green and direct analysis of solid samples.

- The simultaneous determination of organometallic compounds of mercury, tin and lead in natural water was successfully accomplished by an online automated pre-concentration method using large volume injections in a programmable temperature vaporizer (PTV) coupled to GC-ICP-MS. This new methodology could be used as a reference method in control laboratories, ensuring compliance with the European directives and regulations in the Environmental Quality Standards (EQS).

ANEXO I: RESUMEN

El principal objetivo de esta Tesis Doctoral, que tiene por título "Estrategias analíticas para estudiar los metales en matrices ambientales por espectrometría de masas con plasma de acoplamiento inductivo" es desarrollar nuevos métodos analíticos para detectar y cuantificar metales traza y sus formas químicas aplicando los principios de la Química Analítica Verde. Así, el propósito es conseguir métodos simples, rápidos y exactos que proporcionen información validada para tomar decisiones. Este trabajo ha sido llevado a cabo en el grupo de investigación "Química Analítica Aplicada" de la Universidade da Coruña. En concreto, se desarrollarán métodos analíticos para determinar la concentración total y la fracción disuelta o bioaccesible, y también las diferentes especies químicas.

El trabajo está enfocado a dos matrices ambientales, aguas y sedimentos. Para la primera existen leyes claras y estrictas enmarcadas dentro de la Water Framework Directive (WFD), las listas de "potencialmente peligrosos" (PHS), "prioritarios" (PS) y "emergentes", y los estándares de calidad ambiental (EQS) establecidos para cada sustancia. Todo esto hace que sea primordial el desarrollo de nuevos procedimientos analíticos que incluyan técnicas de extracción modernas e instrumentación analítica de vanguardia para poder detectar y cuantificar concentraciones muy bajas de los contaminantes. En el caso de los sedimentos la determinación de la fracción metálica bioaccesible es un buen indicador de su calidad. Desafortunadamente existen muchos puntos de vista diferentes acerca de este término, así como de otros conceptos relacionados, y por otro lado no existe una metodología uniforme para su evaluación. Esta situación hace necesario el desarrollo de nuevas metodologías analíticas sencillas para determinar esta fracción, y que contribuyan a simplificar y uniformizar las guías de calidad de los sedimentos.

De acuerdo con estas consideraciones, se plantearon los ***objetivos específicos*** siguientes:

- Hacer un estudio estadístico preliminar de los modos de calibración clásicos más comunes, lo cual constituye una etapa necesaria en cualquier análisis cuantitativo.

- Desarrollar y validar un procedimiento simple para evaluar la fracción metálica bioaccesible en sedimentos, a través de los metales extraídos simultáneamente (SEM), empleando la espectrometría de masas con plasma de acoplamiento inductivo (ICP-MS), así como proponer un método rápido y sencillo para determinar los sulfuros ácidos volátiles (AVS).

- Aplicar el análisis por dilución isotópica (ID) para evaluar el proceso de extracción de la fracción bioaccesible de Cd u Cr en sedimentos y cuantificarla con un método absoluto. Para ello es necesario estudiar la forma más adecuada de calcular el factor de discriminación de masas en ICP-IDMS.

- Desarrollar una metodología simple y fiable para calcular el contenido total de Cr y Cd en sedimentos por ablación láser ICP-IDMS.

- Implementar un método analítico para realizar la especiación simultánea de compuestos organometálicos de Hg, Sn y Pb usando un inyector de temperatura programada para cromatografía de gases acoplada con ICP-IDMS.

El trabajo experimental de esta tesis y los resultados que se obtuvieron se organizaron en los ***capítulos*** que se detallan a continuación.

Capítulo II: es una revisión crítica. Incluye una introducción acerca de los metales, sus propiedades y su comportamiento químico en el agua y en los sedimentos. Así algunos de estos elementos son esenciales para los seres vivos, a niveles bajos de concentración, pero cuando dichos niveles son más elevados pueden provocar una importante toxicidad. Su principal característica es que no se degradan y por lo tanto se acumulan tanto en el medio ambiente como en los organismos vivos. En concreto, los sedimentos tienen una gran capacidad para acumular metales (hasta un millón de veces más que el volumen equivalente de agua) por lo que han sido caracterizados como sumideros, además a través de ellos los metales pueden entrar en las redes alimentarias ecológicas y humanas. Para los humanos la ruta de entrada de los metales desde los sedimentos es a través del agua que usan para beber,

asearse y nadar; y su disponibilidad está determinada por los procesos de intercambio sedimento-agua que pueden provocar la liberación o la redistribución de los contaminantes que están en el seno del sedimento. Para evaluar los riesgos de contaminación metálica en los sedimentos se deben tener en cuenta dos tipos de fracciones:

- los metales que se encuentran formando parte de la matriz mineral del sedimento, que no están disponibles para la biota y su liberación sólo ocurre por procesos diagenéticos.

- "Intercambiable" o lábil". Las especies metálicas disueltas se combinan con coloides o partículas del sedimento a través de procesos de unión intercambiables. El origen de estos metales es debido a procesos diagenéticos y de desgaste. Esta fracción intercambiable de los metales está sujeta a procesos de especiación en la fase acuosa y de adsorción/absorción en las fases sólidas.

En los últimos años se han realizado esfuerzos enfocados al desarrollo de principios científicos actualizados y directrices para evaluar los riesgos ecológicos de las sustancias químicas en aguas y sedimentos marinos. En el caso de los sedimentos los riesgos asociados varían en función de las condiciones físicas, químicas y biológicas a las que el organismo está expuesto y a su biodisponibilidad. Teniendo en cuenta la importancia de la biodisponibilidad y la bioaccesibilidad en los procesos de evaluación de riesgos, estos términos deben ser definidos con claridad. En este sentido y teniendo en cuenta las recomendaciones de la IUPAC se establecen la siguiente diferenciación:

- Biodisponibilidad: extensión de la absorción de una sustancia (qe está disponible) por parte de un organismo vivo comparada con un sistema de referencia.

- Bioaccesibilidad: potencial de una sustancia de entrar en contacto con un organismo vivo e interactuar con él si el organismo tiene acceso a dicho compuesto.

Estos términos son muy importantes en el proceso de evaluación de riesgo ambiental, que abarca global desde la identificación del peligro hasta la gestión del riesgo. Así el estatus de protección se identifica en términos de conformidad con todos los estándares de calidad medioambiental (EQS) establecidos para las sustancias químicas por la lista europea de prioridad. Los EQS incluyen concentraciones en la columna de agua, en los sedimentos y en la biota que deben proteger la salud humana y el medioambiente.

En relación a los sedimentos de forma general se acepta que la concentración metálica total constituye una predicción poco adecuada del riesgo provocado por los metales. Así sería preferible la evaluación de la bioaccesibilidad, pero la mayor dificultad que se presenta a la hora de hacerlo es que no existe un esquema unificado, sino que existen una gran variedad de aproximaciones, lo que hace muy difícil la comparación de los resultados y el establecimiento de conclusiones.

En el caso de los metales la bioaccesibilidad se puede abordar utilizando el criterio SEM-AVS. Los términos AVS y SEM están definidos de forma operacional y se refieren a las fracciones de sulfuros y de metales que se liberan en una extracción con ácido débil sin calentamiento. Los metales estarán formado parte de los respectivos sulfuros si hay un exceso de AVS con respecto a los metales (SEM), mientras que se mantengan las condiciones anaeróbicas.

En la evaluación del riesgo de los metales en sedimentos es importante también tener en cuenta los niveles de fondo, que se refieren a la concentración utilizada como punto de referencia y a partir de la cual se puede establecer si ha existido algún tipo de liberación, ya sea desde una fuente natural o antropogénica, del contaminante de estudio en un lugar concreto. Además las diferentes formas físicas y químicas de los metales van a afectar a la exposición, bioaccesibilidad, etc., y a su vez dichas formas van a estar influenciadas por las condiciones físico-químicas del medio.

Se incluye también en este capítulo un resumen crítico de los principales procedimientos de tratamiento de muestra para la determinación de metales. Para muestras sólidas se comentan dos tipos de procedimientos:

- Métodos de digestión para la determinación del contenido metálico total basados en la aplicación de microondas. Se comentan sus características y las ventajas que ofrecen frente a los métodos tradicionales de disolución.

- Métodos para la determinación de las fracciones metálicas bioaccesibles, basados en procesos de lixiviación o extracción. Se describe la aplicación de energía de ultrasonidos que proporciona una agitación más eficaz y se comentan las aplicaciones más importantes relacionadas con la determinación de la fracción metálica bioaccesible en sedimentos.

En el caso de muestras de aguas se comparan algunos de los procedimientos más utilizados para la extracción de las diferentes especies metálicas, en términos de eficacia, tiempo, tipo y cantidad de disolventes, etc., como son la extracción líquido-líquido clásica, la extracción en fase sólida (SPE), la microextracción en fase sólida (SPME), la extracción con barras agitadoras (SBSE), la extracción asistida con membrana (MASE) y la microextracción líquido-líquido dispersiva (DLLME).

Así mismo se describe la espectrometría de masas con plasma de acoplamiento inductivo (ICP-MS) como técnica instrumental para la determinación de metales. Se comentan brevemente sus características instrumentales, las principales interferencias y sus ventajas más importantes frente las técnicas espectroscópicas, entre las que se encuentran la capacidad de determinación multielemental, la elevada sensibilidad y la capacidad de obtener información isotópica de forma sencilla.

Finalmente se comentan las características de aplicación de los métodos de cuantificación más comunes, incluyendo la calibración externa, el patrón interno y el método de adiciones estándar. Se aborda el análisis por dilución isotópica como método de cuantificación absoluto, comentando sus grandes ventajas en la calidad de los resultados obtenidos frente a la calibración convencional, y también algunos de sus inconvenientes.

Capítulo III: presenta una demostración matemática completa acerca de la forma óptima de cuantificar analitos utilizando el método de las adiciones estándar. Tradicionalmente se ha utilizado la extrapolación (en lugar de la interpolación) para realizar el cálculo de la concentración, sin embargo esta práctica no es la más adecuada ya que los valores predichos van a verse muy afectados por pequeñas desviaciones de los puntos de calibrado. En este trabajo se estudian ambas aproximaciones (la interpolación y la extrapolación) en términos de las varianzas asociadas a las predicciones. Para ello se plantearon diferentes escenarios, llevando a cabo distintas simulaciones de

errores en tres niveles de concentración del analito. También se hace un estudio sobre el correcto planteamiento matemático que debe utilizarse cuando la cuantificación se realiza mediante interpolación o extrapolación, ya que es una práctica bastante común el realizar la cuantificación mediante extrapolación, pero que utilizando las ecuaciones derivadas de la interpolación para el cálculo de los intervalos de confianza.

Capítulo IV: se desarrolla un procedimiento para evaluar la fracción metálica bioaccesible en sedimentos marinos, a través de los metales extraídos simultáneamente (SEM) y de los sulfuros ácidos volátiles (AVS). El estudio de la extracción se realiza comparando, mediante un análisis multivariante (ANOVA), la agitación magnética y la aplicación de ultrasonidos a través de un baño y de una sonda. La sonda de ultrasonidos proporcionó resultados satisfactorios en un tiempo muy corto (16 min) y permitió realizar la extracción con una cantidad muy pequeña de ácido clorhídrico 1 mol L^{-1}, con lo que se minimiza la cantidad de reactivos utilizada y por lo tanto la generación de residudos. La fracción metálica extraída se compara con la suma de las tres etapas del procedimiento de extracción secuencial del sedimento de referencia BCR 701. Los sulfuros ácidos volátiles se evalúan restando la fracción de azufre que queda en el residuo de la extracción del contenido total de azufre en las muestras. La relación SEM-AVS se usa para evaluar el riesgo de contaminación metálica en muestras de sedimentos procedentes de dos rías gallegas. Se determina también el contenido total de los metales en las muestras analizadas, utilizando un procedimiento de referencia que incluye la digestión total en un horno microondas. Estos valores permiten calcular el porcentaje de la fracción extraída frente al contenido total, lo que constituye una aproximación diferente para la evaluación de la contaminación metálica de los sedimentos.

Capítulo V: en este capítulo se aborda el uso del análisis por dilución isotópica para determinar metales por ICP-MS. En primer lugar, se realiza un estudio estadístico para decidir cuál es el mejor método para calcular el factor de discriminación de masas (factor K), que es un parámetro que afecta a la exactitud en la medida de las relaciones isotópicas que son la base del cálculo en dilución isotópica. La estrategia propuesta está basada en conceptos estadísticos básicos asociados con el ajuste por mínimos cuadrados,

concretamente en el estudio de los residuales de los diferentes modelos que se proponen frecuentemente en la bibliografía: lineal, exponencial, potencial y Russel. Se abordan cuatro ejemplos diferentes en los que se determinan Cd, Cr, Nd y Sm mediante ICP-IDMS. Como resultado de los diferentes test estadísticos aplicados se concluye que para el Cd el modelo de Russel es el más adecuado para calcular el factor K, y para los otros tres elementos el modelo potencial es el óptimo.

A continuación se presentan los métodos desarrollados para cuantificar la fracción bioaccesible de cadmio y cromo en sedimentos mediante ICP-IDMS. Se añade el patrón isotópico enriquecido (trazador) disuelto en la disolución de extracción (HCl 1 mol L^{-1}) para que se produzca el equilibrio con el elemento nativo de la muestra. Así, cualquier posible pérdida de los analitos durante las siguientes etapas del procedimiento no va a causar errores en los valores de concentración calculados, puesto que, una vez alcanzado el equilibrio isotópico, las relaciones isotópicas no varían. Para minimizar las fuentes de error se evaluaron los parámetros que afectan a la precisión y a la exactitud en la medida de las relaciones isotópicas, como son las interferencias espectrales, el tiempo muerto del detector, el factor de discriminación de masas y la selección de la relación óptima muestra/trazador. Por otro lado, al añadir el trazador al final de la extracción, se pudo comprobar que en el caso del Cd se producen pérdidas importantes durante la extracción, debidas probablemente a procesos de evaporación o reabsorción, mientras que para el Cr este efecto es menos significativo. El comportamiento observado para estos dos metales se debe a su diferente interacción con la matriz del sedimento. Las fracciones metálicas extraídas se compararon con la suma de las de las tres etapas del procedimiento de extracción secuencial del sedimento de referencia BCR 701. En ambos casos se alcanzaron correlaciones satisfactorias en torno al 100 %. El método se aplica a la determinación de las fracciones bioaccesibles de Cd y Cr en muestras de sedimentos de dos rías gallegas.

Se desarrolla un método para la determinación directa del contenido total de Cd y Cr en sedimentos utilizando la ablación láser (con un sistema láser convencional con frecuencia de nanosegundos) acoplada a ICP-IDMS. Dicho método está basado en la síntesis de único patrón sólido enriquecido isotópicamente (en Cd y Cr) que a continuación se mezcla de forma sencilla con cada una de las muestras que van a ser analizadas. La preparación del

trazador sólido consiste en añadir una cantidad adecuada de una disolución enriquecida en ciertos isótopos de los elementos estudiados a una alícuota de un sedimento certificado y a continuación se lleva a cabo la eliminación del disolvente. Se estudian dos alternativas para esta etapa de secado la liofilización y la evaporación del disolvente (agua) en un rotavapor. Este último procedimiento, que se realiza tan en sólo 38 min, favorece que se produzca el equilibrio isotópico obteniéndose un trazador con una distribución isotópica homogénea. Se estableció asimismo un protocolo sencillo para la preparación de las pastillas que se someten a la acción del láser, preparando un molde para tal fin. A continuación se realizó un estudio multivariante (diseño de experiencias de Plakett-Burman) para evaluar el efecto de las variables que son críticas durante el proceso de ablación: la energía del láser, el diámetro del spot, la velocidad de repetición y la velocidad de barrido. El resultado fue que ninguna de ellas afecta significativamente a las intensidades proporcionadas por los isótopos de Cd y Cr. El procedimiento se validó satisfactoriamente analizando dos materiales de referencia de sedimento con contenidos certificados de estos dos elementos y se aplicó al análisis de muestras de sedimentos de dos rías gallegas.

Capítulo VI: recoge el trabajo realizado y los resultados alcanzados durante la estancia de investigación en el *Laboratoire de Chimie Analytique Bio-inorganique et Environnement* (LCABIE – *Institut Pluridisciplinaire de Recherche sur l´Environnement et les Matériaux* – Pau, France). Así, se presenta un método analítico para la determinación simultánea de compuestos organometálicos de mercurio (monometil- e inorgánico), estaño (especies metiladas y butiladas) y plomo (tetrametil- y tetraetil-) en aguas de río mediante cromatografía de gases con inyector de temperatura programable acoplada con ICP-IDMS. Es un método automatizado de pre-concentración online que permite inyectar volúmenes grandes de muestra en el cromatógrafo de gases. Se estudió la influencia de varios parámetros como el tiempo y la temperatura de transferencia del inyector PTV, el flujo de gas portador y la cantidad de material de relleno. Se optimizó también el volumen de inyección máximo en los modos de inyección única y múltiple para obtener un compromiso entre resolución cromatográfica y sensibilidad. Se obtuvieron límites de detección muy bajos, del orden de pg L^{-1} para todas las especies estudiadas. Con el fin de demostrar la aplicabilidad del método, se realiza el

análisis de una serie de muestras de agua de río de un ecosistema acuático de interés medioambiental (cuenca y afluentes del río Adour, Pau).

Como ***conclusión general*** se puede afirmar que se ha alcanzado el objetivo global de esta Tesis Doctoral, ya que se han desarrollado métodos analíticos para determinar metales y compuestos organometálicos en sedimentos marinos y aguas de río, siguiendo los principios de la Química Analítica Verde. Además se ha demostrado la aplicación práctica de todos ellos a través del análisis de muestras reales, teniendo en cuenta la dificultad añadida que entraña dicha aplicación.

A continuación se destacan los ***logros más importantes*** alcanzados en la realización de este trabajo:

El estudio matemático acerca de la cuantificación utilizando el método de adiciones estándar (SAM) demostró que el uso de la extrapolación puede dar lugar a predicciones erróneas y a intervalos de confianza significativamente diferentes a los obtenidos por interpolación. Por lo tanto, es altamente recomendable el uso de esta última para garantizar resultados fiables, que son relevantes en control de calidad, validación de métodos y propagación de errores.

Se desarrolló un nuevo método analítico para determinar metales en sedimentos marinos que tiene por objeto contribuir a la simplificación y armonización de las metodologías analíticas requerida para establecer guías internacionales de calidad de los sedimentos. El método simple y rápido propuesto en este trabajo se validó para determinar los metales extraídos simultáneamente (SEM), así como para estimar los sulfuros ácidos volátiles (AVS), proporcionando una nueva metodología para monitorizar la contaminación metálica en sedimentos marinos.

El factor de discriminación de masas, que afecta a la exactitud en ICP-IDMS, se establece utilizando un método rápido, simple y directo basado en el estudio estadístico de los residuales del ajuste por mínimos cuadrados obtenido a partir de varios modelos. Esta aproximación no requiere trabajo

experimental extra y puede ser aplicado fácilmente por los químicos analíticos ya que la toma de decisiones es rápida y fiable.

La aplicación del análisis por dilución isotópica (ID) proporcionó buena exactitud y bajos límites de detección en la determinación de las fracciones bioaccesibles de Cd y Cr en sedimentos, evitando la influencia de posibles pérdidas de los analitos durante el proceso de extracción. Además reduce el tiempo total del análisis.

El análisis directo de muestras sólidas por LA-ICP-IDMS para la determinación de Cd y Cr en sedimentos, basado en la síntesis de un único trazador sólido para analizar todas las muestras, constituye una alternativa prometedora para implementar los procedimientos analíticos directos y absolutos que puede ser aplicada en laboratorios de monitorización ambiental. Esto les permitirá realizar análisis rápidos y directos de muestras sólidas.

La determinación simultánea de compuestos organometálicos de Hg, Sn y Pb en aguas naturales se llevó acabo de forma satisfactoria mediante un método de preconcentración on-line automático usando volúmenes grandes de inyección en un inyector de temperatura programable (PTV) acoplado a GC-ICP-MS. Esta nueva metodología podría ser usada como método de referencia en laboratorios de control, asegurando el cumplimiento de las directivas europeas y de los estándares de calidad ambiental (EQS).

This Doctoral Thesis presents validated analytical strategies to assess metallic contamination (metals and some of their chemical forms) in relevant environmental matrices (marine sediments and river waters) by ICP-MS. Major findings are:

i) A simple method to evaluate the bioaccessible fraction of 6 metals in sediments. Also, an alternative to estimate the acid volatile sulfur content.

ii) ICP-MS with Isotope Dilution improved largely the accuracy of the measurements for Cd and Cr.

iii) A direct method to quantify the total content of Cd and Cr in sediments by LA-ICP/IDMS.

iv) A very sensitive method based on PTV-GC-ICP/IDMS. It reaches the very restrictive limits targeted by WFD for the organometallic compounds of Hg, Sn and Pb.